MAX-PLANCK-INSTITUT
FÜR METEOROLOGIE

The Role of Sailboats in Advancing Our Understanding of the Ocean Carbon Sink

Jacqueline Behncke

Hamburg 2025

Berichte zur Erdsystemforschung 293
Reports on Earth System Science 2025

Hinweis

Die Berichte zur Erdsystemforschung werden vom Max-Planck-Institut für Meteorologie in Hamburg in unregelmäßiger Abfolge herausgegeben.

Sie enthalten wissenschaftliche und technische Beiträge, inklusive Dissertationen.

Die Beiträge geben nicht notwendigerweise die Auffassung des Instituts wieder.

Die "Berichte zur Erdsystemforschung" führen die vorherigen Reihen "Reports" und "Examensarbeiten" weiter.

Anschrift / Address

Max-Planck-Institut für Meteorologie
Bundesstrasse 53
20146 Hamburg
Deutschland

Tel./Phone: +49 (0)40 4 11 73 - 0
Fax: +49 (0)40 4 11 73 - 298

name.surname@mpimet.mpg.de
www.mpimet.mpg.de

Notice

The Reports on Earth System Science are published by the Max Planck Institute for Meteorology in Hamburg. They appear in irregular intervals.

They contain scientific and technical contributions, including PhD theses.

The Reports do not necessarily reflect the opinion of the Institute.

The "Reports on Earth System Science" continue the former "Reports" and "Examensarbeiten" of the Max Planck Institute.

Layout

Bettina Diallo and Norbert P. Noreiks
Communication

Copyright

The Role of Sailboats in Advancing Our Understanding of the Ocean Carbon Sink

Jacqueline Behncke

Hamburg 2025

Jacqueline Behncke
aus Flensburg, Deutschland

Max-Planck-Institut für Meteorologie
The International Max Planck Research School on Earth System Modelling
(IMPRS-ESM)
Bundesstrasse 53
20146 Hamburg

Tag der Disputation: 14. Oktober 2025

Folgende Gutachter empfehlen die Annahme der Dissertation:
Dr. Peter Landschützer
Prof. Dr. Tatiana Ilyina

Vorsitzender des Promotionsausschusses:
Prof. Dr. Hermann Held

Dekan der MIN-Fakultät:
Prof. Dr.-Ing. Norbert Ritter

Titelgrafik: Foto von Andreas Lindlahr

ISSN 1614-1199 - doi: 10.17617/2.3684442

This document was typeset using the `classicthesis` template developed by André Miede and inspired by Robert Bringhurst. Available at https://bitbucket.org/amiede/classicthesis/

ABSTRACT

The ocean absorbs about a quarter of anthropogenic CO_2 emissions each year, mitigating climate change. Since 2018, sailboats have collected >350,000 observations of CO_2 fugacity (fCO_2) mainly during round-the-world races in the Atlantic and the underobserved Southern Ocean, both key regions of carbon uptake. This dissertation examines the role of these sailboat data in advancing our understanding of the ocean carbon sink.

First, I demonstrate the value of high-frequency sailboat observations in capturing fCO_2 variability across different small-scale ocean dynamics. For instance, under different fCO_2 regimes in the Agulhas region, fCO_2 is higher in anticyclonic eddies and lower in cyclonic eddies, with strong gradients at eddy edges. Under algae blooms, varied effects are observed: a Celtic Sea bloom reduces fCO_2, while a mixed coccolithophore bloom on the Patagonian Shelf causes short-term fCO_2 fluctuations up to 100 µatm within half an hour. Small-scale features such as fCO_2 gradients at eddy and bloom edges or bloom-induced fCO_2 fluctuations are often missed in infrequent observations, in regridded data products, or in models. Our findings demonstrate the critical role of high-resolution fCO_2 observations, such as those collected by sailboats, in understanding CO_2 dynamics and improving regional and global air-sea CO_2 flux estimates, particularly in variable, underobserved regions.

Second, I show that including observations from even a single sailboat significantly impacts air-sea CO_2 flux estimates generated by the neural network gap-filling method SOM-FFN, particularly in the Southern Ocean. Adding sailboat observations significantly increases the regional carbon uptake estimate in the North Atlantic and decreases it in the Southern Ocean. While compensating changes in both basins limit the global effect, the Southern Ocean – particularly frontal regions between 40°S–60°S during summertime – exhibited the largest air-sea CO_2 flux changes, averaging 20% of the regional mean. The results stay robust within the expected random measurement uncertainty (±5 µatm) but remain undetectable with a measurement offset of 5 µatm.

Third, using observing system simulations based on the HAMOCC model and novel sailboat tracks, we demonstrate how integrating sailboat data improves estimates of ocean carbon uptake. While we underestimate the ocean carbon sink when mimicking real-world sampling, adding available sailboat data does not substantially improve reconstructions. However, increased sampling reveals a stronger carbon sink, particularly between 40°S and 60°S. The improvement persists with hypothetical measurement uncertainties, but substantial differences arise depending on whether positive or negative biases are applied to the sailboat track data. While we show that two additional circumnavigations already improve the ocean mean sink estimate, we further highlight that the additional data remain insufficient to correct the overestimated CO_2 sink trend, calling for continuation of the ongoing data collection.

These findings highlight the value of racing sailboats as a complementary observing platform that fills essential observational gaps, particularly in highly variable and underobserved ocean regions.

ZUSAMMENFASSUNG

Der Ozean nimmt etwa ein Viertel der vom Menschen verursachten CO_2-Emissionen pro Jahr auf und mildert damit den Klimawandel. Seit 2018 haben Segelboote mehr als 350.000 Beobachtungen der CO_2-Fugazität (fCO_2) gesammelt – hauptsächlich während Weltumsegelungen durch den Atlantik und den unterbeobachteten Südlichen Ozean, zwei Schlüsselregionen für die Kohlenstoffaufnahme. Diese Dissertation untersucht, welchen Beitrag Segelbootdaten zum besseren Verständnis der marinen Kohlenstoffsenke leisten.

Zunächst zeige ich den Mehrwert hochfrequenter Segelbootbeobachtungen für die Erfassung der fCO_2-Variabilität im Zusammenhang mit verschiedenen kleinskaligen marinen Prozessen. In der Agulhas-Region etwa ist fCO_2 in antizyklonalen Eddies erhöht und niedriger in zyklonalen Eddies, mit starken Gradienten an den Rändern der Eddies. Algenblüten zeigen unterschiedliche Effekte: Eine Algenblüte in der Keltischen See senkt fCO_2, während eine gemischte Coccolithophorenblüte auf dem Patagonischen Schelf kurzfristige fCO_2-Schwankungen von bis zu 100 µatm innerhalb von 30 Minuten verursacht. Solche kleinskaligen Merkmale – wie fCO_2-Gradienten an Rändern von Eddies und Blüten oder blüteninduzierte fCO_2-Fluktuationen – werden in unregelmäßigen Beobachtungen, in aufgerasterten Datenprodukten oder in Modellen häufig nicht erfasst. Unsere Ergebnisse unterstreichen die zentrale Bedeutung hochaufgelöster fCO_2-Beobachtungen, wie sie durch Segelboote bereitgestellt werden, für das Verständnis der CO_2-Dynamik und für die Verbesserung regionaler und globaler Schätzungen des CO_2-Flusses zwischen Atmosphäre und Oberflächenozean – insbesondere in variablen, unterbeobachteten Regionen.

Zweitens zeige ich, dass bereits Beobachtungen eines einzelnen Segelboots die Schätzungen des CO_2-Flusses, die mit der neuronalen Netzwerk-Methode SOM-FFN erstellt werden, deutlich verändert, insbesondere im Südlichen Ozean. Die Integration von Segelbootdaten erhöht die geschätzte regionale Kohlenstoffaufnahme im Nordatlantik signifikant und verringert sie im Südlichen Ozean. Während sich kompensierende Änderungen in beiden Becken auf globaler Ebene größtenteils ausgleichen, zeigt der Südliche Ozean – insbesondere die Frontregionen zwischen 40°S und 60°S im Südsommer – die größten Veränderungen im CO_2-Fluss, die im Mittel 20 % des regionalen Mittels betragen. Die Ergebnisse bleiben innerhalb der erwarteten zufälligen Messunsicherheit (±5 µatm) robust, sind bei einem systematischen Messversatz von 5 µatm jedoch nicht mehr nachweisbar.

Drittens zeigen wir mithilfe von Beobachtungssystemsimulationen basierend auf dem HAMOCC-Modell und neuartigen Segelbootrouten, wie die Integration von Segelbootdaten die Schätzung der marinen Kohlenstoffaufnahme verbessert. Wenn reale Probennahmemuster nachgebildet werden, unterschätzen wir die marine Kohlenstoffsenke. Die Ergänzung um bereits verfügbare Segelbootdaten führt zu keiner wesentlichen Verbesserung der Rekonstruktionen; eine verstärkte Probennahme hingegen zeigt eine stärkere Kohlenstoffaufnahme, insbesondere zwischen 40°S und 60°S. Diese Verbesserung bleibt auch unter Berücksichtigung hypothetischer Messunsicherheiten bestehen. Systematisch verzerrte Messungen hingegen – obwohl sie die mittleren jährlichen Flüsse über mehrere Jahre verbessern – verschlechtern die regionalen Flussschätzungen im Südlichen Ozean. Wir zeigen, dass bereits zwei zusätzliche Weltumsegelungen die Schätzung der mittleren marinen Kohlenstoffsenke verbessern; die zusätzlichen Daten reichen jedoch nicht aus, um

den überschätzten Trend der Kohlenstoffaufnahme zu korrigieren. Dies unterstreicht die Notwendigkeit, die laufende Datenerhebung fortzusetzen.
Diese Ergebnisse verdeutlichen den Wert von Segelbooten als ergänzende Beobachtungsplattform, die wesentliche Lücken in hochvariablen und unterbeobachteten marinen Regionen schließt.

PUBLICATIONS

This dissertation is based on the following three first-author studies which are included in the appendix:

APPENDIX A

Behncke, J., Landschützer, P. Physical and biological drivers of fCO_2 variability along sailboat tracks. *(in preparation)*.

APPENDIX B

Behncke, J., Landschützer, P. & Tanhua, T. A detectable change in the air-sea CO_2 flux estimate from sailboat measurements. *Scientific Reports 14*, 3345 (2024). https://doi.org/10.1038/s41598-024-53159-0.

APPENDIX C

Behncke, J., Ilyina, T., Chegini, F. & Landschützer, P. Improved air-sea CO_2 flux estimates from sailboat measurements. *Under review at Science Advances*.

Furthermore, I contributed as a co-author to an additional publication based on my research work:

Landschützer, P., Tanhua, T., **Behncke, J.** & Keppler, L. (2023). Sailing through the southern seas of air-sea CO_2 flux uncertainty. *Philosophical Transactions of the Royal Society A: Mathematical, Physical and Engineering Sciences*, 381 (2249), 20220064. https://doi.org/10.1098/rsta.2022.0064.

ACKNOWLEDGMENTS

The dissertation would not have been possible without the help and support of many people.

First and foremost, I would like to express my deepest gratitude to my supervisor, Peter Landschützer. Thank you for showing me all the good sides of academic research and conveying a healthy perspective on its challenges. Thanks for being the best possible supervisor I could imagine, even from afar. Whether it was scientific guidance, emotional encouragement, reliability, or helping me build connections, your constant support has meant the world to me. The way you lead by example has made you a great role model in science, and for that, I am truly appreciative.

I am also incredibly grateful to my co-advisor, Tatiana Ilyina, for welcoming me into her group. The scientific discussions and the room you provided for me to grow as a scientist have helped me greatly on my journey. Thank you for always being excited about my research!

I sincerely thank the sailors, particularly Boris Herrmann and Team Malizia, for their collaboration and for making room for science during their races. By collecting data in remote ocean regions, you've made this thesis possible.

I am very grateful to my co-authors and my internal and external reviewers. Writing papers with you has been a fantastic experience. I also want to thank everyone who read and commented on drafts of my thesis. Your constructive feedback was incredibly helpful and much appreciated.

I would also like to express my gratitude to my colleagues and friends at the Max Planck Institute for Meteorology, with special thanks to the Ocean Department and the Ocean-Biogeochemistry group. For modelers, you're actually quite okay!

To the ocean carbon observing community: thank you for the great support and inspiring ideas throughout this journey. It's been a privilege to be part of this community and to meet so many brilliant, kind people along the way.

Thank you also to the IMPRS office for all the administrative support.

Last but not least, I want to thank my family and my friends – for always listening, encouraging, and being there throughout this journey. Ein besonderer Dank gilt meiner Oma Angelika, die immer für mich da ist und an mich glaubt.

CONTENTS

LIST OF FIGURES

LIST OF TABLES

LIST OF ACRONYMS

ACC	Antarctic Circumpolar Current
AE	Anticyclonic Eddy
CE	Cyclonic Eddy
CHL	Chlorophyll-a
DIC	Dissolved Inorganic Carbon
fCO_2	Fugacity of CO_2
FFN	Feed-Forward Network
GCB	Global Carbon Budget
HAMOCC	HAMburg Ocean Carbon Cycle
IPCC	The Intergovernmental Panel on Climate Change
MLD	Mixed Layer Depth
MPIOM	Max Planck Institute Ocean Model
OSSE	Observation System Simulation Experiment
pCO_2	Partial Pressure of CO_2
PF	Polar Front
PIC	Particulate Inorganic Carbon
SAF	Sub-Antarctic Front
SLA	Sea Level Anomaly
SOCAT	Surface Ocean CO_2 Atlas
SOOP	Ship of Opportunity Programme
SOM	Self-Organizing Map
SSS	Sea Surface Salinity
SST	Sea Surface Temperature
USV	Unmanned Surface Vehicle
VOS	Voluntary Observing Ships

UNIFYING ESSAY

Unifying Essay

"observations not taken today are lost forever"

— Wunsch et al. (2013)

1 INTRODUCTION

The *Challenger* expedition between 1872 and 1876 marks for many the beginning of modern oceanographic research. A small naval ship was transformed into a pioneering research vessel with laboratories on board to study ocean chemistry, currents, marine life, and more while circumnavigating the globe. While ancient Egyptians, Greeks, and Romans mainly focused on navigation and trade, and explorers like Magellan, Darwin, and Cook contributed to ocean science through their observations and collections, nothing of the *Challenger* expedition's magnitude had been attempted before. It was the first large-scale, systematic attempt to observe the ocean. The expedition circumnavigated the globe, collecting thousands of samples mainly from the ocean floor, and provided insights into deep-sea life, seafloor structure, water chemistry, and ocean currents.

Nowadays, advancements in technology allow us to develop complex mechanistic models that simulate oceanic processes. However, direct observations remain indispensable – not only for validating and refining these models, but also for uncovering new phenomena and mechanisms, and providing the foundational truths about the ocean. Building on the *Challenger*'s legacy, a global collaborative effort has emerged to monitor the oceans. Scientists worldwide contribute extensive observations to large databases such as the Surface Ocean CO_2 Atlas (SOCAT). Additionally, citizen science initiatives, such as those involving racing sailboats (Figure 1.1), have become part of this effort. Sailboats equipped with advanced technology now measure parameters such as the fugacity of CO_2 (fCO_2) to better understand how the ocean exchanges CO_2 with the atmosphere – an endeavor that was beyond reach during the *Challenger* expedition.

150 years after the *Challenger* expedition, we continue to circumnavigate the globe, covering similar distances and traversing vast, underobserved ocean regions, collecting measurements, and exploring these data to deepen and reshape our understanding of the world. In this thesis, I show how the data collected during sailboat circumnavigations enhances our understanding of surface ocean carbon dynamics and advances ocean sciences.

Figure 1.1: The IMOCA 60 sailboat *Seaexplorer – Yacht Club de Monaco* (formerly *Malizia*) from Team Malizia. The IMOCA 60 is a high-performance, 60-foot (18.28 m) monohull class designed for single- or double-handed offshore racing, known for its use in round-the-world regattas such as the *Vendée Globe* and *The Ocean Race*. Since 2018, Team Malizia has collaborated with the Max-Planck-Institute for Meteorology to measure surface ocean fCO_2 during races and transfers. *(Photo credit: Andreas Lindlahr).*

1.1 OCEAN AS A CARBON SINK

"An atmosphere of that gas [i.e., carbon dioxide] would give to our earth a high temperature"

– Foote (1856)

Since the onset of the industrial era, atmospheric carbon dioxide (CO_2) levels have risen from about 280 ppm to about 420 ppm in 2023 (Lan et al., 2024; Sarmiento and Gruber, 2006b). This increase is largely attributed to CO_2 emissions from fossil fuel combustion and to carbon released through deforestation and other land-use changes (Friedlingstein et al., 2025). Only about half of the CO_2 emissions remain in the atmosphere, with the remainder being absorbed by land and oceans (Friedlingstein et al., 2025). The ocean plays a crucial role in mitigating global warming and regulating Earth's climate by absorbing around 26% of anthropogenic CO_2 emissions annually, equivalent to 2.9 ± 0.4 Petagram of carbon per year (Pg C yr^{-1}) (2014-2023) (Friedlingstein et al., 2025).

The ocean continually exchanges CO_2 with the atmosphere through the air-sea

interface. When CO_2 dissolves in seawater, it forms carbonic acid, which further dissociates into bicarbonate and carbonate ions, collectively known as dissolved inorganic carbon (DIC). This process increases the concentration of hydrogen ions, thereby lowering the pH of the ocean and leading to ocean acidification, which reduces the ocean's capacity to absorb more CO_2 and harms calcifying organisms, potentially disrupting the marine food web (Doney et al., 2009).

The partial pressure of CO_2 (pCO_2), measuring the concentration of CO_2 dissolved in seawater, is key to the air-sea CO_2 exchange, as the pCO_2 difference between the ocean and atmosphere determines both the direction and magnitude of this exchange (Williams and Follows, 2011a). To account for the non-ideal behavior of gases, fugacity of CO_2 (fCO_2) is used as a corrected measure of pCO_2 (Pfeil et al., 2013). However, due to the nearly ideal behavior of CO_2 – the difference between partial pressure and fugacity is less than 1% (Weiss, 1974) – both fCO_2 and pCO_2 are commonly used to calculate the air-sea carbon flux and are often treated interchangeably (Takahashi et al., 1997; Fay et al., 2018).[1] The ocean's capacity to absorb CO_2 is influenced by factors such as sea surface temperature and salinity, affecting the solubility and chemical behavior of CO_2 in seawater Together, these factors determine the air-sea CO_2 flux, expressed by the equation:

$$F = k_w \times S \times \Delta fCO_2, \tag{1.1}$$

where F is the air-sea CO_2 flux, k_w is the gas transfer velocity, which depends on wind speed, S is the solubility of CO_2 in seawater, which depends on temperature and salinity, and ΔfCO_2 represents the difference in fugacity of CO_2 at the sea surface and atmosphere (Wanninkhof, 1992).

Increased oceanic fCO_2 can oversaturate surface waters, leading to outgassing, while reduced oceanic fCO_2 results in undersaturation and carbon uptake (Takahashi et al., 2002; Sarmiento and Gruber, 2006a, Figure 1.2a). Globally, regions of carbon uptake and outgassing would nearly balance in a steady-state climate. However, anthropogenic CO_2 emissions create a gradient resulting in net oceanic carbon uptake (Friedlingstein et al., 2025). On top of the long-term increasing trend, the global ocean carbon sink has changed and fluctuated due to natural changes and anthropogenic impacts. In recent decades, it stagnated in the 1990s,

1 Note: In the observational community, it is now standard practice to report observed values as fCO_2, a convention endorsed by the IOCCP (International Ocean Carbon Coordination Project) (Fay et al., 2024). Accordingly, this thesis adopts fCO_2 throughout. For consistency, I refer to fCO_2 even when citing studies that originally report pCO_2. This choice is justified by the fact that both are often used interchangeably, and the difference between them is negligible and often only significant in the subsurface ocean (Dickson et al., 2007; Fay et al., 2024).

strengthened from the early 2000s to the mid-2010s, and has been stagnant since 2016, mainly due to large interannual climate variability (Figure 1.2b, Le Quéré et al., 2007; Landschützer et al., 2016; DeVries et al., 2017; Hauck et al., 2020; McKinley et al., 2020; Gruber et al., 2023; Friedlingstein et al., 2025). Additionally, regional fCO_2 variability, driven by physical and biogeochemical processes, is superimposed on the trend of increased carbon uptake due to human activities (Sarmiento and Gruber, 2006b).

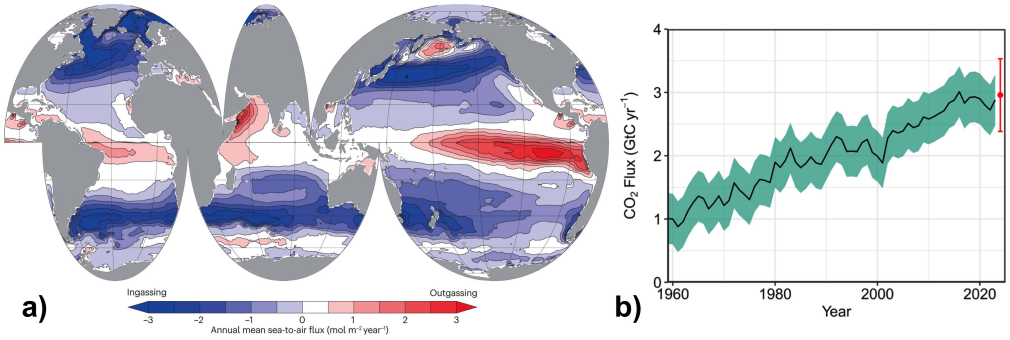

Figure 1.2: Global ocean carbon sink. a) Map of climatological mean air-sea CO_2 flux from 1990 to 2020. *From Gruber et al., 2023).* b) Timeseries of global ocean CO_2 sink. *Uncertainty bounds (±1 standard deviation) are shaded; red dots and error bars show 2024 projections and their uncertainty. From Friedlingstein et al., 2025).*

1.1.1 *Biogeochemical and Physical Drivers of Surface fCO_2*

Surface ocean fCO_2, and consequently the air-sea CO_2 flux, is influenced by a combination of biogeochemical and physical processes (Sarmiento and Gruber, 2006a; Williams and Follows, 2011a). Temperature is the primary physical driver, as the CO_2 solubility decreases with increasing temperature, resulting in higher fCO_2. These temperature changes affect the air-sea CO_2 flux by altering fCO_2 by 4.23% per 1°C (Takahashi et al., 1997; Sarmiento and Gruber, 2006b). Additionally, physical changes such as transport and mixing processes, along with biological activity, affect surface ocean fCO_2. Ocean circulation, including upwelling and mixing, redistributes water masses with varying CO_2 and nutrient levels, which can e.g. stimulate biological activity such as primary production, ultimately impacting fCO_2 (Williams and Follows, 2011a). Photosynthetic uptake of CO_2 biologically reduces surface fCO_2, while remineralization of organic matter in deeper layers can affect surface fCO_2 when DIC is transported to the surface through upwelling (Williams and Follows, 2011a). Biological CO_2 uptake depends on nutrient and light availability, influenced by factors such as seasonal changes, upwelling, and riverine nutrient input (Williams and Follows, 2011b).

Wind speed influences mixing and the rate of gas exchange between the ocean and atmosphere, thereby modifying fCO_2 levels (Williams and Follows, 2011b). The net effect of the combination of these processes creates the regions of CO_2 uptake and outgassing (Figure 1.2a). While the temperature effect predominantly dominates the low latitudes – where stratified waters limit vertical mixing and primary production remains relatively stable – fCO_2 variations in high-latitude regions are mainly driven by physical processes such as transport and mixing, along with biological activity (Sarmiento and Gruber, 2006b).

1.1.2 *Key Regions and Phenomena*

This thesis focuses on the Southern Ocean (purple regions in Figure 1.3) and the North Atlantic (northern part of the blue regions in Figure 1.3), key regions in the global carbon cycle that were sampled using sailboats. Both ocean basins play important roles in carbon uptake and prominently feature small-scale processes – such as eddies and phytoplankton blooms – through which the sailboats passed, capturing fCO_2 variability associated with these features.

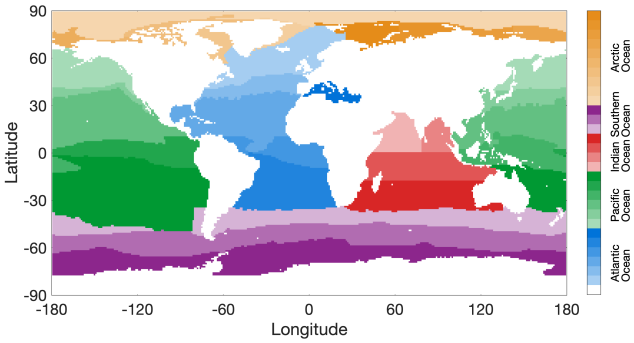

Figure 1.3: Ocean basins classified by similar biogeochemical characteristics. *The masks are from Gregor and Müller, 2025, based on Fay and McKinley, 2014. Different color shades represent subclasses within each basin.*

SOUTHERN OCEAN The Southern Ocean holds a unique position in the global system, as it is entirely surrounded by other oceans, connecting the three major ocean basins and covering approximately one-third of the world's ocean area. It accounts for 75% of excess heat uptake and about 40% of the ocean's uptake of marine anthropogenic CO_2, with the latter projected to increase to 50% by 2100 under high emissions (Frölicher et al., 2015; Landschützer et al., 2016; Mortenson et al., 2025). Between 2001 and 2020, regions south of 35°S absorbed around 1.1 ± 0.25 PgC annually (Gray, 2024).
The Antarctic Circumpolar Current (ACC) is the main current, carrying more water than any other as it flows eastward around the globe at high speeds, a route

taken advantage of by e.g. sailboats (Gray, 2024; Landschützer et al., 2023). It consists of hydrographic frontal bands that create a strong meridional gradient in the air-sea CO_2 flux by separating water masses with distinct properties (Orsi et al., 1995; Kim and Orsi, 2014; Chapman et al., 2020). The Southern Ocean's northern boundary is not consistently defined and varies by studies, extending north with the ACC reaching about 38°S (Talley et al., 2011, see Figure 1.3 for a basin definition based on biogechemical similarities). The broadest definition includes up to 30°S to cover all phenomena up to the Subtropical Front (Talley et al., 2011).
Beyond the large-scale flow of the ACC, the Southern Ocean is home to smaller-scale features, such as eddies, which influence the carbon cycle and dominate small-scale CO_2 flux variability in the region (Chapman et al., 2020; Gray, 2024). Despite its key role in the global carbon cycle, the Southern Ocean remains the most controversial ocean basin in terms of ocean carbon uptake magnitude as well as variability (e.g. DeVries et al., 2019; Hauck et al., 2020; Friedlingstein et al., 2025). This controversy is mainly attributed to the region's undersampling leading to significant uncertainties in observation-based estimates, which will be further discussed in Chapter 2 (e.g. Gloege et al., 2021; Djeutchouang et al., 2022).

NORTH ATLANTIC The North Atlantic is the most intense anthropogenic carbon sink per unit area (Mikaloff Fletcher et al., 2006; Takahashi et al., 2009; Olafsson et al., 2021). The region exhibits high spatial and temporal fCO_2 variability (Friedrich and Oschlies, 2009) and is one of the most regularly observed ocean regions, benefiting from extensive year-round observations via the Ship of Opportunity Programme (SOOP) (Macovei et al., 2020). However, substantial uncertainties persist, particularly in the seasonal variability of the air-sea CO_2 flux in the North Atlantic (as well as in the Southern Ocean) due to limited observations and inadequate representation of seasonal processes in models (Rustogi et al., 2023). Specifically, discrepancies between models and observations are still one to two times greater for seasonal fluxes than annual fluxes in the North Atlantic, despite its better observational coverage and process understanding compared to regions such as the Southern Ocean (Rustogi et al., 2023).
A major contributor to this seasonal variability is the strong biological activity at high latitudes, particularly the springtime phytoplankton blooms in the North Atlantic, which significantly modulate the air-sea CO_2 flux (e.g. Watson et al., 2009; Siegel et al., 2013; McQuatters-Gollop et al., 2007; Shutler et al., 2013; Nicholson et al., 2025).

SMALL-SCALE EDDIES AND ALGAE BLOOMS Both the Southern Ocean and the North Atlantic stand out in the global carbon cycle due to their distinctive physical and biological dynamics. Among the processes shaping carbon fluxes in these regions are small-scale ocean features such as eddies and algae blooms, which drive small-scale variability in air-sea CO_2 exchange (Williams and Follows, 2011a; Gray, 2024). Understanding these features is essential for improving our representation of regional and global carbon fluxes and advancing our knowledge of the mechanisms driving air-sea CO_2 exchange.

Eddies, particularly prevalent in regions such as the Southern Ocean and the Agulhas region, influence CO_2 levels through physical and biological processes (Keppler et al., 2024). Generally, anticyclonic eddies raise surface temperatures and fCO_2 through downwelling, which suppresses nutrients and primary production, though lateral advection can modify fCO_2 either way. Conversely, cyclonic eddies typically promote upwelling, cooling the surface and bringing nutrients upward, thereby decreasing fCO_2 through increased CO_2 solubility and enhanced primary production, but they also bring DIC-rich water to the surface, potentially increasing fCO_2. However, the quantitative and mechanistic effects of different eddies on fCO_2 remain poorly understood and observational investigations are rare (e.g. Guo and Timmermans, 2024b; Gray, 2024; Li et al., 2025). There is no consensus on whether mesoscale eddies act as ocean carbon sinks with varying strength (Jones et al., 2017; Orselli et al., 2019; Ford et al., 2023; Keppler et al., 2024; Li et al., 2025) or as sources (Chen et al., 2007; Pezzi et al., 2021; Kim et al., 2022), or if it depends on the season (Song et al., 2016), or if it varies by type, with anticyclonic eddies acting as a source and cyclonic eddies serving as sinks (Pezzi et al., 2021; Kim et al., 2022).

Phytoplankton blooms can either increase or decrease surface fCO_2, depending on their composition and phases of the bloom. Phytoplankton generally lower fCO_2 through photosynthetic carbon uptake; coccolithophores, as calcifying phytoplankton, likewise lower fCO_2 via photosynthesis, but their calcification process can increase fCO_2 (Frankignoulle et al., 1994; Shutler et al., 2013; Guinder et al., 2025).

These biological and physical processes create high variability in fCO_2 at small spatial and temporal scales. To detect these features and improve our understanding of the spatiotemporal variability of fCO_2 and air-sea CO_2 fluxes, high-resolution data are essential in highly variable regions (Friedrich and Oschlies, 2009; Monteiro et al., 2015; Dong et al., 2024a; Li et al., 2025). However, capturing these small-scale processes remains challenging due to the sparse coverage of current observing systems, particularly in remote and dynamic regions. Many platforms lack the spatial and temporal resolution needed to monitor features such as eddies or phytoplankton blooms, especially where access is limited by harsh

conditions or logistical constraints (Bushinsky et al., 2019b; Chai et al., 2020). Consequently, critical observational gaps persist in regions where high-resolution data are essential for understanding air-sea CO_2 flux variability. Specific observation platforms such as sailboats are suited for resolving this small-scale variability, especially in the remote Southern Ocean, whereas combining multiple platforms allows for capturing fCO_2 variability across a broad range of spatial and temporal scales (Carter et al., 2019).

1.2 THE BIG PICTURE: THE OCEAN CARBON VALUE CHAIN

"The goal is to turn data into information, and information into insight."

– Carly Fiorina

This chapter presents the big picture of ocean carbon observing, namely the *Ocean Carbon Value Chain*, and explains how (sailboat) observations fit into and relate to this framework.

Monitoring surface ocean carbon is key for understanding how the ocean exchanges CO_2 with the atmosphere, its contribution to the carbon cycle, and its response to climate change and human perturbations. This information is essential for quantifying the fluxes and assessing the ocean carbon budget, guiding policymakers and stakeholders in emissions management and climate change mitigation strategies. Over the past three decades, a multi-level system known as the *Ocean Carbon Value Chain* has been developed, consisting of a series of actions (Figure 1.4): (1) collections of in-situ CO_2 measurements using different platforms, (2) data synthesis of these quality-controlled measurements, (3) data analysis, (4) integration of ocean carbon sink estimates into the Global Carbon Budget and the Intergovernmental Panel on Climate Change (IPCC) assessments and (5) annual reporting of these to the Conference of the Parties (COP) (Tanhua et al., 2019; Bakker et al., 2023; IOCCP, 2024). The quality of these scientific assessments depends on the accuracy and availability of ocean carbon data. Community-based efforts have substantially advanced the monitoring and documenting of changes in ocean carbon and our understanding of its role in global carbon cycling.

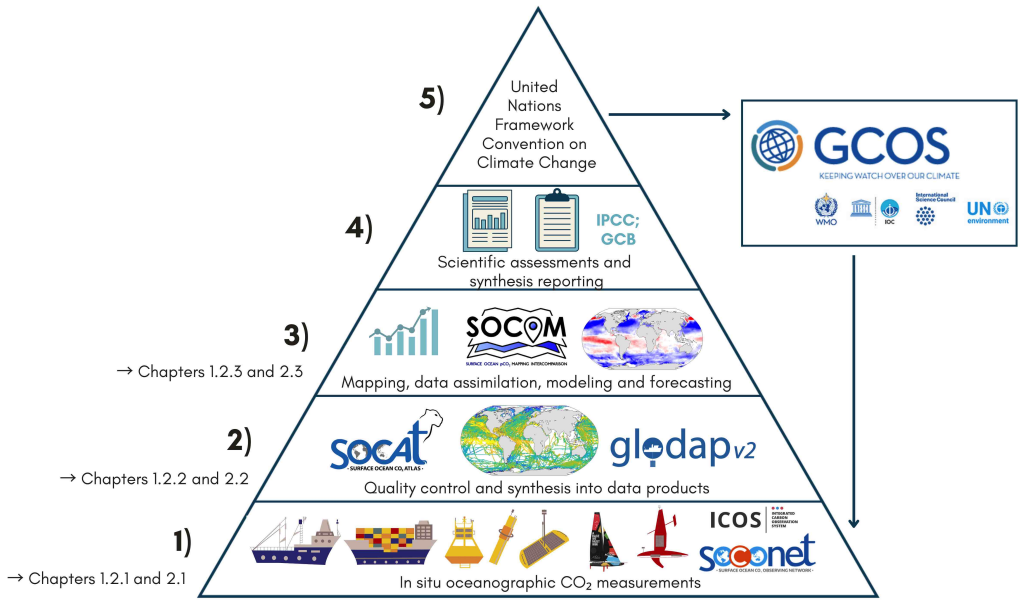

Figure 1.4: The *Ocean Carbon Value Chain* that connects in-situ oceanographic CO_2 measurements to climate negotiations. *Modified after Guidi et al., 2020).*

The collection of ocean carbon data is guided by the broader framework of the Global Ocean Observing System (GOOS) and the Global Climate Observing System (GCOS), which coordinate international efforts to monitor and understand climate-related ocean processes. Within this framework, several ship-based programs such as the Global Ocean Ship-Based Hydrographic Investigations Program (GO-SHIP) (Sloyan et al., 2019) and SOOP (Monteiro, 2010) coordinate the collection of high-quality ocean carbon data from both commercial and research ships. Surface ocean CO_2 measurements are further expanded by the Surface Ocean CO_2 Network (SOCONET), which coordinates sensors deployed on research ships, commercial vessels, and moorings (Wanninkhof et al., 2019).
The fCO_2 measurements from these programs are quality-controlled and integrated into the Surface Ocean CO_2 Atlas (SOCAT) (Bakker et al., 2016), while interior ocean carbon data are synthesized into the Global Ocean Data Analysis Project (GLODAP). These data underpin scientific assessments that inform organizations such as the IPCC (IPCC, 2023), an international collaboration founded by the World Meteorological Organization (WMO), and the United Nations Environment Program (UNEP), helping to shape global environmental policies. For an overview of actors involved in the marine carbon observations value chain, see Schoderer et al., 2024.
Together, these coordinated programs and initiatives form a comprehensive global system providing critical data on the marine carbon cycle, with continuous surface ocean fCO_2 monitoring serving as the foundation for tracking carbon exchange and its changes over time.

1.2.1 *A Short History of fCO_2 Monitoring*

"Look deep into nature, and then you will understand everything better"

– Albert Einstein

The history of in-situ sea surface ocean fCO_2 monitoring has been driven by many technological developments over time, progressing from traditional research ships to unmanned surface vehicles (USV). Historically, fCO_2 data were collected during research ship cruises (Bakker et al., 2016; Pfeil et al., 2013; Sabine et al., 2010), with the first continuous measurements starting in the late 1950s and early 1960s (Takahashi, 1961; Keeling et al., 1965; Keeling and Waterman, 1968; Waterman et al., 1996, www.socat.info/). Traditionally, discrete water samples were lab-analyzed, but automated instruments soon allowed direct, high-accuracy fCO_2 measurements from seawater intakes on moving ships, complementing traditional methods with continuous data (Pierrot et al., 2009; Schoderer et al., 2024). The CO_2 Volunteer Observing Ship Program began in 1992 to recruit commercial shipping vessels for meteorological data collection (Jiang et al., 2019). Since the mid-1990s, fCO_2 data have been gathered from buoys and moorings (Karl and Lukas, 1996; Dickey et al., 1998; Bates et al., 2000; Hood and Merlivat, 2001). In 2007, the global marine carbon community established SOCAT, a voluntary initiative to compile and quality-control the growing volume of fCO_2 data, providing a publicly accessible platform (Bakker et al., 2016). Technological advancements have since introduced marine autonomous platforms, enhancing the observation network (Pierrot et al., 2009; Sutton et al., 2014; Bushinsky et al., 2019b; Whitt et al., 2020; Sutton and Sabine, 2023; Hammermeister et al., 2025). Around 2010, wave gliders joined the fCO_2 observational network (Manley and Willcox, 2010; Monteiro et al., 2015; Chavez et al., 2018). Argo floats, with pH sensors for indirect fCO_2 measurement, became part of the Biogeochemical-Argo program in 2016, including the SOCCOM array in the Southern Ocean (Johnson et al., 2017; Bittig et al., 2019; Bushinsky et al., 2019a; Claustre et al., 2020). Saildrones have been measuring fCO_2 since 2011, with data included in SOCAT from 2017 onwards (Zhang et al., 2019; Sabine et al., 2020; Sutton et al., 2021, www.socat.info/). Since 2018, sailors onboard racing sailboats have collaborated with scientists from the Max-Planck-Institute for Meteorology to collect high-frequency fCO_2 measurements during global racing events, becoming one of the largest providers of fCO_2 data in recent years (Smith et al., 2019; Landschützer et al., 2023, www.socat.info/).

While increasing measurement frequency in monitoring platforms generally enables earlier identification of emergent long-term climate trends, especially in

systems with high short-term variability, different observation platforms – each observing processes over specific temporal and spatial scales – are suited to capturing variability at those particular scales (Carter et al., 2019, Figure 1.5). These platforms complement each other, forming the foundation of the *Ocean Carbon Value Chain*. At the next level, their measurements are synthesized into SOCAT, contributing to the GCB, and ultimately informing IPCC reports, which guide global climate policy (Figure 1.4).

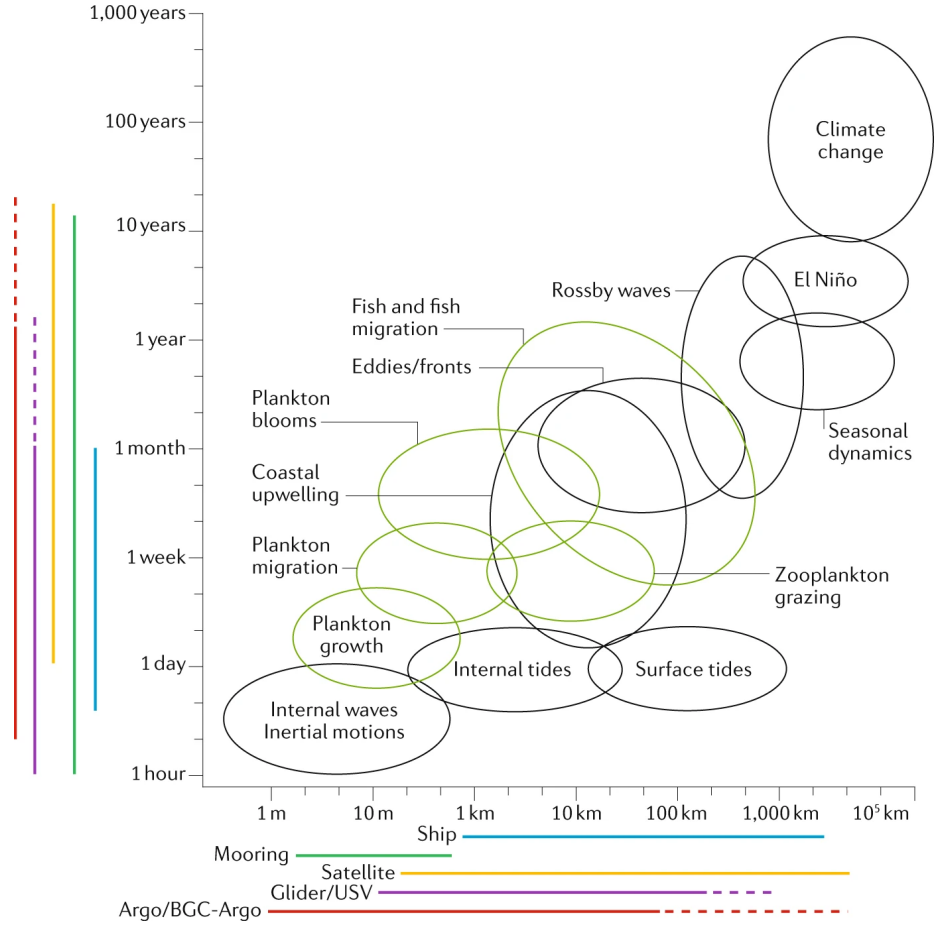

Figure 1.5: Spatial and temporal scale characteristics of ocean observing systems and environmental processes. Black circles represent dynamic and/or physical processes, while green circles represent biological and/or ecological processes. The lines indicate the spatiotemporal coverage of different observational platforms. Dashed lines indicate potential extension of an observational network. *Figure from Chai et al., 2020.*

1.2.2 *Data Synthesis*

On the second level of the *Ocean Carbon Value Chain* observational data is synthesized into quality-controlled databases. GLODAP provides a global synthesis of ocean interior carbon data (Lauvset et al., 2024), while SOCAT focuses on

quality-controlled fCO_2 data at the sea surface (Pfeil et al., 2013; Sabine et al., 2013; Bakker et al., 2016). SOCAT is open access, updated annually, and includes individual dataset files as well as synthesis and gridded data products. The SOCAT version 2025 includes 41.4 million quality-controlled surface ocean fCO_2 observations with an estimated accuracy better than 5 µatm (www.socat.info/). Additionally, SOCAT provides a separate set of 8.2 million fCO_2 values with slightly lower accuracy (5 to 10 µatm), primarily from membrane-based sensors. These data cover the global ocean from 1957 to the present typically with a 1-minute sampling frequency, forming the basis for SOCAT's monthly $1° \times 1°$ gridded product routinely used to estimate global air-sea CO_2 fluxes. For a comprehensive overview of existing ocean carbon data products and their synthesis, see Jiang et al., 2025.

1.2.3 *Gap-Filling*

In-situ fCO_2 measurements in SOCAT cover only about 2% of the global ocean's monthly $1° \times 1°$ grid cells. For that reason, various methods have been developed to fill the gaps in the sparse monthly gridded fCO_2 data (e.g. Landschützer et al., 2013; Friedlingstein et al., 2025; Jiang et al., 2025). The historical increase in surface fCO_2 observations led to the first robust mapping of an ocean fCO_2 climatology in the late 1990s, compiling 30 years of data with 250,000 measurements (Takahashi et al., 1997; Sabine et al., 2010). Due to sparse global and temporal coverage, satellite data such as sea surface temperature, salinity, and chlorophyll-a, which are correlated with surface fCO_2 through physical and biogeochemical processes, are frequently used to estimate missing fCO_2 (Shutler et al., 2020; Shutler et al., 2024).

In addition to using gap-filled observation-based fCO_2 products, the ocean carbon sink is also quantified using approaches such as atmospheric inversions, Earth system models, and global ocean biogeochemical models (Friedlingstein et al., 2025). Historically, ocean biogeochemistry models were the primary source of understanding global ocean carbon dynamics (Gruber et al., 2023).[2] However, the Global Carbon Budget 2013 marked a shift by using not only models and indirect observations but two observation-based fCO_2 products (Park et al., 2010; Rödenbeck et al., 2014; Le Quéré et al., 2014). Since then, the ocean carbon sink has been estimated as the average of both an ensemble mean of observation-based fCO_2 products and an ensemble mean of models (Figure 1.6). Over the past two decades, machine learning based method such as neural networks have

2 In this research field, we distinguish between an 'observation-based community' and a 'model community'. While gap-filling neural networks are indeed models, in this context, they belong to the 'observation community' as they work with observations.

become increasingly prevalent, particularly for filling gaps in fCO_2 observations (e.g. Lefévre et al., 2005; Telszewski et al., 2009; Reichstein et al., 2019; Fay et al., 2021). Today, gap-filling methods span a wide range of approaches with statistical or machine learning techniques being the most common, (Telszewski et al., 2009; Landschützer et al., 2013; Rödenbeck et al., 2015; Gregor et al., 2019; Iida et al., 2021; Chau et al., 2022; Gloege et al., 2022; Gregor et al., 2024), though geospatial and data assimilation methods are also used (Bennington et al., 2022a; Rödenbeck et al., 2022). As of the Global Carbon Budget 2024, alongside the model ensemble mean, an ensemble mean of nine observation-based methods is used to derive estimates of the ocean carbon sink (Friedlingstein et al., 2025, Figure 1.6). While in 2014 only one neural network was used (Landschützer et al., 2013), a decade later, five neural networks now provide estimates to the GCB (Le Quéré et al., 2015; Friedlingstein et al., 2025) including VLIZ-SOMFFN (for more details see Chapter 3.2 or Landschützer et al., 2013). Continuous advancements in machine learning have led to a convergence towards a common bias among these methods, indicating that further optimization of these methods alone is unlikely to improve fCO_2 estimates considerably (Gregor et al., 2019).

Even though all underlying surface fCO_2 measurements originate from SOCAT, the ocean carbon sink estimates vary due to differences in the gap filling methods, gas exchange parameterization, and ancillary products, all introducing sources of uncertainty (Ford et al., 2024, Equation 1.1, Chapter 2.3).

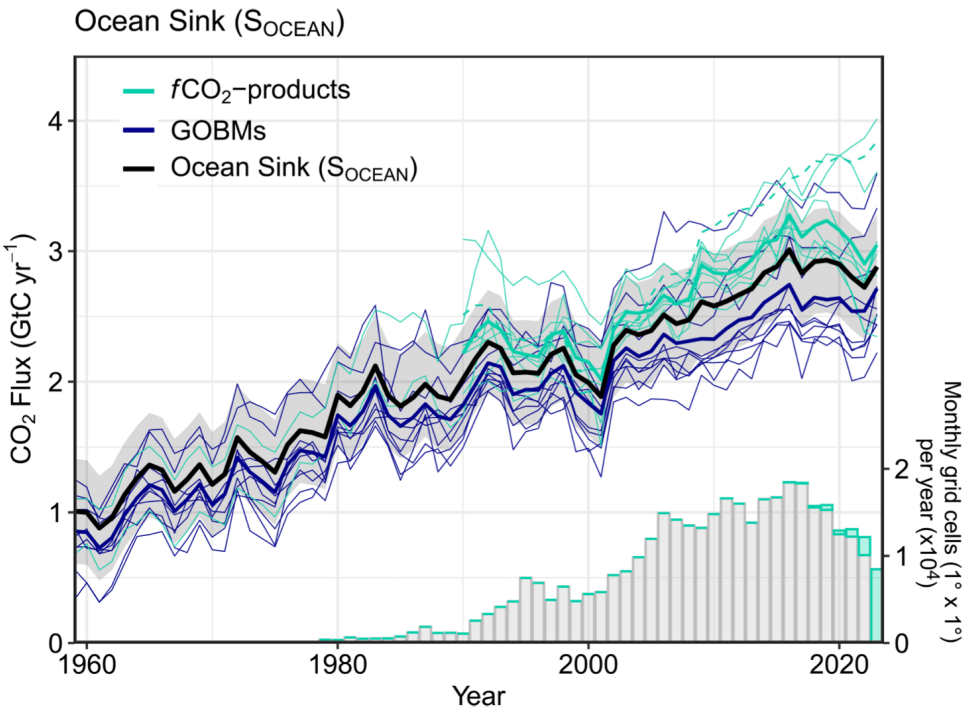

Figure 1.6: Comparison of the air-sea CO_2 flux showing the budget values of the ocean sink estimate (black; with the uncertainty in grey shading), individual ocean models (royal blue), and the ocean fCO_2 products (cyan). The bar plot in the lower right shows the number of monthly gridded values in the SOCAT v2024 database (Bakker et al., 2024). Grey bars indicate the number of grid cells in SOCAT v2023, and coloured bars indicate the newly added grid cells in v2024. *Figure from Friedlingstein et al., 2025.*

2 CHALLENGES IN OCEAN OBSERVING

"One of our largest 'blind spots' in terms of our climate knowledge [...] lies in the Southern Ocean."

– S. Swaart

Each section in the following chapter corresponds to challenges faced on the different levels of the *Ocean Carbon Value Chain* discussed in Chapter 1.2 (Figure 1.4), highlighting research gaps and efforts made to address them.

2.1 DATA COLLECTION CHALLENGES

Challenges in ocean observing at the data collection level include technological and logistical constraints of monitoring platforms (2.1.1), limited spatial and temporal coverage of measurements (2.1.2) and measurement uncertainties associated with sensors (2.1.3). These aspects are discussed in detail in the following sections.

2.1.1 *Limitations of Monitoring Platforms*

In the following, the limitations of various fCO_2 monitoring platforms are discussed (see Figure 1.4 for illustrations of the different monitoring platforms). Each ocean observing platform has specific limitations in terms of spatial coverage, temporal resolution, data quality, or deployment cost. However, their complementary use offers a more comprehensive understanding of the ocean carbon sink.

SHIPS Ships provide the highest data quality due to minimal limitations on sensor size and power constraints. However, their coverage is restricted by commercial shipping routes and sea state conditions, resulting in uneven data distribution on both hemispheres and seasonal biases, particularly in high latitudes (Hauck et al., 2023). They also face high operating costs and contribute to a large carbon footprint.

MOORINGS Moorings (anchored buoys or fixed platforms in the ocean) enhance the observational network by providing fixed-location data and opportunities for sensor validation and calibration (e.g. Schulz et al., 2012; Sutton et al., 2019; Chai et al., 2020; Shadwick et al., 2024). Strategically placed in key regions,

they can significantly reduce uncertainties in air–sea heat flux variability (Wei et al., 2020). However, high maintenance costs limit network expansion, especially in open oceans (Bushinsky et al., 2019b), and they lack spatial context to observed temporal variability (Chai et al., 2020, Figure 1.5).

ARGO FLOATS Compared to shipborne and mooring fCO_2 observations, autonomous-platforms such as wave gliders and Argo floats are capable of adaptive sampling across different scales (Monteiro et al., 2015; Chai et al., 2020, Figure 1.5). Argo floats offer global and seasonal coverage, including polar regions, and are uniquely scalable for studying basin-wide to global processes on seasonal to interannual timescales (Johnson et al., 2017; Bushinsky et al., 2019b; Sarmiento et al., 2023, Figure 1.5). However, the indirect fCO_2 measurements from pH in Argo floats introduce large uncertainties and biases, which exclude them from the Global Carbon Budget (Williams et al., 2017; Friedlingstein et al., 2025). Additionally, the 10-day sampling intervals of these floats do not capture intra-seasonal variability effectively, limiting their effect on reducing uncertainties and biases in fCO_2 estimates (Djeutchouang et al., 2022). While incorporating float-based observations can improve fCO_2 reconstructions, systematic biases degrade their accuracy (Heimdal and McKinley, 2024).

SAILDRONES Saildrones are autonomous observing platforms that can access fast-moving currents that profiling floats or gliders might miss (Bushinsky et al., 2019b). In 2019, a Saildrone measured fCO_2 while circumnavigating Antarctica (Meinig et al., 2019; Sutton et al., 2021). Saildrones are ideal for meridional (north-south) sampling at high temporal resolution (hourly) over large spatial scales, leveraging their speed to cross ocean fronts and capture the spatial variability of fCO_2 across latitudes. This capability helps resolve the seasonal cycle of meridional gradients and minimizes fCO_2 reconstruction errors (Djeutchouang et al., 2022). By adding a few synthetic observations during the Southern Hemisphere winter, Saildrones can reduce a reconstruction bias by up to 86% (Heimdal et al., 2024). Despite their considerable potential in improving the observational network, Saildrones face limitations due to costly measurement campaigns and the absence of a continuous measurement program.

SAILBOATS Unlike Saildrones, sailboats typically perform zonal sampling along the ACC in the Southern Ocean. Sailboats are part of citizen science efforts, with skippers voluntarily collecting fCO_2 data as they follow the fastest possible routes to win racing events, making data collection secondary and preventing deployment for targeted meridional sampling. They capture fast-moving currents with high spatiotemporal resolution (recording sea surface fCO_2 at a 10 second frequency)

but may encounter slow-moving water masses in eddies or during low wind periods. Sailboats are an environmentally friendly, low-emission, and cost-efficient platform with expenses limited to the measurement device (€60,000-€70,000) and maintenance, and they operate without battery dependency, featuring onboard calibration for extended races (Landschützer et al., 2023). Unlike commercial vessels, sailboats navigate less-observed regions in the Southern Ocean, with their recurring circumnavigation races (*Vendée Globe* and *The Ocean Race*, both occurring every 3-4 years) promising more future observations and providing comprehensive spatiotemporal coverage over weeks or months in the underobserved Southern Ocean.
Within the ocean observing network, sailboats provide an important complementary contribution by providing cost-effective, sustainable, and high-resolution data in undersampled key regions such as the Southern Ocean.

2.1.2 *Data Sparsity*

Despite advancements in sensor technology and monitoring platforms, the global observing system remains far from ideal with a substantial measurement imbalance between hemispheres (Figure 2.1). The Northern Hemisphere has been regularly sampled in recent years, largely due to the SOOP program (Pierrot et al., 2009; Jiang et al., 2019), whereas the Southern Hemisphere remains underobserved due to less commercial shipping activity and research missions. The Southern Ocean, accounting for more than 40% of anthropogenic carbon uptake (DeVries, 2014; Frölicher et al., 2015), introduces challenges such as remoteness and harsh sea conditions, particularly during winter, deterring measurement efforts (Bushinsky et al., 2019b).
Figure 2.1 shows the data sparsity in the Southern Ocean. Despite decades of fCO_2 measurements, some regions have never been subjected to any measurements (Figure 2.1a). Even during the austral summer, when measurement activity in the Southern Hemisphere surpasses that of the winter months, extensive areas still lack observations (Figure 2.1b). Figure 2.1c demonstrates the uneven data distribution across the hemisphere, highlighting only few well-observed shipping lanes in the Southern Ocean such as the Drake Passage, while many regions have been measured only once. Additionally, recent years show a new alarming trend: The coverage of surface ocean CO_2 observations has declined by about 35% annually from 2017 to 2021, reverting to early 2000s levels (Dong et al., 2024b; Friedlingstein et al., 2025)(Figure 1.6).

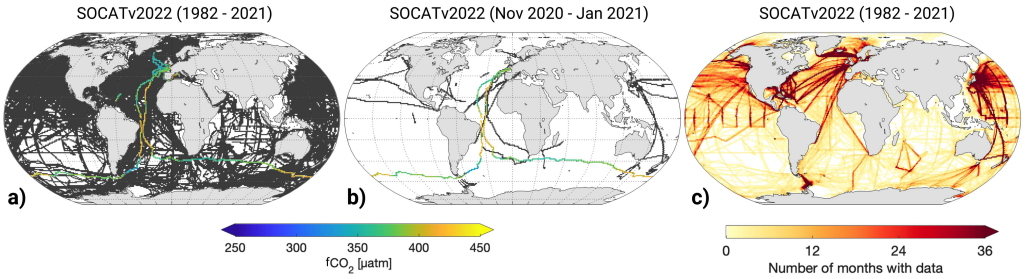

Figure 2.1: Data availability in the SOCATv2022 database. a-b) Maps illustrating data availability in the SOCATv2022 database a) between 1982-2021 and b) between November 2020 to January 2021 (the time of the *Vendée Globe* circumnavigation race). Colored lines represent sailboat fCO_2 measurements from *Seaexplorer*, while observation tracks taken by other observational platforms such as ships, buoys, autonomous measurement platforms etc. are shown in grey. c) Map showing the available number of months with data.

2.1.3 *Measurement Uncertainties*

Another challenge with ocean monitoring platforms is the measurement uncertainties they introduce, which propagate further into gap-filled ocean carbon estimates. For instance, Argo floats, which derive fCO_2 from pH and therefore do not contribute to SOCAT, introduce substantial biases of around 4 µatm and uncertainties up to 11.4 µatm (Williams et al., 2017; Gray et al., 2018; Williams et al., 2018; Fay et al., 2018; Wu and Qi, 2022). In contrast, ships and Saildrones provide high-quality measurements with uncertainties of less than 2 µatm using state-of-the-art air–water equilibrators (Bakker et al., 2016; Sabine et al., 2020; Gkritzalis et al., 2024). An overall accuracy of ±2 µatm for ocean surface fCO_2 is necessary to achieve the community's climate goal, which requires estimating regional fluxes with an accuracy of 0.2 PgC yr^{-1} (Wanninkhof et al., 2019; Bender et al., 2002). Membrane-based systems serve as an alternative to these equilibrator-based systems, and are e.g. used by sailboats (for further details on the measurement device, refer to Landschützer et al., 2023). Earlier studies indicated a lower uncertainty bound of 5 µatm for these systems (Arruda et al., 2019; Olivier et al., 2022), classifying them as flag C and D in SOCAT until 2024, with expected uncertainties under 5 µatm (Lauvset et al., 2018). However, a recent intercomparison revealed higher measurement uncertainties in membrane-based systems (up to 10 µatm), leading to a downgrade to flag E (Gkritzalis et al., 2024; Steinhoff et al., 2025). Lower accuracy data (less than 10 µatm), accounts for 17% of the total fCO_2 data in SOCATv2023 and are excluded from global ocean carbon sink estimates (Bakker et al., 2016; Dong et al., 2024b).
There is ongoing discussion about the acceptable level of measurement uncertainty in climate research, particularly for studying shorter-timescale natural phenom-

ena (Newton et al., 2015; Carter et al., 2019). However, only few studies have explored the impact of measurement uncertainty and bias so far. Carter et al., 2019; Hohensee, 2017 suggest that a larger set of less accurate data may be more beneficial than a smaller set of highly accurate data, particularly when natural variability is high. Dong et al., 2024b found that SOCAT's annual mean CO_2 flux is insensitive to the addition of the lower accuracy data (<10 µatm). Meanwhile, Heimdal and McKinley, 2024 show that targeted autonomous observing can improve fCO_2 reconstructions, even with random uncertainties of ±11 µatm, but not with systematic bias.

Further along the *Ocean Carbon Value Chain*, these measurement uncertainties combined with data sparsity cause substantial uncertainties in mapped ocean carbon estimates (level 3 in Figure 1.4), while the data synthesis process (level 2 in Figure 1.4) simultaneously faces administrative issues.

2.2 DATA SYNTHESIS CHALLENGES: FUNDING, COORDINATION & DATA RESOLUTION

Challenges in ocean observing at the data synthesis level include funding shortfalls, coordination issues and the loss of high-frequency variability due to data regridding.

2.2.1 *Funding & Coordination Issues*

Bakker et al., 2024 warns that ocean CO_2 observing efforts have regressed to levels from a decade ago, and the COVID-19 pandemic has added further strain to the system (Boyer et al., 2023). Although short-term geographic coverage (days to months) remained stable during the pandemic due to the continuation of autonomous platforms, long-term observations (years to decades) were lost due to reduced personnel and supply chain disruptions (Boyer et al., 2023). Additionally, SOCAT faces funding shortfalls and operational vulnerabilities, relying heavily on voluntary contributions, which affects data quality and integration, potentially leading to institutional knowledge loss (Schoderer et al., 2024). The *Ostend Declaration*, supported by over 100 ocean experts, calls for a robust, resilient, and sustainable ocean CO_2 observing system (IOCCP, 2024). Urgent support is requested to maintain SOCAT's role in the Global Carbon Budgets, with proposals for sustainable funding models to establish a strong, resilient, and sustainable framework for ocean CO_2 observations (Bakker et al., 2023).

2.2.2 *Regridding and the Loss of Small-Scale Variability*

SOCAT offers two product types: (i) high-frequency observations in their original resolution and (ii) datasets regridded to a coarser 1-degree grid, with a finer 0.25-degree grid used in coastal areas due to higher variability (Sabine et al., 2013; Bakker et al., 2016). Regridding to a uniform grid offers the advantage of consistent datasets facilitating systematic analysis and global gap-filled ocean carbon sink estimates (Sabine et al., 2013). It is driven by the methodological constraints of gap-filling techniques such as SOM-FFN, which rely on colocated predictor variables in a common spatial and temporal resolution (monthly 1°×1°). However, it comes with a drawback, as it results in the loss of high variability from small-scale processes, which is crucial for accurately capturing ocean carbon dynamics. Regridding can alter the statistical properties of climate variables (Rajulapati et al., 2021) and mask important small-scale processes.

Small-scale variability, captured in high-frequency observations, is crucial for understanding ocean carbon dynamics. For instance, over 30% of air-sea CO_2 flux variability in certain eddy-rich regions is linked to spatial scales smaller than 2° (Guo and Timmermans, 2024b). The lack of comprehensive high-frequency biogeochemical datasets capturing these processes can introduce uncertainties in carbon sink estimates (Resplandy et al., 2014; Monteiro et al., 2015; Hewitt et al., 2022; Dong et al., 2024a; Gray, 2024). Monteiro et al., 2015 demonstrate that a sampling resolution of less than 2 days is required in 30–40% of the Southern Ocean to reduce uncertainty to below 10%, while Djeutchouang et al., 2022 highlight that increasing sampling frequency to this level better resolves intra-seasonal variability and improves air-sea CO_2 flux estimates. Small-scale variability can account for 5–10% of the overall CO_2 flux and can even alter the direction of the CO_2 flux (Wang et al., 2025a; Song et al., 2025; Dombret et al., 2025). High-resolution data are crucial for effectively monitoring carbon cycle dynamics, as they allow for the earlier identification of climate trends, especially in highly variable environments (Carter et al., 2019). In essence, high-frequency observations are invaluable for closing observational gaps and improving our understanding of the ocean carbon cycle, providing benchmarks for models and reanalysis products (e.g. Sutton et al., 2014; Chavez et al., 2018; Djeutchouang et al., 2022; Guo and Timmermans, 2024b; Morgan et al., 2025; Prend et al., 2025).

However, despite their importance, the current reliance on a coarser grid to achieve uniform data and generate gap-filled estimates of the ocean carbon sink results in the loss of details from high-frequency data, sacrificing small-scale variability.

2.3 UNCERTAINTIES IN OCEAN CARBON SINK ESTIMATES

A major challenge in ocean observing at the data analysis level is the uncertainty associated with estimating the ocean carbon sink.

Since 2000s, the discrepancy between modeled ocean carbon uptake and the uptake based on observation-based fCO_2 products has increased (Hauck et al., 2020; Friedlingstein et al., 2025, Figure 1.6). By 2023, the difference between the mean of both products was approximately 0.3 PgC yr^{-1}, roughly 10% of the global sink estimate (Figure 1.6, Kelly et al., 2025; Friedlingstein et al., 2025). The observation-based fCO_2 products estimate a stronger annual mean ocean carbon sink than the models as well as a stronger trend in the ocean sink (Figure 1.6). Resolving this discrepancy is essential for providing accurate information to inform policy-making.

In addition to model biases that introduce errors on the modeling side, which are not discussed here, there are several major sources of biases and uncertainties in observation-based ocean carbon sink estimates such as: (1) biases and uncertainties stemming from gap-filling unobserved ocean regions, (2) uncertainty related to the the gas exchange transfer velocity (3) the uncertainty introduced by the wind product choice (Roobaert et al., 2018; Woolf et al., 2019; Gloege et al., 2021; Hauck et al., 2023; Jersild and Landschützer, 2024; Gloege and Eisaman, 2025). Additional sources of uncertainty include e.g. varying river input and the cool skin effect (Takahashi et al., 2009; Woolf et al., 2016; Watson et al., 2020) as well as measurement uncertainties, though the latter is small compared to the much larger uncertainty stemming from extrapolating limited measurements (Landschützer et al., 2014). The Surface Ocean fCO_2 Mapping intercomparison (SOCOM) analyzed air-sea CO_2 flux variability using 14 fCO_2 gap-filling methods (Rödenbeck et al., 2015). Despite methodological differences, the estimates generally align in capturing seasonal variability, though significant uncertainty remains for interannual variability, particularly in data-sparse regions (Rödenbeck et al., 2015). Fay et al., 2021 introduced a standardized method for estimating air–sea CO_2 fluxes, addressing inconsistencies in flux calculations (by using three wind products and scaling the gas exchange coefficient), which resulted in the creation of the SeaFlux dataset. Methodological adjustments in parameterization and wind product choice cause the global air-sea CO_2 flux to vary by 10–20% (Roobaert et al., 2018; Fay et al., 2021).

In subtropical regions, half of the uncertainty in air–sea CO_2 flux estimates is due to the choice of wind product, whereas in polar regions, nearly half is attributed to the gas exchange transfer velocity (Jersild and Landschützer, 2024). In areas with limited observational coverage, fCO_2 gap-filling-driven uncertainty

is predominant (Jersild and Landschützer, 2024). In the following, we focus on the gap-filling driven uncertainty caused by data sparsity.

Studies show that machine learning, when provided with sufficient data, can skillfully and robustly reconstruct the ocean carbon sink (e.g. Rödenbeck et al., 2015; Fay and McKinley, 2021; Gloege et al., 2021). However, the limited data availability remains a fundamental key-limiting factor in quantifying the ocean carbon sink (e.g. Bushinsky et al., 2019a; Gregor et al., 2019; Hauck et al., 2020; Gloege et al., 2021; Heimdal et al., 2024; Dong et al., 2024b; Fay et al., 2025). While the gap-filling method demonstrates skill in representing low-frequency variability, decadal variability can only be reconstructed with moderate skill in the Southern Ocean due to undersampling (Ritter et al., 2017; Gloege et al., 2021). The uncertainties stemming from the highly undersampled Southern Ocean are substantial (Hauck et al., 2020; Gloege et al., 2021; Hauck et al., 2023; Friedlingstein et al., 2025; Jersild and Landschützer, 2024). According to Gregor et al., 2019 we have "hit a wall" in terms of better resolving surface fCO_2. A way forward in reducing these uncertainties and improving observation-based ocean carbon estimates involves increasing the number of observations, particularly in strategic locations such as the Southern Ocean (e.g. Smith et al., 2019).

2.3.1 *The Impact of Increased Sampling*

Several studies show the impact of additional observations on the estimated ocean carbon uptake, particularly in the Southern Ocean, although there remains some disagreement on the direction of improvement. Studies have shown that observation-based products underestimate the Southern Ocean carbon sink when compared to flux observations from aircraft (Long et al., 2021) and direct measurements (Dong et al., 2024a). Similarly, Heimdal et al., 2024 found that increased targeted meridional and winter sampling with Saildrone can improve the underestimated ocean carbon sink.
In contrast, Hauck et al., 2023 find that SOCAT sampling overestimates the Southern Ocean carbon sink and that additional sampling reduces the ocean carbon sink estimate. Fay et al., 2025 demonstrate that ocean sink reconstructions are highly sensitive to the addition of data from poorly-sampled regions and that additional unbiased data should substantially increase reconstruction accuracy while leading to a weaker ocean carbon sink estimate. Zhong et al., 2024 found that more winter observations would weaken the estimated carbon sink, a finding similar to Bushinsky et al., 2019a, who found that additional float observations also lead to weaker estimates. Deploying 150–200 profiling floats with pH sensors

randomly south of 30°S could reduce ocean carbon sink uncertainty to 0.1 PgC yr^{-1}, tripling the accuracy of current estimates (Majkut et al., 2014). Hauck et al., 2023 demonstrate that optimal sampling, with 1000 evenly distributed sites, can decrease the global air-sea CO_2 flux bias from 9–12% to 2–9%. Djeutchouang et al., 2022 show that ideal sampling to reduce uncertainties includes high-frequency, year-round measurements (including in the underobserved winter) and spatially strategic deployment in key zones such as the Southern Ocean fronts. They also demonstrate that while zonal (east-west) sampling is operationally convenient, combining it with meridional (north-south) sampling enhances the ability to capture fCO_2 variability across latitudes, which is critical for resolving the seasonal cycle of meridional gradients (Djeutchouang et al., 2022), a finding supported by Heimdal et al., 2024.

Reducing the range of carbon flux uncertainties leads to more effective mitigation measures and shows the economic value of research, allowing policymakers to develop tailored mitigation strategies and improve decision-making in managing carbon emissions and resources (Jin et al., 2020).

3.1 RESEARCH QUESTIONS

Monitoring the ocean carbon sink in our changing climate is crucial for informing policy decisions. As discussed in the previous chapters, this process depends on accurate estimates of the ocean carbon sink, which in turn requires extensive data availability.
Sailboats offer a promising solution for collecting underway fCO_2 data in underobserved regions, such as the Southern Ocean, thereby addressing uncertainties in ocean carbon estimates. While competing in recurrent round-the-world racing events, they effectively fill critical observational gaps and support the underresourced SOCAT database by complementing existing systems like ships, moorings, and autonomous platforms.
Once integrated into SOCAT, this data allows for the quantification of the ocean carbon sink, after neural networks reconstruct missing fCO_2 data across time and space. By providing high-frequency observations from underobserved regions, sailboats not only improve our understanding of small-scale oceanic processes but also have the potential to refine ocean carbon sink estimates.

However, the extent to which the data from sailboat impacts the air-sea CO_2 flux estimate and advances our understanding of carbon dynamics remains uncertain. It is still unclear whether these data have a measurable effect on refining ocean carbon sink estimates and how they advance our understanding of the interactions in ocean carbon dynamics.

This dissertation examines the added value of underway fCO_2 sailboat data by 1.) investigating drivers of small-scale fCO_2 variability in high-frequency observations, 2.) detecting changes in global ocean carbon sink estimates from adding sailboat data, and 3.) quantifying improvements in these estimates due to sailboat data. In the following chapters, we address the following research questions:

➜ **What insights into small-scale ocean features driving fCO_2 variability can high-frequency sailboat observations provide?** (Chapter 4 and Appendix A)

I focus on eddies in the Agulhas region and two phytoplankton blooms in the North-East Atlantic and on the Patagonian Shelf, exploring how specific bloom and eddy regimes drive small-scale fCO_2 variability.

➜ **How does the air-sea CO_2 flux estimate change with the addition of sailboat data? Is the impact of adding sailboat data still detectable when considering potential measurement uncertainties?** (Chapter 5 and Appendix B)

I examine whether and how adding fCO_2 data from a single sailboat alters the air-sea CO_2 flux estimate, particularly in the North Atlantic and the Southern Ocean. Additionally, I evaluate how this signal holds up against potential measurement uncertainties and biases.

➜ **How does the air-sea CO_2 flux estimate improve with the addition of sailboat data?** (Chapter 6 and Appendix C)

I quantify the actual improvement from adding existing sailboat data and assess the potential of expanded sailboat observations to improve flux estimates and long-term trends. In addition, I assess how measurement uncertainties and biases in these data affect ocean carbon sink estimates.

3.2 METHODS FOR INVESTIGATING OCEAN CARBON SINK

"What we observe is not nature itself, but nature exposed to our method of questioning."

– Werner Heisenberg

Methodologically, we address our research questions using a multi-faceted approach: 1.) analyzing the high-frequency data directly, 2.) using the regridded SOCAT observations for global ocean carbon sink estimates via neural network gap-filling, and 3.) simulating observation tracks with model data to assess their impact against the model ground truth baseline.

Observation System Simulation Experiments (OSSEs) are used to assess the potential impact of new observational data on existing observing systems by using synthetic observations derived from a model testbed, which acts as the ground truth. They have been used in the past to show the value of optimized sampling strategies in improving the air-sea CO_2 flux estimate (Majkut et al., 2014; Bushinsky et al., 2019a; Denvil-Sommer et al., 2021; Djeutchouang et al., 2022; Hauck et al., 2023; Heimdal et al., 2024; Fay et al., 2025).
In Chapter 6 and Appendix C, we conduct an observation system simulation by subsampling the full hindcast model field of the global ocean biogeochemical model HAMburg Ocean Carbon Cycle (HAMOCC) coupled to the ocean general

circulation model Max Planck Institute Ocean Model (MPIOM) (Ilyina et al., 2013; Paulsen et al., 2017; Mauritsen et al., 2019; Friedlingstein et al., 2025). The subsampling schemes mimic the present-day fCO_2 observations in SOCAT including and excluding different sailboat tracks (Bakker et al., 2016, www.socat.info). The HAMOCC model simulates the oceanic cycles of carbon in the global MPIOM. HAMOCC features biology and inorganic carbon chemistry processes in the water columns and sediment (Heinze et al., 1999; Ilyina et al., 2013). HAMOCC has been evaluated in previous studies and successfully used for climate predictions and projections as well as simulating the past climate (Ilyina et al., 2013; Paulsen et al., 2017; Müller et al., 2018; Mauritsen et al., 2019; Maerz et al., 2020; Liu et al., 2021; Li et al., 2023; Nielsen et al., 2024), and it contributes to the Global Carbon Budget (Friedlingstein et al., 2025).

Based on sparse data – SOCAT observations (Chapter 5 and Appendix B) and subsampled model data (Chapter 6 and Appendix C) – we estimate the global ocean carbon sink with a gap-filling method, the SOM-FFN, from the Global Carbon Budget (Landschützer et al., 2013; Friedlingstein et al., 2025). The SOM-FFN (Self-Organizing Map - Feed-Forward Neural Network) is a two-step neural network approach involving clustering and regression, designed to reconstruct missing fCO_2 from temporally and spatially sparse surface fCO_2 data, enabling the quantification of the global ocean carbon sink (Landschützer et al., 2013; Landschützer et al., 2016). The SOM-FFN product aligns well with other observation-based products, accurately reconstructing surface fCO_2 globally, seasonally and across the Northern Hemisphere (Gregor et al., 2019; Fay et al., 2021; Gloege et al., 2021).

SUMMARY: PHYSICAL AND BIOLOGICAL DRIVERS OF fCO_2 VARIABILITY ALONG SAILBOAT TRACKS

4

"The small scales of the ocean may hold the key to surprises"

— Hewitt et al. (2022)

In a first step to evaluate the added value of fCO_2 underway observations from sailboats in advancing our understanding of the ocean carbon sink, I present case studies that focus on the high-frequency nature of these measurements.

➜ **What insights into small-scale ocean features driving fCO_2 variability can high-frequency sailboat observations provide?** (Chapter 4 and Appendix A)

Between 2018 and 2023, sailboats collected over 300,000 high-frequency fCO_2 observations along ∼112,000 km from low to high latitudes in the Atlantic and Southern Oceans, covering key regions of interest. Combined with satellite data, these in-situ observations revealed small-scale phenomena driving fCO_2 variability, linked to changes in temperature, chlorophyll-a (CHL), and other environmental factors. I focus on three exemplary cases: Agulhas eddies, a Celtic Sea algae bloom, and a coccolithophore bloom on the Patagonian Shelf.

4.1 TEMPERATURE VS. BIOPHYSICAL DOMINATED TRANSECTS

We used the decomposition in thermal and non-thermal (physical and biological) drivers by Takahashi et al., 2002 to identify temperature-dominated ocean regions and features. The sailboat observations reaffirm already established large-scale patterns: across the tropical and subtropical oceans from 40°N to 40°S, fCO_2 variability is predominantly influenced by temperature-driven changes in CO_2 solubility (Takahashi et al., 2002; Gallego et al., 2018; Guo and Timmermans, 2024a). Remarkably, just one or two circumnavigation transects were sufficient to detect and confirm this dominant thermal influence with its boundaries as well as to further identify temperature-dominated ocean features – in this case, anticyclonic eddies and cyclonic eddies in the Agulhas region (Figure 4.1a,c).
While the thermal–non-thermal decomposition effectively distinguishes between regimes dominated by temperature-driven fCO_2 variability and those influenced by combined bio-physical processes, it does not explicitly separate individual physical and biological drivers. The high-resolution sailboat observations enable

us to overcome this limitation by investigating, on a regional basis, the physical and biological processes and how they affect fCO_2 variability. For instance, in biologically active regions such as the Celtic Sea and the Patagonian Shelf, we can examine the influence of biological drivers – algae blooms – on fCO_2 dynamics. Conversely, in thermally dominated regions such as the Agulhas region, we can examine the role of other physical processes, such as small-scale eddy activity, in driving fCO_2 variability.

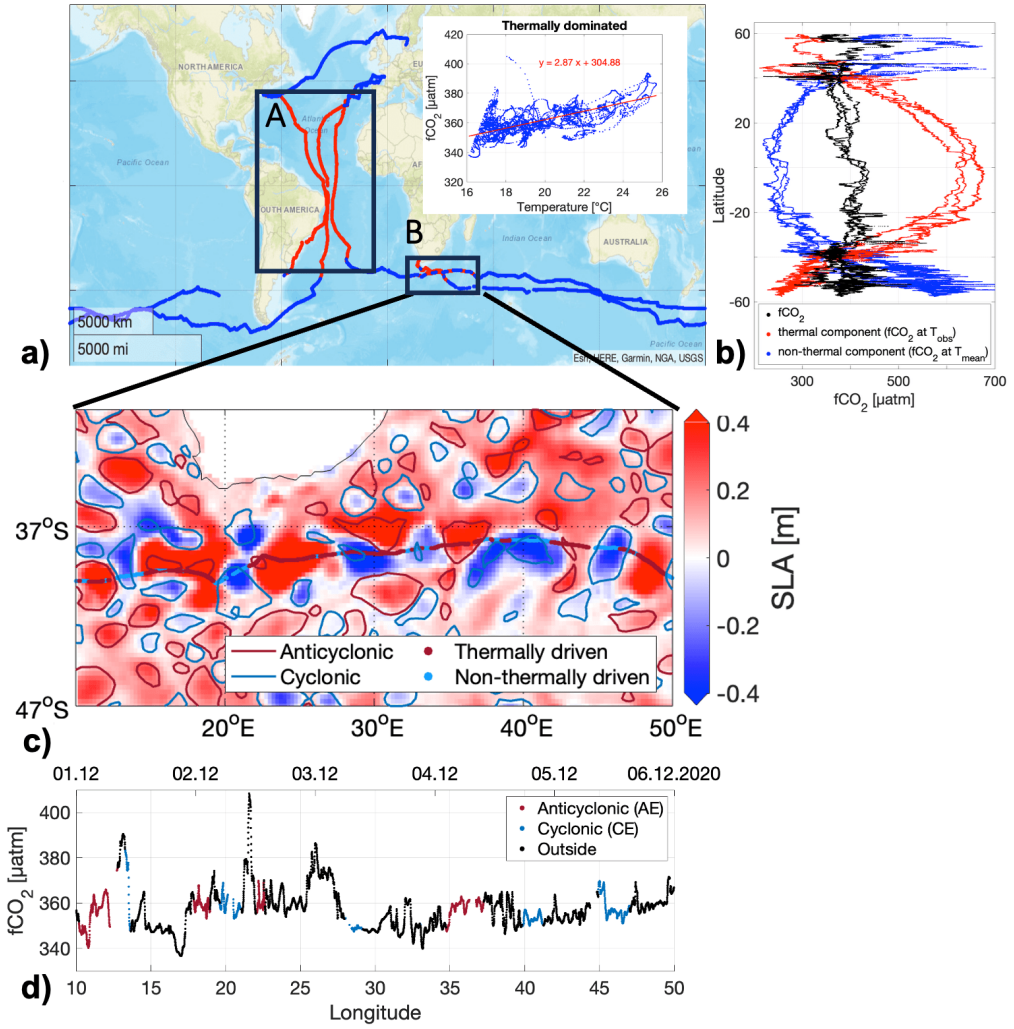

Figure 4.1: Thermal and non-thermal drivers along the sailboat transect. a) Map of the circumnavigation tracks with the thermally dominated tracks in red and the non-thermally dominated tracks in blue. Inlay: Relationship between fCO_2 and temperature in thermally dominated regions of the track (red lines in map). b) fCO_2 as well as thermal and non-thermal fCO_2 components per latitude. c) Thermally and non-thermally dominated features between 10°W to 50°E on top of SLA on the 4th of December 2020. d) fCO_2 measured along the sailboat track.

4.2 THE EFFECT OF EDDIES IN THE AGULHAS REGION ON fCO_2

Considering the ongoing debate regarding the magnitude of fCO_2 and even the direction of the resulting air-sea CO_2 flux within eddies, as well as the limited availability of eddy observations (e.g., Guo and Timmermans, 2024b; Gray, 2024; Li et al., 2025), the high-resolution fCO_2 data collected during sailboat crossings provide a substantial contribution toward refining the spatial variability of fCO_2 within eddies and along their peripheries. The sailboat sailed through 4 anticyclonic (AE) and 7 cyclonic (CE) eddies collecting over 1000 high-frequency fCO_2 observations within these eddies (contours taken from Meta3.2DT Pegliasco et al., 2022) (Table 4.1). The fCO_2 observed along the sailboat tracks (358.3 ± 8.7 µatm) match the upper range of values reported in the literature (Orselli et al., 2019, Table 4.1). Thermally dominated fCO_2 generally aligns with anticyclonic (typically warm-core) eddies, while non-thermally dominated fCO_2 aligns with cyclonic (typically cold-core) eddies (Figure 4.1c). A deviation from this pattern led to the identification of an atypical warm-core cyclonic eddy (around 29°E in Figure 4.1), a common feature in this region (Ni et al., 2021; Liu et al., 2024), highlighting the sailboat's potential in studying both typical and atypical eddies' effects on fCO_2 and air-sea CO_2 flux.

We confirm the traditional view of increased biological activity within cyclonic eddies (e.g. McGillicuddy and Robinson, 1997; Dawson et al., 2018; Belkin et al., 2022, Table 4.1) and their peripheries (Chelton et al., 2011). We emphasize the importance of accounting for the varying impacts of different eddy regimes on fCO_2, as fCO_2 was significantly higher in anticyclonic eddies (358 ± 5 µatm) than in cyclonic eddies (354 ± 3 µatm), and lower in cyclonic eddies compared to the the surroundings (Figure 4.1d). Despite the high standard deviation, the difference is statistically significant and could have a substantial impact when integrated globally.

Our results suggest a stronger carbon sink (or weaker source) in cyclonic eddies generally aligning with Pezzi et al., 2021; Kim et al., 2022 contrary to Keppler et al., 2024; Li et al., 2025; Salinas-Matus et al., 2025.

Strong fCO_2 gradients occurred as the sailboat crossed water mass boundaries with distinct biogeochemical characteristics when entering or leaving an eddy, particularly west of the well-mixed Agulhas current, indicating that these eddy signals are crucial small-scale features that might be overlooked in coarser resolutions as used for global estimates (Figure 4.1c).

Table 4.1: Environmental properties of anticyclonic (AE), cyclonic (CE) eddies, as well as the periphery (trans) and the background (outside) in the Agulhas region. *Transition zones (trans) were defined as 1 hour before/after entering/exiting an eddy. Mean values and standard deviations are displayed.*

Eddy Type	**Nr. of obs.**	**fCO_2** [µatm]	**SST** [°C]	**SSS** [PSU]	**CHL** [mg m^{-3}]	**PIC** [mmol m^{-3}]
AE	679	358 ± 5	18.2 ± 1.6	35.5 ± 0.1	0.27 ± 0.09	0.11 ± 0.08
CE	540	354 ± 3	15.8 ± 0.8	35.2 ± 0.2	0.45 ± 0.12	0.49 ± 0.18
outside	3593	357 ± 9	17.1 ± 1.5	35.5 ± 0.2	0.33 ± 0.15	0.18 ± 0.14
trans	2047	358 ± 9	16.5 ± 2	35.4 ± 0.2	0.37 ± 0.2	0.21 ± 0.21

4.3 ALGAE BLOOM IN THE CELTIC SEA AND ITS EFFECT ON fCO_2

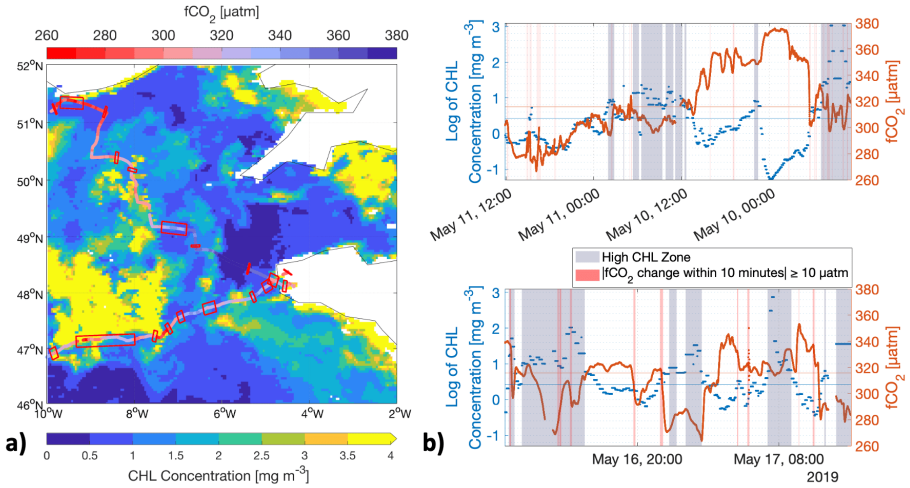

Figure 4.2: Algae bloom in the Celtic Sea in May 2019. a) Map with the background showing an 8-day composite of CHL concentrations from May 9 to May 16, 2019, and the line showing fCO_2 measured by the sailboat. Red boxes mark regions with fCO_2 changes of $\geq$ 10 µatm in $\leq$ 10 minutes. b) Time series of fCO_2 and CHL concentrations (top panel for northern track, bottom for southern track). Red vertical lines indicate fCO_2 changes of $\geq$ 10 µatm in $\leq$ 10 minutes.

A sailboat captured a phytoplankton bloom in the Celtic Sea in May 2019 (Figure 4.2). Increased biological activity, indicated by high CHL concentrations, occurred along coastal lines and mainly between 49°N–47°N and 10°W–7°W (Figure 4.2a). Observed mean CHL concentrations were around 2 mg m^{-3}, with maxima exceeding 7 mg m^{-3} within the bloom patch, similar to concentrations reported in literature (Garcia-Soto and Pingree, 2009). The bloom began around February/March, peaked in April, and ended between June and September, indicating that the sailboat mainly captured the bloom peak (Nicholson et al., 2023).

This algae bloom displayed "classical" bloom behavior, where high CHL concentrations caused reduced fCO_2 (Figure 4.2), and explained 14% of fCO_2 variance. Notably, the most abrupt changes in fCO_2 – fluctuations of ≥10 µatm within 10 minutes – were observed at the boundaries of high CHL zones, where CHL concentrations shifted from around 1 mg m^{-3} to over 7 mg m^{-3} (see gray boxes in Figure 4.2b,c). These changes align with the sailboat crossing into or out of bloom patches (see red boxes in Figure 4.2a), highlighting the edges of high CHL zones as hotspots of increased fCO_2 variability. Increased CHL concentrations caused fCO_2 to decrease from approximately 320 µatm to as low as 265 µatm in high CHL zones (Figure 4.2b). In contrast, CHL-lacking regions (around 5°E) exhibited fCO_2 as high as around 375 µatm (Figure 4.2a and 4.2b top panel).

4.4 COCCOLITHOPHORE BLOOM ON THE PATAGONIAN SHELF AND ITS EFFECT ON fCO_2

In contrast to the Celtic Sea bloom, the Patagonian Shelf presents a more complex scenario. The Patagonian Shelf is known for intense coccolithophore blooms from December to January (Poulton et al., 2013; Balch et al., 2014; Hopkins et al., 2015; Ulibarrena and Conzonno, 2015; Guinder et al., 2025), causing high PIC concentrations that precede a CHL peak (Hopkins et al., 2015). Indeed, in January 2021, the sailboat sailed through a mixed bloom at different stages featured a decaying CHL-dominated bloom (Nicholson et al., 2023) and a peaking coccolithophore bloom (Figure 4.3a).

The coccolithophore bloom forms a westward-facing hook around the Malvinas/-Falkland Islands with relatively low CHL concentrations around 1.5 mg m^{-3} (Figure 4.3), similar to concentrations reported in literature (Romero et al., 2006; Gil et al., 2019). Alongside this, the bloom features high PIC concentrations exceeding 2 mmol C m^{-3} (Figure 4.3b-c), which are comparable to, and even higher than literature values for the Patagonian Shelf (Balch et al., 2014; Hopkins et al., 2015; Oliver et al., 2024). Similarly to the Celtic Sea bloom, large changes in fCO_2 occurred at the edge of high biological activity, in this case high PIC zones (Figure 4.3a, see gray boxes in Figure 4.3b-c). In contrast to the Celtic Sea bloom, the two intersections of the bloom where the sailboat sailed through showed even higher fCO_2 variations (Figure 4.3). While the Celtic Sea bloom produced consistently low fCO_2, the mixed bloom on the Patagonian Shelf caused high fCO_2 fluctuations. The mixed bloom caused opposing influences on fCO_2, leading to the high short-term fCO_2 fluctuations – up to 100 µatm, i.e. up to almost two orders of magnitude larger than the CO_2 variability found in the atmosphere, all

within half an hour (Figure 4.3c). These variations are driven by CO_2 release through calcification and CO_2 uptake through photosynthesis. We found that changes in PIC concentrations account for 46% of the observed short-term fluctuations in fCO_2, while changes in CHL concentrations account for 34% of the observed short-term fluctuations in fCO_2 (Figure 4.3d-e).

Our findings suggest that CHL, commonly used in neural-network methods as a proxy for estimating missing fCO_2 (e.g. Landschützer et al., 2013), does not fully capture the complexity of biological processes, suggesting that PIC should also be considered in these estimations for improved accuracy of CO_2 release due to calcification.

We further conclude that high fCO_2 variability at bloom edges as well as high fCO_2 variability within mixed blooms are crucial small-scale features that might be overlooked in coarser resolutions as used for global estimates. Sailboat-based fCO_2 observations improve our understanding of highly variable and underobserved ocean regions by capturing key small-scale processes at a high spatiotemporal resolution.

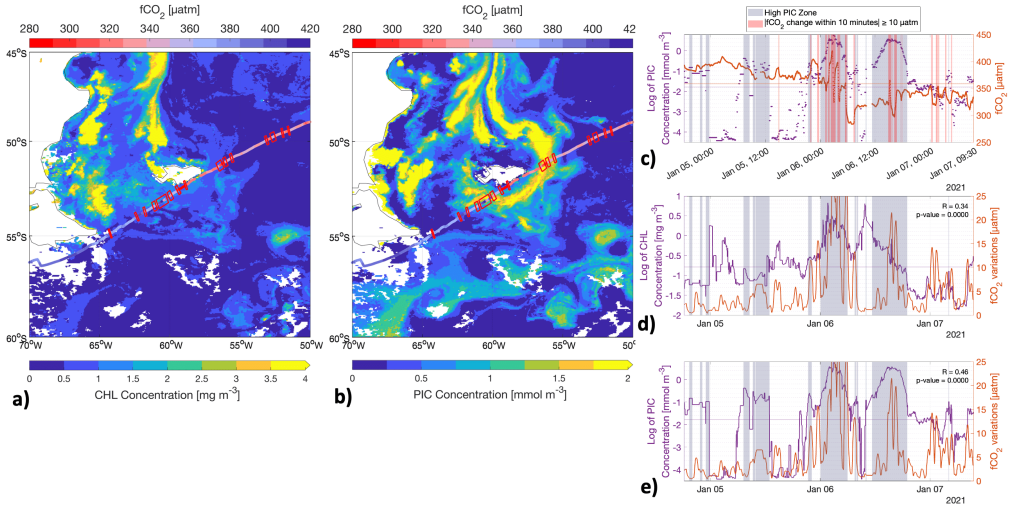

Figure 4.3: Algae bloom on the Patagonian Shelf in January 2021. a-b) Map showing a composite from January 1–8, 2021 of a) CHL and b) PIC concentrations, and the line showing fCO_2 measured by the sailboat. Red boxes mark regions with fCO_2 changes of $\geq$ 10 µatm in $\leq$ 10 minutes. c) Time series of fCO_2 and PIC concentrations. Red vertical lines indicate fCO_2 changes of $\geq$ 10 µatm in $\leq$ 10 minutes. d-e) Time series of fCO_2 variations, calculated with a 60-minute moving standard deviation, and d) CHL and e) PIC concentrations. *The correlation coefficients and p-values between CHL/PIC and fCO_2 variability are shown in the upper right corner of each panel.*

5 SUMMARY: A DETECTABLE CHANGE IN THE AIR-SEA CO_2 FLUX ESTIMATE FROM SAILBOAT MEASUREMENTS

In Chapter 4 (Appendix A), I show that sailboats provide high-frequency observations that capture key small-scale physical and biochemical processes driving fCO_2 variability. However, when integrating surface ocean fCO_2 observations into the global SOCAT database – used for estimating the ocean carbon sink – data must be gridded to a standardized monthly 1°×1° resolution, as required by gap-filling methods such as SOM-FFN to match the fixed spatial and temporal resolution of environmental predictor variables. This raises the following questions:

➜ **How does the air-sea CO_2 flux estimate change with the addition of sailboat data?**

➜ **Is the impact of adding sailboat data still detectable when considering potential measurement uncertainties?**

In Chapter 5 (Appendix B, Behncke et al., 2024), I assess the added value of sailboat observations by evaluating the impact of data from a single sailboat on the ocean carbon sink estimate used in the Global Carbon Budget (Friedlingstein et al., 2022). I show that adding fCO_2 observations from a single sailboat leads to a detectable change in CO_2 flux estimates – especially in the Southern Ocean during austral summer in recent years – even when accounting for measurement uncertainty, though not if the data are biased.

5.1 IMPACT OF ADDING NEW SAILBOAT OBSERVATIONS ON THE AIR-SEA CO_2 FLUX ESTIMATE

We calculated global air-sea CO_2 flux estimates using the SOCATv2022 database, with and without data from a single sailboat (*Seaexplorer-Yacht Club de Monaco*, covering 129 days in the Atlantic and Southern Ocean from 2018 to 2021, primarily from a circumnavigation between November 2020 and January 2021), using the SOM-FFN method. We compare the ensemble means to assess the impact of fCO_2 data from a single platform on air-sea CO_2 flux reconstructions.

Spatially, the addition of sailboat data significantly changed the air-sea CO_2 flux estimate in the North Atlantic and the Southern Ocean (Figure 5.1a-b). In regions such as the Arctic, differences fall within the method's noise, likely due to the weak constraints on air-sea CO_2 flux estimates in highly variable and sparsely

monitored areas (Gloege et al., 2021; Hauck et al., 2023). This highlights the importance of signal-to-noise detection techniques, or alternatively, using synthetic data experiments with large ensembles (Gloege et al., 2021; Heimdal et al., 2024) when comparing different neural network-derived air-sea CO_2 flux estimates.

The addition of sailboat data changed the flux estimate the most in the Southern Ocean between 40°S–60°S (Figure 5.1a-b), supporting research based on synthetic data, which shows that even limited fCO_2 sampling with Saildrone can potentially improve air-sea CO_2 flux reconstructions in the Southern Ocean (Heimdal et al., 2024). Southern Ocean flux estimates vary on average by 0.15 mol C m^{-2} yr^{-1}, which is about 20% of the regional mean. Even well-monitored areas south of Tasmania and New Zealand are affected by the addition of sailboat data, with the largest differences in air-sea CO_2 flux estimates occurring in regions where the sailboat crossed frontal zones (Figure 5.1a). This highlights the importance of capturing frontal dynamics and the insufficient data availability close to frontal zones, given the region's variability. The impact of adding sailboat data is highest around the Sub-Antarctic Front in the Southern Ocean.

Sailboat data reduce the carbon uptake estimate in the Southern Ocean, aligning with Bushinsky et al., 2019a, and increase it in the North Atlantic. Despite dense observations in the North Atlantic, sailboat data still significantly impact regional flux densities, averaging 0.08 mol C m^{-2} yr^{-1} in the North Atlantic (compared to 0.15 mol C m^{-2} yr^{-1}) in the Southern Ocean). Our analysis suggests that the declining number of observations in the North Atlantic (`www.socat.info`) may significantly affect global ocean carbon flux estimates (Canadell et al., 2021).

The regional changes in the two ocean basins compensate each other, limiting the global effect but still resulting in a global difference of up to 0.04 PgC yr^{-1} (2021; -2.55 to -2.51 $\pm$ 0.4 Pg C yr^{-1} (Friedlingstein et al., 2022)).

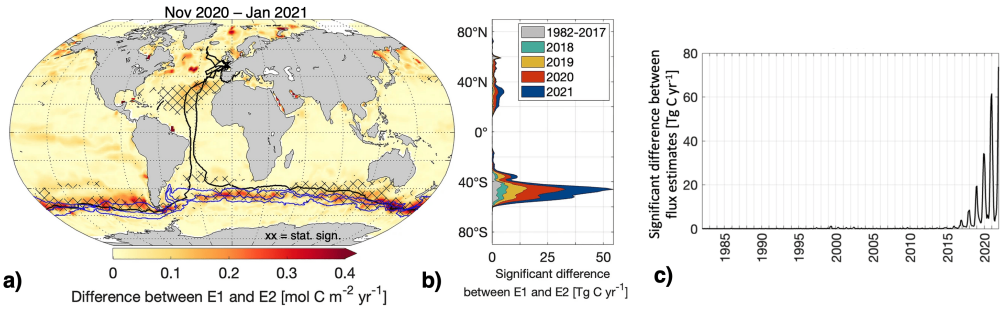

Figure 5.1: Absolute differences in air-sea CO_2 flux between the air-sea CO_2 fluxes E1 (based on SOCATv2022 including Seaexplorer data) and E2 (based on SOCATv2022 excluding Seaexplorer data). (a) Map of absolute differences between air-sea CO_2 flux estimates averaged over Nov 2020–Jan 2021. Hatching shows significance. Black lines indicate sailboat tracks (2018-2021). Blue lines from north to south: Northern Boundary, Subantarctic Front, Polar Front. (b) Significant differences by years and latitude. (c) Time series of significant differences between E1 and E2.

Temporally, sailboat data impacted the flux estimate mainly after 2018, with 91% of significant differences occurring from 2018 to 2021, the period when sailboat measurements were taken, and particularly during the circumnavigation race (Nov 2020 - Jan 2021). Differences appeared up to five years earlier in the Southern Ocean and generally in regions and at times without new data, as the neural network extrapolates over time and space. The limited temporal effect, characterized by smaller differences as we move away from actual data addition, restricts the method's potential for extrapolating past fCO_2 values because atmospheric CO_2, a trend variable, is used as a predictor. This limitation was noted in previous studies using Argo floats (Bushinsky et al., 2019a). We anticipate that a longer time series is necessary to influence interannual to decadal air-sea CO_2 flux trends. The impact of adding sailboat observations is greatest during austral summer, reflecting the seasonal availability of sailboat data.

Unlike Saildrones (Heimdal et al., 2024), sailboats cannot bridge the wintertime discrepancy between float-based and ship-based flux estimates (Bushinsky et al., 2019a). While zonal summertime sampling from sailboats alone may not address seasonal biases, and substantial improvement in Southern Ocean flux reconstructions is better achieved through year-round meridional sampling (Djeutchouang et al., 2022), sailboats can contribute to improved air-sea CO_2 flux reconstructions in the Southern Ocean nonetheless. Sailboats support existing observational platforms (Bakker et al., 2016, `www.socat.info`) and, combined with Argo floats and Saildrones in the Southern Ocean (Djeutchouang et al., 2022), can reduce air-sea CO_2 flux uncertainties.

5.2 SENSITIVITY OF THE AIR-SEA CO_2 FLUX ESTIMATE TO MEASUREMENT UNCERTAINTIES AND BIASES

In the preceding analysis, we assume the sailboat data to be accurate; however, this is not the case in reality. According to SOCAT guidelines, these measurements have an associated uncertainty of 5 µatm (Lauvset et al., 2018), which is at the lower end of values observed in field campaigns (Arruda et al., 2019; Olivier et al., 2022).

Our results show that a random measurement uncertainty of ±5 µatm has a negligible effect on basin-wide air-sea CO_2 flux in the North Atlantic and Southern Ocean. However, it does affect local flux estimates, highlighting the importance of accounting for measurement uncertainty when investigating high-frequency and small spatial scale fluxes.

In contrast, a constant measurement offset of 5 µatm – a worst-case scenario due to system limitations and calibration issues during extended offshore races – substantially affects the air-sea CO_2 flux estimate. The North Atlantic flux estimate is more robust than the Southern Ocean estimate, likely due to the denser observing system, highlighting the need for cross-calibration in remote regions where biases have a larger impact. The potential offset results in a bias of 0.06 PgC yr^{-1} in 2021, which, although representing only approximately 2.5% of the global annual uptake, exceeds the impact from the addition of sailboat data (0.04 PgC yr^{-1}). Thus, the impact from sailboat measurements from 129 days at sea remains undetectable without adherence to the highest measurement standards, thereby supporting the need for a CO_2 reference network (Wanninkhof et al., 2019).

In summary, the effect of sailboat data remains robust when a potential measurement uncertainty of ±5 µatm is considered but becomes undetectable with a 5 µatm offset. Equipping additional sailboats with fCO_2 measurement devices for cross-calibration during races could reduce uncertainties and increase the accuracy of flux estimates. Given that many studies overlook measurement uncertainties in fCO_2 observations, our study highlights the importance of measurement uncertainty analyses to provide more accurate flux estimates.

6 SUMMARY: IMPROVED AIR-SEA CO_2 FLUX ESTIMATES FROM SAILBOAT MEASUREMENTS

In Chapter 5, I show that adding sailboat observations significantly impacts the air-sea CO_2 flux estimate, especially between 40°S and 60°S during the austral summer, even with potential measurement uncertainties of ±5 µatm. However, the actual improvement in the air-sea CO_2 flux estimate remains unquantified and raises the question of:

➜ **How does the air-sea CO_2 flux estimate improve with the addition of sailboat data?**

Using observing system simulations and sailboat tracks, we show how integrating sailboat data improves our ability to estimate the air-sea CO_2 flux. We perform an observation system simulation as described in Chapter 3.2 by subsampling the global ocean biogeochemical model HAMOCC, mimicking present-day fCO_2 observations (Bakker et al., 2016, www.socat.info/), and apply the SOM-FFN neural network to reconstruct the air-sea CO_2 flux. We quantify improvements from 161 days of available, existing sailboat data (including one circumnavigation) and explore potential effects of additional data by subsampling previous years with realistic sailboat tracks. We show how increased sailboat sampling with two additional circumnavigations can correct the underestimated ocean carbon sink, though not yet the overestimated trend, highlighting the need for ongoing long-term data collection. We assess whether reconstructions continue to improve when additional, albeit biased, data is added, to see if increased quantity compensates for lack of quality.

6.1 PERFORMANCE OF NEURAL-NETWORK RECONSTRUCTION

The neural network successfully reconstructed fCO_2 values globally with high fidelity to the model truth, except in the Arctic, a region previously identified as erroneous due to the complexity of the region caused by sea ice dynamics (e.g., Ilyina et al., 2013; Landschützer et al., 2020), and thus excluded from further analysis. However, when mimicking real-world sampling, it overestimates fCO_2 in the undersampled Southern Ocean by around 2–3 µatm (Figure 6.1b). A similar overestimation of fCO_2 was found by Heimdal et al., 2024 using a different reconstruction method and a large ensemble test bed of Earth System Models. In contrast, while similar in magnitude, the mismatch sign differs from Hauck et al., 2023, highlighting model-specific limitations.

To further determine the similarities between model and observational data and validate the method used in Behncke et al., 2024, we quantified the detectable change in the air-sea CO_2 flux estimate caused by adding existing sailboat model data. We demonstrate consistent but smaller signal detection in subsampled model data (due to more consistent predictor-fCO_2 relationships in model data than observations), closely mirroring observations (Behncke et al., 2024), indicating realistic performance on both model and observation data.

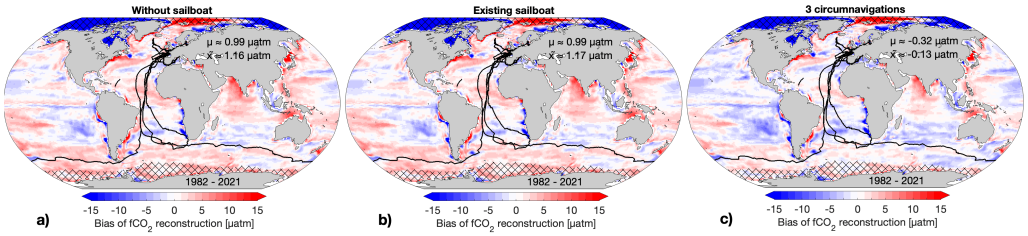

Figure 6.1: **Spatial fCO_2 Bias and Improvement Patterns Resulting from the Integration of Different Sampling Schemes**. **a–c)** Mean bias of subsampled and reconstructed fCO_2 averaged over 1982 until 2021 based on data subsampled after SOCAT **a)** "without sailboat" track data (B) **b)** including "existing sailboat" tracks (A) **c)** including existing sailboat tracks and 2 additional circumnavigations (C or "3 circumnav."). *Black lines represent sailboat tracks. Hatched areas are regions with a climatological maximum sea-ice concentration greater than 50% and are excluded.* μ *represents the mean, while* $\tilde{x}$ *represents the median.* **d)** Latitudinal bias of fCO_2 reconstructions.

6.2 IMPROVEMENT WITH DIFFERENT SAILBOAT SAMPLING

Adding data from "existing sailboat" tracks does not substantially change the reconstructed fCO_2, likely due to the limited sailboat data coverage and late inclusion in SOCAT (Figure 6.1a-b). The global median bias remains elevated (+1.17 µatm instead of +1.16 µatm "without sailboat"), and the spatial bias pattern shows negligible change.

In contrast, enhanced and continuous sampling, as represented by "3 circumnavigations", substantially reduces the fCO_2 bias to -0.13 µatm, particularly by decreasing fCO_2 estimates in the North Atlantic and Southern Ocean – regions directly impacted by the additional data (Figure 6.1c). Moreover, the neural network extrapolates into unaffected regions, reducing biases in regions such as the Indian Ocean and western Pacific (Figure 6.1c). However, this comes at the cost of worsening estimates elsewhere, notably the South Pacific, indicating potential overfitting and compensating effects.

The spatial bias patterns in fCO_2 propagate into the reconstructed air-sea CO_2 fluxes. Globally, the ocean carbon sink is underestimated when mimicking real-

world sampling. Adding "3 circumnavigations" improves and strengthens the estimated ocean carbon sink, especially between 40°S–60°S, aligning with Behncke et al., 2024. However, between 20°S–40°S, the sink is overestimated with "3 circumnavigations" relative to the model truth, which indicates a weaker sink.

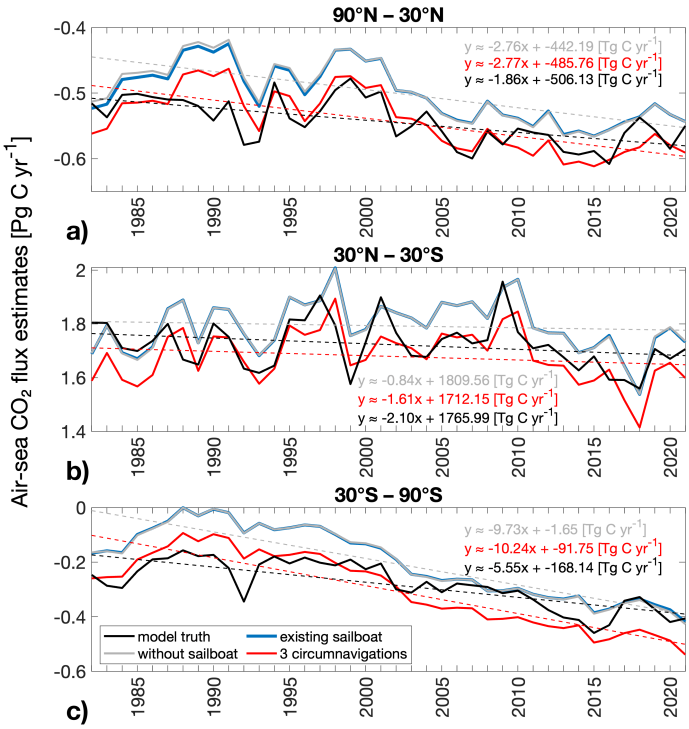

Figure 6.2: **The Impact of Adding Sailboat Data on Air-Sea CO_2 Flux Time Series**. **a–c)** Air-sea CO_2 flux estimates with and without different sailboat tracks in different regions. Dashed lines show the long-term trend. **d–e)** Time series of bias (global and Southern Ocean) in reconstructed air-sea CO_2 flux density. *Dotted lines represent the long-term mean bias. Note that the gray line, indicating the bias of the estimate based on "without sailboat", and the blue line, indicating the bias of the estimate based on "existing sailboat", are in close proximity to each other. Regions with a climatological maximum sea-ice concentration greater than 50% are excluded.*

In the annual time series, including "existing sailboat" data yields no noticeable improvement over the reconstruction "without sailboat" data (Figure 6.2, gray vs. blue lines), with both reconstructions overestimating tropical outgassing and underestimating high-latitude ocean carbon uptake (Figure 6.2). By contrast, adding "3 circumnavigations" (or "2 different circumnavigations", not shown here) brings the global mean air-sea CO_2 flux closer to the model truth, by reducing tropical outgassing (Figure 6.2c) and enhancing uptake in higher latitudes (Figure 6.2a,c). In the Southern Ocean, the mean flux bias is reduced from 0.10 mol C m^{-2} yr^{-1} to 0.00 mol C m^{-2} yr^{-1}. This adjustment slightly overestimates the sink after 2000, which leads to a worsening of the Southern Ocean flux estimate

between 2005 and 2012, with improvements observed before and after.
Notably, the impact of "3 circumnavigations" extends beyond the years with added data, affecting the air-sea CO_2 reconstructions consistently across the entire time series. This behavior is consistent with findings by Heimdal et al. (2024) and contrasts with the more temporally localized effects found in Bushinsky et al. (2019a) and Behncke et al. (2024). We attribute the broader temporal impact to the larger and more consistent training dataset – spanning nearly a decade and based on model output rather than observations – which enables the neural network to more effectively learn and generalize the relationships between predictors and fCO_2.
Our findings reveal that adding measurements shifts and improves the mean time series. However, the shape of the timeseries – and consequently the air-sea CO_2 flux anomalies and trend (represented by dashed lines in Figure 6.2a-c) – remain unchanged and overestimated compared to the model truth trend, particularly in the Southern Ocean, even with data from two additional circumnavigation tracks (Figure 6.2). Despite improvements, data from "3 circumnavigations" are insufficient to improve the trend, indicating that the Global Carbon Budget model and data products are likely to continue diverging even with data from "3 circumnavigations" (Friedlingstein et al., 2022; DeVries et al., 2023). Additional data is necessary to address the overestimated air-sea CO_2 flux trend, with the extent of data needed warranting future investigation. By incorporating more input data over multiple decades with accurate trends into the neural network, the output reconstructions are expected to align more closely with the model's true trend. We conclude that the inclusion of more sailboat data with trend-consistent information could improve the trend accuracy.
This underscores the need for implementing and maintaining multi-decadal observing strategies. Regular sailboat circumnavigations, such as *The Ocean Race* and the *Vendée Globe*, which alternate on a staggered 4-year cycle, present a viable approach. These events ensure a major around-the-world race approximately every one to two years, thereby providing consistent and comprehensive datasets to refine our understanding and improve the accuracy of reconstructions over extended temporal scales. However, sailboats cannot fully cover seasonal measurement gaps, especially in winter at high latitudes. This further underscores the need to support complementary platforms such as autonomous floats (Gray et al., 2018; Bushinsky et al., 2019a) and Saildrones (Sutton et al., 2021), which provide year-round data in challenging conditions. Combining these platforms ensures more complete coverage and improves long-term monitoring of air-sea CO_2 fluxes.
While the finding that adding new measurements improves the air-sea CO_2 flux estimate probably holds irrespective of the baseline model choice, the observed

magnitude of improvement from increased sailboat sampling, however, is highly model-dependent and could vary with different models.

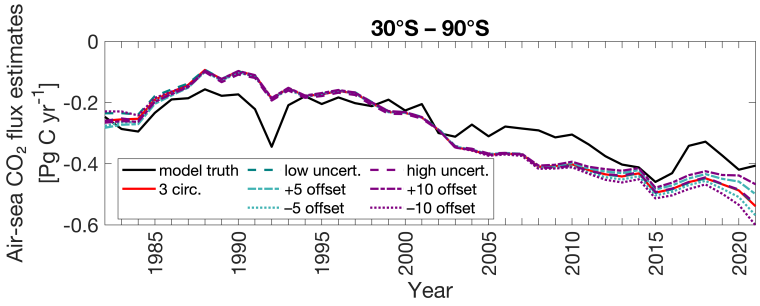

Figure 6.3: **The Effect of Measurement Uncertainties and Biases on the Air-Sea CO_2 Flux Estimate**. Air-sea CO_2 flux estimates based on the model truth (solid black lines), the "3 circumnavigation" sailboat sampling (solid red lines), and the same sampling with added measurement errors. *Measurement errors are applied only to the subsampled sailboat fCO_2 data. Teal lines represent cases with low-end errors (±5 µatm uncertainty or 5 µatm bias), and purple lines represent high-end errors (±10 µatm uncertainty or 10 µatm bias). Random measurement uncertainties are shown as dashed lines (note: they appear on top of each other), while systematic biases are shown as dotted (negative bias) and dash-dotted (positive bias) lines.*

6.3 THE EFFECT OF MEASUREMENT UNCERTAINTIES AND BIASES ON THE AIR-SEA CO_2 FLUX ESTIMATE

We assess the sensitivity of the reconstruction to two types of measurement error applied to the subsampled sailboat data: random measurement uncertainty and systematic bias (i.e., constant offsets). Sailboat data from "3 circumnavigation" tracks continue to improve air-sea CO_2 flux estimates, even when affected by random uncertainties (Figure 6.3, see dashed lines). This holds for both ±5 µatm (best-case scenario, based on previous quality flags) and ±10 µatm (based on updated quality flags) (Arruda et al., 2019; Oliver et al., 2024; Gkritzalis et al., 2024) (Figure 6.3). This finding is consistent with other studies on the impact of random measurement uncertainties (Behncke et al., 2024; Heimdal and McKinley, 2024), showing that adding data from sailboats and Argo floats to the observing system can significantly impact and improve fCO_2 and air-sea CO_2 flux reconstructions, even when the data contain measurement uncertainties, but not if these data are biased. This supports previous findings (Hohensee, 2017; Carter et al., 2019) that data quantity can compensate for reduced data quality.

In contrast, systematic biases have a more pronounced effect, particularly during data-sparse periods before 1990 – a byproduct of the reconstruction method – and in recent years when biased data are introduced. The Southern Ocean is par-

ticularly sensitive: air-sea CO_2 flux estimates begin to diverge from the unbiased reconstruction around 2005 (Figure 6.3), whereas divergence in the tropics and northern high latitudes becomes visible only after 2018–2019. This high sensitivity in the Southern Ocean estimate is consistent with previous findings (Behncke et al., 2024).

Surprisingly, the reconstruction does not respond to measurement biases as one might expect: while negative biases worsen the estimates as anticipated, positive biases can, counterintuitively, result in improved reconstructions (Figure 6.3). In the Southern Ocean, a negative bias exacerbates the already slightly overestimated ocean carbon uptake in recent years, while a positive bias reduces this overestimate, bringing the estimate closer to the model truth (Figure 6.3). Along the sailboat tracks themselves, both bias directions degrade the flux estimate as expected (with +10 µatm and –10 µatm biases yielding mean flux biases of +0.14 and –0.16 mol C m^{-2} yr^{-1}, respectively). Therefore, the improvement observed in the positive bias scenario must originate elsewhere.

Indeed, we find that positive-biased sailboat data improve the reconstruction in high-fCO_2 regions such as the Southern Ocean outgassing zone, the South Atlantic, and the Equatorial Pacific. In these areas, biased data can incidentally shift the reconstruction closer to the model truth. As a result, biased data seemingly improve global reconstructions while they reduce accuracy regionally where the measurements are taken. This behavior highlights the sensitivity of the neural network (Landschützer et al., 2013) – and likely other machine learning models – to biases in predictors and targets.

When the data distribution is skewed and observational constraints are weak, neural network extrapolation can have disproportionate and occasionally beneficial effects, even when the input data are systematically biased. However, this sensitivity depends on the extent and direction of bias, the spatial coverage, and the underlying model used as the testbed. It is important to consider the underlying data density distribution, the model used for the testbed analysis as well as the machine learning background bias (relative to the model truth), and the direction of any measurement bias before interpreting the machine learning extrapolation, and we highly recommend considering these in future observing system design studies.

In summary, while random measurement uncertainties have a negligible influence on reconstruction skill, systematic biases introduce complex and regionally dependent impacts. Biases in sailboat data can improve estimates (by compensating for structural underestimation of fCO_2 in high-fCO_2 areas in our testbed setup), but at the same time, they can worsen estimates during data-sparse periods and in sensitive regions like the Southern Ocean.

7 SUMMARY AND CONCLUSIONS

This dissertation presents a comprehensive answer to the question of the added value of underway fCO_2 data collected by racing sailboats. First, we focus on the additional value gained from the high-frequency nature of these fCO_2 observations for better understanding small-scale ocean carbon dynamics, showcasing three case studies on eddies and phytoplankton blooms. Second, we assess the impact of sailboat data on global carbon flux estimates, as provided in the Global Carbon Budget (GCB) (Friedlingstein et al., 2025), which contribute to IPCC assessments that inform policy decisions (IPCC, 2023). Third, we quantify the improvements in these estimates that result from the addition of sailboat data. In the following, the research questions outlined in Chapter 3.1 are revisited and answered.

7.1 ANSWERING THE RESEARCH QUESTIONS

➜ **What insights into small-scale ocean features driving fCO_2 variability can high-frequency sailboat observations provide?**

In Chapter 4, it is shown that resolving different bloom and eddy regimes with high-frequency observations is key to capturing small-scale fCO_2 variability. In the Agulhas region, we find elevated fCO_2 in anticyclonic eddies (358 ± 5 µatm) and decreased fCO_2 in cyclonic eddies (354 ± 3 µatm), with strong fCO_2 gradients occurring at eddy edges. An algae bloom in the Celtic Sea displayed "classical" bloom behavior, where high chlorophyll concentrations led to reduced fCO_2 (from 320 ± 27 µatm to as low as 265 µatm, averaging 305 ± 16 µatm). In contrast, the Patagonian Shelf presented a more complex scenario, with a mixed bloom at different stages: a decaying chlorophyll-dominated bloom co-occurring with a peaking coccolithophore bloom, characterized by particularly high PIC concentrations of >2 mmol C m^{-3}. This combination caused opposing effects on fCO_2, resulting in short-term fluctuations of up to 100 µatm within half an hour. In both blooms, large fCO_2 changes were associated with bloom edges.
We conclude that incorporating both CHL and PIC as complementary bloom proxies allows for a more accurate representation of bloom-driven fCO_2 variability. Small-scale features – such as fCO_2 gradients at eddy and bloom edges or bloom-induced fCO_2 fluctuations – are often missed in infrequent observations, when regridding to coarser resolutions, or in models. Our findings highlight the critical role of high-resolution fCO_2 observations in understanding spatiotempo-

ral CO_2 dynamics and improving estimates of regional and global air-sea CO_2 fluxes, particularly in variable and underobserved regions.

➜ **How does the air-sea CO_2 flux estimate change with the addition of sailboat data? Is the impact of adding sailboat data still detectable when considering potential measurement uncertainties?**

In Chapter 5 we show that even a single sailboat makes a significant difference when estimating the air-sea CO_2 flux, particularly in the Southern Ocean. Adding sailboat observations significantly increases the regional carbon uptake estimate in the North Atlantic and decreases it in the Southern Ocean. While compensating changes in both basins limit the global effect, the Southern Ocean - particularly frontal regions between 40°S–60°S during summertime - exhibited the largest air-sea CO_2 flux changes, averaging 20% of the regional mean. Assessing the sensitivity of the air-sea CO_2 flux estimate to measurement uncertainty, the results stay robust within the expected random measurement uncertainty (±5 µatm) but remain undetectable with a measurement offset of 5 µatm. We thus conclude that sailboats fill essential measurement gaps in remote ocean regions.

➜ **How does the air-sea CO_2 flux estimate improve with the addition of sailboat data?**

While we detect changes in the air-sea CO_2 flux estimate caused by the addition of sailboat observations in Chapter 5, Chapter 6 extends this analysis, providing a definitive answer regarding if and to what extent sailboat data improve air-sea CO_2 flux estimates.
Using observing system simulations and artificial sailboat tracks, we demonstrate how sailboat data improve estimates of the ocean carbon sink. While we at present underestimate the ocean carbon sink when mimicking real-world sampling in the HAMOCC model, adding available sailboat data does not substantially improve reconstructions. However, increased sampling reveals a stronger carbon sink, particularly between 40°S and 60°S. The improvement persists with hypothetical measurement uncertainties, but substantial differences arise depending on whether positive or negative biases are applied to the sailboat track data. While we show that two additional circumnavigations already improve the ocean mean sink estimate, we further highlight that the additional data remain insufficient to correct the overestimated CO_2 sink trend, calling for continuation of the ongoing data collection.

As shown, sailboats help close essential observational gaps – particularly in the underobserved Southern Ocean – a priority highlighted by many studies (e.g.

Gregor et al., 2019; Gloege et al., 2021; Djeutchouang et al., 2022; Hauck et al., 2023; Dong et al., 2024b; Fay et al., 2025). Among the general advantages of citizen science, sailboats offer clear benefits for ocean carbon monitoring: they are cost-efficient, environmentally friendly, operate in poorly sampled regions, provide broad spatial coverage during round-the-world races, and capture small-scale variability at high frequency. Although sailboats cannot perform ideal sampling – such as meridional, winter, or other targeted deployments (e.g. Djeutchouang et al., 2022) – they effectively complement existing observing networks, particularly in the Southern Ocean, alongside Saildrones and Argo floats, offering strong potential to improve long-term ocean carbon sink estimates. By providing high-resolution fCO_2 data from underobserved ocean regions, sailboat observations strengthen the scientific foundation of climate policy, enabling policymakers to develop more targeted and effective mitigation and adaptation measures.

7.2 OUTLOOK AND FINAL REMARKS

This section presents an outlook by discussing key insights and implications from high-frequency sailboat observations and by outlining recommendations for future studies to improve sailboat-based sampling and our understanding of the global carbon sink.

Need for Enhanced Ocean fCO_2 Monitoring

Enhanced and sustained ocean carbon monitoring is key to improving estimates of the ocean carbon sink at regional and global scales, which feed into assessments such as the GCB and are critical for understanding the ocean's role in the climate system and informing policy decisions. This need is especially urgent as large parts of the ocean, such as the Southern Ocean, remain underobserved, introducing substantial uncertainties in carbon flux estimates. In addition to sparse data coverage, small-scale, high-frequency variability – often missed by current observing systems – challenges our ability to accurately estimate the ocean carbon sink. At the same time, climate change is altering the ocean carbon cycle in complex, regionally and temporally variable ways, thereby increasing the urgency for enhanced and sustained observational efforts. Among the ocean processes affected by climate change are, for instance, intensified Agulhas leakage (Biastoch et al., 2009; Rouault et al., 2009; Sebille et al., 2009; Beech et al., 2022), shifts in Southern Ocean eddy activity (Beech et al., 2025; Mortenson et al., 2025), and more frequent phytoplankton blooms on the Patagonian Shelf and in the Celtic Sea (Dai et al., 2023; Nocera et al., 2024; Demasy et al., 2025). Additionally, rising marine heatwaves (Frölicher et al., 2018) and enhanced mesoscale temperature variance (Guo et al., 2022) further alter the thermal component of

fCO_2 variations, impacting mesoscale CO_2 exchange. These rapid and spatially variable changes demand an observing system that captures small-scale processes driving carbon flux variability. Sailboats equipped to measure at a high frequency complement the ocean observing network by providing continuous measurements capable of detecting emerging climate-driven changes in ocean carbon dynamics earlier than most other platforms (Carter et al., 2019).

Importance of Resolving Small-Scale fCO_2 Dynamics

High-frequency sailboat observations capture small-scale fCO_2 dynamics associated with eddies and phytoplankton blooms, which are often missed by lower-frequency datasets. These dynamics may be obscured or underestimated due to infrequent sampling, coarse spatiotemporal gridding (e.g., the monthly 1°x1° grid used in SOCAT), and in neural network gap-filling methods and mechanistic models. As a result, key processes – such as strong fCO_2 gradients at eddy and bloom edges and high variability during coccolithophore blooms – are underrepresented. Looking ahead, accurately resolving these processes with the aid of sailboats and uncrewed surface vehicles (e.g. Patterson et al., 2025) at fine temporal and spatial scales is necessary. This will become particularly relevant, as biogeochemical models are developed at kilometer scale and enable more accurate estimates of the ocean carbon budget.

Addressing Measurement Uncertainty

Addressing measurement uncertainty remains a key challenge for evaluating the effectiveness of ocean carbon monitoring platforms. The studies here assumed fCO_2 measurement uncertainties of ±5 µatm (Behncke et al., 2024) and ±10 µatm (Behncke et al., 2024; Behncke et al., n.d.) – ±5 µatm being consistent with SOCAT quality flags at the time and prior field studies (Lauvset et al., 2018; Arruda et al., 2019; Olivier et al., 2022), while recent research suggests ±10 µatm is a more realistic uncertainty (Gkritzalis et al., 2024). Given the rarity and importance of such analyses, future work should continue to conduct detailed uncertainty assessments that cover both low-end and high-end scenarios. This should include sensitivity analyses that systematically apply fixed fCO_2 biases, and Monte Carlo simulations introducing varying measurement uncertainties with different random perturbations in each run to quantify the impact of varying uncertainty levels on regional and global air-sea CO_2 flux estimates, along with detailed temporal and spatial bias assessments to determine how uncertainty affects flux estimates by season and region (e.g., winter versus summer fluxes in the Southern Ocean). These analyses will be essential to assess how measurement errors propagate into global and regional carbon flux estimates. Additionally, cross-platform intercomparisons should be performed to better understand how accuracy compares across observing systems. Our analyses focused on the theoretical impact of an expected uncertainty on global carbon flux estimates. We emphasize the importance of reducing biases and uncertainties through improved instrument design to improve the accuracy of the global ocean carbon sink estimates.

OSSEs for Optimizing Sailboat Sampling and Data Requirements

Beyond addressing measurement uncertainties, substantially increasing data coverage remains crucial to improve air-sea CO_2 flux estimates. Although valuable, sailboat observations collected by the end of 2021 – even with data from two additional circumnavigation races – remain insufficient to correct the overestimation of the air-sea CO_2 flux trend when reconstructing the model truth, represented by the HAMOCC model. Future research should determine how many additional races are necessary to address this issue, using OSSEs as effective tools to evaluate sampling strategies. We recommend using OSSEs to assess the benefits of sailboat fleet deployments and to guide complementary sampling designs for other platforms, considering race routes and timing (e.g., as planned in the EU project TRICUSO, 2024).

Future Opportunities with Sailboat Fleets

The recurring nature of major circumnavigation races – such as the *Vendée Globe* and *The Ocean Race*, both held every 3–4 years – and the availability of a fleet present promising opportunities for sustained, high-resolution ocean observations in the future. For instance, during the *Vendée Globe 2024*, four sailboats measured fCO_2, with many other sailboats gathering additional environmental data including plankton imaging data (e.g., Tanhua et al., 2020; Umbert et al., 2022; Pollina et al., 2022; Landschützer et al., 2023; IMOCA, 2024; Hernani et al., 2025). To further improve monitoring of algae blooms and their impact on air-sea CO_2 exchange, future deployments should incorporate fluorescence sensors or plankton imaging systems alongside fCO_2 instruments on sailboats. An upcoming trimaran campaign in the North-East Atlantic in summer 2025 will help to advance our understanding of fCO_2 dynamics during bloom events, with data made available via the innovation platform (`www.soop-platform.earth`). We also highlight the potential benefits of varying race routes through the Southern Ocean and of simultaneous fCO_2 measurements from multiple sailboats following closely aligned, yet slightly offset tracks. Looking ahead, this approach facilitates cross-calibration of instruments, a crucial step to reduce measurement uncertainties inherent in sailboat data and improve data quality for long-term monitoring efforts.

Advancing Neural Network Techniques

Building on the need for enhanced and optimized sampling strategies, advances in neural network techniques offer promising avenues to further improve ocean carbon flux reconstructions. Indeed, research shows that incorporating metrics related to eddy activity into neural networks improves the accuracy of fCO_2 reconstructions, especially on a regional and seasonal scale (Wang et al., 2025b). Future research should focus on improving global mapping and gap-filling methods by leveraging the high-resolution data provided by sailboats. Integrating these data with additional biological proxies such as PIC alongside CHL in these neural networks and employing high-resolution neural network techniques can improve

the representation of mesoscale features and variability associated with eddies and phytoplankton blooms at a high resolution. Sensitivity analyses should be conducted in future studies to evaluate the effectiveness of these approaches. Recent developments such as a global 8-day fCO_2 dataset at a finer spatial resolution of 0.25°×0.25° (Gregor et al., 2024) show the potential of higher-resolution datasets to improve carbon flux estimates, particularly at subseasonal timescales and in spatially highly variable regions. Moving towards even higher-resolution neural network models – such as those by Duke et al., 2023; Duke et al., 2024 with resolutions of approximately 1/12° × 1/12° – is especially valuable in key dynamic regions, enabling more accurate reconstructions of ocean carbon fluxes and better capturing small-scale variability critical for understanding air-sea CO_2 exchange. However, these high-resolution neural networks need sufficient training data, calling for continuous sampling on sailboats.

Advancing Ocean Carbon Modeling

While data-driven approaches like neural networks are valuable for reconstructing fCO_2 and consequently air-sea CO_2 flux estimates, process-based ocean models remain essential for testing sampling strategies and understanding underlying mechanisms. In the OSSE in Behncke et al., n.d., I used HAMOCC with a 1°×1° grid resolution, estimating that at least 2–3 circumnavigations are needed to improve global mean estimates. However, this resolution is too coarse to resolve complex small-scale features crucial for accurately evaluating sampling strategies. Future work should employ high-resolution models (<10 km) to better capture eddies and phytoplankton blooms. The new ICOsahedral Nonhydrostatic (ICON)-Sapphire Earth system model, which includes the HAMOCC biogeochemistry component, supports ocean simulations with grid spacings down to 1.25 km, enabling resolution of submesoscale processes (Hohenegger et al., 2023; Nielsen et al., 2025). Using such models for future high-resolution OSSEs will allow more realistic representation of small-scale ocean dynamics and improve the design of observational strategies aimed at capturing variability in the ocean carbon cycle.

Need for Multi-Model Comparisons

While adding new sailboat measurements is likely to improve air-sea CO_2 flux estimates regardless of the baseline model, the degree of improvement depends strongly on model choice. We used HAMOCC as the assumed truth, which reasonably reproduces the spatial distribution of annual mean fCO_2 (Ilyina et al., 2013) but underestimates Southern Ocean surface fCO_2 (Ilyina et al., 2013) and amplifies the seasonal cycle (Rustogi et al., 2023). This may exaggerate or obscure improvements across seasons compared to a model accurately capturing fCO_2 dynamics, potentially distorting long-term trends. Additionally, our analysis employed only one neural network method (Landschützer et al., 2013); alternative methods might respond differently to added data. To increase confidence in our findings, future studies should conduct inter-model comparisons using multiple ocean biogeochemistry models and alternative gap-filling techniques, as used in

the Global Carbon Budget (e.g., Friedlingstein et al., 2025). Such intercomparisons will help determine the sensitivity of flux estimates and trends to model and method choice, thereby strengthening observational design recommendations.

Closing Remarks

I would like to close with the cautionary words quoted by Wunsch et al., 2013 at the start of this dissertation: **observations not taken today are lost forever**. As demonstrated here, sailboat observations contribute meaningfully to advancing our understanding of the ocean carbon sink and its dynamics and refining global estimates used by policymakers to manage emissions and climate mitigation. Yet, it is an ongoing effort. Observations not taken will inevitably lead to gaps in our understanding and hinder our ability to make informed decisions. Continued, consistent and widespread observations are essential, if we are to protect our planet and guide policy with confidence and precision.

APPENDIX A, APPENDIX B & APPENDIX C

Appendix A

PHYSICAL AND BIOLOGICAL DRIVERS OF fCO_2 VARIABILITY ALONG SAILBOAT TRACKS

Behncke, J. & Landschützer, P. Physical and biological drivers of fCO_2 variability along sailboat tracks. *(in preparation)*.

Physical and biological drivers of fCO_2 variability along sailboat tracks

Jacqueline Behncke[1,2], Peter Landschützer[3,2],

[1] *Max Planck Institute for Meteorology, Bundesstrasse 53, 20146, Hamburg, Germany*
[2] *International Max Planck Research School for Earth System Modelling, Bundesstrasse 53, 20146, Hamburg, Germany*
[3] *Flanders Marine Institute (VLIZ), Jacobsenstraat 1, 8400, Ostend, Belgium*

ABSTRACT

Sailboats collected more than 300,000 high-frequency observations of the CO_2 fugacity (fCO_2) across ∼112,000 km during races in the Atlantic and Southern Ocean between 2018 and 2023, observing several small-scale ocean features. We identified key physical and biogeochemical processes influencing fCO_2, such as Agulhas eddies and algae blooms, by examining fCO_2 changes driven by temperature, chlorophyll, and other environmental factors using in-situ and satellite data.

A single sailboat transect confirmed regional temperature-dominance in the CO_2 variability between 40°N–40°S and the Agulhas retroflection, where the sailboat encountered 4 anticyclonic and 7 cyclonic eddies. We find elevated fCO_2 in anticyclonic eddies (358 ± 5 µatm) compared to cyclonic eddies, and decreased fCO_2 in cyclonic eddies (354 ± 3 µatm), with strong fCO_2 gradients occurring at eddy edges. An algae bloom in the Celtic Sea displayed "classical" bloom behavior, where high chlorophyll concentrations (>7 mg m^{-3}) led to reduced fCO_2 (from 320 ± 27 µatm to as low as 265 µatm, averaging 305 ± 16 µatm). In contrast, the Patagonian Shelf presented a more complex scenario, with a mixed bloom at different stages: a decaying chlorophyll-dominated bloom co-occurring with a peaking coccolithophore bloom, characterized by high particulate inorganic carbon concentrations (>2 mmol m^{-3}). This combination caused opposing effects on fCO_2, resulting in short-term fluctuations of up to 100 µatm within the bloom. In both blooms, large fCO_2 changes were associated with bloom edges.

Small-scale features – such as fCO_2 gradients at eddy and bloom edges or bloom-induced fCO_2 fluctuations – are often missed in infrequent observations, when regridding to coarser resolutions, or in models. Our findings demonstrate the critical role of high-resolution fCO_2 observations, such as those collected by sailboats, in understanding spatiotemporal CO_2 process dynamics and improving estimates of regional and global air-sea CO_2 fluxes, particularly in variable and underobserved regions.

A.1 INTRODUCTION

The ocean acts as a major sink for carbon dioxide (CO_2), taking up approximately a quarter of anthropogenic carbon emissions and mitigating climate

change (Friedlingstein et al., 2025). Rising atmospheric CO_2 is the main driver behind the increase in the ocean carbon sink over the past decades (DeVries et al., 2023; Gruber et al., 2023; Müller et al., 2023); however, the uptake and outgassing of carbon by the ocean are not spatially uniform due to processes on small scales such as enhanced biological activity, localized mixing, and ocean circulation. This small-scale variability is insufficiently captured by current observational networks due to general undersampling and a specific lack of high-resolution measurements of the fugacity of CO_2 (fCO_2)—leading to large uncertainties in ocean carbon sink estimates and a limited understanding of the underlying carbon cycle dynamics (e,g, Resplandy et al., 2014; Djeutchouang et al., 2022; Dong et al., 2024b; Fay et al., 2025; Song et al., 2025; Dombret et al., 2025). These uncertainties can be substantially reduced by increasing sampling resolution (Monteiro et al., 2015). Moreover, high-frequency measurements can improve the detection of emerging climate signals, especially in regions with high short-term variability (Carter et al., 2019).

Most existing fCO_2 observations come from research and commercial ships, which typically record measurements at intervals ranging from several minutes to hours and cover spatial scales from kilometers to basin scale (Bushinsky et al., 2019b; Chai et al., 2020). Since 2018, sailboats fill critical gaps in this monitoring system by providing high-frequency fCO_2 observations, that capture variability at small spatiotemporal scales (tens of meters, every 10 seconds). While it has been shown how the sailboat data affect and improve air-sea CO_2 flux estimates when regridded to a coarser resolution (monthly 1°x1° grid) contributing to the Global Carbon Budget (Behncke et al., 2024; Friedlingstein et al., 2025; Behncke et al., n.d.), these estimates are too coarse to resolve small-scale features and the added value of the high-frequency measurements from sailboats in improving our understanding of observed small-scale processes has yet to be quantified.
During round-the-world circumnavigation races such as the *Vendée Globe* in winter 2020/21, *The Ocean Race* in spring 2023, and several shorter races in the North Atlantic, sailboats collected valuable high-frequency observations while capturing small-scale eddies in the Agulhas region and algae blooms in the Celtic Sea and on the Patagonian Shelf along the sailboat tracks.

The observed small-scale ocean features – eddies and algae blooms – contribute substantially to fCO_2 variability (Resplandy et al., 2014). These features modulate fCO_2, i.e. the dominant control of air-sea CO_2 exchange, and can thereby amplify or dampen CO_2 fluxes between the ocean and atmosphere (e.g. Shutler et al., 2013; Gray, 2024). For instance, more than 30% of air-sea CO_2 flux variability in eddy-rich ocean regions is attributed to small spatial scales (Guo and

Timmermans, 2024b), and small-scale variability can contribute up to 5–10% of the total CO_2 flux, and even reverse its direction (Wang et al., 2025a; Song et al., 2025; Dombret et al., 2025). Incorporating eddy activity proxies into neural networks has been shown to improve fCO_2 reconstructions, especially on a regional and seasonal scale (Wang et al., 2025b). Resolving small-scale ocean features is important for accurately constraining the ocean carbon sink.

Among small-scale features, mesoscale eddies are particularly complex and influential in modulating fCO_2 variability, as they can cause outgassing through physical processes or carbon uptake via both physical and biological mechanisms (Keppler et al., 2024). Agulhas eddies, formed by the retroflection of the Agulhas current, transport warm, salty water from the Indian Ocean to the Atlantic, affecting fCO_2. Generally, anticyclonic eddies with a warm core raise surface temperatures and fCO_2 through downwelling, which suppresses nutrients and primary production, although lateral advection can modify fCO_2 in either direction. Conversely, cyclonic eddies typically promote upwelling, cooling the surface and bringing nutrients upward, thereby decreasing fCO_2 through increased CO_2 solubility and enhanced primary production, but they also bring DIC-rich water to the surface, potentially increasing fCO_2. Despite their importance, the quantitative and mechanistic effects of different eddy types on fCO_2 remain poorly understood and observational eddy investigations are rare in key regions such as the Southern Ocean (Smith et al., 2023; Guo and Timmermans, 2024b; Gray, 2024). Guo and Timmermans, 2024b state that there is ongoing debate about whether mesoscale eddies act as ocean carbon sinks (Jones et al., 2017; Orselli et al., 2019; Smith et al., 2023; Ford et al., 2023; Keppler et al., 2024; Li et al., 2025) as sources (Chen et al., 2007; Moreau et al., 2017; Pezzi et al., 2021; Kim et al., 2022), if it depends on the season (Song et al., 2016), or if it varies by type, with anticyclonic eddies acting as a source and cyclonic eddies serving as sinks (Pezzi et al., 2021; Kim et al., 2022). Eddy-induced upwelling in cyclones can also enhance biological activity, thereby reducing fCO_2 (McGillicuddy and Robinson, 1997; Oschlies and Garçon, 1998; Dawson et al., 2018; Belkin et al., 2022; Li et al., 2025), and advection can increase chlorophyll in the eddy periphery (Chelton et al., 2011). However, the impact of eddies on phytoplankton biomass, much like their impact on fCO_2 remains unclear (Su et al., 2021). Contrary to expectations, cyclonic eddies do not always show increased chlorophyll concentrations compared to anticyclones, with various regional mechanisms causing high productivity in anticyclones as well (Meredith et al., 2003; Waite et al., 2007; Siegel et al., 2011; Gaube et al., 2013; Dufois et al., 2014; Dufois et al., 2016; Song et al., 2016; Doddridge and Marshall, 2018; Su et al., 2021) or reduced productivity in cyclones (Song et al., 2016; Moreau et al., 2017).

Biological phenomena such as algae blooms also play a critical role in shaping surface fCO_2 and consequently the air-sea CO_2 exchange on a small scale. These blooms can both increase or decrease surface ocean fCO_2 depending on bloom composition and bloom stages. For instance, the Patagonian Shelf supports intense phytoplankton blooms from December to January (Ulibarrena and Conzonno, 2015; Guinder et al., 2025), which influence the air-sea CO_2 flux (Schloss et al., 2007; Bianchi et al., 2009; Kahl et al., 2017; Oliveira Carvalho et al., 2022; Berghoff et al., 2023; Guinder et al., 2025). Coccolithophores, in particular, are prevalent there (Garcia et al., 2011; Souza et al., 2012; Balch et al., 2014; Guinder et al., 2025). Although algae blooms generally decrease fCO_2 through photosynthesis; coccolithophores, being calcifying phytoplankton, can both decrease fCO_2 via photosynthesis and increase fCO_2 through their calcification process (Frankignoulle et al., 1994; Shutler et al., 2013). Moreover, the North Atlantic, including the Celtic Sea in the North East Atlantic in May, experiences algae blooms that drive changes in fCO_2 (Rees et al., 1999; McQuatters-Gollop et al., 2007; Garcia-Soto and Pingree, 2009; Suykens et al., 2010; Shutler et al., 2013; Perrot et al., 2018). While fCO_2 in subtropical regions is largely temperature dominated, fCO_2 changes in both these subpolar regions are largely driven by biological activity (Fay and McKinley, 2017; Guo and Timmermans, 2024a).

The examples above show how high-resolution spatiotemporal data are key to better understanding and resolving small-scale processes and their effect on carbon dynamics. High-frequency observations—such as those collected by sailboats in key regions dominated by eddies and algae blooms—are essential not only to improve our understanding of fCO_2 variability but also to provide robust benchmarks for the next generation of models and reanalysis products (e.g. Sutton et al., 2014; Chavez et al., 2018; Djeutchouang et al., 2022; Guo and Timmermans, 2024b; Prend et al., 2025; Morgan et al., 2025).
In this study, we analyze high-frequency sailboat-based fCO_2 measurements from 2018–2023 across the Atlantic and Southern Ocean to investigate the drivers of CO_2 variability in mesoscale features. Specifically, we focus on the fCO_2 drawdown during an algae bloom in the Celtic Sea, a mixed coccolithophore bloom on the Patagonian Shelf, and the role of eddies in the Agulhas region in shaping fCO_2 dynamics. We demonstrate how integrating satellite Earth observations with in situ sailboat data improves our understanding of ocean carbon fluxes, offering insights for improved representation in high-resolution Earth system models.

A.2 DATA AND METHODS

A.2.1 *Observational satasets: Underway fCO_2 measurements and satellite data*

Sampling of fCO_2 was conducted using the membrane-based OceanPack^{TM} Race system, developed by SubCtech industries, aboard the IMOCA 60 class sailboat from Team Malizia "*Malizia-Seaexplorer*" during *The Ocean Race* (round-the-world race from February 26 - May 29, 2023; Leg 3: February 26 - April 2, 2023, Leg 4: April 24 - May 10, 2023, Leg 5: May 21 - May 29, 2023) as well as on their former sailboat "*Seaexplorer – Yacht Club de Monaco*" during the *Vendée Globe* race (round-the-world race from November 8, 2020 - January 28, 2021), as well as during four races in the North Atlantic and four transfers (between 2018 and 2021) (see Figure A.1 and Supplementary Table A.2).

The water inlet, located at the keel at a depth of ∼2 meters below the sea surface, feeds the sample into a debubbler unit equipped with a conductivity–temperature–depth (CTD) sonde (Sea&Sun customized CTD48). A membrane separates the sampled seawater from a closed air-loop, facilitating gas exchange until equilibrium is achieved. The air is then circulated by a membrane pump through a LI-COR L840 infrared gas analyzer. The measurement system is equipped with a two-point underway calibration: 1. zero reference calibration, and 2. calibration with a known reference gas (using a 2-liter bottle containing a compressed, pre-calibrated air mixture) to enable daily calibration over extended periods without replacing the bottle. For a more detailed description of the measurement system, refer to Landschützer et al., 2023.
In the observational community, reporting measured values as fCO_2 has become standard practice, a convention endorsed by the International Ocean Carbon Coordination Project (IOCCP) (Fay et al., 2024). Accordingly, we adopt fCO_2 throughout this study. For consistency, we refer to fCO_2 even when citing studies that originally report pCO_2. We justify this approach as the two terms are often used interchangeably, with differences being negligible and often only significant in the subsurface ocean (Dickson et al., 2007; Fay et al., 2024).

Besides fCO_2, temperature, and salinity data provided by the sailboats, we further analyze satellite data, co-located with the sailboat measurements. Chlorophyll-a (CHL), particulate inorganic carbon (PIC) (`http://www.globcolour.info`; parameter CHL1 and PIC with the AVW L3 merging method in 4 km resolution, 8-daily), wind (Hersbach et al., 2023), and gridded daily Sea Level Anomaly (SLA) data (Copernicus Climate Change Service, 2018) were used to identify small-scale

ocean features. Additionally, NOAA 1/4° Daily Optimum Interpolation Sea Surface Temperature (OISSTv2.1) (Huang et al., 2021), available at NOAA/ NCEI (https://www.ncei.noaa.gov/data/sea-surface-temperature-optimum-interpolation/v2.1/access/avhrr/) was used to obtain more information about sea surface temperature (SST) in the proximity of the sailboat tracks.
We used regional ocean masks available at https://github.com/RECCAP2-ocean/R2-shared-resources/tree/master (last accessed: January 27, 2025, Gregor and Müller, 2025) with most regional ocean masks based on Fay and McKinley, 2014 and the coastal mask based on Laruelle et al., 2017, to characterize the regional data distribution. The Southern Ocean is defined as the following biomes by Fay and McKinley, 2014: Southern Hemisphere ice biome (SSH ICE), Southern Hemisphere subpolar seasonally stratified biome (SH SPSS), Southern Hemisphere subtropical seasonally stratified biome (SH STSS). The Atlantic starts north of SH STSS and has the boundaries defined by the World Ocean Atlas (Levitus et al., 2009; Gregor and Müller, 2025).

A.2.2 *Small-scale ocean feature detection*

We identified small-scale ocean features by examining temperature-, physical, and biological-driven changes in fCO_2 explained in the following sections.

A.2.2.1 *Thermal and non-thermal drivers*

Thermal (gas solubility) and non-thermal (bio-physical) processes affect surface fCO_2 with the relative contribution of these processes varying seasonally and regionally (e.g. Takahashi et al., 2002; Peter et al., 2025). Following Takahashi et al., 2002 we estimate fCO_2 at T_{mean} (non-thermal bio-physical component; T_{mean} being the mean observed temperature) and fCO_2 at T_{obs} (thermal component, T_{obs} being the given observed temperature) during both circumnavigations (Equations A.1). While fCO_2 at T_{obs} is driven by temperature gradients, fCO_2 at T_{mean} is influenced by physical processes such as mixing as well as biological processes. We performed k-means clustering on thermal and non-thermal components to determine which is the dominant driver within each cluster (Supplementary Figure A.6).

$$\begin{aligned} (fCO_2 \text{ at } T_{\text{mean}}) &= (fCO_2)_{\text{obs}} \times \exp[0.0423(T_{\text{mean}} - T_{\text{obs}})] \\ (fCO_2 \text{ at } T_{\text{obs}}) &= (\text{Mean annual } fCO_2) \times \exp[0.0423(T_{\text{obs}} - T_{\text{mean}})] \end{aligned} \tag{A.1}$$

A.2.2.2 *Eddies in the Agulhas region*

We used the locations of the dominant (thermal and non-thermal) drivers to identify the region of the Agulhas retroflection and Agulhas Return Current and potential eddies. We then used the all-satellite Mesoscale Eddy Trajectory Atlas, version 3.2 (Meta3.2DT; Pegliasco et al., 2022; DOI: 10.24400/527896/a01-2022.005.220209), to identify eddies in the Agulhas region from December 1st to 6th, 2020 (10°E-50°E). Meta3.2DT identifies eddy centers by detecting minima or maxima in the filtered absolute dynamic topography (ADT), distinguishing cyclonic eddies (CEs) and anticyclonic eddies (AEs). We selected Meta3.2DT eddies that persist for at least 10 days to guarantee they are stable formations with a sufficient duration to significantly influence ocean biogeochemistry. For further details on the eddy location method, see Chaigneau et al., 2009; Pegliasco et al., 2022; Keppler et al., 2024. Additionally, we used gridded daily SLA data from Copernicus Climate Change Service, 2018 to gather more information about the eddies.

When the sailboat crossed an eddy's contour line, the track segment within was classified as either cyclonic eddy (CE) or anticyclonic eddy (AE), except for transition zones defined as 1 hour before and after entering or exiting an eddy. The remaining segments were labeled 'outside'. Typical cold-core cyclonic eddies and warm-core anticyclonic eddies have SLA and SST anomalies at the center with the same sign (Ni et al., 2021; Liu et al., 2024). Eddies, such as warm-core cyclonic eddies, are considered atypical if the anomalies at their centers have opposite signs (Ni et al., 2021). To check for this atypical behavior (indicated by thermally-driven parts of the sailboat track coinciding with negative SLA), we checked the SST anomaly (Huang et al., 2021).

A.2.2.3 *Algae blooms*

We examined the role of biological activity in driving fCO_2 variability by analyzing CHL and PIC concentrations (`http://www.globcolour.info`). To identify regions with potential algae blooms, we pre-selected regions where sailors reported algae blooms. We identified algae blooms by analyzing the correlation between fCO_2 and CHL and PIC, as well as between short-term fluctuations in fCO_2 and CHL and PIC. Due to gaps in the satellite ocean color data, we selected the values closest in time and space to the sailboat track (for the *Vendée Globe* track: the median Euclidean distance from the track to the nearest CHL value is 2.52 km (IQR 1.48–3.65 km; for the Patagonian shelf area (70°W–50°W: the median Euclidean distance is 2.42 km (IQR 1.71–3.18 km); for the *Bermudes1000* track in the North Atlantic: the median Euclidean distance is 2.27 km (IQR 1.59–2.79 km).) The distances seem adequate since algae blooms e.g. on the Patagonian

shelf have been described as extensive, covering approximately 55,000 km^2 (Garcia et al., 2008). We focused on regions with an increase/decrease in fCO_2 of ≥10 µatm/10min and high concentrations of PIC and CHL. We used a satellite-derived phenology data product to determine the phenological stage of the blooms (Nicholson et al., 2023; Nicholson et al., 2025).

A.3 RESULTS

A.3.1 *Oceanographic conditions across the sailboat transects*

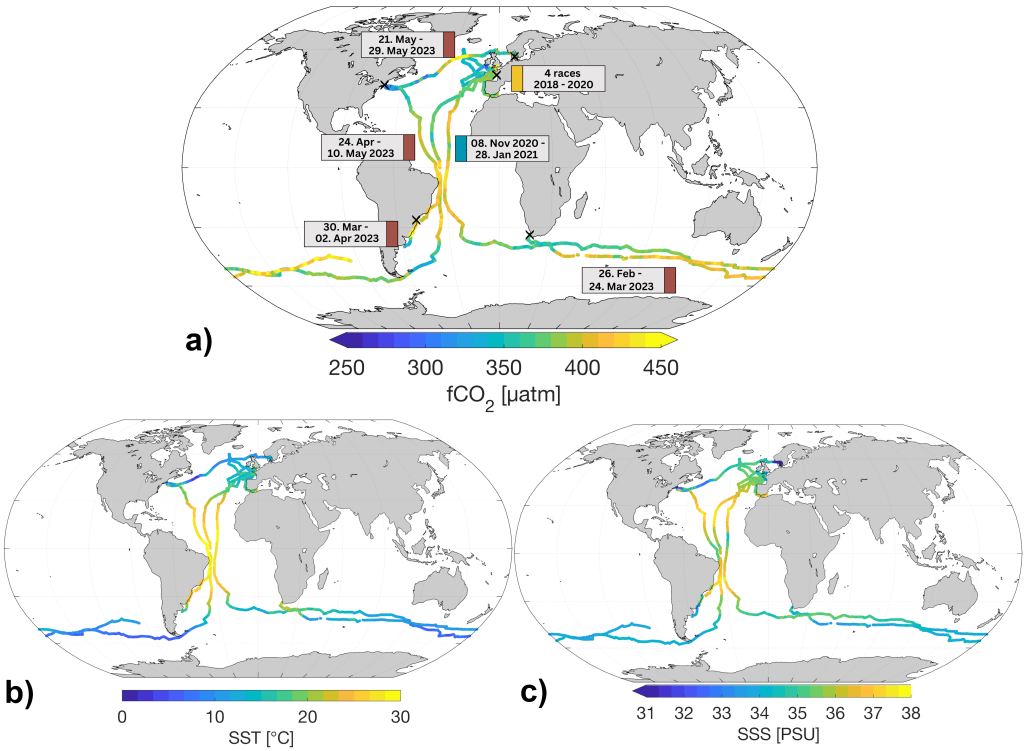

Figure A.1: **Sailboat Tracks. a)** fCO_2 data **b)** SST data and **c)** SSS data from four North Atlantic races and four transfers (yellow tag), and two Antarctic circumnavigations sailed by Team Malizia. *Vendée Globe 2020/21 (blue tag) is a non-stop race, whereas The Ocean Race 2023 (brown tags) is a multi-leg race. (No measurements were taken during the first two legs and the last of The Ocean Race 2023.)*

The sailboats sailed mainly through the Atlantic and Southern Ocean during the winter of 2020/21 and spring of 2023, participating in four North Atlantic races, which involved four transfers to the race's starting point, and two round-the-world circumnavigations ((Figure A.1a and Supplementary Table A.2). The sampling across both hemispheres was relatively balanced with 59% from the Northern Hemisphere and 41% from the Southern Hemisphere, showing the focus on the less well-observed Southern Hemisphere in contrast to most observing

platforms (www.socat.info, Supplementary Figure A.7). Seasonally, the samples were collected as follows: 5% in winter, 36% in spring, 38% in summer, and 21% in autumn, with all seasons referring to both Northern and Southern Hemisphere conditions (Supplementary Figure A.7). This distribution indicates an overall seasonal summer bias in the dataset. Regional distribution showed that 69% of the samples were from the Atlantic Ocean, 30% from the Southern Ocean, 1% from the Pacific Ocean, and less than 1% from the Indian Ocean (Supplementary Figure A.7). 62% of the samples were from open ocean areas, while 38% were from coastal regions (either 300 km distance from the coastline or the 1000m isobaths, Supplementary Figure A.7).
The environmental parameters recorded included SST of 15.8 ± 5.9°C, SSS of 35.1 ± 1.2 PSU, and fCO_2 of 372.8 ± 39.7 µatm (Figure A.1). Satellite products show wind speeds of 7.2 ± 2.9 m/s at the time and location of the races, and CHL concentration of 0.6 ± 1.2 mg m^{-3}, with the latter co-located only during two races (*Bermudes1000* and *Vendée Globe*).

Using the well-established thermal decomposition method by Takahashi et al., 2002, by using the temperature sensitivity of CO_2, we can further investigate the dominant drivers along the track. Decomposition of fCO_2 from the circumnavigations into a thermal and non-thermal component shows that between 40°N and 40°S in the Atlantic, fCO_2 variability is primarily driven by temperature controlling CO_2 solubility, with thermal drivers dominating over non-thermal influences (Figure A.2a–b, Box A), in agreement with Takahashi et al., 2002; Gallego et al., 2018.
Interestingly, the observations from few circumnavigations are sufficient to identify this division and moreover, to identify temperature-dominated small-scale ocean features, in this case Agulhas eddies (see box B in Figure A.2a). The relationship between fCO_2 and temperature in thermally dominated regions is as follows: 0.94% CO_2 change per 1°C change (see Inlay in A.2a).

In general, the north-south transect in the Atlantic shows fewer drivers of fCO_2 than the east-west (E-W) transect, as its fCO_2 is mainly driven by temperature gradients. In contrast, the E-W transects in high latitudes are influenced by biological and physical driven processes (see blue lines for biological and physical drivers and red lines for thermal drivers in Figure A.2a).
While the thermal–non-thermal decomposition effectively distinguishes between regimes where fCO_2 is dominated by temperature variability and those influenced by combined bio-physical processes, it does not further distinguish between individual physical and biological drivers. The high-resolution sailboat observations enable us to overcome this limitation by investigating, on a regional basis, the

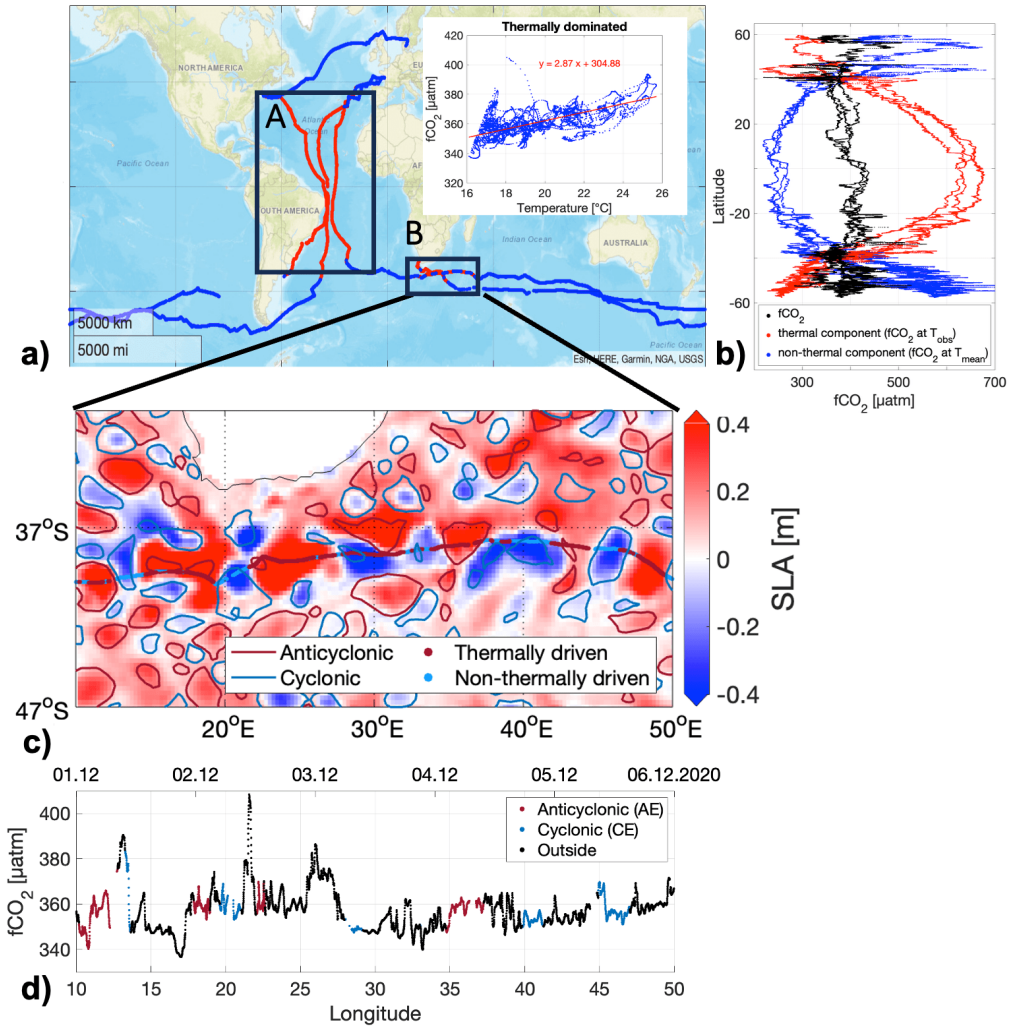

Figure A.2: **Thermal and Non-Thermal Drivers Along the Sailboat Transect.** **a)** Map of the circumnavigation tracks with the thermally dominated tracks in red and the non-thermally dominated tracks in blue. Inlay: Relationship between fCO_2 and SST in thermally dominated regions of the track (red lines in map). **b)** fCO_2 as well as thermal and non-thermal fCO_2 components per latitude. **c)** Thermally and non-thermally dominated features between 10°W to 50°E on top of SLA on the 4th of December 2020. **d)** fCO_2 measured along the sailboat track.

physical and biological processes and how they affect fCO_2 variability. For instance, in biologically active regions such as the Celtic Sea and the Patagonian Shelf, we can examine the influence of biological drivers – algae blooms – on fCO_2 dynamics. Conversely, in thermally dominated regions like the Agulhas region, we can examine the role of other physical processes, such as small-scale eddy activity, in driving fCO_2 variability.

A.3.2 *Eddies in the Agulhas region*

We identify the location of the region of the Agulhas retroflection and Agulhas Return Current between 10°E and 50°E (see box B in Figure A.2a,c-d) with thermal drivers dominating fCO_2 variability along segments of the fCO_2 track. We confirm the location of the Agullhas retroflection with 1/4° daily OISST v2.1 data (Supplementary Figure A.8). Plumes of higher sea surface temperatures coincide with thermally dominated sections (Supplementary Figure A.8). From December 1st to December 6th, 2020, the sailboat navigated through 12 $|SLA| > 0.2$m) in that area, comprising 6 positive and 6 negative SLA of that magnitude (Supplementary Figure A.9). The positive SLA covered more area than the smaller negative ones (Supplementary Figure A.9).
While SLAs indicate the presence of eddies, there can be deviations. Using the META3.2 DT we identified 4 anticyclonic and 7 cyclonic eddies through which the sailboat sailed (Figure A.2c – for daily resolution see Supplementary Figure A.10).
Interestingly, the thermal-dominated parts of the fCO_2 tracks largely coincide with positive SLA and anticyclonic eddies, and the non-thermal-dominated parts of the track largely coincide with cyclonic eddies (Figure A.2c and Supplementary Figure A.11). We observe an exception around 29°E where the fCO_2 in a cyclonic eddy is thermally dominated (Figure A.2c and Supplementary Figure A.11). Upon closer inspection, SST anomalies and SLA near the center of the cyclonic eddy exhibit opposite signs (Supplementary Table A.3), indicating an atypical warm-core cyclonic eddy. The temperature within this eddy is notably higher than compared to the other cyclonic eddies in that region (Figure **??**). It should be noted that META3.2 eddy contours have a daily resolution and might therefore lag behind or not fully align with the higher-resolved temperature data. Nonetheless, the temperature difference between typical and atypical cyclonic eddies is around 2–3°C (Figure A.12) and might be even greater if the eddy contours matched the resolution of the temperature data.

Figure A.3 shows time series of environmental parameters along sailboat tracks crossing different eddy regimes: anticyclonic eddies, cyclonic eddies, transition zones, and outside regions.
fCO_2 averaged 358.3±8.7 µatm along the sailboat track between 10°E and 50°E. Using a two-sample t-test, we find that the mean fCO_2 in the Agulhas region is significantly higher in AE (358 ± 5 µatm) than CE (354 ± 3 µatm) by 4 µatm ($p = 0.0000$), although the differences lie within the range of the standard deviation. The mean fCO_2 of CE is significantly lower than both the outside

Table A.1: Environmental properties of anticyclonic (AE), cyclonic (CE) eddies, as well as the periphery (trans) and the background (outside) in the Agulhas region. *Transition zones (trans) were defined as 1 hour before/after entering/exiting an eddy. Mean values and standard deviations are displayed.*

Eddy Type	**Nr. of obs.**	**fCO_2** [µatm]	**SST** [°C]	**SSS** [PSU]	**CHL** [mg m^{-3}]	**PIC** [mmol m^{-3}]	**Wind Speed** [m s^{-1}]
AE	679	358 ± 5	18.2 ± 1.6	35.5 ± 0.1	0.27 ± 0.09	0.11 ± 0.08	10 ± 1.7
CE	540	354 ± 3	15.8 ± 0.8	35.2 ± 0.2	0.45 ± 0.12	0.49 ± 0.18	8.8 ± 0.7
outside	3593	357 ± 9	17.1 ± 1.5	35.5 ± 0.2	0.33 ± 0.15	0.18 ± 0.14	10.1 ± 1.6
trans	2047	358 ± 9	16.5 ± 2.0	35.4 ± 0.2	0.37 ± 0.20	0.21 ± 0.21	9.8 ± 1.6

(357 ± 9 µatm) and transition zones (358 ± 9 µatm) ($p = 0.0000$) (Figure A.3 and Table A.1). Unsurprisingly, anticyclones exhibited higher temperatures than cyclones, except for the cyclonic eddy on December 3rd, 2020 (Figure A.3a). Differences between anticyclonic and cyclonic eddy temperatures are around 2.4°C. Salinity variations closely follow temperature changes, with sharp decreases and increases occurring simultaneously (Figure A.3a-b). In cyclones, salinity dropped sharply with temperature, whereas in anticyclones, salinity increased with rising temperature. We find that the SST and SSS means of AE (SST: 18.2 ± 1.6°C, SSS: 35.5 ± 0.1) are significantly higher than those of CE (SST: 15.8 ± 0.8°C, SSS: 35.2 ± 0.2), transition zones, and outside ($p = 0.0000$) (Table A.1). The SST and SSS means of CE are significantly lower than those of the outside, AE, and transition zones ($p = 0.0000$) (Table A.1).

Peaks in fCO_2 and strong gradients were observed to coincide with sharp changes in SLA during transitions, as the sailboat entered or exited eddies, particularly before December 4th, 2020, west of approximately 30°E (Figure A.3c). This area is west of the retroflection and further from the relatively well-mixed Agulhas current. SLA appeared to generally follow wind speed with similar timing of changes and both exhibiting gradual changes (Figure A.3c-d). Wind speeds in AE (10 ± 1.7 m/s) are significantly higher than in CE (8.8 ± 0.7 m/s). CE mean wind speeds are lower than those in AE, transition zones, and outside (Table A.1).

Additionally, higher biological activity was observed in cyclones compared to anticyclones and outside of eddies, with cyclones showing increased CHL concentrations (Figure A.3e). However, the impact on fCO_2 was generally weak. In cyclonic eddies on December 2nd, 5th, and 6th, CHL concentrations increased to approximately 0.6 mg m^{-3} (Figure A.3e), with a slight decrease in fCO_2. In contrast, in the atypical warm-core cyclonic eddy, particularly while exiting the eddy, CHL concentrations reached up to 1.6 mg m^{-3}, reducing fCO_2 from around 370 µatm before entering the eddy to 350 µatm during the CHL peak when exiting the eddy (Figure A.3e).

PIC concentrations were similarly elevated in cyclones and their surrounding tran-

sition zones compared to anticyclones and areas outside of eddies (Figure A.3f). Inside cyclonic eddies, PIC concentrations reached up to 1 mmol m^{-3}, but again, the effect on fCO_2 was not very prominent (Figure A.3f). The CHL and PIC concentrations of AE (CHL: 0.27 ± 0.09 mg m^{-3}, PIC: 0.11 ± 0.08 mmol m^{-3}) are significantly lower than those of CE (CHL: 0.45 ± 0.12 mg m^{-3}, PIC: 0.49 ± 0.18 mmol m^{-3}), transition zones, and outside ($p = 0.0000$). The CHL and PIC means of CE are significantly higher than those of AE, outside, and transition zones ($p = 0.0000$) (Table A.1).

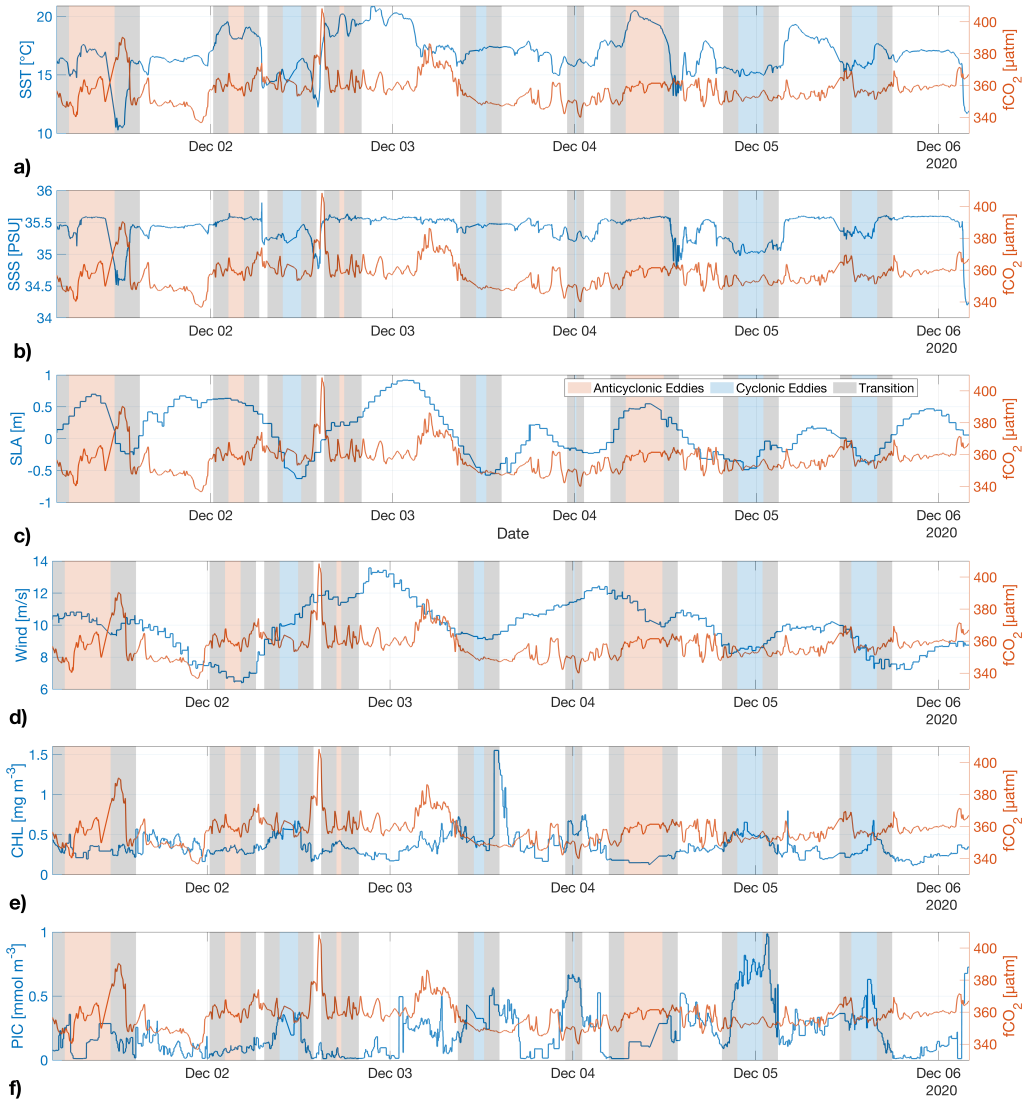

Figure A.3: **Effect of Agulhas Eddies on fCO_2.** Time series of fCO_2 (orange) and **a)** SST, **b)** SSS, **c)** SLA, **d)** wind speed, **e)** CHL concentration, and **f)** PIC concentration and salinity between 10°E and 50°E. *Red-shaded segments are classified as inside an anticyclonic eddy, blue-shaded shaded are classified as inside a cyclonic eddy, and gray is the transition area. The eddy on December 3rd, 2020 appears to be an atypical warm-core cyclonic eddy.*

A.3.3 *Algae bloom in North-East Atlantic/Celtic Sea*

The *Bermudes1000* sailboat race in May 2019 was characterized by high CHL concentrations, indicating high primary productivity during the bloom season (Figure A.4a). Regions characterized by elevated CHL concentrations generally exhibit low fCO_2 (305 ± 16 µatm), compared to low CHL regions (320 ± 27 µatm, Figure A.4b), consistent with the expected biological drawdown of CO_2 during productive periods.

High CHL concentrations occurred along the coast and between 49°N and 47°N and 10°W and 7°W through which the sailboat sailed at the northeast and south edges (Figure A.4a). We observed mean CHL concentrations around 2 mg m^{-3} along the track. Notably, the most distinct changes in fCO_2 were observed at the boundaries of these high CHL zones (see gray boxes in Figure A.4b,c), where CHL concentrations changed from around 1 mg m^{-3} to more than 7 mg m^{-3}. Abrupt increases or decreases in fCO_2 – fCO_2 fluctuations of ≥10 µatm within 10 minutes – align with the sailboat crossing into or out of bloom patches (see red boxes in Figure A.4a), highlighting that the edges of high CHL zones are hotspots of high fCO_2 variability.
Increased CHL concentrations caused fCO_2 to decrease from around 320 µatm to as low as 265 µatm (Figure A.4b). We observed much higher CHL concentrations (up to 21 mg m^{-3}) in coastal zones; however, without a sudden decrease in fCO_2, indicating the difference between coastal and open ocean dynamics and the presence of other drivers. Furthermore, it is well known that ocean color algorithms have problems in near-shore regions. The lowest observed CHL concentrations around 6°E coincided with the highest fCO_2 of up to 380 µatm (dark blue patch in Figure A.4a). CHL accounts for 14% of the variance in fCO_2 (Supplementary Figure A.13), reflecting a statistically significant but moderate relationship, consistent with observations from other bloom events (Lüger et al., 2004; Schneider et al., 2006; Lueger et al., 2008).

To investigate other bloom types, such as coccolithophores, we examined different ocean color products and analyzed the correlation between PIC and fCO_2, which proved to be insignificant and did not account for any variance in fCO_2 (see Supplementary Figure A.13). Although high PIC concentrations, indicative of coccolithophore blooms, are mainly found along the coast, the sailboat only encounters elevated PIC concentrations around 48°N in the Bay of Biscay, coinciding with sudden changes in fCO_2 (Supplementary Figure A.14). For the rest of the region, we observe low PIC concentrations, indicating that calcification

played a minor role during this bloom (Supplementary Figure A.14).
Examining the phenological stage of the bloom in that region in 2019 (Nicholson et al., 2023; Nicholson et al., 2025), we observe that the bloom began around February/March, peaked in April, and terminated between June and September, indicating that the sailboat mainly captured the bloom peak in May (Supplementary Figure A.15).

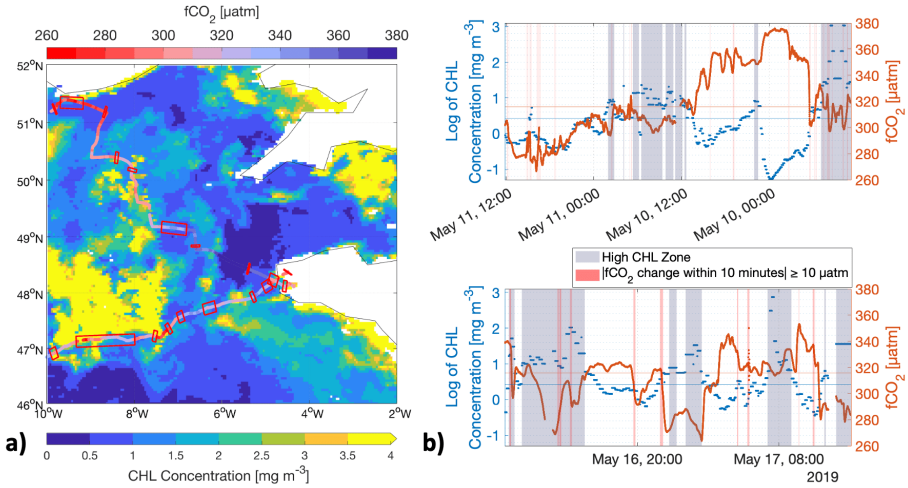

Figure A.4: **Algae Bloom in the Celtic Sea in May 2019.** a) Map with the background showing an 8-day composite of CHL concentrations from May 9 to May 16, 2019, and the line showing fCO_2 measured by the sailboat. Red boxes mark regions with fCO_2 changes of $\geq$10 µatm in $\leq$ 10 minutes. b) Time series of fCO_2 and CHL concentrations (top panel for northern track, bottom for southern track). Red vertical lines indicate fCO_2 changes of $\geq$10 µatm in $\leq$ 10 minutes.

A.3.4 *Coccolithophore bloom on the Patagonian Shelf*

In January 2021, during the *Vendée Globe* race, we observed abrupt changes in fCO_2 over a short time period on the Patagonian Shelf. Interestingly, though, and in contrast to the algae bloom in the Celtic Sea, the relationship between CHL and fCO_2 is less apparent (Figure A.5a and Supplementary Figure A.16a). There is no correlation between CHL and fCO_2 (insignificant, $R^2 = 0$). Examining the phenological stage of the CHL-based bloom on the Patagonian Shelf in 2020/21 (Nicholson et al., 2025), we observe that a CHL-dominated bloom began around September, peaked in November, and terminated in February (Supplementary Figure A.17). This indicates that a CHL-based bloom was in a decaying stage in January when the sailboat passed through it. The correlation between PIC and fCO_2 (significant, $R^2 = 0.09$) is still weak, but still insightful (Supplementary Figure A.16) with increased PIC generally reducing fCO_2. Regions with elevated

PIC concentrations exhibited fCO_2 of 354 ± 27 µatm, characterized by a relatively high standard deviation compared to the productive zones of the Celtic Sea. Similarly, regions without high PIC concentrations exhibited comparable fCO_2 of 360 ± 31 µatm.

Notably, high fluctuations in fCO_2 are associated with elevated CHL concentrations and particularly with elevated PIC concentration, indicating the presence of both a CHL- and PIC-based bloom (Figure A.5). While bloom patches with high CHL concentrations in the Celtic Sea led to consistently low fCO_2 (Figure A.4b), the mixed bloom on the Patagonian Shelf, in contrast, caused high fCO_2 fluctuations (Figure A.5c-e). Changes in PIC concentrations account for 46% of the observed short-term fluctuations in fCO_2, while changes in CHL concentrations account for 34% (Figure A.5d-e). These variations are driven by CO_2 release through calcification and CO_2 uptake through photosynthesis. In this scenario, fCO_2 varies up to 100 µatm, i.e. up to almost two orders of magnitude larger than the CO_2 variability found in the atmosphere, and all within half an hour within the bloom (Figure A.5c).

The satellite data show high PIC concentrations in the coastal region of the Patagonian Shelf, particularly in the Grande Bay as well as in the river mouth of Magellan Strait (Figure A.5b). The bloom navigated by the sailboat forms a westward-facing hook around the Malvinas/Falkland Islands (Figure A.5b-c). Maximum PIC concentrations exceed 2 mmol m^{-3}, with average concentrations of 0.8 mmol m^{-3} in high PIC zones. The two intersections where the sailboat sailed through the bloom indicated by increased PIC concentrations show high fCO_2 variations. Similarly to the Celtic Sea bloom, large changes in fCO_2 occurred at the edge of high PIC zones (Figure A.5b, see gray boxes in Figure A.5c).
As the sailboat enters the bloom around 60°W, fCO_2 increases from 370 µatm to approximately 420 µatm. It then sharply drops and fluctuates 2–3 times by up to 100 µatm before reaching around 320 µatm upon leaving the bloom (Figure A.5c). Upon re-entering the high PIC bloom area around 63°W, fCO_2 fluctuates again, stabilizing around 320 µatm. Generally, fCO_2 is higher west of 60°W compared to east of 60°W despite slightly higher temperatures east of 60°W (Figure A.5b-c and Supplementary Figure A.18).

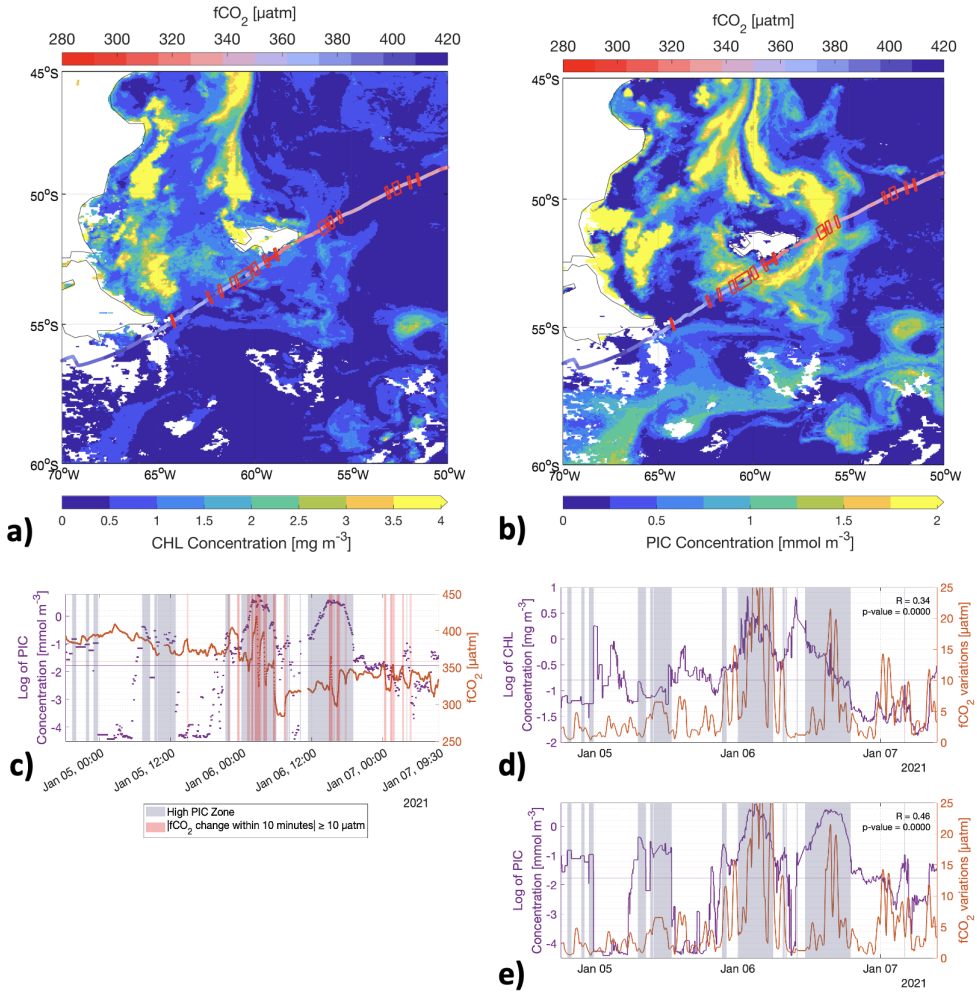

Figure A.5: **Algae Bloom on the Patagonian Shelf in January 2021.** a-b) Map showing a composite from January 1–8, 2021 of a) CHL and b) PIC concentrations, and the line showing fCO_2 measured by the sailboat. Red boxes mark regions with fCO_2 changes of $\geq$10 µatm in $\leq$ 10 minutes. c) Time series of fCO_2 and PIC concentrations. Red vertical lines indicate fCO_2 changes of $\geq$10 µatm in $\leq$ 10 minutes. d-e) Time series of fCO_2 variations, calculated with a 60-minute moving standard deviation, and d) CHL and e) PIC concentrations. *The correlation coefficients and p-values between CHL/PIC and fCO_2 variability are shown in the upper right corner of each panel.*

The elevated PIC concentration of the main bloom body (around the river mouth of the Magellan Strait as well as around the Malvinas/Falkland) matches increased temperatures (Supplementary Figure A.18). Lower PIC occurs east and southwest of the bloom where temperatures are generally lower (Supplementary Figure A.18).

A.4 DISCUSSION

The high-resolution fCO_2 measurements collected during sailboat races provide a unique opportunity to observe how physical and biological processes drive sea surface fCO_2, i.e. the dominant control on the air-sea CO_2 exchange, at small spatial and temporal scales. These data reveal the importance of small-scale processes – often unresolved by coarser observational networks and models – in driving surface fCO_2 variability.

While the thermal–non-thermal decomposition is useful as a valuable first-order approach for identifying broad regimes of fCO_2 variability, it provides limited insight into the specific underlying drivers other than distinguishing temperature-driven changes from general other influences. The sailboat observations reaffirm already established large-scale patterns: across the tropical and subtropical oceans from 40°N to 40°S, fCO_2 variability is predominantly influenced by temperature-driven changes in CO_2 solubility (Takahashi et al., 2002; Gallego et al., 2018; Guo and Timmermans, 2024a). Remarkably, just one or two circumnavigation transects were sufficient to detect and confirm this dominant thermal influence with its boundaries as well as to further identify more thermally driven small-scale features such as Agulhas eddies (see box B in Figure A.2a).

Moreover, the high-frequency observations presented here provide the resolution needed to move beyond a binary thermal/non-thermal framework, enabling more detailed, region-specific investigations that better differentiate and characterize the physical and biological drivers of observed fCO_2 variability.

A.4.1 *Agulhas eddy regimes influence fCO_2*

The Agulhas region is characterized by large spatial and temporal eddy-driven fCO_2 variations, controlled mainly by temperature, biology and circulation. As demonstrated in our study, these variations depend on the eddy regime.

fCO_2 measured along the sailboat track in the Agulhas region (358.3 ± 8.7 µatm) is generally consistent with previously reported values, although it falls toward the upper end of the observed range (Orselli et al., 2019). Our findings generally support studies (Pezzi et al., 2021; Kim et al., 2022) demonstrating increased fCO_2 in anticyclones (358 ± 5µatm), and decreased fCO_2 in cyclones (354 ± 3 µatm). This finding is, however, in disagreement with observational studies from Keppler et al., 2024 analyzing Southern Ocean eddies and Li et al., 2025 analyzing eddies from the Kuroshio Extension, both showing increased carbon uptake in anticyclones and weaker carbon uptake in cyclones.

The observed stronger winds in anticyclones can either amplify an anticyclonic

CO_2 source signal by releasing more CO_2 to the atmosphere or the stronger winds act to mitigate the reduced uptake caused by higher fCO_2 depending on the direction of the prevailing air-sea CO_2 flux.

We confirm the classical perspective of heightened biological activity in cyclones (McGillicuddy and Robinson, 1997; Oschlies and Garçon, 1998; Dawson et al., 2018; Belkin et al., 2022) and their periphery (Chelton et al., 2011) possibly due to upwelling in cyclonic eddy increasing nutrients in surface water and thereby biological activity (McGillicuddy and Robinson, 1997; Oschlies and Garçon, 1998; Dawson et al., 2018; Belkin et al., 2022), with the suggested mechanisms for increased biological activity in anticyclonic eddies appearing to be of lesser importance in this region during the study period (Waite et al., 2007; Siegel et al., 2011; Gaube et al., 2013; Doddridge and Marshall, 2018; Su et al., 2021).

fCO_2 in anticyclonic eddies was significantly higher than in cyclonic eddies by 4 µatm and fCO_2 in cyclonic eddies was significantly lower than outside of eddies and in transition zones. While the results are statistically significant, it has to be noted that the standard deviation is relatively high. However, globally integrated these differences may have a substantial impact on the ocean carbon uptake. The effect might differ and be smaller in other ocean regions where the difference between warm-core and cold-core eddies is less pronounced.

Strong fCO_2 gradients when entering or leaving eddies occur when the sailboat crossed the boundaries of different distinct water masses with distinct biogeochemical signals, particularly west of the relatively well-mixed Agulhas current, as well as different eddy signals are important small-scale features that might be lost in coarser resolutions.

We show that the fCO_2 decomposition in thermal and non-thermal fCO_2 (Takahashi et al., 2002) can be used to first-order identify SLA and eddies in the Agulhas region. It highlights the potential of sailboats in examining the understudied effects of both typical and atypical anticyclonic and cyclonic eddies on fCO_2 and the air-sea CO_2 flux. The encounter with atypical warm-core cyclonic eddies in the Agulhas region as shown in this study is not unusual, as globally, around 20% of eddies are atypical (Ni et al., 2021) and long-lived eddies display atypical behavior for about 40% of their lifetimes, with these eddies predominantly concentrated in the South Atlantic Ocean (Ni et al., 2021; Liu et al., 2024). Given their occurrence and abundance in the Agulhas region, we recommend conducting more observations to investigate and better understand the impact of these eddies on biological processes and CO_2 uptake.

One limitation of our study is the current definition of transition zones, which are currently time-dependent (60 minutes before and after entering or exiting an eddy). This approach may not accurately capture the dynamics, as we show

that wind conditions differ between anticyclonic eddies and cyclonic eddies, with higher wind speeds in anticyclonic eddies and lower in cyclonic eddies, resulting in faster transitions through anticyclonic eddies compared to cyclonic eddies. Additionally, we did not identify the life stage of the eddies, which could be significant since the impact of eddies on fCO_2 varies with their age (Liu et al., 2025). Future studies should address these limitations, especially as more sailboat observations become available, to enhance our understanding of eddy dynamics and their influence on the carbon system.

A.4.2 *Algae bloom in the Celtic Sea*

Although coccolithophore blooms regularly occur between April and June in the Bay of Biscay (Harlay et al., 2010; Suykens et al., 2010; Perrot et al., 2018) – a part of the observed region—it is unlikely to be a coccolithophore dominated bloom through which "*Seaexplorer*" sailed due to the relatively low PIC concentrations. In the Celtic bloom, observed CHL maxima exceeded 4 mg m^{-3}, similar to concentrations reported in literature (Garcia-Soto and Pingree, 2009). Most observations along the track ranged from 1 to 2 mg m^{-3}, matching modal peak concentrations for spring blooms in the region (Garcia-Soto and Pingree, 2009). High CHL concentrations (up to 21 mg m^{-3}) in coastal areas did not coincide with reduced fCO_2, likely due to limited photosynthesis, river discharge, or algorithmic uncertainties in nearshore waters.

While Watson et al., 1991 show a close and inverse relationship between fCO_2 and CHL, we could only observe a modest correlation between CHL and fCO_2 in the Celtic Sea. Similarly, other studies reported a weaker or even no correlation between CHL and fCO_2 (Lüger et al., 2004; Schneider et al., 2006; Schloss et al., 2007; Lueger et al., 2008; Takao et al., 2020). Schloss et al., 2007 attribute the lack of a relationship to a differing influence of different phytoplankton groups on fCO_2. Lüger et al., 2004; Schneider et al., 2006; Lueger et al., 2008 attribute the weak relationship to the differing temporal behavior of these signals. They argue that a decrease in CHL will not directly correlate with an fCO_2 increase because of longer timescales of upwelling, mixing, or air-sea gas exchange. The drastic changes in fCO_2 ($\geq$10 µatm within 10 minutes) might occur due to the patchiness of algae blooms at small-scales (Breier et al., 2018; Robinson et al., 2021).

A.4.3 *Coccolithophore bloom on the Patagonian Shelf*

While the Celtic Sea displayed "classical" bloom behavior with high CHL concentrations reducing fCO_2 through photosynthesis, the bloom along the Patagonian Shelf paints a more complex picture. The relatively low CHL concentrations of around 1.5 mg m^{-3} are similar to concentrations reported in literature around the Malvinas/Falkland at the end of austral summer (Romero et al., 2006; Gil et al., 2019). The low CHL concentrations and phenology metrics may suggest the decay of a bloom, however, they do not necessarily indicate its absence, as shown in previous studies (Garcia et al., 2011). Indeed, the high PIC concentration observed in January 2021 suggests a coccolithophore bloom, which aligns with the typical bloom patterns on the Patagonian Shelf – a region known for intense algal blooms from December to January (Poulton et al., 2013; Balch et al., 2014; Hopkins et al., 2015; Ulibarrena and Conzonno, 2015; Oliver et al., 2024; Guinder et al., 2025). Zones with high biological activity, indicated by elevated PIC concentrations, coincide with high fCO_2 fluctuations and in part increased fCO_2, indicating the effect of CO_2 release due to calcification. This demonstrates the contrasting effect of the coccolithophore bloom compared to elevated CHL concentrations.

We confirm that a CHL peak preceded the observed high PIC concentration, that likely represents the coccolithophore peak, along the Patagonian Shelf in January 2021 (Hopkins et al., 2015). This pattern is consistent with the bloom dynamics of *Emiliania huxleyi* and supports the notion that blooms of coccolithophores and other phytoplankton species can co-occur (Hopkins et al., 2015). The bloom resulted in high PIC concentrations exceeding 2 mmol C m^{-3}, which is comparable to, and even higher than literature values where concentrations exceeding 1 mmol C m^{-3} are common along the Patagonian Shelf, typically attributed to *Emiliania huxleyi* (Balch et al., 2014; Hopkins et al., 2015; Oliver et al., 2024). As observed in other blooms, the pattern of PIC concentration follows the 200m isobath (Gil et al., 2019) and the spatial extent of the bloom appears to coincide with warmer temperatures, aligning with (Oliver et al., 2024), who noted that the spatial extent of coccolithophore blooms in that region is defined by temperature limitation.

A.4.4 *Implications and Recommendations for Future*

A.4.4.1 *Implications for models and neural network gap-filling*

Small-scale variations are often missed by lower-frequency observations, can be lost during regridding in synthesis products (e.g., the monthly 1°×1° grid in SO-

CAT; Bakker et al., 2016), or through gap-filling procedures, and are frequently not accurately represented in models used to estimate carbon budgets. For instance, strong fCO_2 gradients at the edges of blooms and eddies and short-term bloom dynamics cannot be resolved at a monthly 1°×1° resolution. This limitation makes low-resolution models less ideal for estimating local fCO_2 dynamics, as small-scale processes are not adequately represented. This could lead to underestimating changes in the carbon budget, which is crucial for understanding climate change impacts. To address discrepancies between global ocean biogeochemistry models and observations (Hauck et al., 2020; Rodgers et al., 2023; Friedlingstein et al., 2025), processes at various scales should be taken into account (e.g. Jersild et al., 2021; Hewitt et al., 2022; Ford et al., 2023; Rodgers et al., 2023; Smith et al., 2023; Couespel et al., 2024; Beech et al., 2025; Nielsen et al., 2025) as well as high-resolution measurements, particularly in highly variable regions such as e.g. eddy-rich regions (e.g. Leseurre et al., 2022; Guo and Timmermans, 2024b; Morgan et al., 2025; Song et al., 2025). Looking ahead, accurately resolving these processes with the aid of sailboats and uncrewed surface vehicles (e.g. Patterson et al., 2025) at small temporal and spatial scales is necessary. This will become increasingly important, as biogeochemical models are developed at kilometer scale and enable more accurate estimates of the ocean carbon budget. Research shows that incorporating metrics related to eddy activity into neural networks improves the accuracy of fCO_2 reconstructions, especially on a regional and seasonal scale (Wang et al., 2025b).

We demonstrate that the CO_2 dynamics can vary between different types of blooms. Specifically, coccolithophore blooms, which are characterized by high PIC concentrations, can have an opposite effect on fCO_2 compared to CHL, and mixed blooms can obscure the signals. Our findings indicate that CHL, often used in neural-network methods as a proxy for estimating missing fCO_2 (e.g. Rödenbeck et al., 2015; Fay et al., 2021), does not fully capture the biological processes and is not an ideal predictor or proxy. We recommend including PIC as a predictor in these estimations to improve the representation of different bloom dynamics and variability associated with eddies at a high resolution.

Recent developments, such as a global 8-day fCO_2 dataset at a finer spatial resolution of 0.25°×0.25° (Gregor et al., 2024) show the potential of higher-resolution datasets to improve carbon flux estimates. Moving towards even higher-resolution neural network models – such as those by Duke et al., 2023; Duke et al., 2024 with resolutions of approximately $1/12° \times 1/12°$ – is especially valuable in key dynamic regions, enabling more accurate reconstructions of ocean carbon fluxes and better capturing small-scale variability critical for understanding air-sea CO_2 exchange. However, these high-resolution neural networks need sufficient training data, calling for continuous sampling on sailboats.

A.4.4.2 *Importance of enhanced monitoring and future applications of sailboats*

Climate change is altering the ocean carbon cycle in complex and regionally variable ways, thereby increasing the urgency for expanded high-frequency in situ fCO_2 observations. With the rise in marine heatwaves (Frölicher et al., 2018) and enhanced mesoscale temperature variance (Guo et al., 2022), the thermal component of fCO_2 variations is likely being altered as well, potentially impacting mesoscale-driven CO_2 exchange (Guo and Timmermans, 2024b). As the ocean's temperature dynamics shift, the contribution of thermal and non-thermal influences on fCO_2 may be disrupted, potentially affecting the ocean's role in global carbon cycling.

At the same time, climate change is driving shifts in the small-scale physical and biological phenomena that modulate fCO_2 and thereby CO_2 fluxes, making it increasingly important to expand observational networks that effectively monitor these dynamics, with particular focus on biologically active and eddy-rich regions, to better understand their evolving influence on regional flux variability and the carbon cycle (e.g. Gray, 2024; Prend et al., 2025). This becomes especially important as phenomena such as the Agulhas leakage intensify (Biastoch et al., 2009; Rouault et al., 2009; Sebille et al., 2009; Beech et al., 2022) and Southern Ocean eddy activity is projected to shift polewards and intensify (Beech et al., 2025; Mortenson et al., 2025). Meanwhile, coastal regions like the Patagonian Shelf and the Celtic Sea are experiencing increased bloom frequency and shifts in phytoplankton community composition (Dai et al., 2023; Nocera et al., 2024; Demasy et al., 2025).

Prend et al., 2025 recommend a coordinated deployment of USVs in key regions with high eddy-driven air–sea flux variability. We highlight that sailboats, although not subject to targeted deployment due to their independent sailing routes, provide a large spatiotemporal high-resolution dataset that complements the existing network of USVs, moorings and ships. With upcoming races featuring a fleet of sailboats equipped with various measurement devices – as exemplified by the *Vendée Globe 2024*, where four sailboats measured fCO_2 and one carried a plankton imaging platform (Pollina et al., 2022) – we anticipate capturing many more small-scale processes and gaining a deeper understanding of their dynamics. Because these sailboats sail through eddies and blooms at different times, the combined data will effectively create a time-lapse view of evolving physical and biological features, offering unique insights into temporal changes that are difficult to capture with fixed or single-platform observations.

Sailboats are able to monitor these changes, complementing the ocean observing network by providing high-frequency measurements that can detect emerging climate-driven changes in ocean carbon dynamics earlier than many other

platforms (Carter et al., 2019). We recommend adding fluorescence sensors and plankton imaging systems (e.g. Pollina et al., 2022) alongside fCO_2 measurement devices to better understand the role of biology in modulating fCO_2, especially the counteracting effects of CHL and PIC in blooms of various stages.

A.5 CONCLUSION

Many ocean regions lack sufficient observational coverage, particularly in areas where high variability occurs at small spatial and temporal scales, challenging accurate assessment of carbon fluxes. Emerging observational platforms such as sailboats measuring during racing events provide a unique opportunity to capture these small-scale processes, complementing traditional ship-based and autonomous systems (Olivier et al., 2022; Landschützer et al., 2023; Zhang et al., 2023; Prend et al., 2025; Patterson et al., 2025).

In this study, we demonstrate how high-resolution fCO_2 measurements collected by sailboats across the Atlantic and Southern Ocean between 2018 and 2023 capture small-scale ocean features such as eddies and algae blooms and provide new insights into the physical and biological drivers of sea surface fCO_2 variability. Our observations confirm the thermal dominance of fCO_2 variability between approximately 40°N and 40°S and identify the Agulhas region as a key area influenced by temperature and other physical phenomena, namely small-scale eddy activity. Meanwhile, in regions such as the Celtic Sea and the Patagonian Shelf, biological processes exert a dominant influence on fCO_2 variability.

The high-frequency sailboat observations reveal the key role of eddies and algae blooms in driving fCO_2 variability. In the Agulhas region, distinct eddy regimes demonstrate characteristic variations in fCO_2. Cyclonic eddies emerge as biologically productive regions with lower fCO_2. Anticyclonic eddies show increased fCO_2 concentrations than cyclonic eddies, while cyclonic eddies have lower fCO_2 compared to anticyclones and their surroundings.

These patterns, along with sharp fCO_2 gradients at the eddy edges, suggest potential misrepresentations in coarser-scale models and regridded data products as used for the Global Carbon Budget (Friedlingstein et al., 2025), consequently underestimating regional and global carbon flux changes. The identification of atypical eddies further highlights the complexity of these systems and underscores the need for detailed, high-resolution monitoring.

Beyond eddies, we observed significant fCO_2 variability associated with algae blooms in the Celtic Sea and along the Patagonian Shelf. The Celtic Sea bloom followed a "classical" pattern where high CHL concentrations caused reduced

fCO_2. In contrast, the Patagonian Shelf featured a more complex, mixed-stage bloom, where a decaying CHL-dominated bloom and a peaking coccolithophore bloom (high in PIC) counteracted each other's effects on fCO_2, causing large short-term fluctuations up to 100 µatm.
These small-scale variations (e.g. strong fCO_2 gradients at the edges of eddies and bloom dynamics) are often missed in infrequent measurements, when regridded to coarser resolutions, or in models, leading to inaccuracies in estimating fCO_2. We conclude that CHL, commonly used as a predictor for estimating fCO_2 (e.g. Rödenbeck et al., 2015; Fay et al., 2021), does not fully capture biological processes, suggesting that PIC should also be considered in these estimations for improved accuracy of CO_2 release due to calcification.
This study presents a detailed case for three distinct small-scale features, highlighting the potential of the sailboat dataset. Given the accelerating impacts of climate change on bloom dynamics, eddy intensity, and temperature regimes, expanding high-frequency in situ fCO_2 observations is critical. While ships and autonomous platforms provide targeted measurements, sailboats offer valuable complementary coverage, sampling across space and time with a natural time-lapse effect as fleets encounter dynamic features at different moments. Upcoming sailboat races with a fleet, equipped with different sensors such as fluorescence and plankton imaging systems (the latter already used during *Vendée Globe 2024*), will further enhance our capacity to resolve and understand biological and physical influences on ocean carbon fluxes.

Sailboat-based fCO_2 observations improve our understanding of highly variable and underobserved ocean regions by capturing key small-scale processes at a high spatiotemporal resolution. These insights are vital for refining models and improving regional to global estimates of the ocean carbon sink in a rapidly changing climate.

A.6 DATA AVAILABILITY

The sailboat data used and discussed in this article are freely available via www.socat.info. The code will be made publicly available upon submission or publication of this work.

A.7 ACKNOWLEDGEMENTS

We thank Team Malizia for their support, especially skipper Boris Herrmann for collecting the valuable data presented here. The Surface Ocean CO_2 Atlas

(SOCAT) is an international effort, endorsed by the International Ocean Carbon Coordination Project (IOCCP), the Surface Ocean Lower Atmosphere Study (SOLAS) and the Integrated Marine Biosphere Research (IMBeR) program, to deliver a uniformly quality-controlled surface ocean CO_2 database. The many researchers and funding agencies responsible for the collection of data and quality control are thanked for their contributions to SOCAT. The altimetric Mesoscale Eddy Trajectories Atlas (META3.2 DT) was produced by SSALTO/DUACS and distributed by AVISO+ (https://aviso.altimetry.fr) with support from CNES, in collaboration with IMEDEA (DOI: 10.24400/527896/a01-2022.005.220209 for the META3.2 DT allsat version and 10.24400/527896/a01-2022.006.220209 for the META3.2 DT twosat version).

A.8 SUPPLEMENTARY INFORMATION

Table A.2: Overview of sailing races and fCO_2 observations collected by Team Malizia. $\sum$ 305,405 fCO_2 observations over 112,369 km measured during 2 round-the-world races, 4 North Atlantic Races, and 4 transfers

Name of Race	**Period of Time**	**# of fCO_2 observations**	**Distance covered (between samples)**	**Region**
Défi Azimuth	21-Sep-2018 – 22-Sep-2018	5,192	297 km	North Atlantic
Bermudes 1000	09-May-2019 – 17-May-2019	67,561	4,158 km	North Atlantic
Rolex Fastnet	03-Aug-2019 – 05-Aug-2019	17,249	1,296 km	North Atlantic
Transfer Brest	03-May-2019 – 04-May-2019	3,685	165 km	North Atlantic
Transfer Les Sables	09-Oct-2020 – 11-Oct-2020	711	344 km	North Atlantic
Transfer Monaco	02-Jun-2019 – 11-Jun-2019	5,996	2,391 km	North Atlantic
Transfer Bretagne	14-Aug-2018 – 16-Aug-2018	9,422	402 km	North Atlantic
Vendée Arctic	03-Jul-2020 – 15-Jul-2020	15,001	6,157 km	North Atlantic
Vendée Globe	08-Nov-2020 – 28-Jan-2021	109,919	53,480 km	Atlantic, Southern Ocean
The Ocean Race (multi-legged)	26-Feb-2023 – 29-May-2023	69,377	43,679 km	Atlantic, Southern Ocean

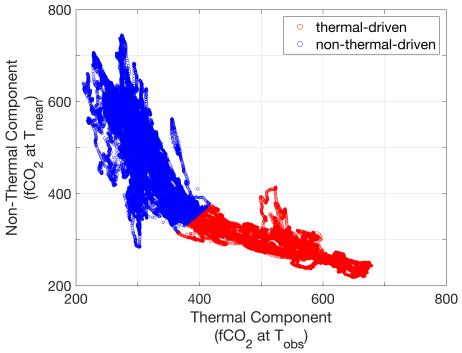

Figure A.6: K-Means clustering of fCO_2 data from two circumnavigation races into thermal and non-thermal driven components.

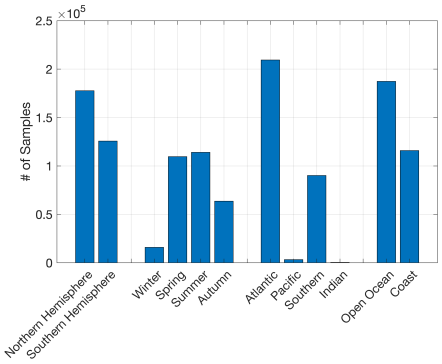

Figure A.7: Distribution of sailboat data categorized by hemisphere, season, ocean basin, and distinguishing between open ocean and coastal regions.

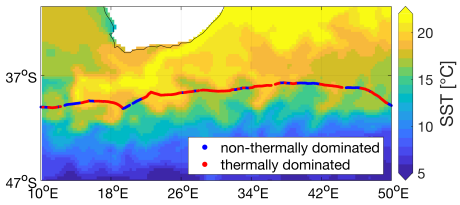

Figure A.8: Thermally and non-thermally dominated sailboat tracks, with satellite SST, averaged from December 1 to December 6, 2020, shown as the background.

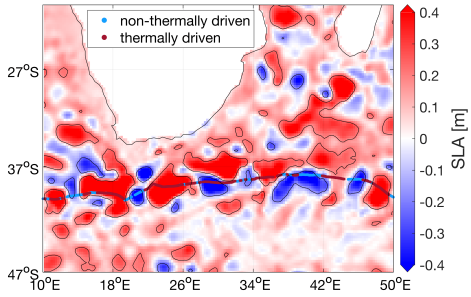

Figure A.9: SLA in the Agulhas region with sailboat tracks colored by whether fCO_2 is non-thermally or thermally dominated. *Background shows SLA from December 4, 2020, with 0.2 m contour lines.*

Table A.3: Sea surface temperature and sea level anomalies of eddies in the Agulhas region from December 1st to December 6th, 2020. *The bold line marks an atypical eddy, characterized by anomalies of opposite sign, indicative of a warm-core cyclonic eddy.*

Date	SST Anomaly	Sea Level Anomaly
01-Dec-2020	-3.1315	-0.2368
02-Dec-2020	-1.5745	-0.5411
03-Dec-2020	**0.1290**	**-0.4496**
04-Dec-2020	-1.9715	-0.4853
04-Dec-2020	-1.1651	-0.1486
05-Dec-2020	-1.1336	-0.3520
05-Dec-2020	-1.7167	-0.4622

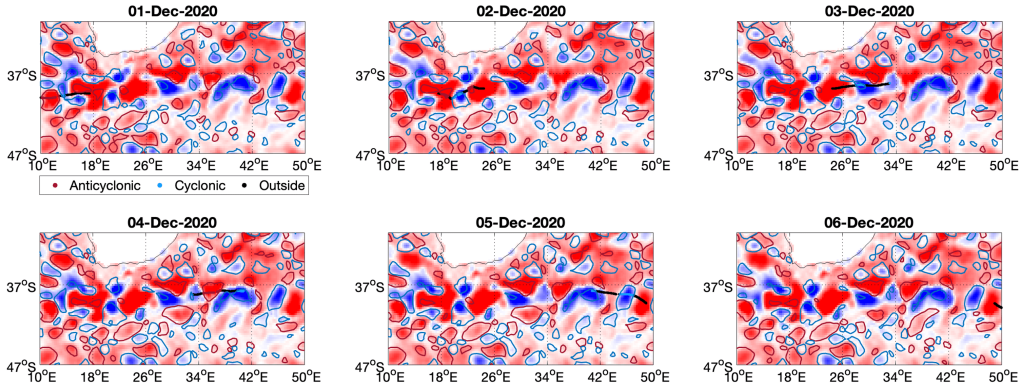

Figure A.10: Sailboat tracks colored by location relative to eddies (inside AE, inside CE, outside) overlaid on daily sea level anomaly (background) and META3.2 DT all-satellite long-lived eddy contours.

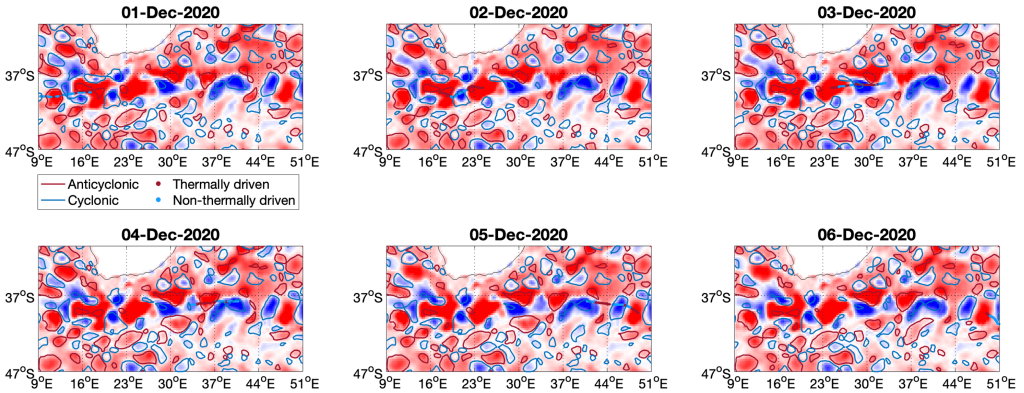

Figure A.11: Dominant fCO_2 drivers (thermal or non-thermal) derived by Takahashi decomposition (Takahashi et al., 2002) along the sailboat track in the Agulhas region (lines of points) on top of daily sea level anomaly (background) and META3.2 DT all-satellite long-lived eddy contours.

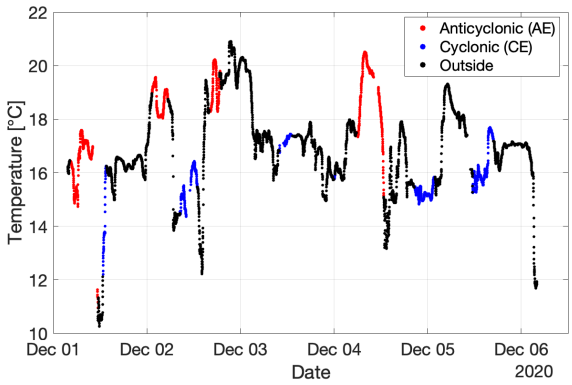

Figure A.12: Temperature time series along sailboat tracks in the Agulhas region.

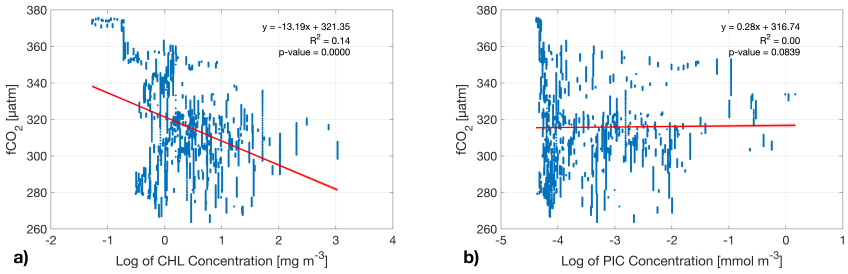

Figure A.13: Relationship between fCO_2 and satellite-derived (a) (CHL) and (b) PIC in the Celtic Sea during an algae bloom in May 2019.

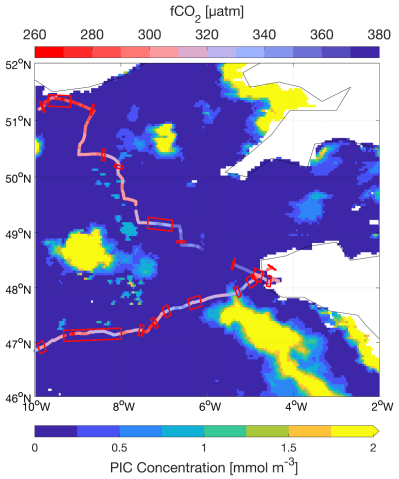

Figure A.14: Map of the Celtic Sea algae bloom with the background showing an 8-day composite of PIC concentration data from May 9 to May 16, 2019, and the line showing fCO_2 measured by the sailboat *Seaexplorer*. Red boxes indicate regions where fCO_2 changed by $\geq$10 µatm in $\leq$ 10 minutes minutes.

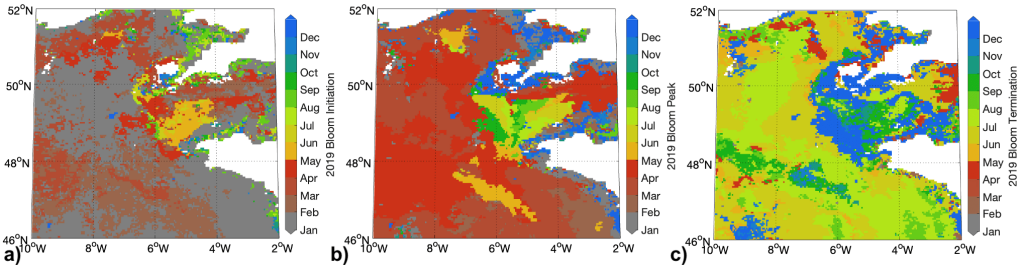

Figure A.15: Maps of Celtic Sea bloom phases in 2019. (a) Bloom initiation, (b) bloom peak, (c) bloom termination. Phenological metrics are derived from Nicholson et al., 2025.

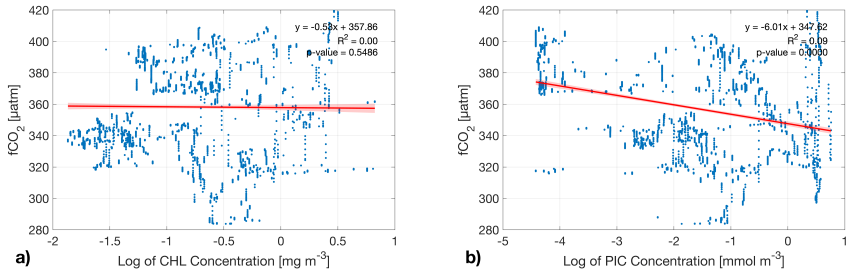

Figure A.16: Relationship between fCO_2 and satellite (a) CHL and (b) PIC on the Patagonian Shelf during an algae bloom in January 2021.

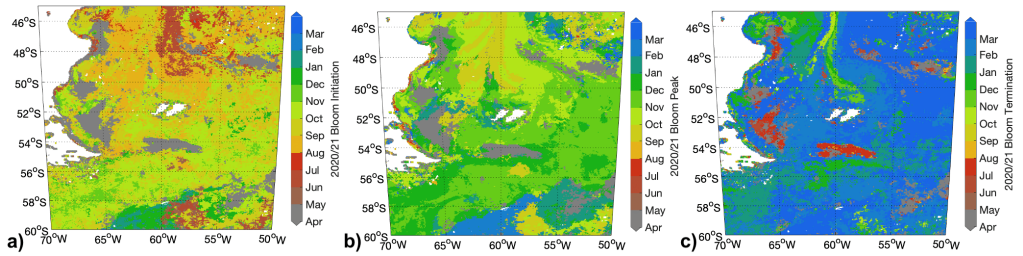

Figure A.17: Maps of Patagonian Shelf bloom phases in 2020/21. (a) Bloom initiation, (b) bloom peak, (c) bloom termination. Phenological metrics are derived from Nicholson et al., 2025.

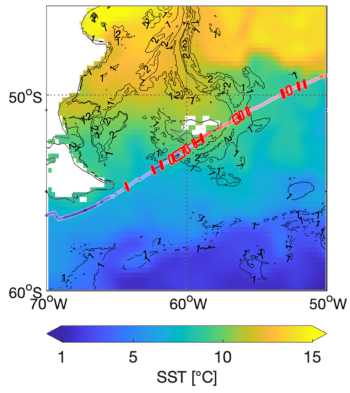

Figure A.18: Satellite SST (Huang et al., 2021) averaged from January 6 to January 5, 2021. Contours depict PIC concentrations derived from an 8-day composite from January 1 to January 8, 2021.

Appendix B

A DETECTABLE CHANGE IN THE AIR-SEA CO_2 FLUX ESTIMATE FROM SAILBOAT MEASUREMENTS

Behncke, J., Landschützer, P. & Tanhua, T. A detectable change in the air-sea CO_2 flux estimate from sailboat measurements. *Scientific Reports 14*, 3345 (2024). https://doi.org/10.1038/s41598-024-53159-0.

A detectable change in the air-sea CO_2 flux estimate from sailboat measurements

Jacqueline Behncke[1,2], Peter Landschützer[3,2] & Toste Tanhua[4]

[1] *Max Planck Institute for Meteorology, Bundesstrasse 53, 20146, Hamburg, Germany*
[2] *International Max Planck Research School for Earth System Modelling, Bundesstrasse 53, 20146, Hamburg, Germany*
[3] *Flanders Marine Institute (VLIZ), Jacobsenstraat 1, 8400, Ostend, Belgium*
[4] *GEOMAR Helmholtz Centre for Ocean Research, Wichhofstrasse 1-3, 24148, Kiel, Germany*

ABSTRACT

The sailboat *Seaexplorer* collected underway sea surface partial pressure of CO_2 (pCO_2) data for 129 days (2018–2021), including an Antarctic circumnavigation. By comparing ensembles of data-driven air-sea CO_2 fluxes computed with and without sailboat data and applying a detection algorithm, we show that these sailboat observations significantly increase the regional carbon uptake in the North Atlantic and decrease it in the Southern Ocean. While compensating changes in both basins limit the global effect, the Southern Ocean - particularly frontal regions (40°S–60°S) during summertime - exhibited the largest air-sea CO_2 flux changes, averaging 20% of the regional mean. Assessing the sensitivity of the air-sea CO_2 flux to measurement uncertainty, the results stay robust within the expected random measurement uncertainty (± 5 µatm) but remain undetectable with a measurement offset of 5 µatm. We thus conclude that sailboats fill essential measurement gaps in remote ocean regions.

B.1 INTRODUCTION

The ocean plays a critical role in regulating Earth's climate by absorbing more than a quarter of anthropogenically emitted carbon dioxide (CO_2) from the atmosphere on an annual basis (Friedlingstein et al., 2022; Gruber et al., 2023; DeVries et al., 2023). However, climate change has already started to alter the carbon uptake capacity of the ocean (Friedlingstein et al., 2022; Le Quéré et al., 2007), thus monitoring the sea surface CO_2 content is crucial for understanding the Earth system as a whole. Although there has been a significant community effort resulting in the collection and synthesis of sea surface CO_2 observations (Bakker et al., 2016; Pierrot et al., 2009) in recent decades, and methods to upscale the existing measurements (Landschützer et al., 2016; Bennington et al., 2022b; Iida et al., 2021; Rödenbeck et al., 2022; Gregor and Gruber, 2021; Chau

et al., 2022) we find a significant difference between hemispheres. While the Northern Hemisphere has been regularly sampled in the recent past being the result of the community-driven measurement efforts resulting from the Ship Of Opportunity (SOOP) program (Pierrot et al., 2009; Jiang et al., 2019), key regions in the ocean carbon and heat uptake such as the Southern Ocean remain undersampled (Bakker et al., 2016; Pfeil et al., 2013; Sabine et al., 2013). The resulting uncertainty in air-sea CO_2 fluxes is problematic (Gloege et al., 2021; Hauck et al., 2023) and limits our ability to resolve and interpret observed and modelled variations in the carbon sink (McKinley et al., 2020; DeVries et al., 2017; Mongwe et al., 2018). This is concerning as the Southern Ocean alone is estimated to be responsible for 40% of the marine anthropogenic CO_2 and 75% of the marine excess heat uptake (Landschützer et al., 2016; Frölicher et al., 2015).

New techniques, including new sensors on biogeochemical floats, have started to address this observational gap, but their indirect measurements of pCO_2 - calculated from pH and salinity measurements—remain uncertain (Bushinsky et al., 2019a; Gray et al., 2018; Williams et al., 2017). Additionally, Antarctic operations from Saildrones (Sutton et al., 2021) have contributed to filling the measurement gaps and are suggested to improve the air-sea CO_2 flux estimates (Heimdal et al., 2024), however, thus far no continuous measurement program exists. Given the limitations of the existing observational network and the moderate success of gap-filling methods in further improving pCO_2 estimates (Gloege et al., 2021; Hauck et al., 2023), it is essential to explore new opportunities to fill observational gaps.

Here we show that a novel observing platform is capable of improving our estimates of the air-sea CO_2 exchange. Since 2018, the high-performance IMOCA class 60 sailboat "*Seaexplorer-Yacht Club de Monaco*"(until 2019 "*Malizia*") has collected pCO_2 observations (hereinafter: *Seaexplorer* data) while competing for 129 days in round-the-world racing events, including an Antarctic circumnavigation race from November 2020 to January 2021 (Landschützer et al., 2023). We show that the use of a single platform ("*Seaexplorer-Yacht Club de Monaco*"), and the participation in a single race in the Southern Ocean has a measurable effect on data-driven air-sea CO_2 flux estimates. This impact persists even when considering its expected measurement uncertainty of ± 5 µatm (Lauvset et al., 2018). Thus sailboats have the potential to complement and improve the existing observing system. Nevertheless, we further illustrate that high standard measurements are crucial in detecting changes in the air-sea flux and that measurement biases still pose a challenge for detecting improvements in the air-sea CO_2 flux estimates.

B.2 RESULTS

GLOBAL EFFECT OF ADDING SAILBOAT pCO_2 DATA Figure B.1a,b show the air-sea CO_2 fluxes calculated based on the upscaling of all available pCO_2 measurements including (ensemble 1=E1) and excluding *Seaexplorer* data (ensemble 2=E2). The ensembles were generated using SOM-FFN, a 2-step neural network method (Landschützer et al., 2013) — see "Methods" — regularly used in the Global Carbon Budget (Friedlingstein et al., 2022) and the recent IPCC assessment (Canadell et al., 2021). The significant impact of adding all underway pCO_2 observations from the sailboat on the air-sea CO_2 flux from November 2020 through January 2021 is further illustrated in Fig. B.1c. We chose this time period from November 2020 to January 2021 as it showed the largest flux impact by adding sailboat data, which is related to the circumnavigation race where *Seaexplorer* participated (see black lines in Fig. B.1 and in Supplementary Fig. B.1). Interestingly, significant differences between E1 and E2 in the North Atlantic (largely negative shown in blue: E1<E2) and the Southern Ocean (largely positive shown in red: E1>E2) in the air-sea CO_2 fluxes are opposing each other (Fig. B.1), resulting in an insignificant change when integrated globally (i.e. an annual flux difference in 2021 from - 2.55 to - 2.51±0.4 Pg C yr^{-}1), which has also been suggested by Landschützer et al., 2023.

Considering that both the North Atlantic and the Southern Ocean are predominantly carbon sinks from 2018 onwards, the addition of *Seaexplorer* data reveals increased carbon uptake in the North Atlantic and reduced uptake in the Southern Ocean (Fig. B.1 and Supplementary Fig. B.1) similar to previous findings (Bushinsky et al., 2019a).

Differences in the flux estimates are visible across all ocean regions even away from the sailboat tracks. The neural network's ability to estimate changes in air-sea CO_2 flux distant from the sailboat tracks originates from its methodology, combining clustering and regression. This process involves assimilating data from observations made in distant yet biogeochemically comparable ocean regions. However, in many regions, these differences fall within the noise of the method (Storey, 2002) (see "Methods") and are thus not detected as significant changes (hatches in Figs. B.1 and B.2). This is most visible in the high-latitude ocean regions and is likely due to the poor constraint of the air-sea CO_2 flux estimate in highly heterogeneous and sparsely observed regions (Gloege et al., 2021; Hauck et al., 2023). Focusing on the detectable changes, irrespective of the background fluxes, the absolute magnitude of the difference between flux estimates provides a better insight (Fig. B.2).

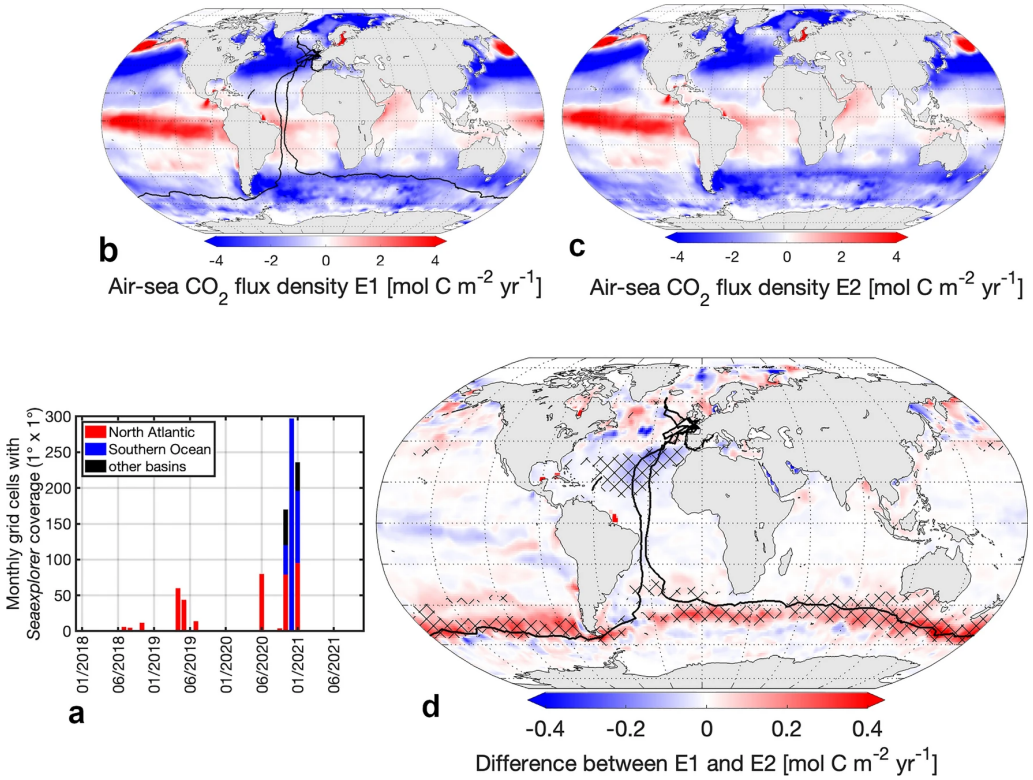

Figure B.1: (a) Timeseries of *Seaexplorer* data availability per basin and b-d) air-sea CO_2 fluxes in ensemble 1 (E1) and 2 (E2) and their difference averaged over Nov 2020–Jan 2021. (b) Air-sea CO_2 flux in E1 (based on SOCATv2022 including *Seaexplorer* data). (c) Air-sea CO_2 flux in E2 (based on SOCATv2022 excluding *Seaexplorer* data). Positive=carbon outgassing, negative=carbon uptake. (d) Difference between E1 and E2. Hatching indicates significant differences. Blue indicates increased carbon uptake due to the addition of *Seaexplorer* data, red indicates reduced carbon uptake due to the addition of *Seaexplorer* data. Black lines in (b,d) represent sailboat tracks from 2018 to 2021. Figures generated using a mapping package for MATLAB (Pawlowicz, 2020).

IMPACT OF ADDING SAILBOAT pCO_2 DATA IN THE SOUTHERN OCEAN

In less frequently monitored regions such as the Southern Ocean, even adding Southern Ocean CO_2 measurements from a single track results in a significant difference between E1 and E2 (Fig. B.2a)—acknowledging a possible influence of sailboat observations from other oceanic regions that were equally excluded.

This aligns with previous findings based on synthetic data (Heimdal et al., 2024) demonstrating that few additional pCO_2 sampling by Saildrone would potentially improve the air-sea CO_2 flux reconstructions most in the Southern Ocean (south of 35°S). The reconstructions of our air-sea CO_2 flux differ most significantly between 40°S and 60°S and with maximum differences of 0.77 mol C m^{-2} yr^{-1}, reflecting the rate of carbon exchange between the atmosphere and the ocean per unit area, in the time period from 1982 to 2021 in the Southern Ocean (Figs. B.2b and B.3a). Overall, the absolute air-sea CO_2 fluxes significantly differed on

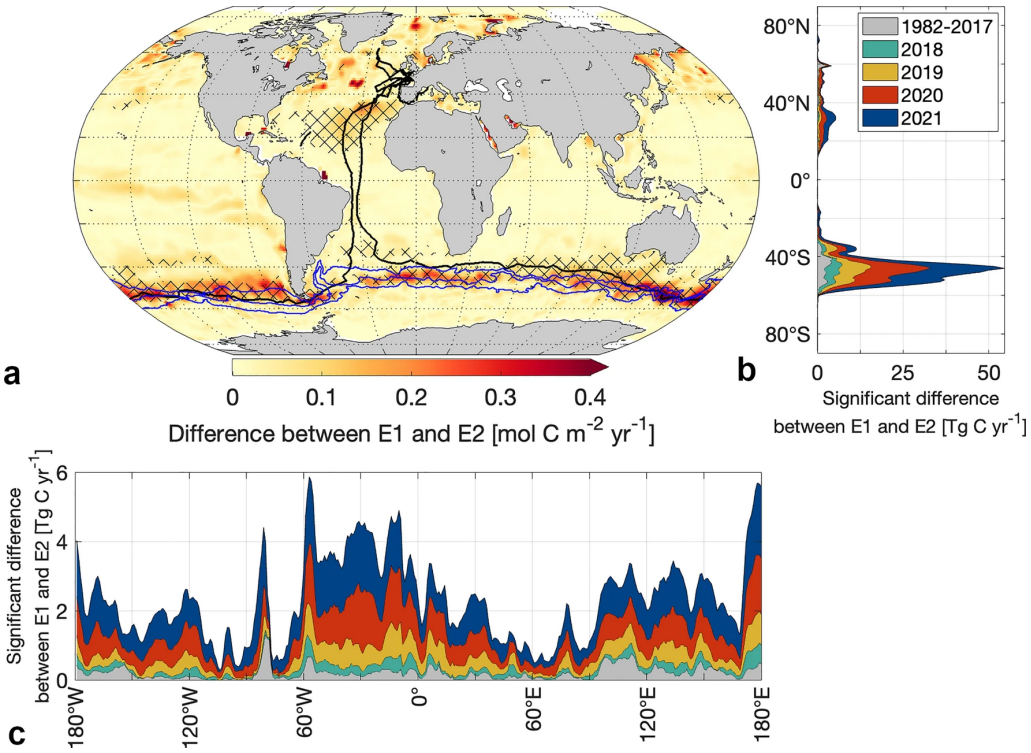

Figure B.2: The absolute magnitude of differences between the air-sea CO_2 flux E1 (based on SOCATv2022 including *Seaexplorer* data) and the air-sea CO_2 flux E2 (based on SOCATv2022 excluding *Seaexplorer* data). (a) Map shows the absolute magnitude of differences between carbon flux estimates averaged over Nov 2020–Jan 2021. Hatching indicates significance. Black lines represent sailboat tracks from 2018 to 2021. Blue lines from north to south: Northern Boundary, Subantarctic Front, Polar Front. Figure generated using a mapping package for MATLAB (Pawlowicz, 2020). (b,c) Significant differences between air-sea CO_2 flux estimates per year and (b) latitude and (c) longitude.

average by 0.15 mol C m^{-2} yr^{-1} in the Southern Ocean (Supplementary Fig. B.2), which is roughly 20% of the regional mean flux density, thus leaving a significant imprint on the regional flux.

The impact of including the *Seaexplorer* data in the air-sea CO_2 flux calculations is the largest within the vicinity of the Subantarctic Front (2-degree grid cells or approximately 200 km radius) closely followed by the Northern Boundary (Figs. B.2a and B.3c). Although the sailboat did not cross the Polar Front, significant differences emerge in its vicinity (Figs. B.2a and B.3c) due to the extrapolation of the data using the neural network algorithm. This pattern coincides with the coverage of the *Seaexplorer* data, as the region along the Subantarctic Front contained most *Seaexplorer* data with an overall 11% of the area covered by sailboat tracks when binned into a 1×1 degree grid, followed by 9% along the Northern Boundary, and 2% in the vicinity of the Polar Front.

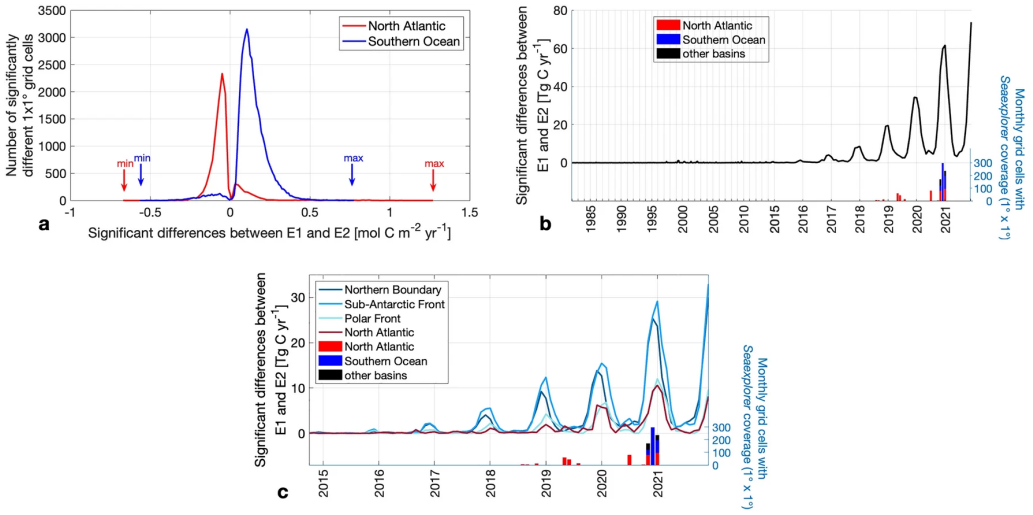

Figure B.3: Magnitude of significant differences between the air-sea CO_2 flux E1 (based on SOCATv2022 including *Seaexplorer* data) and the air-sea CO_2 flux E2 (based on SOCATv2022 excluding *Seaexplorer* data). (a) Histogram of the magnitude of significant flux differences in the Southern Ocean and the North Atlantic. (b,c) Time series of the magnitude of significant differences between carbon flux estimates (based on SOCATv2022 with and without *Seaexplorer* data) as well as the *Seaexplorer* data availability per basin (b) on a global scale and (c) on regional scales.

Regionally, we find the largest differences during the Antarctic circumnavigation race between Nov 2020–Jan 2021 exceeding 0.4 mol C m^{-2} yr^{-1} in the interfrontal region south of Tasmania and New Zealand (Figs. B.1 and B.2a). Although the region south of Tasmania and New Zealand is relatively well-observed for the Southern Hemisphere (Bakker et al., 2016), the data availability close to frontal zones is insufficient considering the variability within this region (Chapman et al., 2020). The frontal zones are characterized by enhanced vertical mixing and high biological productivity. In fact, the pCO_2 signal measured by *Seaexplorer-Yacht Club de Monaco* there is oversaturated and distinctly higher than the surrounding area (Landschützer et al., 2023). Our results demonstrate the high potential of sailboat pCO_2 data in improving the air-sea CO_2 flux estimate in frontal regions.

Although our results confirm the finding that regional differences in the air-sea CO_2 flux are attributed to the frontal zones in the Southern Ocean, the previously proposed changes south of the Polar Front (Landschützer et al., 2023) probably stem from noise in the methodology and not from a detectable signal. This underscores the need for signal-to-noise detection methods as presented here, or alternatively, the use of synthetic data experiments using large ensembles (Gloege et al., 2021; Heimdal et al., 2024) when comparing different air-sea CO_2 flux estimates from neural networks.

IMPACT OF ADDING SAILBOAT pCO_2 DATA IN THE NORTH ATLANTIC Compared to the Southern Ocean, individual races in the North Atlantic are less impactful (Figs. B.2 and B.3c), largely owing to the already denser observing network in place where the addition of a single measurement track does not cause large significant changes in the already robust reconstruction. Nevertheless, we still observe that sailboat pCO_2 measurements have a significant regional impact since *Seaexplorer* data covers a total of 7% of the North Atlantic area (when binned into 1×1° pixels), in comparison to only 3% of the Southern Ocean area.

The air-sea CO_2 fluxes significantly differed regionally peaking at 1.26 mol C m^{-2} yr^{-1} in the North Atlantic between 1982 and 2021 (Fig. B.3a), which is thus higher than the maximum flux difference of 0.77 mol C m^{-2} yr^{-1} in the Southern Ocean. However, the mean difference of 0.08 mol C m^{-2} yr^{-1} in the North Atlantic is substantially smaller than observed in the Southern Ocean (0.15 mol C m^{-2} yr^{-1}) (Supplementary Fig. B.2), considering the historic coverage of the SOOP program. In recent years however, we also find a reduction in North Atlantic measurements (`www.socat.info`; Bakker et al., 2016), thus even in the better observed North Atlantic the sailboat data might gain more importance.

TEMPORAL EVOLUTION Comparing the flux reconstructions E1 and E2 over time, we see the greatest impact of adding *Seaexplorer* data from 2018 to 2021 in the air-sea CO_2 flux estimates in the latter years of the time series (Fig. B.3). About 91% of the significant differences between E1 and E2 occurred between 2018 and 2021, which is when the sailboat pCO_2 observations were measured. The pCO_2 data collected by *Seaexplorer-Yacht Club de Monaco* affects the air-sea CO_2 flux estimate only up to ca. 5 years prior to the Antarctic circumnavigation race. This is not immediately obvious, since the applied method extrapolates information both in space and time. It learns from all available observations when clustering the ocean into biogeochemical provinces and estimating the missing pCO_2 values by using previously established relationships between already available pCO_2 and other environmental variables within each province. However, a similar observation, where differences become smaller as we look further back in time, has been made when BGC Argo data were added (Bushinsky et al., 2019a). This is explained by trend variables (i.e. atmospheric xCO_2) used in the method (Landschützer et al., 2013) limiting the potential of the method when extrapolating the missing pCO_2 values into the past (Bushinsky et al., 2019a). As a consequence, we expect that a longer time series is required to change the interannual to decadal air-sea CO_2 flux trends. Nevertheless, with upcoming races announced (round-the-globe racing events taking place every other year) and with the increasing willingness among skippers to contribute with observations, we see

a long term potential to increase pCO_2 data in remote ocean regions to overcome this limitation.

The addition of *Seaexplorer* data has the highest impact on austral summer, whereas it has little to no impact on austral wintertime fluxes (Fig. B.3b,c), mirroring the seasonal availability of data and illustrating the weak connectivity between seasons identified in our neural network. Therefore, sailboat measurements – unlike Saildrone campaigns (Sutton et al., 2021; Heimdal et al., 2024) – currently are unable to bridge the wintertime discrepancy between float-based and ship-based flux estimates (Bushinsky et al., 2019a). Even though sailboat pCO_2 data have limited added value during harsh winter conditions in the Southern Ocean where no sailboat racing events take place, we show that sailboats support the existing observing system of Argo floats (Bushinsky et al., 2019a; Gray et al., 2018; Johnson et al., 2017), Saildrones (Sutton et al., 2021; Meinig et al., 2019), moorings, drifting buoys, and wave gliders.

SENSITIVITY OF AIR-SEA CO_2 FLUX TO MEASUREMENT UNCERTAINTY

Finally, we also tested whether potential measurement uncertainties or even measurement bias have an effect on the air-sea CO_2 flux estimate. We considered a random measurement uncertainty of ±5 µatm (ensemble E3) and a constant measurement offset of 5 µatm (ensemble E4) (Fig. B.4) as the data set quality flag assigned by SOCAT is 5 µatm. Figure B.4a illustrates that a random measurement uncertainty of ±5 µatm does not affect the air-sea CO_2 flux at a basin-wide level in the North Atlantic and the Southern Ocean, as the mean difference (E1–E3) is near zero for both basins (Fig. B.4a). However, locally the air-sea CO_2 flux can be significantly impacted by up to 0.65 mol C m^{-2} yr^{-1} in the North Atlantic during individual months and up to 0.32 mol C m^{-2} yr^{-1} in the Southern Ocean (Fig. B.4a). This highlights the importance of accounting for measurement uncertainty when investigating high-frequency and small spatial scale fluxes which will become increasingly important as we move towards marine carbon accounting, marine carbon dioxide removal and national carbon stocktake efforts (United Nations Framework Convention on Climate Change, 2015; Lebling et al., 2022).

We also explore potential limitations of the system and imperfect calibration over long offshore racing events by testing a constant measurement offset of 5 µatm. This causes a global bias up to 0.06 Pg C yr^{-1} (E1–E4) in 2021 (Supplementary Table B.1). On the one hand this is only roughly 2.5% of the global annual uptake, showing the rather small sensitivity of the air-sea CO_2 flux, to biases in a single platform. However it is larger than the global flux change from adding *Seaexplorer* data of 0.04 Pg C yr^{-1} (Supplementary Table B.1). Thus, our comparison

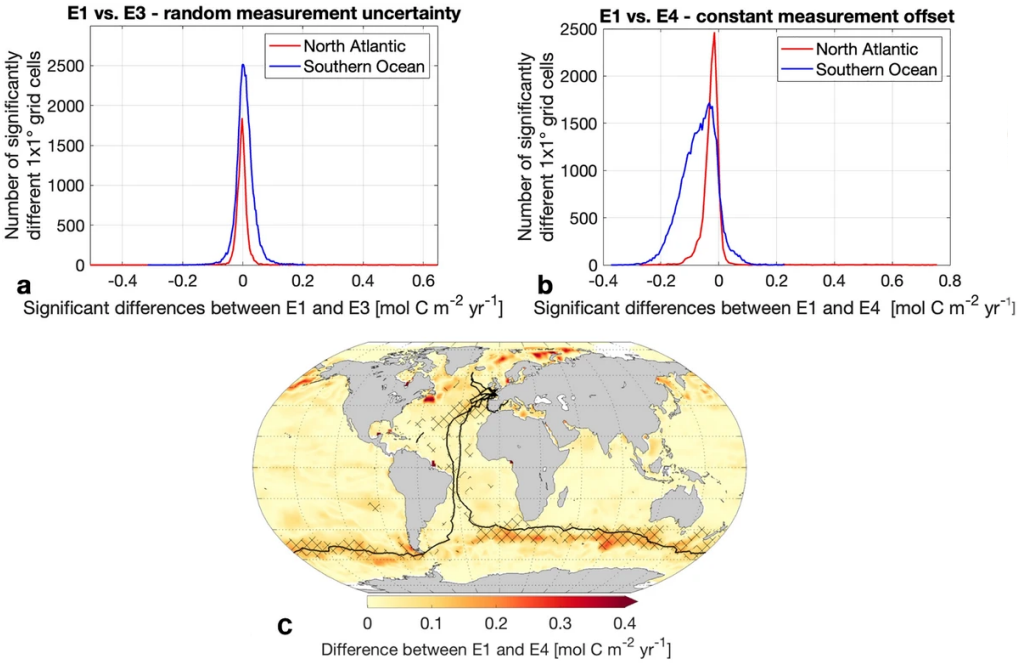

Figure B.4: Sensitivity of air-sea CO_2 flux to measurement uncertainty. (a,b) Histogram of significant differences between flux estimate E1 (based on SOCATv2022 with original *Seaexplorer* data) and E3 and E4 (based on SOCATv2022 with modified *Seaexplorer* data) in the Southern Ocean and the North Atlantic. (a) E3 modification = addition of random measurement uncertainty, (b) E4 modification = addition of constant measurement offset. (c) Map shows the absolute magnitude of differences between the original flux estimate E1 and the E4 flux estimate including a sailboat measurement offset averaged over Nov 2020–Jan 2021. Hatching indicates significance. Black lines represent sailboat tracks. Figures generated using a mapping package for MATLAB (Pawlowicz, 2020).

highlights that flux changes from measurements from 129 days at sea remain undetectable if the measurement system does not follow the highest standards, supporting the need for a CO_2 reference network (Wanninkhof et al., 2019). However, while important globally, the constant measurement biases are still smaller at basin scale. The mean absolute difference in the air-sea CO_2 flux attributed to the offset is 0.03 mol C m^{-2} yr^{-1} in the North Atlantic and only 0.07 mol C m^{-2} yr^{-1} in the Southern Ocean (Fig. B.4b), which is smaller than the mean differences caused by adding *Seaexplorer* data. Particularly in the North Atlantic, the flux estimate proves to be more robust towards a potential measurement offset than the Southern Ocean flux estimate. This robustness is again attributed to the already denser observations from different platforms. This however also indicates the need for cross-calibration of measurements in remote regions, as measurement biases have a larger impact there. Locally, the air-sea CO_2 flux densities (based on E1-E4) significantly differed up to 0.76 mol C m^{-2} yr^{-1} in the North Atlantic during individual months and up to 0.38 mol C m^{-2} yr^{-1} in the Southern

Ocean. The significant differences occur in proximity to the sailboat tracks and peak between 40°S and 60°S (Fig. B.4c). Equipping more sailboats with a pCO_2 measurement device during the round-the-world races would help to reduce the impact of potential measurement uncertainties and increase the accuracy of our flux estimate. Considering that many studies thus far do not include or assess the impact of measurement uncertainty in their pCO_2 observations (Landschützer et al., 2016; Rödenbeck et al., 2015), we hereby show the importance of measurement uncertainty analyses at a regional scale to provide a more accurate estimate of high-frequency fluxes.

B.3 DISCUSSION

We quantify the impact of underway pCO_2 data from sailboats on the air-sea CO_2 exchange by comparing the air-sea CO_2 flux estimates based on pCO_2 measurements of the SOCAT database – with and without the *Seaexplorer* data. We show that measuring pCO_2 underway, and in particular during round-the-world sailing events, improved air-sea CO_2 flux reconstruction at regional scales, particularly in under-sampled regions like the Southern Ocean. However, we find that also in the more densely observed North Atlantic, significant flux density changes occur locally. The flux reconstructions differ the most between 40°S and 60°S, particularly within 200 km of the Subantarctic Front during austral summertime, where the largest disagreement in air-sea CO_2 flux reconstructions exist (DeVries et al., 2019; Ritter et al., 2017). While the addition of *Seaexplorer* data regionally increases the estimated carbon sink in the North Atlantic, it reduces the carbon sink in the Southern Ocean similar to previous studies (Bushinsky et al., 2019a). Even though sailboat data cannot help to close the winter discrepancy between float-based and ship-based flux estimates (Bushinsky et al., 2019a), due to the seasonal sampling bias, it supports the existing observational platforms (`www.socat.info`). Utilizing this data, particularly in combination with various other platforms, particularly from Argo floats and Saildrones in the Southern Ocean (Djeutchouang et al., 2022), can reduce air-sea CO_2 flux uncertainties. While the zonal summertime sampling alone may not suffice to address seasonal biases, and substantial improvement in the Southern Ocean flux reconstructions is better achieved through year-round meridional sampling (Djeutchouang et al., 2022), sailboats still contribute to an improved reconstruction of the air-sea CO_2 fluxes in the Southern Ocean.

Rare underway pCO_2 observations collected close to the frontal zones changed the air-sea CO_2 flux estimate the most and can help to better understand these

regions and their role in carbon uptake and the longer-term variation of the air-sea CO_2 exchange. Compared to the Southern Ocean, races in the North Atlantic were less impactful due to the historical stronger observing network there. However, since the majority of races took place there, we still see sailboat pCO_2 observations having a significant impact on regional air-sea CO_2 flux densities. Thus, our analysis suggests that a declining number of observations in the North Atlantic as we currently see (www.socat.info), may lead to a significant impact on the global ocean carbon flux estimates (Canadell et al., 2021).

Added random measurement uncertainty (±5 µatm) has a low impact on the overall air-sea CO_2 flux estimate due to compensating errors. However, we illustrate the importance of including measurement uncertainty locally when investigating high-resolution fluxes. On the contrary, a potential measurement bias of 5 µatm results in a global flux bias larger than the detectable change due to 129 days of sailboat measurements. Although a measurement uncertainty of 5 µatm marks the lower end of achievable uncertainty ranges (Arruda et al., 2019; Olivier et al., 2022), we show that even with this lower-end uncertainty fails to reveal any detectable impact when adding 129 days of *Seaexplorer* data. The impact of the measurement bias was more pronounced in the data-sparse Southern Ocean flux estimate, whereas the North Atlantic flux estimate proved to be more robust towards a measurement offset as a result of the denser existing measurement network (Bakker et al., 2016). Thus, our findings indicate that the quantity of the data has a greater influence on accuracy than the data quality in densely observed ocean areas.

We show the importance of cross-calibration and having a fleet simultaneously measuring pCO_2 while closely sailing together. In this study, we detect any changes in the air-sea CO_2 flux and attribute them to the integration of sailboat pCO_2 observations. Although we show the difference induced by the *Seaexplorer* data, a conclusive answer to if, and to how much, the *Seaexplorer* data reduce the overall present-day uncertainty in the air-sea CO_2 flux is still not provided. This should be explored in future studies. Considering the recurrence of sailboat races, they have the potential to improve reconstructive air-sea CO_2 flux estimates on longer timescales in the future.

B.4 MATERIALS AND METHODS

SURFACE-OCEAN CARBON DIOXIDE DATA Two sea surface carbon dioxide datasets were used in this study: (1) pCO_2 measurements from underway

shipboard and mooring data contained in the 1×1 degree gridded Surface Ocean CO_2 Atlas SOCATv2022 from 1982 to 2021 (Bakker et al., 2016) and (2) underway pCO_2 measurements from the sailboat "*Seaexplorer-Yacht Club de Monaco*" (until 2019 "Malizia") during offshore sailing and training events from 2018 to 2021. The former dataset includes the latter data as well, hence we artificially create a third dataset, where we exclude the *Seaexplorer* measurements from the SOCAT gridded dataset.

To quantify the changes in air-sea CO_2 fluxes based on the addition of *Seaexplorer* data, we used these 2 datasets as starting points, i.e. (1) SOCATv2022 including *Seaexplorer* data (E1), and (2) SOCATv2022 excluding *Seaexplorer* data (E2). To assess the impact of a potential measurement accuracy of ±5 µatm we created two more datasets by (3) adding a random uncertainty of ±5 µatm to the *Seaexplorer* data (E3) (similar to differences observed during measurement campaigns (Arruda et al., 2019; Olivier et al., 2022) where multiple pCO_2 systems were compared to the membrane system used on sailboats) and by (4) adding a constant measurement offset of 5 µatm to the *Seaexplorer* data (E4), which is in theory possible but less likely considering the prescribed daily two-point calibration. The 5 µatm are based on the expected accuracy of flag C data in SOCAT, however, larger differences with the same systems have also been observed in field studies (Arruda et al., 2019; Olivier et al., 2022). The system used here is configured with pressure measurements in the gas phase of the equilibration and makes daily zero and span gas calibrations. For a more detailed description of the measurements and the instrument setup and justification of the 5 µatm offset, we refer to Landschützer et al., 2023.

PCO$_2$ MAPPING AND AIR-SEA CO$_2$ FLUX CALCULATION Mapped estimates of the sea surface pCO_2 were created by applying the SOM-FFN method to all four datasets. Here we provide a brief overview of the method, whereas a more detailed description including evaluation can be found in (Landschützer et al., 2013; Landschützer et al., 2014).

In the first step, a self-organizing map (SOM) clusters the ocean into 16 biogeochemical provinces based on common patterns in predictor variables. We used sea-surface temperature (SST) data (Reynolds et al., 2007) (https://psl.noaa.gov/data/gridded/data.noaa.oisst.v2.html), sea-surface salinity (SSS) data (Good et al., 2013) (https://www.metoffice.gov.uk/hadobs/en4/ - Analyses with Gouretski and Reseghetti (2010) bias corrections applied), a mixed layer depth (MLD) climatology (Boyer Montégut et al., 2004) (https://cerweb.ifremer.fr/deboyer/mld/Surface_Mixed_Layer_Depth.php),

and a pCO_2 climatology (Takahashi et al., 2009) (https://www.ncei.noaa.gov/access/ocean-carbon-acidification-data-system/oceans/LDEO_Underway_Database/sumflux_2006c.txt) as predictors. In the second step, a feed-forward neural network (FFN) establishes non-linear relationships between the predictors and pCO_2 observations within each province separately. It uses these relationships to reconstruct the missing pCO_2 values within each province. The predictors for the FFN were SST, SSS, the MLD climatology as well as chlorophyll-a (http://www.globcolour.info); parameter CHL1 with the GSM L3 merging method), and the atmospheric CO_2 concentration (Dlugokencky et al., 2021) (https://gml.noaa.gov/ccgg/mbl/data.php). Prior to 1997, we used a monthly climatology from 1998 to 2002 for chlorophyll-a, given that chlorophyll-a became available only after the launch of satellites in 1997. The data for the FFN are divided into a training dataset to train on and a validation dataset used for validation within the method (Landschützer et al., 2013).

From the four reconstructed pCO_2 maps described above we estimate the air-sea CO_2 flux based on a bulk gas transfer formulation with a quadratic relationship between windspeed and transfer velocity (Landschützer et al., 2013; Wanninkhof, 1992) where we scale the mean gas transfer to a global average rate of 16.5 cm hr^{-1} (Naegler, 2009). We use wind data (Hersbach et al., 2023), monthly mean sea level pressure data (Kalnay et al., 1996) as well as sea ice concentration data (Titchner and Rayner, 2014) for the air-sea CO_2 flux calculation. We calculate the difference between the flux estimate based on SOCAT with and without *Sea-explorer* data (E1 vs. E2) to quantify the impact on the air-sea CO_2 flux. We further calculate the difference between the flux estimate based on *Seaexplorer* data with and without added measurement uncertainties (E1 vs. E3 and E4) to assess the impact of the expected measurement accuracy on the air-sea CO_2 flux.

SIGNAL-TO-NOISE-DETECTION To detect statistically significant differences and reduce the impact of random errors arising from methodological choices, we use a Monte Carlo approach to reconstruct and calculate each of the air-sea CO_2 flux estimates (i.e. with *Seaexplorer* data, without *Seaexplorer* data, random error and constant offset—see above) 40 times with a varying split between the training and validation dataset to create for ensembles, i.e. ensemble E1 = *Seaexplorer* data, E2 = *Seaexplorer* data excluded, E3 = random measurement uncertainty, and E4 = fixed measurement bias. We gradually increased the number of runs and based on trial and error we found that the absolute difference between the two means of the ensembles between runs is nearly constant for 40 runs (Supplementary Fig. B.3). To ensure the statistical significance of our results, we conducted a two-sample t-test and adjusted the resulting p-values in order to

control the False Discovery Rate, i.e. the expected proportion of false discoveries among all significant results, to 5% (Storey, 2002). The signal corresponds to adjusted p-values below 5%, indicating significance, while non-significant differences represent noise (Supplementary Fig. B.4). The noise level is highest at the beginning of the time series as SOCAT contains few observations before 1990 (Bakker et al., 2016), whereas the signal increases after 2016 as new *Seaexplorer* data made a difference (Supplementary Fig. B.4).

REGIONAL FOCUS Finally, we set our focus on two main regions of interest, i.e. the North Atlantic, where most sailboat races took place, and on the Southern Ocean, where the longest race, the Antarctic circumnavigation race, took place. Furthermore, Rustogi et al., 2023 has highlighted significant uncertainties in the air-sea CO_2 flux in both regions. We focused on three zonal bands in the Southern Ocean: the Polar Front, the Subantarctic Front, and the Northern Boundary (Park et al., 2019) including the respective areas within a 2-degree (or roughly 200 km) radius. We utilized the zonal bands enclosing the fronts as geographical reference points only to delineate zones in the Southern Ocean and to attribute differences caused by the addition of *Seaexplorer* data to these zones. Note that overlap between the frontal regions occurs. In the North Atlantic, we define the region as the area between 70°N, 0°, 85°W, and 20°E. The extent of the Southern Ocean is defined by south of 35°S. To determine the data availability per region, we calculate the percentage of $1\times1^\circ$ pixels that were filled with *Seaexplorer* data at least once, regardless of the monthly availability.

B.5 DATA AVAILABILITY

All data used and discussed in this article are freely available via `www.socat.info`. The datasets generated and/or analysed during the current study are available in the Zenodo repository, `https://doi.org/10.5281/zenodo.10036578`.

B.6 ACKNOWLEDGEMENTS

We would like to thank Team Malizia and in particular skipper Boris Herrmann for their engagement in collecting valuable data. The Surface Ocean CO_2 Atlas (SOCAT) is an international effort, endorsed by the International Ocean Carbon Coordination Project (IOCCP), the Surface Ocean Lower Atmosphere Study (SOLAS) and the Integrated Marine Biosphere Research (IMBeR) program, to deliver a uniformly quality-controlled surface ocean CO_2 database. The many researchers and funding agencies responsible for the collection of data and quality control are

thanked for their contributions to SOCAT. The VLIZ ICOS work is supported by Research Foundation Flanders (FWO) contract I001821N. VLIZ ICOS data and metadata are available on the ICOS Carbon Portal (https://www.icos-cp.eu/). TT acknowledges German federal and state funding for developing the innovation platform Shaping an Ocean of Possibilities, SOOP. JB gratefully acknowledges funding from the International Max Planck Research School on Earth System Modelling (IMPRS-ESM).

B.7 SUPPLEMENTARY INFORMATION

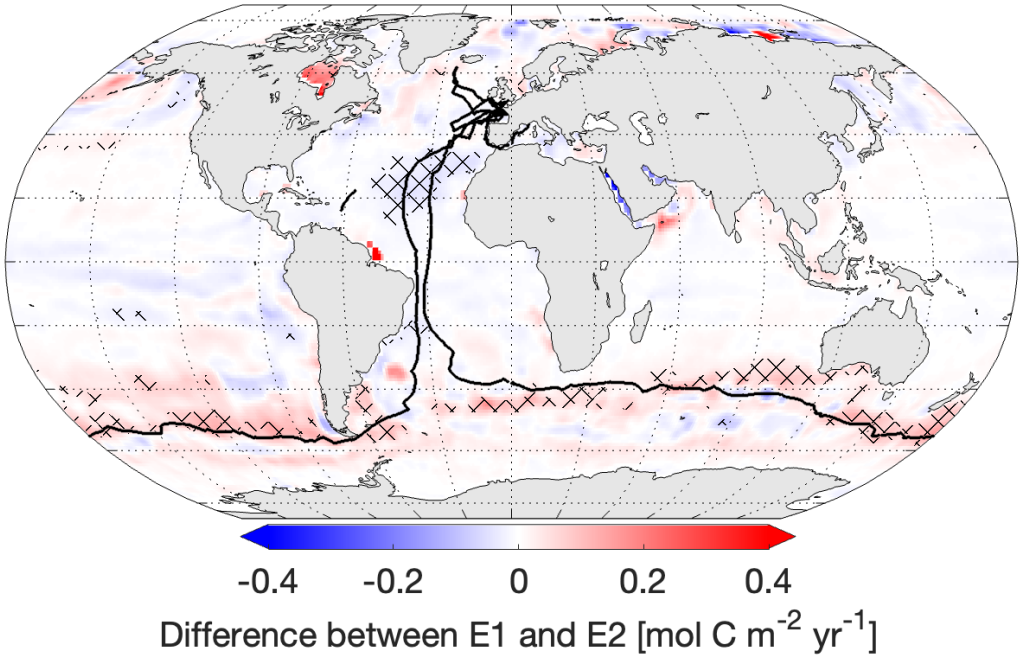

Figure B.1: Difference between the air-sea CO_2 fluxes in ensemble E1 (based on SOCATv2022 including *Seaexplorer* data) and in ensemble E2 (based on SOCATv2022 excluding *Seaexplorer* data) averaged over 2018 - 2021. Hatching indicates significant differences. Blue indicates increased carbon uptake due to the addition of *Seaexplorer* data, red indicates reduced carbon uptake due to the addition of *Seaexplorer* data. Black lines represent sailboat tracks from 2018 - 2021. Figure generated using a mapping package for MATLAB (Pawlowicz, 2020).

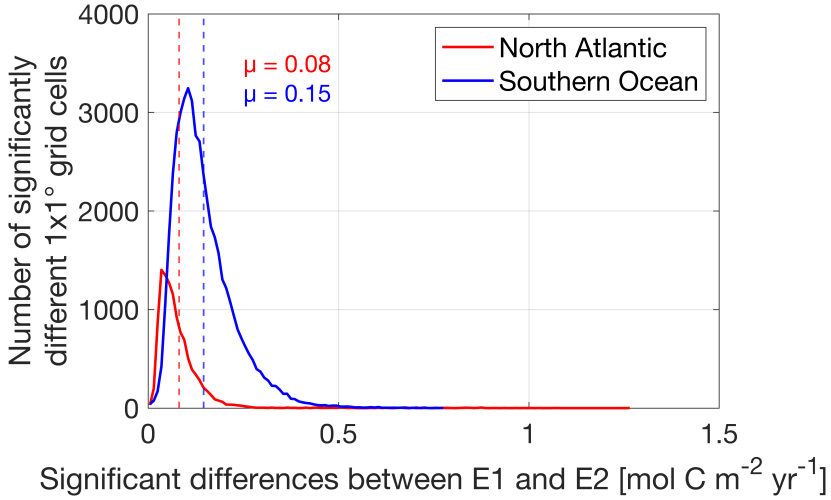

Figure B.2: Histogram of the absolute magnitude of significant differences between the air-sea CO_2 flux E1 (based on SOCATv2022 including *Seaexplorer* data) and the air-sea CO_2 flux E2 (based on SOCATv2022 excluding *Seaexplorer* data) in the Southern Ocean and the North Atlantic.

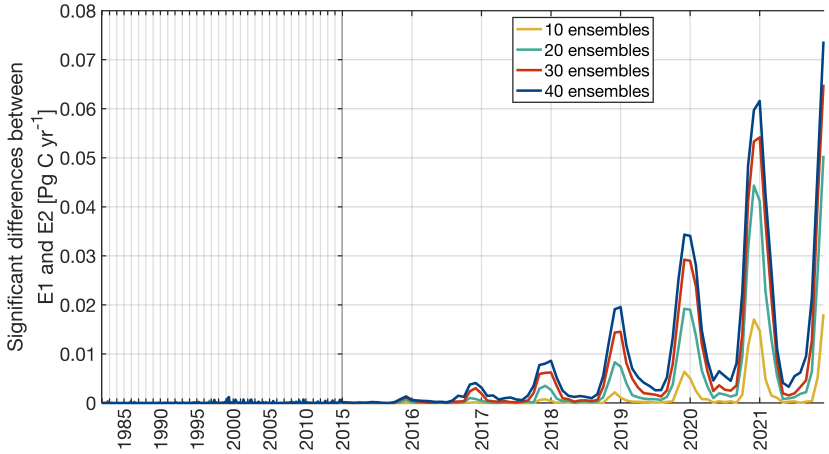

Figure B.3: Time series of the magnitude of significant differences between the air-sea CO_2 fluxes E1 and E2 (including and excluding sailboat pCO_2 data) based on the ensemble size of flux reconstructions. Changes in the magnitude of significant differences decrease with an increasing number of flux reconstructions as the random uncertainty is less well constrained.

Table B.1: Integrated flux bias in Pg C yr^{-1} in 2021.

	Due to missing *Seaexplorer* data (comparison E1 and E2)	Due to random measurement uncertainty (comparison E1 and E3)	Due to fixed measurement bias (comparison E1 and E4)
Global	0.04	0.01	- 0.06
North Atlantic	0.00	0.00	- 0.01
Southern Ocean	0.05	0.02	- 0.03

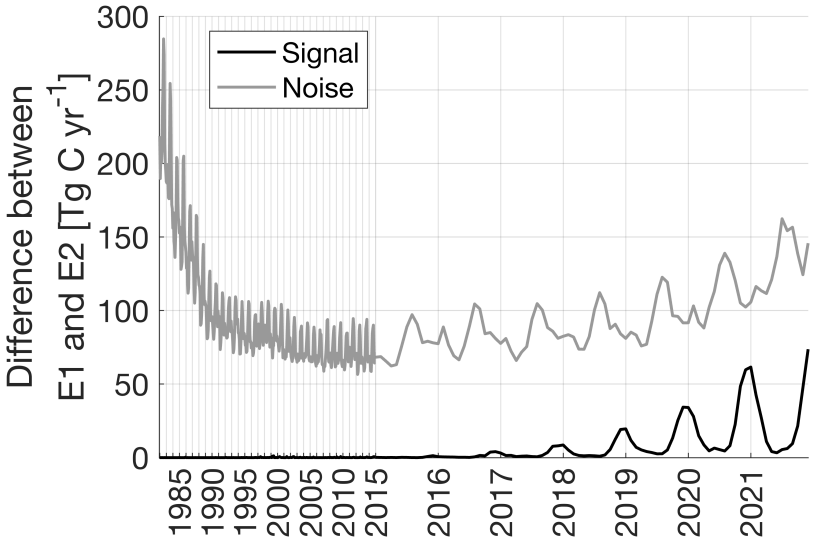

Figure B.4: Temporal development of signal and noise.

Appendix C

IMPROVED AIR-SEA CO_2 FLUX ESTIMATES FROM SAILBOAT MEASUREMENTS

Behncke, J.,Ilyina, T., Chegini, F. & Landschützer, P. Improved air-sea CO_2 flux estimates from sailboat measurements. *under review at Science Advances.*

Improved air-sea CO_2 flux estimates from sailboat measurements.

Jacqueline Behncke[1,2], Tatiana Ilyina[3,4,1], Fatemeh Chegini[4] & Peter Landschützer[6,1]

[1] *Max Planck Institute for Meteorology, Bundesstrasse 53, 20146, Hamburg, Germany*
[2] *International Max Planck Research School for Earth System Modelling, Bundesstrasse 53, 20146, Hamburg, Germany*
[4] *Universität Hamburg, Bundesstrasse 55, 20146 Hamburg, Germany*
[5] *Helmholtz-Zentrum Hereon, Max-Planck-Straße 1, 21502 Geesthacht, Germany*
[6] *Flanders Marine Institute (VLIZ), Jacobsenstraat 1, 8400, Ostend, Belgium*

ABSTRACT

Despite their significance in the climate system, remote ocean regions and their ability to absorb anthropogenic carbon dioxide remain highly uncertain. To address this issue, citizen science initiatives, including sailboats, expand the observational network. Using observing system simulations and novel sailboat tracks, we demonstrate how integrating sailboat data improves estimates of ocean carbon uptake. While we underestimate the ocean carbon sink when mimicking real-world sampling, adding available sailboat data does not substantially improve reconstructions. However, increased sampling reveals a stronger carbon sink, particularly between 40°S and 60°S. The improvement persists with hypothetical measurement uncertainties, but substantial differences arise depending on whether positive or negative biases are applied to the race track data. While we show that two additional circumnavigations already improve the ocean mean sink estimate, we further highlight that the additional data remain insufficient to correct the overestimated CO_2 sink trend, calling for continuation of the ongoing data collection.

C.1 INTRODUCTION

The ocean plays a critical role in regulating Earth's climate by acting as a substantial carbon sink that annually absorbs over a quarter of anthropogenically emitted carbon dioxide (CO_2) from the atmosphere (Friedlingstein et al., 2025; Gruber et al., 2023). However, climate change alters the carbon uptake capacity of the ocean (Le Quéré et al., 2007; Gruber et al., 2023; Friedlingstein et al., 2025), making the monitoring of the sea surface partial pressure of CO_2 (pCO_2) or the fugacity of CO_2 (fCO_2) indispensable in order to assess the impacts of climate change. Despite this need, a declining trend in observations in recent years

and an imbalance in sampling efforts across the hemispheres persist (Bakker et al., 2016; Dong et al., 2024b). While the Ship Of Opportunity (SOOP) program has successfully contributed to systematic sampling in the Northern Hemisphere (Jiang et al., 2019), the Southern Ocean remains more irregularly sampled (Pfeil et al., 2013; Sabine et al., 2013; Bakker et al., 2016; Dong et al., 2024b), leading to biases in the reconstruction of the air-sea CO_2 flux (Gloege et al., 2021; Hauck et al., 2023; Jersild and Landschützer, 2024; Ford et al., 2024). Specifically, insufficient sampling leads to a 31% overestimation of the Southern Ocean decadal variability (Gloege et al., 2021) and a strong overestimation of decadal trends (Hauck et al., 2023). Considering the key role of remote ocean basins such as the Southern Ocean in ocean carbon and heat uptake (Frölicher et al., 2015; Landschützer et al., 2016; Williams et al., 2024), and the moderate success of gap-filling methods in further improving fCO_2 estimates (Gregor et al., 2019; Gloege et al., 2021; Hauck et al., 2023), new observational efforts have been undertaken to expand the observational network.

Sailboat races are emerging as a novel means to address observational gaps by providing a unique source of oceanographic data, particularly in remote ocean regions, as part of citizen science efforts (Landschützer et al., 2023; Behncke et al., 2024). Despite their predominant occurrence in the North Atlantic, regular repeating circumnavigation races (*Vendée Globe* – every 4 years, *The Ocean Race* – every 3–4 years) also provide valuable data in the Southern Ocean – both regions prone to uncertainty in the air-sea CO_2 flux (Rustogi et al., 2023; Pérez et al., 2024) and drivers on multiple timescales (Ostle et al., 2022). Hence, sailboats complement the observational network consisting so far of research ships, voluntary observing ships, drifting and moored buoys (e.g. Yang et al., 2024), gliders (e.g. Daniel et al., 2011; Chavez et al., 2018; Monteiro et al., 2015; Nicholson et al., 2022), biogeochemical floats (e.g. Williams et al., 2017; Gray et al., 2018; Bushinsky et al., 2019a) and Saildrones (Sutton et al., 2021; Heimdal et al., 2024; Nickford et al., 2024) and have been shown to significantly impact the air-sea CO_2 flux estimate, particularly between 40°S and 60°S during austral summer (Behncke et al., 2024). Previous research has shown that even when considering potential measurement uncertainties within the range of ±5 µatm the impact of new Southern Ocean measurements on the air-sea CO_2 flux is still detectable, unlike when considering a systematic measurement bias (Behncke et al., 2024). What we still lack, however, is information on whether sailboat measurements actually improve the air-sea CO_2 flux estimates which has yet to be quantified. Here, we address this challenge.

Recent *Observing System Simulation Experiments* investigate the impact of differ-

ent sampling strategies on carbon fluxes by using a model testbed as a benchmark to quantify the improvement (Bushinsky et al., 2019a; Denvil-Sommer et al., 2021; Djeutchouang et al., 2022; Hauck et al., 2023; Heimdal et al., 2024; Henson et al., 2024; Yun et al., 2024). These investigations typically involve subsampling a fCO_2 model testbed based on synthetic sampling schemes and reconstructing the air-sea CO_2 flux with neural network gap-filling methods (e.g. Landschützer et al., 2013) to compare against the model truth. However, previous studies often focus on optimal, yet not operational sampling scenarios rather than feasible real-world sampling schemes such as our repeating circumnavigations. Thus, although studies show promising improvements linked to optimized sampling (Hauck et al., 2023; Wei et al., 2020), the implementation is often not feasible. The frequency of sailboat races allows us to quantify the extent to which realistic sampling by sailboats, particularly in the Southern Ocean, improves the estimate of the air-sea CO_2 flux, providing a path forward in improved monitoring of the Southern Ocean CO_2 uptake.

Here, we conduct an observation system simulation by subsampling the global ocean biogeochemical model HAMOCC coupled to the ocean general circulation model MPIOM that contributes to the Global Carbon Budget (Ilyina et al., 2013; Paulsen et al., 2017; Mauritsen et al., 2019; Friedlingstein et al., 2025) mimicking the present-day observations (`www.socat.info`; Bakker et al., 2016) of the sea surface fugacity of CO_2 (fCO_2) and apply the 2-step neural network method SOM-FFN (self-organizing map – feed-forward neural network) (Landschützer et al., 2013; Landschützer et al., 2020) to reconstruct different air-sea CO_2 flux estimates. We quantify the improvement from our existing 161 days of sailboat data from several sailboats on the air-sea CO_2 flux estimate as well as the potential effect of more data by subsampling data from previous years using realistic sailboat tracks (Fig. C.1). Our analysis further explores the effect of potential random measurement uncertainties and systematic biases associated with the sailboat data. We investigate whether reconstructions continue to improve when additional, albeit biased, data is added, to assess whether the increase in quantity compensates for the lack of quality. Here we show that continuous and long-term observing improves the mean air-sea CO_2 flux estimate; however, our analysis reveals that the reconstructed trend from the neural network method remains overestimated even after adding 3 circumnavigation races, highlighting the need for multi-decadal observing strategies.

C.2 RESULTS

In this study, we show how incorporating different synthetic sailboat data improves the reconstructions of a known-truth model field in an observing system simulation experiment. We take the full hindcast model fCO_2 field from MPIOM HAMOCC and subsample it at times and locations where (based on a 1x1 degree grid location) historical and synthetic observations exist. Fig. C.1 presents the different pseudo-observation tracks used in this study to subsample the model field. Using the SOM-FFN method, i.e. a two-step neural network method (see Landschützer et al., 2013 for details), we then gap-fill these subsampled data to reconstruct the complete model fCO_2 field. Fig. C.1a presents the reconstructed global fCO_2 based on subsampled model data mimicking the real-world observations from SOCAT ("existing sailboat"). After deriving the air-sea CO_2 flux estimates from the subsampled and gap-filled fCO_2 field, our analysis proceeds in three steps: (1) assessing the neural network's performance with present-day sampling against the model truth; (2) quantifying improvements in air-sea CO_2 flux estimates from adding different sailboat data tracks; and (3) assessing the impact of measurement uncertainties and biases.

C.2.1 *Performance of Neural-Network Reconstruction*

We evaluated the neural network method's performance in reconstructing fCO_2 (based on available present-day observation tracks from SOCATv2022 "existing sailboat") by comparing the fCO_2 model truth with the "existing sailboat" fCO_2 estimate. By comparing fCO_2 data distributions, we observe a relatively strong agreement (Supplementary Fig. C.6). The neural network successfully reconstructed fCO_2 values close to the model truth, with the exception of the polar north (Supplementary Fig. C.6), i.e. a region that has been identified as erroneous in previous studies (Ilyina et al., 2013; Landschützer et al., 2020) and is thus not further considered here (see Methods). Probability density functions for the original model fCO_2 and the model-subsampled neural-network-reconstructed fCO_2 show dissimilarities with Bhattacharyya distances ranging from 0.00 to 0.14. The Bhattacharyya distance (BD) (Bhattacharyya, 1943) measures the similarity between two probability distributions, with lower values indicating greater similarity. In this context, the distances ranging from 0.00 to 0.14 suggest a high degree of similarity between the distribution of the model fCO_2 and reconstructed fCO_2. The fCO_2 distributions in the tropics show the highest agreement with relatively low Bhattacharyya distances, suggesting a robust representation of the observed patterns, and almost identical means (0.23–1.11 µatm difference) between model

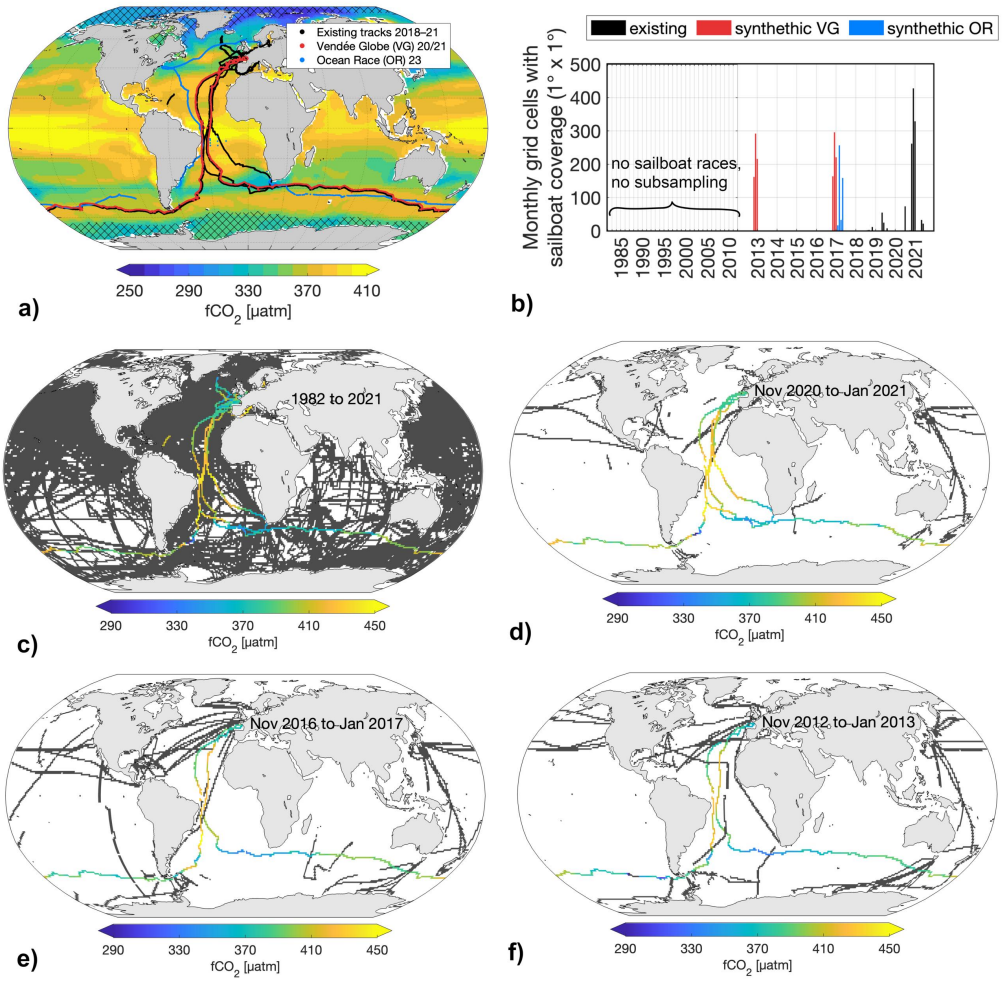

Figure C.1: **Sailboat Sampling Schemes**. **a)** Reconstructed fCO_2 based on SOCAT-sampling. The lines represent different sailboat tracks, which are used alongside the rest of SOCATv2022 tracks in the subsampling process. *(Note: The Vendée Globe track (red) was plotted with a small offset from its original position to avoid overlap with the "existing sailboat" tracks, even though Vendée Globe 2020/21 is included in "existing sailboat" tracks). Hatched areas are regions with a climatological maximum sea-ice concentration greater than 50% and are excluded.* **b)** Sailboat data availability per month. Sampling scheme A "existing sailboat" = black data. Sampling scheme C "3 circumnav." = black + red data. Sampling scheme D "2 diff. circumnav." = black + blue. Sampling scheme B "without sailboat" excludes all colored sailboat track data. **c–f)** Tracks used to subsample the model during different time periods for the "3 circumnavigations" run. *Gray lines indicate SOCAT tracks; colored lines represent subsampled sailboat fCO_2 tracks.*

and reconstruction followed by the fCO_2 distributions in the middle latitudes (Supplementary Fig. C.6). In the Southern polar region, dissimilarities are more pronounced, featuring BD between 0.04 and 0.05 and higher offsets between mean fCO_2 values ranging from 0.92 to 3.78 µatm (Supplementary Fig. C.6).

Both over- and underestimation of fCO_2 occur along the coastal ocean (Fig. C.2), a region that is highly variable (Roobaert et al., 2019; Roobaert et al., 2024). We find that the neural network in combination with the present-day sampling overestimates fCO_2 in the under-sampled Southern Ocean by around 2–3 µatm (Fig. C.2b and Supplementary Fig. C.7). A similar overestimation of fCO_2 was found by Heimdal et al., 2024 using a different reconstruction method and a large ensemble test bed of Earth System Models. In contrast, while similar in magnitude to our results, the sign of the mismatch is opposite to a study conducted by Hauck et al., 2023 using a different single hindcast model, illustrating the limitations of such an analysis to a single model. However, here we are interested in potential improvements in space and time from adding measurement compared to the baseline. Additionally, we do not test the effect of different gas transfer schemes, as our study solely focuses on the improvement in the fCO_2 from increased sailboat sampling. We find that additional sailboat data from "3 circumnavigations" already reduces the fCO_2 in the Southern Ocean, hence improving the reconstruction (Supplementary Fig. C.8).

Behncke et al., 2024 quantified the detectable change caused by the addition of existing sailboat data based on real-world observations. To validate this and determine the similarities between observation and model data, we applied the same method to our subsampled model data and compared both (Supplementary Fig. C.9). The neural network demonstrated consistent but smaller signal detection in subsampled model data, mirroring observations closely, thus underscoring the method's realistic performance on both model and observation data (Supplementary Fig. C.9).
The effect of the sailboat sampling scheme on the model reconstruction is more subtle, complicating detection as the relationships between driver variables and fCO_2 are more consistent in the model setup, compared to the real world. Measured fCO_2 is subject to variability and uncertainties, such as measurement uncertainties and temporal averaging when producing gridded fields; fCO_2 measurements taken at one point in time are averaged per month, reducing accuracy. Additionally, the effect in observations may be more pronounced because effects of hypothetical biogeochemical and physical processes and their variability that could be missing or unresolved in models might be captured in the real world (Ilyina et al., 2013; Hauck et al., 2020; DeVries et al., 2023; Mayot et al., 2023).

C.2.2 *Effect of Sailboat Sampling on fCO_2 Estimates*

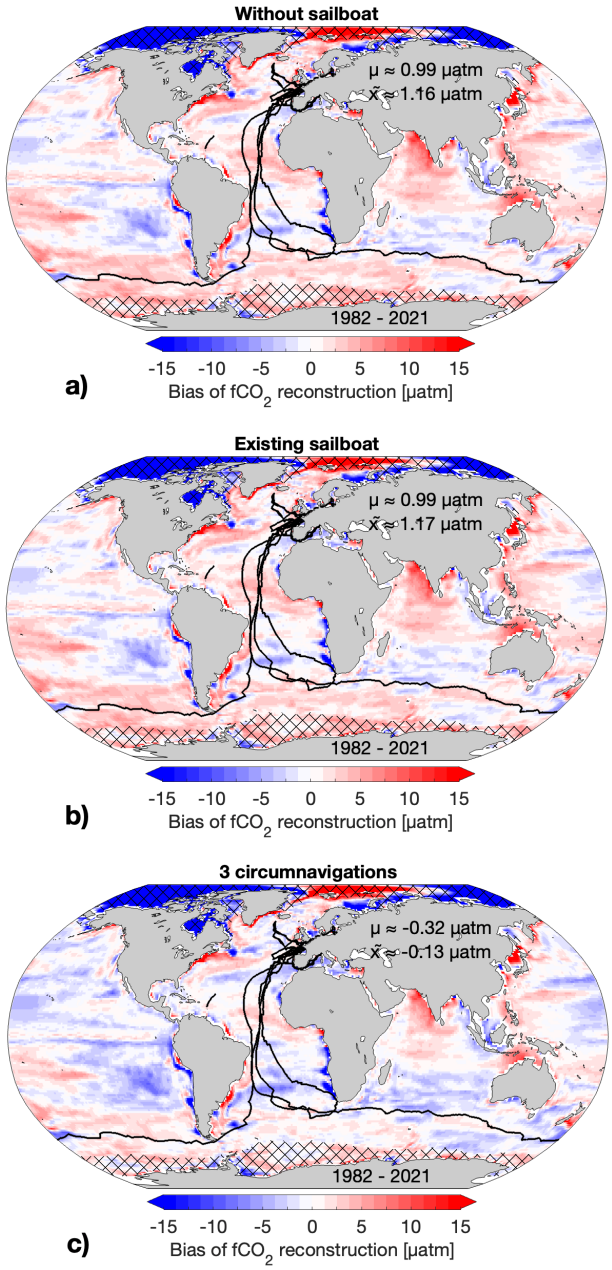

Figure C.2: **Spatial fCO_2 Bias and Improvement Patterns Resulting from the Integration of Different Sampling Schemes. a–c)** Mean bias of subsampled and reconstructed fCO_2 averaged over 1982 until 2021 based on data subsampled after SOCAT **a)** "without sailboat" track data (B) **b)** including "existing sailboat" tracks (A) **c)** including existing sailboat tracks and 2 additional circumnavigations (C or "3 circumnav."). *Black lines represent sailboat tracks. Hatched areas are regions with a climatological maximum sea-ice concentration greater than 50% and are excluded. μ represents the mean, while $\tilde{x}$ represents the median.*

Adding data from the existing sailboat tracks does not substantially reduce the fCO_2 bias when averaged over the full time period 1982-2021, probably due to their small number and their late addition to the SOCAT database (Figs. C.2a,b). The global mean fCO_2 is overestimated by 0.99 µatm regardless of the inclusion of sailboat data, and particularly in the Southern Ocean by around 3 µatm (Figs. C.2a,b and Supplementary Fig. C.7). Similarly, the median bias is 1.17 µatm with sailboat data and 1.16 µatm without it. The spatial bias pattern stays nearly identical (Fig. C.2a). In contrast, adding sailboat fCO_2 data from "3 circumnavigation" tracks substantially reduces biases mainly in the North Atlantic and in the Southern Ocean, mirroring the data addition in these regions (Figs. C.2a-c). The fCO_2 estimate improves with the addition of "3 circumnavigations" particularly between 40°S – 60 °S (Fig. C.2 and Supplementary Fig. C.7) similar to findings in Behncke et al., 2024. Due to the neural network's capacity to extrapolate over time and space, fCO_2 estimates in other regions e.g. in the Indian Ocean and West Pacific, where we do not have new data, improve as well (Figs. C.2b-c). However, we also observe compensating effects, indicating a trade-off in other regions, e.g. the South Pacific (Figs. C.2b-c). While the neural network learns new features and minimizes errors, it also adopts inaccurate representations of processes due to overfitting tendencies, resulting in increased biases in e.g. parts of the East Pacific, where the fCO_2 is underestimated. Globally, however, the median bias decreases to near zero, when adding data from "3 circumnavigation" tracks (Fig. C.2).

C.2.3 *Effect of Sailboat Sampling on Air-Sea CO_2 Flux Estimates*

Using these fCO_2 reconstructions and model wind data, we compute the air–sea CO_2 flux estimates by applying a bulk gas transfer formulation (Wanninkhof, 1992; Landschützer et al., 2013, Supplementary Fig. C.10). Fig. C.3 shows the latitudinal air-sea CO_2 flux estimates and the best guess closest to the model truth with the direction of improvement. Mirroring the spatial improvement pattern seen in the fCO_2 estimate (Fig. C.2), the air-sea CO_2 flux estimate improves the most with the addition of "3 circumnavigations", particularly between 40°S – 60 °S (Fig. C.3), similar to findings in Behncke et al., 2024. This results in a more negative air–sea CO_2 flux, indicating an enhanced global ocean carbon sink (Fig. C.3). In contrast, we observe no improvement of the reconstruction between 20°S – 40°S (Fig. C.3), where the model truth sink is weaker than estimated with more sailboat data.

In addition to spatial patterns, we evaluate the influence of added sailboat data

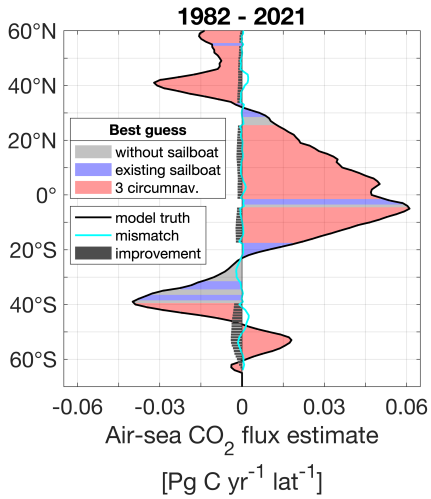

Figure C.3: **Latitudinal Air-Sea CO_2 Flux Estimates for the Period From 1982 to 2021**. The black line represents the model truth. The area under the black curve is shaded to depict the "best guess" estimate closest to the model truth, with the color corresponding to one of three scenarios: A ("existing sailboat"), B ("without sailboat"), or C ("3 circumnav."). The cyan line highlights the persistent mismatch between the "best guess" estimate and the model truth. Gray bars illustrate the improvement in estimates from scenario B ("without sailboat") to the "best guess." *For example, bars pointing in the negative direction indicate that the "best guess" reduced the estimate by that amount. A cyan line pointing to the left indicates that the estimate is still too negative, while a line pointing to the right indicates that the estimate is still too positive.*

on the temporal trajectory of the air–sea CO_2 flux (Fig. C.4). Similar to the estimated fCO_2, the air-sea CO_2 flux does not show substantial improvement with the addition of existing sailboat tracks (see proximity of gray and blue lines in Figs. C.4a-e). However, the global mean air-sea CO_2 flux density bias slightly decreases from 0.06 to -0.02 mol C m^{-2} yr^{-1}, and in the Southern Ocean, it improved from 0.10 to 0.00 mol C m^{-2} yr^{-1} when data from two additional circumnavigation tracks ("3 circumnavigations") were included (Figs. C.4d-e). Without this data, we observe that the annual air-sea CO_2 flux is almost consistently too positive, indicating excessive outgassing and/or insufficient uptake (see gray lines in Fig. C.4). However, when data from "3 circumnavigation" tracks are added, the air-sea CO_2 flux estimate decreases by approximately 0.1 mol C m^{-2} yr^{-1}. This adjustment brings the estimate closer to the model truth (Fig. C.4) by reducing the excessive outgassing in the tropics (Fig. C.4b) and increasing the insufficient uptake north and south of 30° before 2000 (Figs. C.4a,c). It also results in an exaggeration of the total carbon sink after 2000 on a global scale (Figs. C.4a-c,d) and in the Southern Ocean (Figs. C.4c,e) as a trade-off.

The inclusion of additional sailboat data not only affects the air-sea CO_2 flux where the data has been added, but the neural network extrapolates in the past, affecting the air-sea CO_2 reconstructions consistently over time. Even though no

new data were added prior to 2012/2013, the data addition in the later years influenced the pre-2000 air-sea CO_2 flux estimate (Figs. C.4a-e), similar to results shown in Heimdal et al., 2024, probably due to the sparse data during that period, as less than 1% of the monthly 1°x1° grid cells contain measurements (Dong et al., 2024b). In contrast to the findings in Bushinsky et al., 2019a; Behncke et al., 2024, where the effect of additional data on the air-sea CO_2 flux was primarily detected in the most recent years, attributed to the use of atmospheric CO_2 as a predictor with trend behavior, our study demonstrates improvement over the entire timeseries. This more generalized impact, similar to Heimdal et al., 2024, is mainly attributed to the increased data volume spanning multiple years, as well as methodological differences such as the different nature of data.

The larger dataset, covering e.g. a decade starting in the "3 circumnavigation"-run, offers broader temporal coverage. This allows the model to learn generalized patterns and make informed predictions further back in time, enhancing its ability to extrapolate beyond the immediate training period. Additionally, the use of model data, instead of observations, provides consistent relationships between fCO_2 and predictors that enable the neural network to learn and generalize patterns more effectively.

In the Southern Ocean, the air-sea CO_2 flux density is improved before 2000 and in some of the better observed recent years when adding “3 circumnavigations”; however, it notably worsens between 2005 and 2012 as a trade-off for improving the full timeseries (Figs. C.4c and C.4e and Supplementary Figs. C.11c-d). Globally, the estimate is most improved before 2000, but it also continues to show improvement afterwards (Figs. C.4a-d and Supplementary Figs. C.11a-b).

Our findings further reveal a remarkable behavior: While we observe a shift in the mean due to the addition of the measurements, the shape of the timeseries and consequently the air-sea CO_2 flux anomalies and trend (represented by dashed lines in Figs. C.4a-c) remains unchanged and continues to be overestimated compared to the model truth trend, particularly in the Southern Ocean, even with the addition of data from two additional circumnavigation tracks (Fig. C.4).

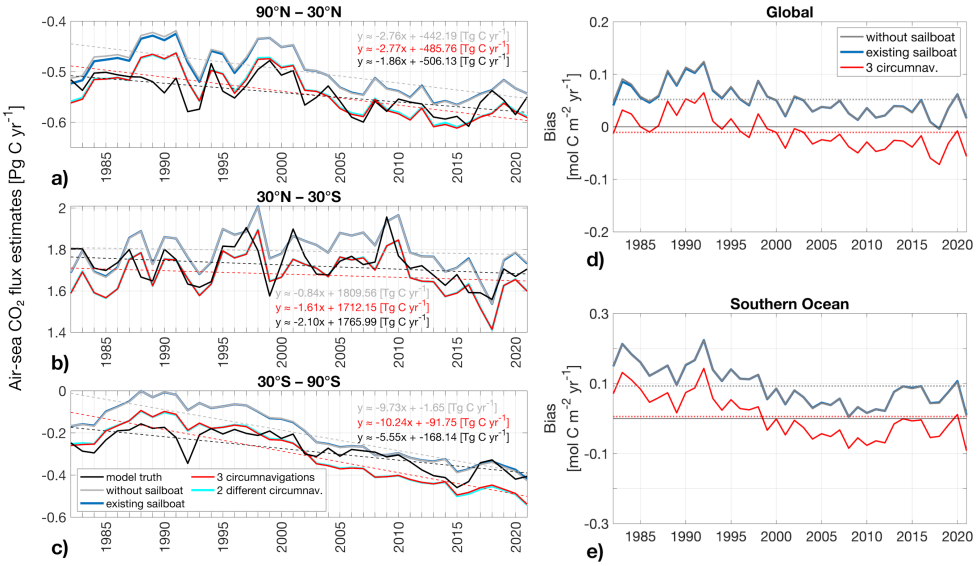

Figure C.4: **The Impact of Adding Sailboat Data on Air-Sea CO_2 Flux Time Series. a–c)** Air-sea CO_2 flux estimates with and without different sailboat tracks in different regions. Dashed lines show the long-term trend. **d–e)** Time series of bias (global and in Southern Ocean) in reconstructed air-sea CO_2 flux density. *Dotted lines represent the long-term mean bias. Note that the gray line, indicating the bias of the estimate based on "without sailboat", and the blue line, indicating the bias of the estimate based on "existing sailboat", are in close proximity to each other. Regions with a climatological maximum sea-ice concentration greater than 50% are excluded.*

Adding data from one additional but different circumnavigation track, such as from *The Ocean Race 2023* instead of *Vendée Globe 2020/21* (Fig. C.1), to the existing sailboat data improves the air-sea CO_2 flux estimates as effectively as adding data from two identical *Vendée Globe 2020/21* tracks (see cyan and red lines in Fig. C.4).

C.2.4 *The Effect of Measurement Uncertainties and Biases on the Air-Sea CO_2 Flux Estimate*

We explore the effect of two types of measurement errors applied to the subsampled sailboat fCO_2 data on the resulting air-sea CO_2 reconstructions: random measurement uncertainties, representing zero-mean fluctuations in the measurements, and systematic biases, representing constant offsets. Random uncertainties are assumed to be normally distributed around zero, while biases introduce a fixed, consistent deviation from the true value. Specifically, we consider six scenarios (Fig. C.5):

(i) a low-end measurement uncertainty of ±5 µatm (best-case scenario);

(ii–iii) a constant positive or negative bias of 5 µatm (low-end systematic offset);

(iv) a high-end measurement uncertainty of ±10 µatm;
(v–vi) a constant positive or negative bias of 10 µatm (high-end systematic offset).

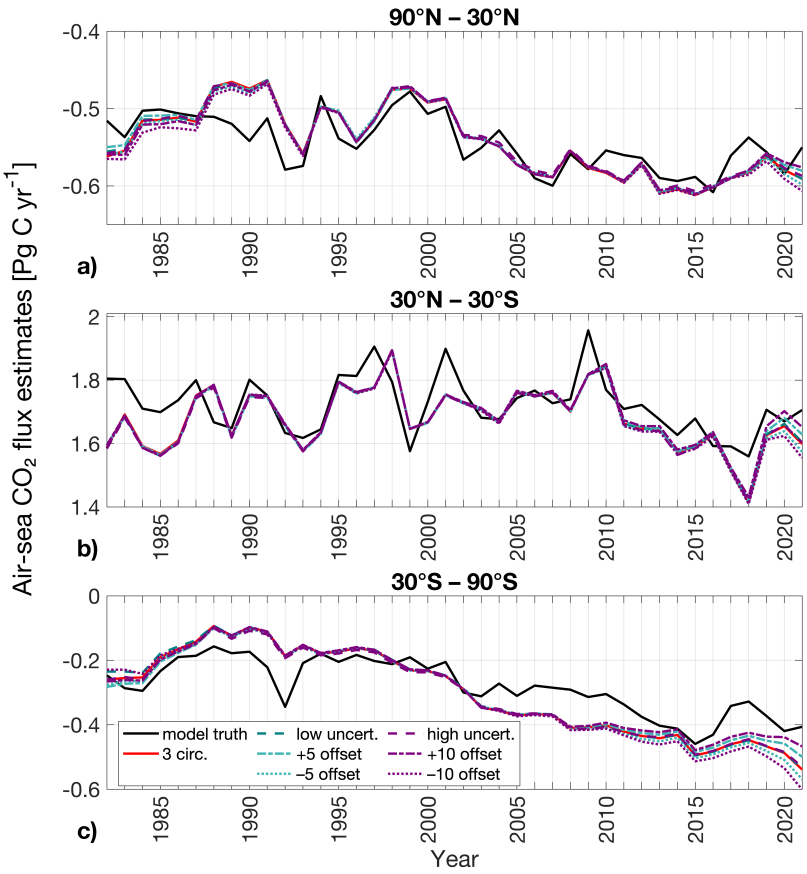

Figure C.5: **The Effect of Measurement Uncertainties and Biases on the Air-Sea CO_2 Flux Estimate. a–c)** Air-sea CO_2 flux estimates based on the model truth (solid black lines), the "3 circumnavigation" sailboat sampling (solid red lines), and the same sampling with added measurement errors. *Measurement errors are applied only to the subsampled sailboat fCO_2 data. Teal lines represent cases with low-end errors (±5 µatm uncertainty or 5 µatm bias), and purple lines represent high-end errors (±10 µatm uncertainty or 10 µatm bias). Random measurement uncertainties are shown as dashed lines (note: they appear on top of each other), while systematic biases are shown as dotted (negative bias) and dash-dotted (positive bias) lines.*

5 µatm is at the lower range of uncertainties observed in the field (Arruda et al., 2019; Olivier et al., 2022), thus representing a "best case" estimate, while 10 µatm is at the higher end with a systematic offset representing the "worst-case" scenario of limited calibration and maintenance as well as system limitations. Sailboat data from "3 circumnavigation" tracks with an associated random measurement uncertainty ranging between ±5 µatm still improve the air-sea CO_2 flux estimate, presenting a similar picture to unaffected reconstructions, both showing improved reconstructions in the data-sparse period before 2000 and in recent years (see the teal dashed following the red line in Figs. C.5a-c). This is consistent with

other studies examining the effect of random measurement uncertainties, showing that the addition of data can improve air-sea CO_2 flux estimates, even when those data are affected by high random measurement uncertainties (Behncke et al., 2024; Heimdal and McKinley, 2024).
While adding a negative bias to the measurements worsens the reconstruction as expected (dotted lines in Fig. C.5), interestingly, introducing positive measurement offsets of either 5 µatm or 10 µatm to the sailboat data improves the air-sea CO_2 flux reconstructions (dash-dotted lines in Fig. C.5). The impact of the systematic offsets – both negative and positive – is most pronounced before 1990 in high latitudes (Figs. C.5a,c) and in recent years where biased sailboat data were added starting around 2015 (Figs. C.5a-c), indicating that the bias is not extrapolated in time, but in space. Positive biases lead to reduced CO_2 uptake in recent years, particularly in the high latitudes (dash-dotted lines in Figs. C.5a,c) and increased outgassing in the tropics (dash-dotted lines in Fig. C.5b), while negative biases cause the opposite.
Similar to Behncke et al., 2024, we also find that Southern Ocean air-sea CO_2 estimates are most sensitive to measurement errors, particularly measurement biases, with biased estimates diverging from the unbiased estimate around 2005 (Fig. C.5c), while estimates in the northern high latitudes and tropics only visibly diverge around 2018/2019 (Figs. C.5a-b).

Interestingly, positive measurement biases counteract the overestimation of the carbon uptake in high latitudes and underestimation of outgassing in the tropics with "3 circumnavigations" in recent years, bringing the air-sea CO_2 flux estimates even closer to the model truth (see dash-dotted lines and red solid line compared to black line in Figs. C.5a-c). This highlights that the impact of biased observations is more complex than one would expect at first sight. Negative offsets, on the other hand, in "3 circumnavigations" lead to an overestimation of the ocean carbon uptake in high latitudes and underestimation of the outgassing in the tropics especially in recent years.
Focusing on the sailboat tracks alone, we find that both the high and low biased scenarios lead to similar errors, but as expected in opposite directions. A 10 µatm positive bias leads to a mean flux bias of 0.14 mol C m^{-2} yr^{-1} and a negative measurement bias leads to a flux bias of -0.16 mol C m^{-2} yr^{-1}. Therefore, the difference must come from other places, where the neural network extrapolates the information gained by sailboat tracks. This is visualized in Supplementary Fig. C.12. While adding negative biases worsens the reconstruction, adding positive biases actually improves the reconstruction in the Southern Ocean outgassing region, the South Atlantic and the Equatorial Pacific.

These results indicate that the neural network method used here (Landschützer et al., 2013) and potentially other machine learning methods are sensitive to systematic biases and their extrapolation. Biased measurements may compensate for missing information (in our case high-end fCO_2) elsewhere, improving the reconstruction for the wrong reason (Supplementary Fig. C.13). Thus, even biased observations can improve reconstructions when data availability is limited and data distribution is skewed (Supplementary Fig. C.13), as evidenced by the proximity of the dash-dotted and dotted lines to the solid red lines in Fig. C.5, however our analysis shows that this result is strongly linked to the underlying model testbed, the machine learning algorithm and the direction of the bias.

In conclusion, the improvement in the air-sea CO_2 flux reconstruction caused by the addition of data from "3 circumnavigations" persists even when the sailboat data contain uncertainties. Although biased data can still contribute to improved overall reconstructions, for the wrong reason through spatial extrapolation, the bias impact becomes substantial when observational constraints are weak: under-observed regions and data-sparse periods are particularly sensitive. A positive measurement bias may coincidentally shift the reconstruction closer to the model truth. However, negative biases – especially those approaching the upper limit of what is expected from the measurement system – worsen the air-sea CO_2 flux estimates.

It is important to note that, unlike studies such as Dong et al., 2024b; Watson et al., 2020, which applied bias corrections to the entire underlying observational dataset, our study introduces measurement errors only to a limited subset of sailboat data, similar to Behncke et al., 2024 We show that our method – as maybe other machine learning approaches – is sensitive to biased predictors and targets; however, the neural network's sensitivity depends on the extent of biased data, and the measurement coverage, and the underlying model used as ground truth.

C.3 DISCUSSION

Here, we quantify the improvement in the air-sea CO_2 flux estimate by adding sailboat observations in an observing system simulation experiment. We find that a commonly used neural network method, using the available real-world sampling scheme, underestimates the model-truth ocean carbon sink, which aligns with findings by Heimdal et al., 2024. However, increased sampling with sailboats improves the global estimate and increases the ocean carbon sink from 1982 to the end of 2021, particularly in the North Atlantic and in the Southern Ocean be-

tween 40°S–60°S. For instance, by adding data from "3 circumnavigation" tracks, the global mean air-sea CO_2 flux density bias decreases from 0.06 to -0.02 mol C m^{-2} yr^{-1}, and in the Southern Ocean from 0.10 to 0.00 mol C m^{-2} yr^{-1}.

Despite the observed shift in the mean air-sea CO_2 flux when adding more data, the overestimated air-sea CO_2 flux trend persists even with the addition of two additional circumnavigations. We conclude that data from two additional circumnavigations are insufficient to improve the trend, suggesting that the Global Carbon Budget model and data products are likely to continue diverging even with the incorporation of more circumnavigation data (DeVries et al., 2023; Friedlingstein et al., 2025). Additional data is needed to improve the trend. Currently, the trend in the reconstructions deviates from the model trend. By incorporating more input data over multiple decades that inherently follow the correct trend into the neural network, the output reconstructions are expected to align more closely with the model's true trend. Thus, we conclude that the inclusion of more sailboat data with trend-consistent information could improve the trend accuracy.
This underscores the need for implementing multi-decadal observing strategies. Regular sailboat circumnavigations, such as *The Ocean Race* and the *Vendée Globe*, which alternate on a staggered 4-year cycle, present a viable approach. These events ensure a major round-the-world race approximately every one to two years, thereby providing consistent and comprehensive datasets to refine our understanding and improve the accuracy of reconstructions over extended temporal scales. However, sailboats cannot fully cover seasonal measurement gaps, especially in winter at high latitudes. This further underscores the need to support complementary platforms such as autonomous floats (Gray et al., 2018; Bushinsky et al., 2019a) and Saildrones (Sutton et al., 2021), which provide year-round data in challenging conditions. Combining these platforms ensures more complete coverage and improves long-term monitoring of air-sea CO_2 fluxes.

Previous studies have shown that adding data from sailboats and Argo floats to the observing system can significantly impact and improve fCO_2 and air-sea CO_2 flux reconstructions, even when the data contain measurement uncertainties, but not if these data are biased (Behncke et al., 2024; Heimdal and McKinley, 2024). Here we show that adding more data, even if they contain uncertainties, can improve air-sea CO_2 flux reconstructions and strengthen the overall observing system. This supports previous findings (Hohensee, 2017; Carter et al., 2019) that data quantity can compensate for reduced data quality. However, biased data come with a trade-off. They can still help improve overall reconstructions, but for the wrong reason. Compensating for the lack of high-end fCO_2 samples in the

machine learning training data, biased measurements led to an improved reconstruction in high fCO_2 regions. As a result, biased data seemingly improve global reconstructions while they reduce accuracy regionally where the measurements are actually taken. Such improvements have to be taken with caution as they are likely machine learning and model-dependent and may not be translatable into the real world, creating a false acceptance for measurement biases. Instead, we show in our study that in order to interpret reconstructions with biased measurements, it is essential to consider the underlying data density distribution, the model used for the testbed analysis as well as the machine learning background bias (relative to the model truth), and the direction (positive or negative) of any measurement bias before interpreting the machine learning extrapolation, and we highly recommend to consider these in future observing system design studies.

While the finding that adding new measurements improves the air-sea CO_2 flux estimates probably holds irrespective of the baseline model choice, the observed magnitude of improvement from increased sailboat sampling, however, is highly model-dependent and could vary with different models. We work under the assumption that HAMOCC represents a known truth for our experiment; however, the HAMOCC model is known to underestimate surface ocean fCO_2 in the Southern Ocean (Ilyina et al., 2013) and exhibits an amplified seasonal cycle (Rustogi et al., 2023). This could affect the results by making the improvements appear more pronounced or less consistent across seasons than they would with a model that accurately captures seasonal variations in fCO_2, potentially distorting the long-term trend. Furthermore, we only employ one neural network method (Landschützer et al., 2013) on the model data, and different neural network methods might respond differently to data addition. We recommend more extensive analyses in the future including different neural network approaches and different model data, i.e. the products used in the Global Carbon Budget (Friedlingstein et al., 2025).
While we studied how underway fCO_2 measurements from sailboats affect and improve reconstructions, we have yet to identify the specific ocean features responsible for this effect. To determine why these changes and improvements occur, future research should focus on another added value of the data: the high-resolution nature of sailboat data, which resolves important small-scale ocean features driving variability in the air-sea CO_2 flux (e.g. Gray, 2024).

The global fCO_2 measurement coverage is biased towards the Northern Hemisphere, which leads to reconstruction errors; however, the addition of sailboat data provides better data coverage in the Southern Ocean with the potential to improve air-sea CO_2 flux reconstructions in the future. The frequency of the

sailboat races meets the demand for more affordable and innovative platforms (Whitt et al., 2020; Gregor et al., 2019; Meinig et al., 2019; Roemmich et al., 2019; Hassoun et al., 2024). Considering that the Southern Ocean carbon uptake will increase (Mongwe et al., 2018; Silvy et al., 2024) and the observational coverage recently declined (`www.socat.info` Bakker et al., 2016), more observations are needed to closely monitor the ocean carbon sink over multiple decades and sailboat races provide the opportunity to do that. We conclude that while the addition of sailboat data has the potential to improve air-sea CO_2 flux reconstructions, particularly in the Southern Ocean, further expansion of the sailboat-based observational network is essential to help minimize discrepancies in Global Carbon Budget sink estimates. Continued efforts to increase the volume and coverage of sailboat measurements will be crucial in refining our understanding of oceanic carbon dynamics.

C.4 MATERIALS AND METHODS

C.4.1 *Datasets and Sampling Masks*

In this study, our primary aim is to quantify the improvement in our air-sea CO_2 flux estimate caused by adding different sailboat data to our flux reconstructions. To achieve this, we utilize the model fCO_2 field as our starting point and apply different subsampling schemes (Fig. C.1) to get pseudo-observations. Most of the races took place in the North Atlantic between 2018 and the end of 2021. However, the Antarctic circumnavigation race, *Vendée Globe*, primarily navigated the Southern Ocean and occurred in 2020/2021, repeating every four years. Another significant round-the-world race contributing substantial Southern Ocean data is *The Ocean Race*, held in 2023 and recurring approximately every three years. This study focuses on the period from 1982 to 2021, utilizing *The Ocean Race* tracks solely to subsample earlier years.

Data X - "truth": Ground truth fCO_2 values from the HAMOCC (HAMburg Ocean Carbon Cycle model) model coupled to the ocean general circulation model MPIOM, contributing to Global Carbon Budget simulation at a monthly 1x1 degree resolution from 1982 until the end of 2021 (Ilyina et al., 2013; Paulsen et al., 2017; Mauritsen et al., 2019; Friedlingstein et al., 2025).
The HAMburg Ocean Carbon Cycle (HAMOCC) model simulates the oceanic cycles of carbon in the global Max Planck Institute Ocean Model (MPIOM). HAMOCC features biology and inorganic carbon chemistry processes in the water column and sediment (Six and Maier-Reimer, 1996; Ilyina et al., 2013). Marine

primary producers are represented by two state variables: bulk phytoplankton and diazotrophs. The growth of bulk phytoplankton is limited by temperature and light as well as by the availability of nutrients including nitrate, phosphate, and iron linked by constant Redfield ratios across organic compartments. The growth of nitrogen-fixing cyanobacteria is parameterized analogously to that of the bulk phytoplankton, but at a lower rate and is extended by representing their buoyancy. Zooplankton grazes on bulk phytoplankton, producing particulate organic matter which enters the detritus pool. Opal particles or $CaCO_3$ is produced during detritus formation, depending on silicate availability. HAMOCC simulates the upper sediment by 12 biologically active layers and a burial layer to represent the dissolution and decomposition of inorganic and organic matter as well as the diffusion of pore water constituents (Heinze et al., 1999). The HAMOCC model has been extensively evaluated in previous studies and successfully used for climate predictions and projections as well as simulating the past climate (Ilyina et al., 2013; Paulsen et al., 2017; Mauritsen et al., 2019; Müller et al., 2018; Maerz et al., 2020; Liu et al., 2021; Li et al., 2023; Nielsen et al., 2024).

Data A - "existing sailboat": Subsampled model fCO_2 (X) generated using the SOCATv2022 sampling scheme, including sailboat data. We used underway fCO_2 measurement tracks from the IMOCA 60 sailboats "*Seaexplorer-Yacht Club de Monaco*" (until 2019 "*Malizia*") and "*Newrest - Art & Fenêtres*" (now "*Nexans - Art & Fenêtres*") during offshore sailing and training events from 2018 to 2021. Together, all sailboats collected 161 days of fCO_2 measurements until the end of 2021.

Data B - "without sailboat": Subsampled model fCO_2 (X) generated using the SOCATv2022 sampling scheme, excluding sailboat data

Data C - "3 circumnavigations": Subsampled model fCO_2 (X) generated using the SOCATv2022 sampling scheme including existing sailboat data and two additional Antarctic circumnavigations (*Vendée Globe*; 2012/13, 2016/17, 2020/21) (from which only the latter one is from the existing track and also included in A; the track of the *Vendée Globe 2020/21*, where fCO_2 measurements were taken, was used to subsample the model data in earlier years when *Vendée Globe* races occurred without fCO_2 measurements.)

Data D - "2 different circumnavigations": Subsampled model fCO_2 (X) generated using the SOCATv2022 sampling scheme including sailboat data and 2 different round-the-world races (*Vendée Globe 2020/21* and the preliminary *The Ocean Race 2017/18*) (for the latter one we used existing tracks from 2023).

In the following, we added random measurement uncertainties and biases to the subsampled sailboat fCO_2 data in "3 circumnavigations":

Data E - "3 circumnav + low uncert.": Data C, but with an added random measurement uncertainty ranging from ±5 µatm (lower end of what is expected from the measurement device) to the data from sailboat tracks

Data F - "3 circumnav + 5 offset": Data C, but with an added + 5 µatm measurement offset to the data from sailboat tracks

Data G - "3 circumnav − 5 offset": Data C, but with an added – 5 µatm measurement offset to the data from sailboat tracks

Data H - "3 circumnav + high uncert": Data C, but with an added random measurement uncertainty ranging from ±10 µatm (higher end of what is expected from the measurement device) to the data from sailboat tracks

Data I - "3 circumnav + 10 offset": Data C, but with an added + 10 µatm measurement offset to the data from sailboat tracks

Data J - "3 circumnav − 10 offset": Data C, but with an added – 10 µatm measurement offset to the data from sailboat tracks

C.4.2 *The reconstruction of sea surface fCO_2 and air-sea CO_2 fluxes*

The gaps in all subsampled sea surface fCO_2 maps (data A-J) were filled using the 2-step neural network method called SOM-FFN (Landschützer et al., 2013). In the first step, a self-organizing map (SOM) classified the ocean into biogeochemical provinces based on common patterns in predictor variables, including HAMOCC sea-surface temperature, sea-surface salinity, mixed layer depth, and a fCO_2 climatology (Ilyina et al., 2013; Paulsen et al., 2017; Mauritsen et al., 2019; Friedlingstein et al., 2025). The second step involved a feed-forward neural network (FFN) establishing non-linear relationships between predictors and subsampled fCO_2 data within each province. Predictors were HAMOCC sea-surface temperature, sea-surface salinity, mixed layer depth, atmospheric CO_2 concentration, and phytoplankton plus cyanobacteria biomass integrated over a depth of 37 meters. This specific depth, limited to the upper ocean biology and excluding the deep chlorophyll maxima, was chosen due to the limitations of equivalently and

previously used ocean color observations for case-1 water, which are restricted to the first optical depth below 40 meters (Nababan et al., 2021). Based on the reconstructed fCO_2 A-J and model truth X, we computed flux estimates A-J and X by applying a bulk gas transfer formulation with a quadratic relationship between wind speed and transfer velocity to the reconstructed maps (A-J), as well as the model truth X (Wanninkhof, 1992; Landschützer et al., 2013)(37,49). The mean gas transfer was standardized to a global average rate of 16.5 cm hr^{-1} (Naegler, 2009). While the neural network reconstructed fCO_2 closely matches the model fCO_2, the reconstructed air-sea CO_2 flux differs from the model flux. This discrepancy arises because of the bulk gas transfer parametrization with a standardized mean gas transfer velocity of 16.5 cm hr^{-1}, which is not ideal for the model fCO_2. Acknowledging that our primary focus is not on realistically estimating the air-sea CO_2 flux but rather on assessing the impact of different sampling schemes on the flux estimate, we decided to eliminate this uncertainty by applying the same parametrization on the model fCO_2 (Wanninkhof, 1992). This allowed us to establish a comparable "original" flux model truth for our analysis.

We focus both on the air-sea CO_2 flux and the fCO_2 because of the high sensitivity of air-sea CO_2 flux estimates to errors in fCO_2. In high wind regions, small fCO_2 errors can lead to large flux errors due to high gas transfer velocity, while the same fCO_2 error in low wind regions results in smaller flux errors. Furthermore, the direction of the fCO_2 error improvement (negative or positive) significantly impacts the air-sea CO_2 flux estimate. A small negative improvement in fCO_2 can either decrease or increase the flux estimate depending on whether the ocean fCO_2 is greater or less than the atmospheric fCO_2, respectively. Similarly, a small positive improvement can increase or decrease the flux estimate based on the same conditions. By focusing on both estimates, we ensure a comprehensive assessment, minimizing the risk of overlooking critical factors that could skew the air-sea CO_2 flux estimates.

In this study, we define the air-sea CO_2 flux density as the instantaneous flux into or out of the ocean (in units of mol C m^{-2} yr^{-1}), where positive flux indicates outgassing and negative flux indicates uptake (Fig. C.10), generally aligning its direction with fCO_2. In contrast, the air–sea CO_2 flux—as well as the ocean carbon sink when referring to a negative integrated signal—is quantified as the spatially integrated flux over a given area (in PgC) and typically follows the opposite direction.

C.4.3 *Statistical Analyses*

We exclude regions with a climatological maximum sea-ice concentration greater than 50%, from most of our analysis as sparse observations (Bakker et al., 2016) and the influence of seasonal changes in sea-ice coverage introduce high uncertainties into the neural network reconstruction in that region (Duke et al., 2024; Ford et al., 2024; Jersild and Landschützer, 2024; Roobaert et al., 2024) and due to the model's less realistic representation of the high latitudes (Ilyina et al., 2013). The ice zone in the Southern Ocean coincides with the high uptake region south of 60°S (Fig. C.1a).

C.4.4 *Neural Network Performance Evaluation*

To evaluate the performance of the neural network in reconstructing the HAMOCC fCO_2 we use Probability Density Functions and calculate the Bhattacharyya distance (BD) (Bhattacharyya, 1943), which measures the similarity between the probability density functions of the reconstruction and the original model fCO_2. Lower BD values indicate a higher degree of similarity between the probability density functions. We further compare the detectable signal in the air-sea CO_2 flux estimate caused by the addition of sailboat data in our subsampled model data to the signal in observation data from a previous study using a signal-to-noise detection described in Behncke et al., 2024.

C.4.5 *Improvement Quantification*

We employed a Monte Carlo approach, generating 10- to 40-member ensembles for each of the 10 subsampling scenarios. For scenarios A ("existing sailboat"), B ("without sailboat"), C ("3 circumnavigations"), D ("2 different circumnavigations"), E ("3 circumnavigations + low measurement uncertainty"), and F ("3 circumnavigations + positive 5 µatm offset"), we generated 40 ensemble members each. For scenarios G ("3 circumnavigations – 5 µatm offset"), H ("3 circumnavigations + high measurement uncertainty"), I ("3 circumnavigations + 10 µatm offset"), and J ("3 circumnavigations – 10 µatm offset"), we generated 10 ensemble members each, as the standard deviation across 10 versus 40 ensembles differs only slightly and using fewer members allows for more computationally efficient analysis.

We generated the ensembles by varying training and validation dataset splits to enhance the reliability of our air-sea CO_2 flux estimates and identify potential random errors caused by the sensitivity of the neural-network approach to differ-

ent subsets of the data. The ensemble mean served as the best estimate for each sampling scenario.
The bias is calculated as the mean of the reconstruction R (i.e., A, B, C) minus the model truth (X): Bias = mean(R) - mean(X) and measures the over- and underestimation in the reconstructions over different time periods. It is important to note that values near zero not only indicate a good reconstruction but could also indicate that positive and negative differences cancel out. We calculated the mean bias as well as the median bias to minimize the impact of regional outliers caused by regions of high uncertainty (Fig. C.2).

C.5 ACKNOWLEDGMENTS

We express our gratitude to the sailors, particularly Boris Herrmann and Fabrice Amedeo, and their teams, Team Malizia and Nexans - Wewise, for their dedicated involvement in collecting valuable data. The Surface Ocean CO_2 Atlas (SOCAT) is an international effort, endorsed by the International Ocean Carbon Coordination Project (IOCCP), the Surface Ocean Lower Atmosphere Study (SOLAS) and the Integrated Marine Biosphere Research (IMBeR) program, to deliver a uniformly quality-controlled surface ocean CO_2 database. The many researchers and funding agencies responsible for the collection of data and quality control are thanked for their contributions to SOCAT.

Funding

Research Foundation Flanders (FWO) contract I001821N (VLIZ ICOS, PL)
Deutsche Forschungsgemeinschaft (DFG, German Research Foundation) under Germany's Excellence Strategy – EXC 2037 'CLICCS - Climate, Climatic Change, and Society' – Project Number: 390683824 (TI)
EU Horizon 2020 research and innovation programme under grant agreement No. 101003536 (ESM2025–Earth System Models for the Future) (TI)
EU Horizon Europe research and innovation programme under grant agreement No. 101188028 (TRICUSO) (PL, JB) International Max Planck Research School on Earth System Modelling (IMPRS-ESM) (JB)

Author contributions

Conceptualization: JB, PL
Methodology: JB, PL, TI, FC
Investigation: JB, PL

Visualization: JB
Supervision: PL, TI
Writing—original draft: JB, PL, TI, FC
Writing—review & editing: JB, PL, TI, FC

Competing interests

All authors declare they have no competing interests.

Data and materials availability

The source code for the neural network method can be found at ref. (Jersild, 2023). The MPIM-HAMOCC model output can be found at Project, 2022. Results from the neural-network based SOM-FFM method are publicly available online 10.5281/zenodo.15131072.

C.6 SUPPLEMENTARY

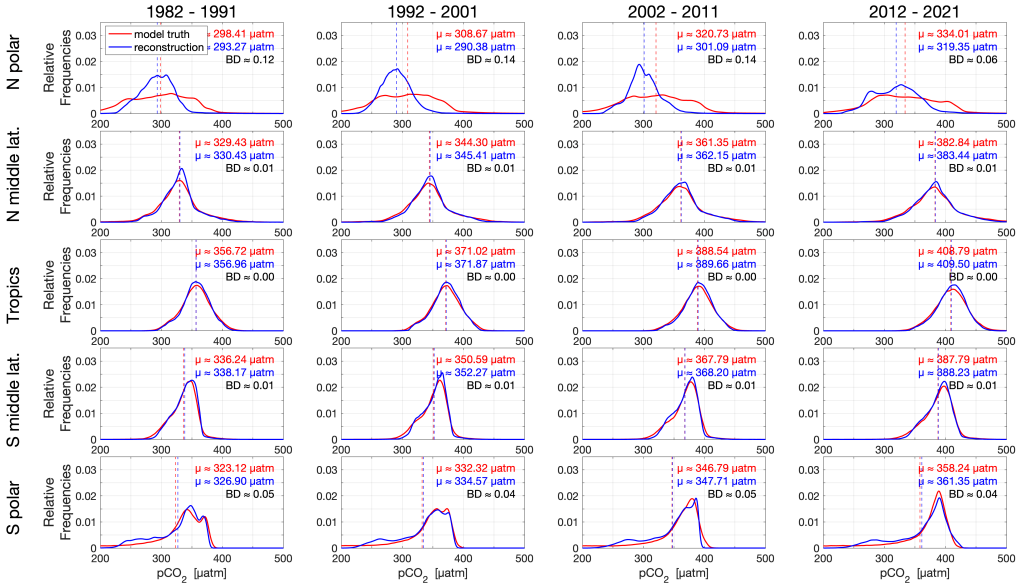

Figure C.6: **Reconstruction Uncertainty Assessment**. Kernel density estimate of fCO_2 data distributions of model truth fCO_2 (X; red) and subsampled and NN-reconstructed fCO_2 (A *"existing sailboat"*; blue) for different regions and time periods. *Regions with a climatological maximum sea-ice concentration greater than 50% are included. Latitudinal zones are divided into increments of 30°, ranging from 90°N to 90°S. The time periods were chosen to demonstrate how the addition of sailboat data impacts the fCO_2 and, by extension, the air-sea CO_2 flux across the entire time period, independently of the specific years in which data were added.*

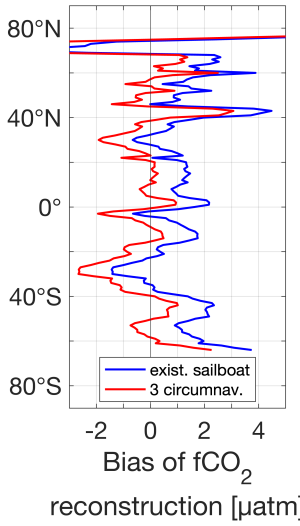

Figure C.7: **Latitudinal Bias of the fCO_2 Reconstructions "existing sailboat" and "3 circumnavigations" compared to model truth.**

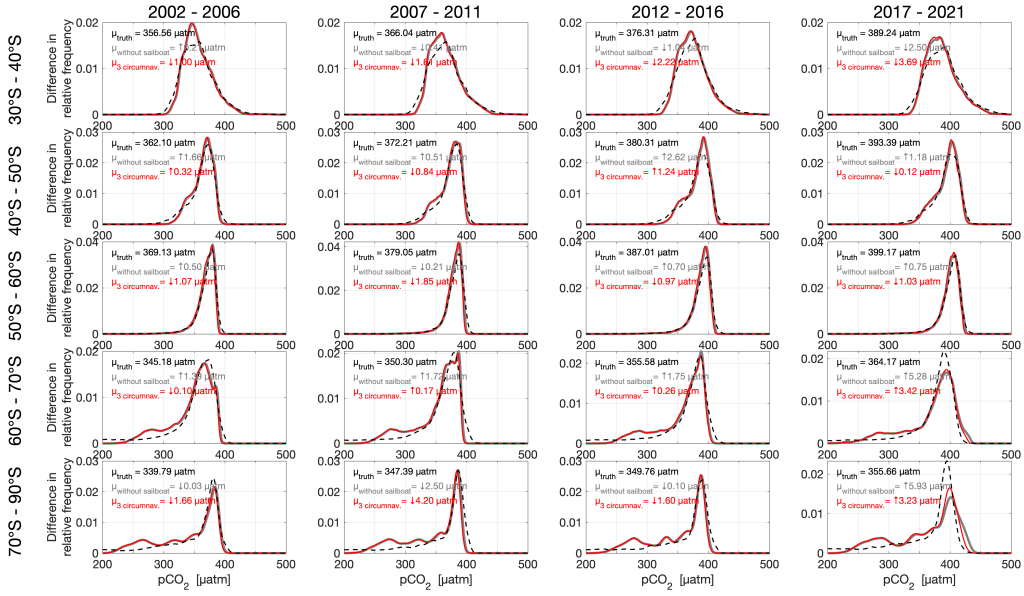

Figure C.8: **Effect of "3 circumnavigations" on Southern Ocean fCO_2 distribution (2002–2021)**. Difference between the data distribution of fCO_2 estimates based on sampling scheme B "without sailboat" (gray) and C "3 circumnavigations" (red) in the Southern Ocean between 2002–2021. *Regions with a climatological maximum sea-ice concentration greater than 50% are included. Additional sailboat data reduce the fCO_2 estimate in the Southern Ocean (see change from gray line to red line).*

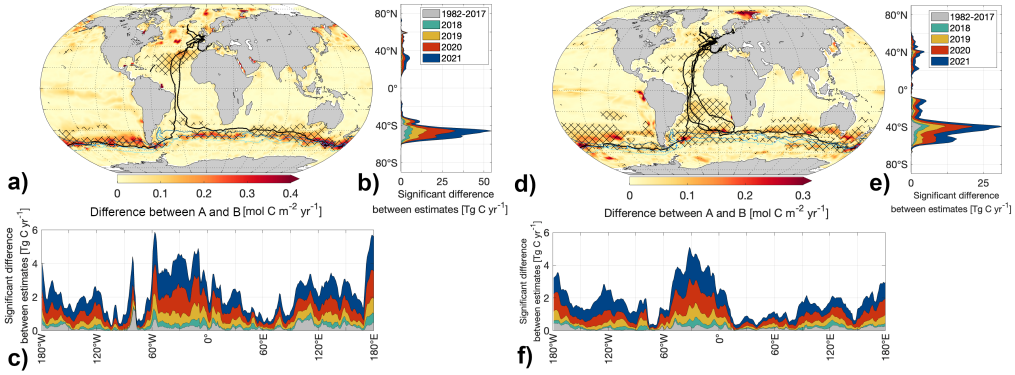

Figure C.9: **Comparing the Impact of Observational and Model-Based Sailboat Data Addition on Air-Sea CO_2 Flux Estimates**. The detectable change in the air-sea CO_2 flux estimate caused by adding the existing sailboat data to the reconstructions. **a–c)** Observation-based reconstructions (Behncke et al., 2024) and **d–f)** (subsampled) model-based reconstructions. **a)** and **d)** Maps show the detectable change in the air-sea CO_2 flux estimate caused by adding the existing sailboat data to the reconstructions averaged over November 2020 to January 2021 (the time of the *Vendée Globe* circumnavigation). Hatching indicates significant differences. **b,c)** and **e,f)** Significant differences between air-sea CO_2 flux estimates per year and (**b, e**) latitude and (**c, f**) longitude. *Blue lines from north to south: Northern Boundary, Subantarctic Front, Polar Front (Park et al., 2019). Note the different ranges on axes.* ***a–c)*** *includes tracks from a single sailboat (Behncke et al., 2024), while* ***d–f)*** *include tracks from all sailboats measuring fCO_2 and contributing to SOCAT (Bakker et al., 2016) up until the end of 2021 (used in this study).*

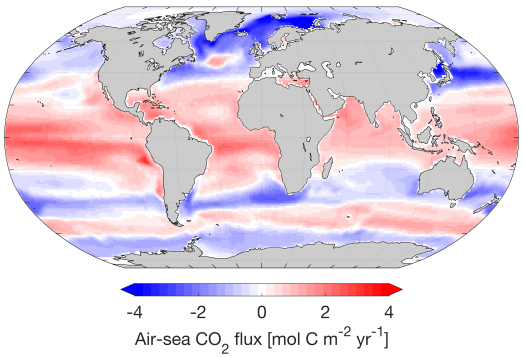

Figure C.10: **Reconstructed air-sea CO_2 flux density based on SOCAT-sampling.**

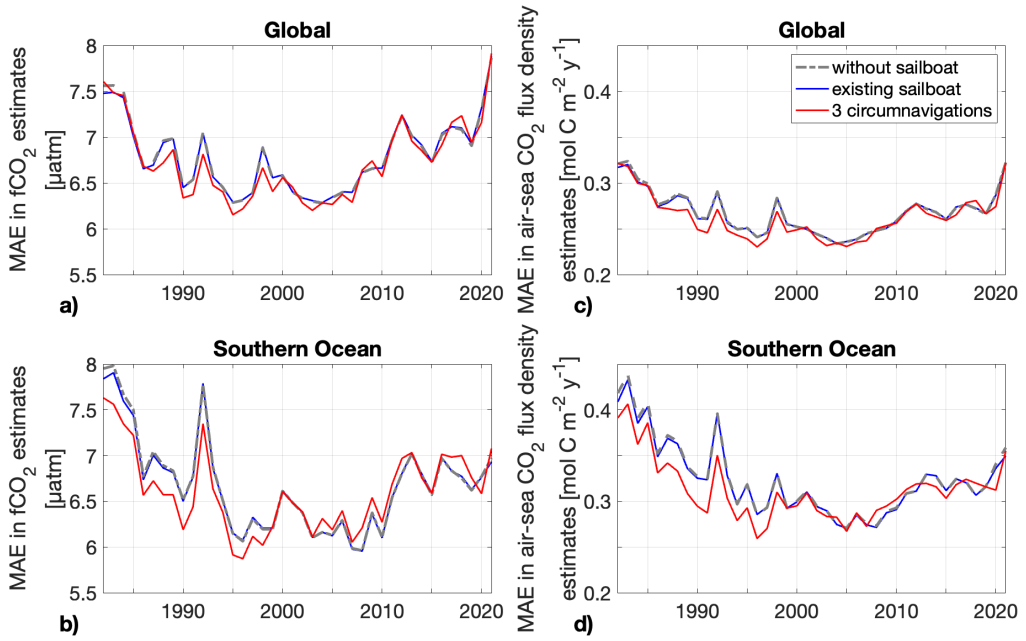

Figure C.11: **Annual Time Series of Mean Absolute Errors (MAE) in Reconstructed a–b)** fCO_2 (left column) and **c–d)** air-sea CO_2 flux density (right column).

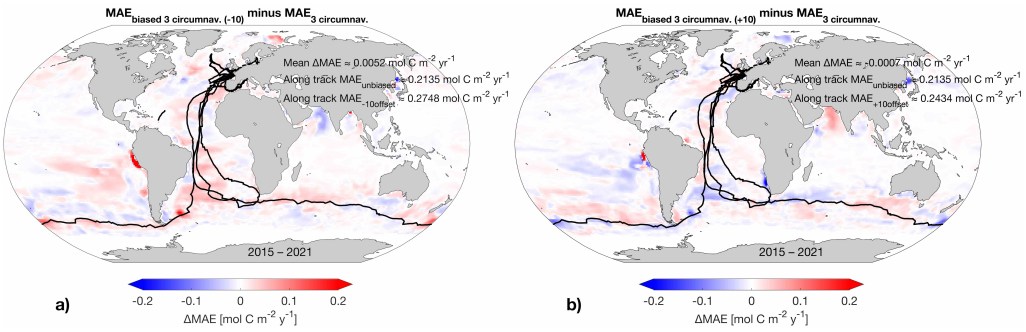

Figure C.12: **Spatial Difference in the MAE of Reconstructed Air-Sea CO_2 Fluxes between Biased (±10 µatm) and Unbiased "3 Circumnavigation" Scenarios**. Spatial difference in the MAE of reconstructed air-sea CO_2 fluxes between biased (±10 µatm) and unbiased "3 circumnavigation" scenarios. ΔMAE was calculated as $MAE_{\text{biased reconstruction}} - MAE_{\text{unbiased reconstruction}}$. *Positive (red) values indicate regions where the unbiased run yielded lower reconstruction errors (i.e., performed better), while negative (blue) values indicate areas where the biased run performed better. Track-averaged MAE and bias values are shown to the right of each map and indicate that the addition of biased observations systematically increases both the bias and MAE along the sailboat track.* ***a)*** *−10 µatm bias scenario;* ***b)*** *+10 µatm bias scenario.*

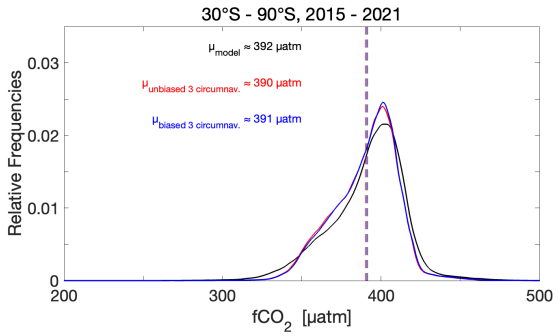

Figure C.13: **Kernel density estimate of data distribution of model truth fCO_2, unbiased "3 circumnavigations", and +10 µatm biased "3 circumnavigations" south of 30°S between 2015 and 2021**. Regions with a climatological maximum sea-ice concentration greater than 50% are excluded. Biased "3 circumnavigations" (blue) shift the data distribution closer to the model truth (black) than unbiased "3 circumnavigations" (red).

BIBLIOGRAPHY

Arruda, Ricardo, Dariia Atamanchuk, Margot Cronin, Tobias Steinhoff, and Douglas Wallace (2019). "At-sea intercomparison of three underway pCO_2 systems: Intercomparison of pCO_2 systems." In: *Limnology and Oceanography: Methods* 18. DOI: 10.1002/lom3.10346.

Bakker, D. C. E. et al. (2024). *Surface Ocean CO_2 Atlas Database Version 2024 (SOCATv2024) (NCEI Accession 0293257)*. Data set. URL: https://doi.org/10.25921/9wpn-th28.

Bakker, Dorothee C. E. et al. (2016). "A multi-decade record of high-quality fCO_2 data in version 3 of the Surface Ocean CO_2 Atlas (SOCAT)." In: *Earth System Science Data* 8.2, pp. 383–413. ISSN: 1866-3508. DOI: 10.5194/essd-8-383-2016.

Bakker, Dorothee et al. (2023). *Case for SOCAT as an integral part of the value chain advising UNFCCC on ocean CO_2 uptake*. URL: http://www.ioccp.org/images/Gnews/2023_A_Case_for_SOCAT.pdf (visited on 04/07/2025).

Balch, W. M., D. T. Drapeau, B. C. Bowler, E. R. Lyczkowski, L. C. Lubelczyk, S. C. Painter, and A. J. Poulton (2014). "Surface biological, chemical, and optical properties of the Patagonian Shelf coccolithophore bloom, the brightest waters of the Great Calcite Belt." In: *Limnology and Oceanography* 59.5, pp. 1715–1732. ISSN: 1939-5590. DOI: 10.4319/lo.2014.59.5.1715.

Bates, Nicholas R, Liliane Merlivat, Laurence Beaumont, and A.Christine Pequignet (2000). "Intercomparison of shipboard and moored CARIOCA buoy seawater fCO_2 measurements in the Sargasso Sea." In: *Marine Chemistry* 72.2. Second International Symposium on Carbon Dioxide in the Oceans, pp. 239–255. ISSN: 0304-4203. DOI: https://doi.org/10.1016/S0304-4203(00)00084-0.

Beech, Nathan, Thomas Rackow, Tido Semmler, Sergey Danilov, Qiang Wang, and Thomas Jung (2022). "Long-term evolution of ocean eddy activity in a warming world." In: *Nature Climate Change* 12.10, pp. 910–917. ISSN: 1758-6798. DOI: 10.1038/s41558-022-01478-3.

Beech, Nathan, Thomas Rackow, Tido Semmler, and Thomas Jung (2025). "High-latitude Southern Ocean eddy activity projected to evolve with anthropogenic climate change." In: *Communications Earth & Environment* 6.1, p. 237. ISSN: 2662-4435. DOI: 10.1038/s43247-025-02221-4.

Behncke, Jacqueline, Tatiana Ilyina, Fatemeh Chegini, and Peter Landschützer (n.d.). "Improved air-sea CO_2 flux estimates from sailboat measurements." Manuscript under review at *Science Advances*.

Behncke, Jacqueline, Peter Landschützer, and Toste Tanhua (2024). "A detectable change in the air-sea CO_2 flux estimate from sailboat measurements." In: *Sci-*

entific Reports 14.1, p. 3345. ISSN: 2045-2322. DOI: 10.1038/s41598-024-53159-0.

Belkin, N. et al. (2022). "Influence of cyclonic and anticyclonic eddies on plankton in the southeastern Mediterranean Sea during late summertime." In: *Ocean Science* 18.3, pp. 693–715. DOI: 10.5194/os-18-693-2022.

Bender, M. et al. (2002). *A large scale carbon observing plan: In situ oceans and atmosphere (LSCOP)*. Technical Note. Springfield: Nat. Tech. Info. Service, p. 201. URL: https://repository.library.noaa.gov/view/noaa/23522.

Bennington, Val, Tomislav Galjanic, and Galen A. McKinley (2022a). "Explicit Physical Knowledge in Machine Learning for Ocean Carbon Flux Reconstruction: The pCO_2-Residual Method." In: *Journal of Advances in Modeling Earth Systems* 14.10, e2021MS002960. DOI: https://doi.org/10.1029/2021MS002960.

Bennington, Val, Lucas Gloege, and Galen A. McKinley (2022b). "Variability in the Global Ocean Carbon Sink From 1959 to 2020 by Correcting Models With Observations." In: *Geophysical Research Letters* 49.14, e2022GL098632. DOI: https://doi.org/10.1029/2022GL098632.

Berghoff, Carla F., Denis Pierrot, Lucía Epherra, Ricardo I. Silva, Valeria Segura, Rubén M. Negri, M. Constanza Hozbor, Mario O. Carignan, Leticia Barbero, and Vivian A. Lutz (2023). "Physical and biological effects on the carbonate system during summer in the Northern Argentine Continental Shelf (Southwestern Atlantic)." In: *Journal of Marine Systems* 237, p. 103828. ISSN: 0924-7963. DOI: 10.1016/j.jmarsys.2022.103828.

Bhattacharyya, Anil (1943). "On a measure of divergence between two statistical populations defined by their probability distributions." In: *Bulletin of the Calcutta Mathematical Society* 35, pp. 99–109.

Bianchi, Alejandro A., Diana Ruiz Pino, Hernán G. Isbert Perlender, Ana P. Osiroff, Valeria Segura, Vivian Lutz, Moira Luz Clara, Carlos F. Balestrini, and Alberto R. Piola (2009). "Annual balance and seasonal variability of sea-air CO_2 fluxes in the Patagonia Sea: Their relationship with fronts and chlorophyll distribution." In: *Journal of Geophysical Research: Oceans* 114.C3. ISSN: 2156-2202. DOI: 10.1029/2008JC004854. (Visited on 02/20/2025).

Biastoch, A., C. W. Böning, F. U. Schwarzkopf, and J. R. E. Lutjeharms (2009). "Increase in Agulhas leakage due to poleward shift of Southern Hemisphere westerlies." In: *Nature* 462.7272, pp. 495–498. ISSN: 1476-4687. DOI: 10.1038/nature08519.

Bittig, Henry C. et al. (2019). "A BGC-Argo Guide: Planning, Deployment, Data Handling and Usage." In: *Frontiers in Marine Science* 6. ISSN: 2296-7745. DOI: 10.3389/fmars.2019.00502.

Boyer Montégut, Clément de, Gurvan Madec, Albert S. Fischer, Alban Lazar, and Daniele Iudicone (2004). "Mixed layer depth over the global ocean: An examination of profile data and a profile-based climatology." In: *Journal of Geophysical Research: Oceans* 109.C12. ISSN: 2156-2202. DOI: 10.1029/2004JC002378.

Boyer, Tim et al. (2023). "Effects of the Pandemic on Observing the Global Ocean." In: *Bulletin of the American Meteorological Society* 104.2. Place: Boston MA, USA Publisher: American Meteorological Society, E389 –E410. DOI: 10.1175/BAMS-D-21-0210.1.

Breier, Rebekka E., Cristian C. Lalescu, Devin Waas, Michael Wilczek, and Marco G. Mazza (2018). "Emergence of phytoplankton patchiness at small scales in mild turbulence." In: *Proceedings of the National Academy of Sciences* 115.48, pp. 12112–12117. DOI: 10.1073/pnas.1808711115.

Bushinsky, Seth M., Peter Landschützer, Christian Rödenbeck, Alison R. Gray, David Baker, Matthew R. Mazloff, Laure Resplandy, Kenneth S. Johnson, and Jorge L. Sarmiento (2019a). "Reassessing Southern Ocean Air-Sea pCO_2 Flux Estimates With the Addition of Biogeochemical Float Observations." In: *Global Biogeochemical Cycles* 33.11, pp. 1370–1388. ISSN: 1944-9224. DOI: 10.1029/2019GB006176.

Bushinsky, Seth M., Yuichiro Takeshita, and Nancy L. Williams (2019b). "Observing Changes in Ocean Carbonate Chemistry: Our Autonomous Future." In: *Current Climate Change Reports* 5.3, pp. 207–220. ISSN: 2198-6061. DOI: 10.1007/s40641-019-00129-8.

Canadell, J.G. et al. (2021). "Global Carbon and other Biogeochemical Cycles and Feedbacks." In: *Climate Change 2021: The Physical Science Basis. Contribution of Working Group I to the Sixth Assessment Report of the Intergovernmental Panel on Climate Change*. Ed. by V. Masson-Delmotte et al. Cambridge, United Kingdom and New York, NY, USA: Cambridge University Press, pp. 673–816. DOI: 10.1017/9781009157896.007.

Carter, B. R., N. L. Williams, W. Evans, A. J. Fassbender, L. Barbero, C. Hauri, R. A. Feely, and A. J. Sutton (2019). "Time of Detection as a Metric for Prioritizing Between Climate Observation Quality, Frequency, and Duration." In: *Geophysical Research Letters* 46.7, pp. 3853–3861. DOI: https://doi.org/10.1029/2018GL080773.

Chai, Fei, Kenneth S. Johnson, Hervé Claustre, Xiaogang Xing, Yuntao Wang, Emmanuel Boss, Stephen Riser, Katja Fennel, Oscar Schofield, and Adrienne Sutton (2020). "Monitoring ocean biogeochemistry with autonomous platforms." In: *Nature Reviews Earth & Environment* 1.6, pp. 315–326. ISSN: 2662-138X. DOI: 10.1038/s43017-020-0053-y.

Chaigneau, Alexis, Gérard Eldin, and Boris Dewitte (2009). "Eddy activity in the four major upwelling systems from satellite altimetry (1992–2007)." In: *Progress in Oceanography* 83.1, pp. 117–123. ISSN: 0079-6611. DOI: https://doi.org/10.1016/j.pocean.2009.07.012.

Chapman, Christopher, Mary-Anne Lea, Amelie Meyer, Jean-baptiste Sallée, and Mark Hindell (2020). "Defining Southern Ocean fronts and their influence on biological and physical processes in a changing climate." In: *Nature Climate Change* 10, pp. 1–11. DOI: 10.1038/s41558-020-0705-4.

Chau, Thi Tuyet Trang, Marion Gehlen, and Frédéric Chevallier (2022). "A seamless ensemble-based reconstruction of surface ocean pCO_2 and air–sea CO_2 fluxes over the global coastal and open oceans." In: *Biogeosciences* 19.4, pp. 1087–1109. ISSN: 1726-4170. DOI: 10.5194/bg-19-1087-2022.

Chavez, Francisco P., Jeff Sevadjian, Chris Wahl, Jules Friederich, and Gernot E. Friederich (2018). "Measurements of pCO_2 and pH from an autonomous surface vehicle in a coastal upwelling system." In: *Deep Sea Research Part II: Topical Studies in Oceanography* 151. Studies of the California Current System Part 3, pp. 137–146. ISSN: 0967-0645. DOI: https://doi.org/10.1016/j.dsr2.2017.01.001.

Chelton, Dudley, Peter Gaube, Michael Schlax, Jeffrey Early, and Roger Samelson (2011). "The Influence of Nonlinear Mesoscale Eddies on Near-Surface Oceanic Chlorophyll." In: *Science (New York, N.Y.)* 334, pp. 328–32. DOI: 10.1126/science.1208897.

Chen, Feizhou, Wei-Jun Cai, Claudia Benitez-Nelson, and Yongchen Wang (2007). "Sea surface pCO_2-SST relationships across a cold-core cyclonic eddy: Implications for understanding regional variability and air-sea gas exchange." In: *Geophysical Research Letters* 34.10. DOI: https://doi.org/10.1029/2006GL028058.

Claustre, Hervé, Kenneth S. Johnson, and Yuichiro Takeshita (2020). "Observing the Global Ocean with Biogeochemical-Argo." In: *Annual Review of Marine Science* 12.Volume 12, 2020, pp. 23–48. ISSN: 1941-0611. DOI: https://doi.org/10.1146/annurev-marine-010419-010956.

Copernicus Climate Change Service (2018). *Sea level gridded data from satellite observations for the global ocean from 1993 to present*. Copernicus Climate Change Service (C3S) Climate Data Store (CDS). Accessed on 10-Apr-2025. DOI: 10.24381/cds.4c328c78.

Couespel, Damien, Marina Lévy, and Laurent Bopp (2024). "Stronger Oceanic CO_2 Sink in Eddy-Resolving Simulations of Global Warming." In: *Geophysical Research Letters* 51.4, e2023GL106172. DOI: https://doi.org/10.1029/2023GL106172.

Dai, Yanhui et al. (2023). "Coastal phytoplankton blooms expand and intensify in the 21st century." In: *Nature* 615.7951, pp. 280–284. ISSN: 1476-4687. DOI: 10.1038/s41586-023-05760-y.

Daniel, Tom, Justin Manley, and Neil Trenaman (2011). "The Wave Glider: enabling a new approach to persistent ocean observation and research." In: *Ocean Dynamics* 61.10, pp. 1509–1520. ISSN: 1616-7228. DOI: 10.1007/s10236-011-0408-5.

Dawson, H. R. S., P. G. Strutton, and P. Gaube (2018). "The Unusual Surface Chlorophyll Signatures of Southern Ocean Eddies." In: *Journal of Geophysical Research: Oceans* 123.9, pp. 6053–6069. DOI: https://doi.org/10.1029/2017JC013628.

DeVries, Tim (2014). "The oceanic anthropogenic CO_2 sink: Storage, air-sea fluxes, and transports over the industrial era." In: *Global Biogeochemical Cycles* 28.7, pp. 631–647. ISSN: 1944-9224. DOI: 10.1002/2013GB004739.

DeVries, Tim, Mark Holzer, and Francois Primeau (2017). "Recent increase in oceanic carbon uptake driven by weaker upper-ocean overturning." In: *Nature* 542.7640, pp. 215–218. ISSN: 1476-4687. DOI: 10.1038/nature21068.

DeVries, Tim et al. (2019). "Decadal trends in the ocean carbon sink." In: *Proceedings of the National Academy of Sciences* 116.24, pp. 11646–11651. DOI: 10.1073/pnas.1900371116.

DeVries, Tim et al. (2023). "Magnitude, Trends, and Variability of the Global Ocean Carbon Sink From 1985 to 2018." In: *Global Biogeochemical Cycles* 37.10, e2023GB007780. ISSN: 1944-9224. DOI: 10.1029/2023GB007780.

Demasy, Clément, Marie Boye, Ambroise Delisée, Jean-François Maguer, Melilotus Thyssen, and Léa Gest (2025). "Responses of the Natural Phytoplankton Assemblage to Patagonian Dust Input and Anthropogenic Changes in the Southern Ocean." In: *Earth's Future* 13.6, e2024EF005762. DOI: https://doi.org/10.1029/2024EF005762.

Denvil-Sommer, A., M. Gehlen, and M. Vrac (2021). "Observation system simulation experiments in the Atlantic Ocean for enhanced surface ocean pCO_2 reconstructions." In: *Ocean Science* 17.4, pp. 1011–1030. DOI: 10.5194/os-17-1011-2021.

Dickey, T. et al. (1998). "Initial results from the Bermuda Testbed Mooring program." In: *Deep Sea Research Part I: Oceanographic Research Papers* 45.4, pp. 771–794. ISSN: 0967-0637. DOI: https://doi.org/10.1016/S0967-0637(97)00096-4.

Dickson, A.G., C.L. Sabine, and J.R. Christian, eds. (2007). *Guide to best practices for ocean CO_2 measurements*. 3. PICES Special Publication, p. 191.

Djeutchouang, Laique M., Nicolette Chang, Luke Gregor, Marcello Vichi, and Pedro M. S. Monteiro (2022). "The sensitivity of pCO_2 reconstructions to

sampling scales across a Southern Ocean sub-domain: a semi-idealized ocean sampling simulation approach." en. In: *Biogeosciences* 19.17, pp. 4171–4195. ISSN: 1726-4189. DOI: 10.5194/bg-19-4171-2022.

Dlugokencky, E.J., K. W. Thoning, X. Lan, and P. P. Tans (2021). *NOAA Greenhouse Gas Reference from Atmospheric Carbon Dioxide Dry Air Mole Fractions from the NOAA GML Carbon Cycle Cooperative Global Air Sampling Network*. Data Path: ftp://aftp.cmdl.noaa.gov/data/trace_gases/co2/flask/surface/. Data Path: https://gml.noaa.gov/aftp/data/trace_gases/co2/flask/surface/.

Doddridge, Edward W. and David P. Marshall (2018). "Implications of Eddy Cancellation for Nutrient Distribution Within Subtropical Gyres." In: *Journal of Geophysical Research: Oceans* 123.9, pp. 6720–6735. DOI: https://doi.org/10.1029/2018JC013842.

Dombret, Jeanne et al. (2025). "Data-based estimates of ocean carbon uptake biased high from neglect of submonthly atmospheric pressure variability." In: DOI: 10.22541/essoar.175308893.36793607/v1.

Doney, Scott C., Victoria J. Fabry, Richard A. Feely, and Joan A. Kleypas (2009). "Ocean Acidification: The Other CO_2 Problem." In: *Annual Review of Marine Science* 1.Volume 1, 2009, pp. 169–192. ISSN: 1941-0611. DOI: https://doi.org/10.1146/annurev.marine.010908.163834.

Dong, Yuanxu, Dorothee C. E. Bakker, Thomas G. Bell, Mingxi Yang, Peter Landschützer, Judith Hauck, Christian Rödenbeck, Vassilis Kitidis, Seth M. Bushinsky, and Peter S. Liss (2024a). "Direct observational evidence of strong CO_2 uptake in the Southern Ocean." In: *Science Advances* 10.30. Publisher: American Association for the Advancement of Science, eadn5781. DOI: 10.1126/sciadv.adn5781.

Dong, Yuanxu, Dorothee C. E. Bakker, and Peter Landschützer (2024b). "Accuracy of Ocean CO_2 Uptake Estimates at a Risk by a Reduction in the Data Collection." In: *Geophysical Research Letters* 51.9, e2024GL108502. ISSN: 1944-8007. DOI: 10.1029/2024GL108502.

Dufois, François, Nick J. Hardman-Mountford, Jim Greenwood, Anthony J. Richardson, Ming Feng, Steven Herbette, and Richard Matear (2014). "Impact of eddies on surface chlorophyll in the South Indian Ocean." In: *Journal of Geophysical Research: Oceans* 119.11, pp. 8061–8077. DOI: https://doi.org/10.1002/2014JC010164.

Dufois, François, Nick J. Hardman-Mountford, Jim Greenwood, Anthony J. Richardson, Ming Feng, and Richard J. Matear (2016). "Anticyclonic eddies are more productive than cyclonic eddies in subtropical gyres because of winter mixing." In: *Science Advances* 2.5, e1600282. DOI: 10.1126/sciadv.1600282.

Duke, P. J., R. C. Hamme, D. Ianson, P. Landschützer, M. M. M. Ahmed, N. C. Swart, and P. A. Covert (2023). "Estimating marine carbon uptake in the northeast Pacific using a neural network approach." In: *Biogeosciences* 20.18, pp. 3919–3941. DOI: 10.5194/bg-20-3919-2023. URL: https://bg.copernicus.org/articles/20/3919/2023/.

Duke, P. J., R. C. Hamme, D. Ianson, P. Landschützer, N. C. Swart, and P. A. Covert (2024). "High-Resolution Neural Network Demonstrates Strong CO_2 Source-Sink Juxtaposition in the Coastal Zone." In: *Journal of Geophysical Research: Oceans* 129.7, e2024JC021134. DOI: https://doi.org/10.1029/2024JC021134.

Fay, A. R. and G. A. McKinley (2014). "Global open-ocean biomes: mean and temporal variability." In: *Earth System Science Data* 6.2, pp. 273–284. DOI: 10.5194/essd-6-273-2014. URL: https://essd.copernicus.org/articles/6/273/2014/.

— (2021). "Observed Regional Fluxes to Constrain Modeled Estimates of the Ocean Carbon Sink." In: *Geophysical Research Letters* 48.20, e2021GL095325. ISSN: 1944-8007. DOI: 10.1029/2021GL095325.

Fay, A. R., D. R. Munro, G. A. McKinley, D. Pierrot, S. C. Sutherland, C. Sweeney, and R. Wanninkhof (2024). "Updated climatological mean ΔfCO_2 and net sea–air CO_2 flux over the global open ocean regions." In: *Earth System Science Data* 16.4, pp. 2123–2139. DOI: 10.5194/essd-16-2123-2024.

Fay, Amanda R., Thea Hatlen Heimdal, Viviana Acquaviva, Abby P. Shaum, and Galen A. McKinley (2025). "Sensitivity of ocean carbon sink estimates to rare observations." In: preprint. URL: https://www.authorea.com/users/529535/articles/1288775-sensitivity-of-ocean-carbon-sink-estimates-to-rare-observations (visited on 05/12/2025).

Fay, Amanda R, Nicole S Lovenduski, Galen A McKinley, David R Munro, Colm Sweeney, Alison R Gray, Peter Landschützer, Britton B Stephens, Taro Takahashi, and Nancy Williams (2018). "Utilizing the Drake Passage Time-series to understand variability and change in subpolar Southern Ocean pCO_2." In: *Biogeosciences* 15.12, pp. 3841–3855.

Fay, Amanda R. and Galen A. McKinley (2017). "Correlations of surface ocean pCO_2 to satellite chlorophyll on monthly to interannual timescales." In: *Global Biogeochemical Cycles* 31.3, pp. 436–455. ISSN: 1944-9224. DOI: 10.1002/2016GB005563.

Fay, Amanda R. et al. (2021). "SeaFlux: harmonization of air–sea CO_2 fluxes from surface pCO_2 data products using a standardized approach." In: *Earth System Science Data* 13.10. Publisher: Copernicus GmbH, pp. 4693–4710. ISSN: 1866-3508. DOI: 10.5194/essd-13-4693-2021.

Foote, Eunice (1856). "Circumstances Affecting the Heat of Sun's Rays." In: *American Journal of Art and Science*. 2nd Series XXII.LXVI, pp. 382–383.

Ford, Daniel J., Josh Blannin, Jennifer Watts, Andrew J. Watson, Peter Landschützer, Annika Jersild, and Jamie D. Shutler (2024). "A Comprehensive Analysis of Air-Sea CO_2 Flux Uncertainties Constructed From Surface Ocean Data Products." In: *Global Biogeochemical Cycles* 38.11, e2024GB008188. ISSN: 1944-9224. DOI: 10.1029/2024GB008188.

Ford, Daniel J., Gavin H. Tilstone, Jamie D. Shutler, Vassilis Kitidis, Katy L. Sheen, Giorgio Dall'Olmo, and Iole B. M. Orselli (2023). "Mesoscale Eddies Enhance the Air-Sea CO_2 Sink in the South Atlantic Ocean." In: *Geophysical Research Letters* 50.9, e2022GL102137. DOI: https://doi.org/10.1029/2022GL102137.

Frankignoulle, Michel, Christine Canon, and Jean-Pierre Gattuso (1994). "Marine calcification as a source of carbon dioxide: Positive feedback of increasing atmospheric CO_2." In: *Limnology and Oceanography* 39.2, pp. 458–462. DOI: https://doi.org/10.4319/lo.1994.39.2.0458.

Friedlingstein, P. et al. (2022). "Global Carbon Budget 2022." In: *Earth System Science Data* 14.11, pp. 4811–4900. DOI: 10.5194/essd-14-4811-2022.

Friedlingstein, P. et al. (2025). "Global Carbon Budget 2024." In: *Earth System Science Data* 17.3, pp. 965–1039. DOI: 10.5194/essd-17-965-2025.

Friedrich, T. and A. Oschlies (2009). "Neural network-based estimates of North Atlantic surface pCO_2 from satellite data: A methodological study." In: *Journal of Geophysical Research: Oceans* 114.C3. DOI: https://doi.org/10.1029/2007JC004646.

Frölicher, Thomas L, Erich M Fischer, and Nicolas Gruber (2018). "Marine heatwaves under global warming." In: *Nature* 560.7718, pp. 360–364.

Frölicher, Thomas L., Jorge L. Sarmiento, David J. Paynter, John P. Dunne, John P. Krasting, and Michael Winton (2015). "Dominance of the Southern Ocean in Anthropogenic Carbon and Heat Uptake in CMIP5 Models." In: *Journal of Climate* 28.2, pp. 862–886. ISSN: 0894-8755, 1520-0442. DOI: 10.1175/JCLI-D-14-00117.1.

Gallego, M. A., A. Timmermann, T. Friedrich, and R. E. Zeebe (2018). "Drivers of future seasonal cycle changes in oceanic pCO_2." In: *Biogeosciences* 15.17, pp. 5315–5327. DOI: 10.5194/bg-15-5315-2018.

Garcia-Soto, Carlos and Robin D. Pingree (2009). "Spring and summer blooms of phytoplankton (SeaWiFS/MODIS) along a ferry line in the Bay of Biscay and western English Channel." In: *Continental Shelf Research* 29.8, pp. 1111–1122. ISSN: 0278-4343. DOI: https://doi.org/10.1016/j.csr.2008.12.012.

Garcia, Carlos Alberto Eiras, Virginia Maria Tavano Garcia, Ana Inés Dogliotti, Amábile Ferreira, Silvia I. Romero, Antonio Mannino, Marcio S. Souza, and

Mauricio M. Mata (2011). "Environmental conditions and bio-optical signature of a coccolithophorid bloom in the Patagonian shelf." In: *Journal of Geophysical Research: Oceans* 116.C3. ISSN: 2156-2202. DOI: 10.1029/2010JC006595.

Garcia, Virginia M.T., Carlos A.E. Garcia, Mauricio M. Mata, Ricardo C. Pollery, Alberto R. Piola, Sergio R. Signorini, Charles R. McClain, and M. Débora Iglesias-Rodriguez (2008). "Environmental factors controlling the phytoplankton blooms at the Patagonia shelf-break in spring." In: *Deep Sea Research Part I: Oceanographic Research Papers* 55.9, pp. 1150–1166. ISSN: 0967-0637. DOI: https://doi.org/10.1016/j.dsr.2008.04.011.

Gaube, Peter, Dudley B Chelton, Peter G Strutton, and Michael J Behrenfeld (2013). "Satellite observations of chlorophyll, phytoplankton biomass, and Ekman pumping in nonlinear mesoscale eddies." In: *Journal of Geophysical Research: Oceans* 118.12, pp. 6349–6370. DOI: https://doi.org/10.1002/2013JC009027.

Gil, Mónica Noemí et al. (2019). "Chapter 34 - Southern Argentina: The Patagonian Continental Shelf." In: *World Seas: an Environmental Evaluation (Second Edition)*. Ed. by Charles Sheppard. Academic Press, pp. 783–811. ISBN: 978-0-12-805068-2. DOI: 10.1016/B978-0-12-805068-2.00040-1.

Gkritzalis, T., D.C.E. Bakker, S.K. Lauvset, and T. Steinhoff (2024). *SOCAT Quality Control Cookbook for version 2025 of the Surface Ocean CO_2 Atlas*. URL: https://socat.info/wp-content/uploads/2025/01/2024_SOCAT_QC_Cookbook_Update.pdf.

Gloege, L. and M. D. Eisaman (2025). "Regional Uncertainty Analysis in the Air–Sea CO_2 Flux." In: *Earth and Space Science* 12.6, e2024EA004032. DOI: https://doi.org/10.1029/2024EA004032.

Gloege, L., M. Yan, T. Zheng, and G. A. McKinley (2022). "Improved Quantification of Ocean Carbon Uptake by Using Machine Learning to Merge Global Models and pCO_2 Data." In: *Journal of Advances in Modeling Earth Systems* 14.2, e2021MS002620. DOI: https://doi.org/10.1029/2021MS002620.

Gloege, Lucas et al. (2021). "Quantifying Errors in Observationally Based Estimates of Ocean Carbon Sink Variability." In: *Global Biogeochemical Cycles* 35.4, e2020GB006788. ISSN: 1944-9224. DOI: 10.1029/2020GB006788.

Good, Simon A., Matthew J. Martin, and Nick A. Rayner (2013). "EN4: Quality controlled ocean temperature and salinity profiles and monthly objective analyses with uncertainty estimates." In: *Journal of Geophysical Research: Oceans* 118.12, pp. 6704–6716. DOI: https://doi.org/10.1002/2013JC009067.

Gray, Alison R. (2024). "The Four-Dimensional Carbon Cycle of the Southern Ocean." In: *Annual Review of Marine Science* 16.Volume 16, 2024. Publisher:

Annual Reviews Type: Journal Article, pp. 163–190. ISSN: 1941-0611. DOI: https://doi.org/10.1146/annurev-marine-041923-104057.

Gray, Alison R., Kenneth S. Johnson, Seth M. Bushinsky, Stephen C. Riser, Joellen L. Russell, Lynne D. Talley, Rik Wanninkhof, Nancy L. Williams, and Jorge L. Sarmiento (2018). "Autonomous Biogeochemical Floats Detect Significant Carbon Dioxide Outgassing in the High-Latitude Southern Ocean." In: *Geophysical Research Letters* 45.17, pp. 9049–9057. ISSN: 1944-8007. DOI: 10.1029/2018GL078013.

Gregor, L., A. D. Lebehot, S. Kok, and P. M. Scheel Monteiro (2019). "A comparative assessment of the uncertainties of global surface ocean CO_2 estimates using a machine-learning ensemble (CSIR-ML6 version 2019a) – have we hit the wall?" In: *Geoscientific Model Development* 12.12, pp. 5113–5136. DOI: 10.5194/gmd-12-5113-2019.

Gregor, Luke and Nicolas Gruber (2021). "OceanSODA-ETHZ: a global gridded data set of the surface ocean carbonate system for seasonal to decadal studies of ocean acidification." In: *Earth System Science Data* 13.2, pp. 777–808. ISSN: 1866-3508. DOI: 10.5194/essd-13-777-2021.

Gregor, Luke and Jens Daniel Müller (2025). *RECCAP2 Regional Masks*. URL: https://github.com/RECCAP2-ocean/R2-shared-resources/blob/master/data/regions/RECCAP2_region_masks_all_v20221025.nc.

Gregor, Luke, Jamie Shutler, and Nicolas Gruber (2024). "High-Resolution Variability of the Ocean Carbon Sink." In: *Global Biogeochemical Cycles* 38.8, e2024GB008127. DOI: https://doi.org/10.1029/2024GB008127.

Gruber, Nicolas, Dorothee C. E. Bakker, Tim DeVries, Luke Gregor, Judith Hauck, Peter Landschützer, Galen A. McKinley, and Jens Daniel Müller (2023). "Trends and variability in the ocean carbon sink." In: *Nature Reviews Earth and Environment* 4, pp. 119–134. ISSN: 2662-138X. DOI: 10.3929/ethz-b-000595538.

Guidi, L. et al. (2020). "Big Data in Marine Science." In: Future Science Brief 6 of the European Marine Board. Ed. by S. JJ Heymans, B. Alexander, Á. Muñiz Piniella, P. Kellett, and J. Coopman. DOI: 10.5281/zenodo.3755793.

Guinder, Valeria, Carola Ferronato, Ana Dogliotti, Valeria Segura, and Vivian Lutz (2025). "The phytoplankton of the Patagonian Shelf-Break Front." In: preprint. URL: https://www.authorea.com/users/641655/articles/655938-the-phytoplankton-of-the-patagonian-shelf-break-front.

Guo, Yiming, Scott Bachman, Frank Bryan, and Stuart Bishop (2022). "Increasing trends in oceanic surface poleward eddy heat flux observed over the past three decades." In: *Geophysical Research Letters* 49.16, e2022GL099362.

Guo, Yiming and Mary-Louise Timmermans (2024a). "Global ocean pCO_2 variation regimes: Spatial patterns and the emergence of a hybrid regime." In: *Journal of Geophysical Research: Oceans* 129.5, e2023JC020679.

— (2024b). "The Role of Ocean Mesoscale Variability in Air-Sea CO_2 Exchange: A Global Perspective." In: *Geophysical Research Letters* 51.10, e2024GL108373. ISSN: 1944-8007. DOI: 10.1029/2024GL108373.

Hammermeister, Emily M., Stathys Papadimitriou, Martin Arundell, Jake Ludgate, Allison Schaap, Matthew C. Mowlem, Sara E. Fowell, Edward Chaney, and Socratis Loucaides (2025). "New Capability in Autonomous Ocean Carbon Observations Using the Autosub Long-Range AUV Equipped with Novel pH and Total Alkalinity Sensors." In: *Environmental Science & Technology*. Publisher: American Chemical Society. ISSN: 0013-936X. DOI: 10.1021/acs.est.4c10139.

Harlay, J. et al. (2010). "Biogeochemical study of a coccolithophore bloom in the northern Bay of Biscay (NE Atlantic Ocean) in June 2004." In: *Progress in Oceanography* 86.3, pp. 317–336. ISSN: 0079-6611. DOI: https://doi.org/10.1016/j.pocean.2010.04.029.

Hassoun, Abed El Rahman, Toste Tanhua, Inga Lips, Emma Heslop, George Petihakis, and Johannes Karstensen (2024). "The European Ocean Observing Community: urgent gaps and recommendations to implement during the UN Ocean Decade." In: *Frontiers in Marine Science* 11. ISSN: 2296-7745. DOI: 10.3389/fmars.2024.1394984.

Hauck, Judith, Cara Nissen, Peter Landschützer, Christian Rödenbeck, Seth Bushinsky, and Are Olsen (2023). "Sparse observations induce large biases in estimates of the global ocean CO_2 sink: an ocean model subsampling experiment." In: *Philosophical Transactions of the Royal Society A: Mathematical, Physical and Engineering Sciences* 381.2249, p. 20220063. DOI: 10.1098/rsta.2022.0063.

Hauck, Judith et al. (2020). "Consistency and Challenges in the Ocean Carbon Sink Estimate for the Global Carbon Budget." In: *Frontiers in Marine Science* 7. ISSN: 2296-7745. DOI: 10.3389/fmars.2020.571720.

Heimdal, T. H., G. A. McKinley, A. J. Sutton, A. R. Fay, and L. Gloege (2024). "Assessing improvements in global ocean pCO_2 machine learning reconstructions with Southern Ocean autonomous sampling." In: *Biogeosciences* 21.8, pp. 2159–2176. DOI: 10.5194/bg-21-2159-2024.

Heimdal, Thea H. and Galen A. McKinley (2024). "The importance of adding unbiased Argo observations to the ocean carbon observing system." In: *Scientific Reports* 14.1, p. 19763. ISSN: 2045-2322. DOI: 10.1038/s41598-024-70617-x.

Heinze, C., E. Maier-Reimer, A. M. E. Winguth, and D. Archer (1999). "A global oceanic sediment model for long-term climate studies." In: *Global Biogeochemical Cycles* 13.1, pp. 221–250. ISSN: 1944-9224. DOI: 10.1029/98GB02812.

Henson, Stephanie, Kelsey Bisson, Matthew L. Hammond, Adrian Martin, Colleen Mouw, and Andrew Yool (2024). "Effect of sampling bias on global estimates of ocean carbon export." In: *Environmental Research Letters* 19.2. Publisher: IOP Publishing, p. 024009. DOI: 10.1088/1748-9326/ad1e7f. URL: https://dx.doi.org/10.1088/1748-9326/ad1e7f.

Hernani, Maider, Nicolas Werner-Pelletier, Marta Umbert, Nina Hoareau, Anna Olivé-Abelló, and Jordi Salat (2025). "Inter-annual hydrographic changes in the Southern Ocean: analysis of Vendée Globe Race and Barcelona World Race data." In: *Antarctic Science*, pp. 1–18. DOI: 10.1017/S0954102025100138.

Hersbach, H. et al. (2023). *ERA5 hourly data on single levels from 1940 to present.* data set. DOI: 10.24381/cds.adbb2d47.

Hewitt, Helene, Baylor Fox-Kemper, Brodie Pearson, Malcolm Roberts, and Daniel Klocke (2022). "The small scales of the ocean may hold the key to surprises." In: *Nature Climate Change* 12, pp. 496–499. DOI: 10.1038/s41558-022-01386-6.

Hohenegger, C. et al. (2023). "ICON-Sapphire: simulating the components of the Earth system and their interactions at kilometer and subkilometer scales." In: *Geoscientific Model Development* 16.2, pp. 779–811. DOI: 10.5194/gmd-16-779-2023.

Hohensee, Dorothee (2017). "Vergleich von pCO_2 Sensoren für die Oberfläche des Ozeans - Eine Wirtschaftlichkeitsuntersuchung." MA thesis. Christian-Albrechts-Universität Kiel. URL: https://oceanrep.geomar.de/id/eprint/40887/.

Hood, E. M. and L. Merlivat (2001). "Annual to interannual variations of fCO_2 in the northwestern Mediterranean Sea: Results from hourly measurements made by CARIOCA buoys, 1995–1997." In: *Journal of Marine Research* 59.1, pp. 113–131. DOI: 10.1357/002224001321237399.

Hopkins, Jason, Stephanie A. Henson, Stuart C. Painter, Toby Tyrrell, and Alex J. Poulton (2015). "Phenological characteristics of global coccolithophore blooms." In: *Global Biogeochemical Cycles* 29.2. Publisher: John Wiley & Sons, Ltd, pp. 239–253. ISSN: 0886-6236. DOI: 10.1002/2014GB004919.

Huang, Boyin, Chunying Liu, Viva Banzon, Eric Freeman, Garrett Graham, Bill Hankins, Tom Smith, and Huai-Min Zhang (2021). "Improvements of the Daily Optimum Interpolation Sea Surface Temperature (DOISST) Version 2.1." In: *Journal of Climate* 34.8. Publisher: American Meteorological Society

Section: Journal of Climate, pp. 2923–2939. ISSN: 0894-8755, 1520-0442. DOI: 10.1175/JCLI-D-20-0166.1.

IMOCA (2024). *The IMOCA sailors – key contributors to global oceanographic science*. Press release, published October 23, 2024. Accessed on 20-Jun-2025. URL: https://www.imoca.org/en/news/news/the-imoca-sailors-key-contributors-to-global-oceanographic-science.

IOCCP (2024). *Declaration on Operationalising the Surface Ocean Carbon Value Chain*. URL: http://www.ioccp.org/images/Gnews/Declaration_on_Operationalising_the_Surface_Ocean_Carbon_Value_Chain.pdf (visited on 04/27/2025).

Iida, Yosuke, Yusuke Takatani, Atsushi Kojima, and Masao Ishii (2021). "Global trends of ocean CO_2 sink and ocean acidification: an observation-based reconstruction of surface ocean inorganic carbon variables." In: *Journal of Oceanography* 77.2, pp. 323–358. ISSN: 1573-868X. DOI: 10.1007/s10872-020-00571-5.

Ilyina, Tatiana, Katharina D. Six, Joachim Segschneider, Ernst Maier-Reimer, Hongmei Li, and Ismael Núñez-Riboni (2013). "Global ocean biogeochemistry model HAMOCC: Model architecture and performance as component of the MPI-Earth system model in different CMIP5 experimental realizations." In: *Journal of Advances in Modeling Earth Systems* 5.2, pp. 287–315. ISSN: 1942-2466. DOI: 10.1029/2012MS000178.

Intergovernmental Panel on Climate Change (2023). *AR6 Synthesis Report: Climate Change 2023*. URL: https://www.ipcc.ch/report/sixth-assessment-report-cycle/.

Jersild, A. (2023). *SOMFFN (version 2022)*. URL: https://github.com/aljersild/SOMFFNv2022.

Jersild, Annika, Sara Delawalla, and Takamitsu Ito (2021). "Mesoscale Eddies Regulate Seasonal Iron Supply and Carbon Drawdown in the Drake Passage." In: *Geophysical Research Letters* 48.24, e2021GL096020. DOI: https://doi.org/10.1029/2021GL096020.

Jersild, Annika and Peter Landschützer (2024). "A Spatially Explicit Uncertainty Analysis of the Air-Sea CO_2 Flux From Observations." In: *Geophysical Research Letters* 51.4, e2023GL106636. DOI: https://doi.org/10.1029/2023GL106636.

Jiang, L.-Q. et al. (2025). "Synthesis of data products for ocean carbonate chemistry." In: *Earth System Science Data Discussions* 2025, pp. 1–72. DOI: 10.5194/essd-2025-255.

Jiang, Zong-Pei, Jiajun Yuan, Susan E. Hartman, and Wei Fan (2019). "Enhancing the observing capacity for the surface ocean by the use of Volunteer

Observing Ship." In: *Acta Oceanologica Sinica* 38.7, pp. 114–120. ISSN: 1869-1099. DOI: 10.1007/s13131-019-1463-3.

Jin, Di, Porter Hoagland, and Ken O. Buesseler (2020). "The value of scientific research on the ocean's biological carbon pump." In: *Science of The Total Environment* 749, p. 141357. ISSN: 0048-9697. DOI: https://doi.org/10.1016/j.scitotenv.2020.141357.

Johnson, Kenneth S. et al. (2017). "Biogeochemical sensor performance in the SOCCOM profiling float array." In: *Journal of Geophysical Research: Oceans* 122.8, pp. 6416–6436. ISSN: 2169-9291. DOI: 10.1002/2017JC012838.

Jones, Elizabeth M. et al. (2017). "Mesoscale features create hotspots of carbon uptake in the Antarctic Circumpolar Current." In: *Deep Sea Research Part II: Topical Studies in Oceanography* 138, pp. 39–51. ISSN: 0967-0645. DOI: https://doi.org/10.1016/j.dsr2.2015.10.006.

Kahl, Lucía C., Alejandro A. Bianchi, Ana Paula Osiroff, Diana Ruiz Pino, and Alberto R. Piola (2017). "Distribution of sea-air CO_2 fluxes in the Patagonian Sea: Seasonal, biological and thermal effects." In: *Continental Shelf Research* 143, pp. 18–28. ISSN: 0278-4343. DOI: 10.1016/j.csr.2017.05.011.

Kalnay, E. et al. (1996). "The NCEP/NCAR 40-year reanalysis project." In: *Bulletin of the American Meteorological Society* 77, pp. 437–470. URL: https://www.cpc.ncep.noaa.gov/products/wesley/reanalysis.html.

Karl, David M. and Roger Lukas (1996). "The Hawaii Ocean Time-series (HOT) program: Background, rationale and field implementation." In: *Deep Sea Research Part II: Topical Studies in Oceanography* 43.2, pp. 129–156. ISSN: 0967-0645. DOI: https://doi.org/10.1016/0967-0645(96)00005-7.

Keeling, C. D., N. W. Rakestraw, and L. S. Waterman (1965). "Carbon Dioxide in Surface Waters of the Pacific Ocean 1. Measurements of the Distribution." In: *Journal of Geophysical Research* 70, pp. 6087–6097.

Keeling, C. D. and L. S. Waterman (1968). "Carbon Dioxide in Surface Ocean Waters 3. Measurements on Lusiad Expedition 1962-63." In: *Journal of Geophysical Research* 73, pp. 4529–4541.

Kelly, K.J., A.A. Larkin, D. Munro, E. Ombres, L. Wright-Fairbanks, R.A. Feely, S. Clevenger, E. Keister, and K. Tedesco (2025). *NOAA Oceanic and Atmospheric Research Ocean Carbon Observing Science Plan FY25 to FY30*. NOAA Special Report. Washington DC: NOAA. URL: https://doi.org/10.25923/g4z3-b739.

Keppler, Lydia, Yassir A. Eddebbar, Sarah T. Gille, Nicola Guisewhite, Matthew R. Mazloff, Veronica Tamsitt, Ariane Verdy, and Lynne D. Talley (2024). "Effects of Mesoscale Eddies on Southern Ocean Biogeochemistry." In: *AGU Advances* 5.6, e2024AV001355. ISSN: 2576-604X. DOI: 10.1029/2024AV001355.

Kim, Dongseon, Seon-Eun Lee, Sosul Cho, Dong-Jin Kang, Geun-Ha Park, and Sok Kuh Kang (2022). "Mesoscale eddy effects on sea-air CO_2 fluxes in the northern Philippine Sea." In: *Frontiers in Marine Science* Volume 9 - 2022. ISSN: 2296-7745. DOI: 10.3389/fmars.2022.970678.

Kim, YS and AH Orsi (2014). "On the variability of Antarctic Circumpolar Current fronts inferred from 1992–2011 altimetry." In: *Journal of Physical Oceanography* 44.12, pp. 3054–3071.

Lan, X., P. Tans, and K. W. Thoning (2024). *Trends in globally-averaged CO_2 determined from NOAA Global Monitoring Laboratory measurements, Version 2024-09*. [data set]. URL: https://gml.noaa.gov/ccgg/trends/global.html (visited on 01/21/2025).

Landschützer, P., N. Gruber, D. C. E. Bakker, and U. Schuster (2014). "Recent variability of the global ocean carbon sink." In: *Global Biogeochemical Cycles* 28.9, pp. 927–949. ISSN: 1944-9224. DOI: 10.1002/2014GB004853.

Landschützer, P., N. Gruber, D. C. E. Bakker, U. Schuster, S. Nakaoka, M. R. Payne, T. P. Sasse, and J. Zeng (2013). "A neural network-based estimate of the seasonal to inter-annual variability of the Atlantic Ocean carbon sink." In: *Biogeosciences* 10.11, pp. 7793–7815. ISSN: 1726-4170. DOI: 10.5194/bg-10-7793-2013.

Landschützer, Peter, Nicolas Gruber, and Dorothee C. E. Bakker (2016). "Decadal variations and trends of the global ocean carbon sink." In: *Global Biogeochemical Cycles* 30.10, pp. 1396–1417. ISSN: 1944-9224. DOI: 10.1002/2015GB005359.

Landschützer, Peter, Goulven G. Laruelle, Alizee Roobaert, and Pierre Regnier (2020). "A uniform pCO_2 climatology combining open and coastal oceans." In: *Earth System Science Data* 12.4. Publisher: Copernicus GmbH, pp. 2537–2553. ISSN: 1866-3508. DOI: 10.5194/essd-12-2537-2020.

Landschützer, Peter, Toste Tanhua, Jacqueline Behncke, and Lydia Keppler (2023). "Sailing through the southern seas of air-sea CO_2 flux uncertainty." In: *Philosophical Transactions of the Royal Society A: Mathematical, Physical and Engineering Sciences* 381.2249, p. 20220064. DOI: 10.1098/rsta.2022.0064.

Laruelle, G. G., P. Landschützer, N. Gruber, J.-L. Tison, B. Delille, and P. Regnier (2017). "Global high-resolution monthly pCO_2 climatology for the coastal ocean derived from neural network interpolation." In: *Biogeosciences* 14.19, pp. 4545–4561. DOI: 10.5194/bg-14-4545-2017.

Lauvset, S. K. et al. (2024). "The annual update GLODAPv2.2023: the global interior ocean biogeochemical data product." In: *Earth System Science Data* 16.4, pp. 2047–2072. DOI: 10.5194/essd-16-2047-2024.

Lauvset, S., K. Currie, N. Metzl, SI. Nakaoka, D. Bakker, K. Sullivan, A. Sutton, K. O'Brien, and A. Olsen (2018). *SOCAT Quality Control Cookbook*. URL: https://socat.info/wp-content/uploads/2020/12/2018_SOCAT_QC_Cookbook_final_with-v2021-contact-details.pdf.

Le Quéré, C. et al. (2014). "Global carbon budget 2013." In: *Earth System Science Data* 6.1, pp. 235–263. DOI: 10.5194/essd-6-235-2014.

Le Quéré, C. et al. (2015). "Global carbon budget 2014." In: *Earth System Science Data* 7.1, pp. 47–85. DOI: 10.5194/essd-7-47-2015.

Le Quéré, Corinne et al. (2007). "Saturation of the Southern Ocean CO_2 sink due to recent climate change." In: *Science* 316.5832, pp. 1735–1738. ISSN: 0036-8075. DOI: 10.1126/science.1136188.

Lebling, Katie, Eliza Northrop, Colin McCormick, and Elizabeth Bridgwater (2022). "Towards Responsible and Informed Ocean-Based Carbon Dioxide Removal: Research and Governance Priorities." In: *World Resources Institute*. DOI: 10.46830/wrirpt.21.00090.

Lefévre, Nathalie, Andrew J. Watson, and Adam R. Watson (2005). "A comparison of multiple regression and neural network techniques for mapping in situ pCO_2 data." In: *Tellus B: Chemical and Physical Meteorology* 57.5, pp. 375–384. ISSN: null. DOI: 10.3402/tellusb.v57i5.16565.

Leseurre, Coraline, Claire Lo Monaco, Gilles Reverdin, Nicolas Metzl, Jonathan Fin, Claude Mignon, and Léa Benito (2022). "Summer trends and drivers of sea surface fCO_2 and pH changes observed in the southern Indian Ocean over the last two decades (1998–2019)." In: *Biogeosciences* 19.10, pp. 2599–2625. ISSN: 1726-4170. DOI: 10.5194/bg-19-2599-2022. (Visited on 11/26/2024).

Levitus, Sydney, Tim P. Boyer, and et al. (2009). *World Ocean Atlas 2009*. https://accession.nodc.noaa.gov/0094866. NOAA National Centers for Environmental Information. Dataset.

Li, Hongmei, Tatiana Ilyina, Tammas Loughran, Aaron Spring, and Julia Pongratz (2023). "Reconstructions and predictions of the global carbon budget with an emission-driven Earth system model." In: *Earth System Dynamics* 14.1. Publisher: Copernicus GmbH, pp. 101–119. ISSN: 2190-4979. DOI: 10.5194/esd-14-101-2023.

Li, Xueyin, Bolan Gan, Zhengguang Zhang, Zhimian Cao, Bo Qiu, Zhaohui Chen, and Lixin Wu (2025). "Oceanic uptake of CO_2 enhanced by mesoscale eddies." In: *Science Advances* 11.24, eadt4195. DOI: 10.1126/sciadv.adt4195.

Liu, Bo, Katharina D. Six, and Tatiana Ilyina (2021). "Incorporating the stable carbon isotope ^{13}C in the ocean biogeochemical component of the Max Planck Institute Earth System Model." In: *Biogeosciences* 18.14. Publisher: Copernicus GmbH, pp. 4389–4429. ISSN: 1726-4170. DOI: 10.5194/bg-18-4389-2021.

Liu, Xiaoke, Huisheng Wu, Yanguo Fan, Yunlong Ji, Wenliang Zhou, Lejie Wang, and Long Cui (2025). "The impact of long-lived cycle mesoscale eddies on air–sea CO_2 flux in the South Atlantic: focus on the full life cycle of the eddy." In: *Environmental Research Letters* 20.3, p. 034033. DOI: 10.1088/1748-9326/adb59d.

Liu, Yingjie, Xiaofeng Li, Chuanyu Liu, and Qian Liu (2024). "Transitions in surface thermal signatures during the evolution of long-lived eddies in the global ocean." In: *Deep Sea Research Part I: Oceanographic Research Papers* 206, p. 104279. ISSN: 0967-0637. DOI: https://doi.org/10.1016/j.dsr.2024.104279.

Long, Matthew et al. (2021). "Strong Southern Ocean carbon uptake evident in airborne observations." In: *Science (New York, N.Y.)* 374, pp. 1275–1280. DOI: 10.1126/science.abi4355.

Lueger, H., R. Wanninkhof, A. Olsen, J. Triñanes, T. Johannessen, Douglas W.R. Wallace, and Arne Körtzinger (2008). "The sea-air CO_2 flux in the North Atlantic estimated from satellite and Argo profiling data." In: OAR AOML-96. Place: Miami, FL., USA Publisher: Atlantic Oceanographic and Meteorological Laboratory Type: NOAA Technical Memorandum, p. 28.

Lüger, Heike, Douglas W. R. Wallace, Arne Körtzinger, and Yukihiro Nojiri (2004). "The pCO_2 variability in the midlatitude North Atlantic Ocean during a full annual cycle." In: *Global Biogeochemical Cycles* 18.3. DOI: https://doi.org/10.1029/2003GB002200.

Macovei, Vlad A, Susan E Hartman, Ute Schuster, Sinhué Torres-Valdés, C Mark Moore, and Richard J Sanders (2020). "Impact of physical and biological processes on temporal variations of the ocean carbon sink in the mid-latitude North Atlantic (2002–2016)." In: *Progress in Oceanography* 180, p. 102223.

Maerz, Joeran, Katharina D. Six, Irene Stemmler, Soeren Ahmerkamp, and Tatiana Ilyina (2020). "Microstructure and composition of marine aggregates as co-determinants for vertical particulate organic carbon transfer in the global ocean." In: *Biogeosciences* 17.7. Publisher: Copernicus GmbH, pp. 1765–1803. ISSN: 1726-4170. DOI: 10.5194/bg-17-1765-2020.

Majkut, Joseph D., Brendan R. Carter, Thomas L. Frölicher, Carolina O. Dufour, Keith B. Rodgers, and Jorge L. Sarmiento (2014). "An observing system simulation for Southern Ocean carbon dioxide uptake." In: *Philosophical Transactions of the Royal Society A: Mathematical, Physical and Engineering Sciences* 372.2019, p. 20130046. DOI: 10.1098/rsta.2013.0046.

Manley, Justin and Scott Willcox (2010). "The Wave Glider: A persistent platform for ocean science." In: *OCEANS'10 IEEE SYDNEY*, pp. 1–5. DOI: 10.1109/OCEANSSYD.2010.5603614.

Mauritsen, Thorsten et al. (2019). "Developments in the MPI-M Earth System Model version 1.2 (MPI-ESM1.2) and Its Response to Increasing CO_2." In: *Journal of Advances in Modeling Earth Systems* 11.4, pp. 998–1038. DOI: https://doi.org/10.1029/2018MS001400.

Mayot, N. et al. (2023). "Climate-driven variability of the Southern Ocean CO_2 sink." In: *Philosophical Transactions of the Royal Society A: Mathematical, Physical and Engineering Sciences* 381.2249. Publisher: Royal Society, p. 20220055. DOI: 10.1098/rsta.2022.0055.

McGillicuddy, D. J. and A. R. Robinson (1997). "Eddy-induced nutrient supply and new production in the Sargasso Sea." In: *Deep Sea Research Part I: Oceanographic Research Papers* 44.8, pp. 1427–1450. ISSN: 0967-0637. DOI: https://doi.org/10.1016/S0967-0637(97)00024-1.

McKinley, Galen A., Amanda R. Fay, Yassir A. Eddebbar, Lucas Gloege, and Nicole S. Lovenduski (2020). "External Forcing Explains Recent Decadal Variability of the Ocean Carbon Sink." In: *AGU Advances* 1.2, e2019AV000149. DOI: https://doi.org/10.1029/2019AV000149.

McQuatters-Gollop, Abigail, D.E. Raitsos, Martin Edwards, and Martin Attrill (2007). "Spatial patterns of diatoms and dinoflagellate seasonal cycles in the North - East Atlantic Ocean." In: *Marine Ecology Progress Series* 339, pp. 301–306.

Meinig, Christian et al. (2019). "Public–Private Partnerships to Advance Regional Ocean-Observing Capabilities: A Saildrone and NOAA-PMEL Case Study and Future Considerations to Expand to Global Scale Observing." In: *Frontiers in Marine Science* 6. ISSN: 2296-7745. DOI: 10.3389/fmars.2019.00448.

Meredith, Michael P., Jon L. Watkins, Eugene J. Murphy, Nathan J. Cunningham, Andrew G. Wood, Rebecca Korb, Mick J. Whitehouse, Sally E. Thorpe, and Frédéric Vivier (2003). "An anticyclonic circulation above the Northwest Georgia Rise, Southern Ocean." In: *Geophysical Research Letters* 30.20. DOI: https://doi.org/10.1029/2003GL018039.

Mikaloff Fletcher, Sara E, Nicolas Gruber, Andrew R Jacobson, Scott C Doney, Stephanie Dutkiewicz, Markus Gerber, M Follows, Fortunat Joos, Keith Lindsay, D Menemenlis, et al. (2006). "Inverse estimates of anthropogenic CO_2 uptake, transport, and storage by the ocean." In: *Global biogeochemical cycles* 20.2.

Mongwe, N. P., M. Vichi, and P. M. S. Monteiro (2018). "The seasonal cycle of pCO_2 and CO_2 fluxes in the Southern Ocean: diagnosing anomalies in CMIP5 Earth system models." In: *Biogeosciences* 15.9, pp. 2851–2872. DOI: 10.5194/bg-15-2851-2018.

Monteiro, Pedro M. S., Luke Gregor, Marina Lévy, Stacy Maenner, Christopher L. Sabine, and Sebastiaan Swart (2015). "Intraseasonal variability linked to sampling alias in air-sea CO_2 fluxes in the Southern Ocean." In: *Geophysical Research Letters* 42.20, pp. 8507–8514. DOI: https://doi.org/10.1002/2015GL066009.

Monteiro, Pedro (2010). "A Global Sea Surface Carbon Observing System: Assessment of Changing Sea Surface CO_2 and Air-Sea CO_2 Fluxes." In: pp. 702–714. ISBN: 978-3-86987-200-1. DOI: 10.5270/OceanObs09.cwp.64.

Moreau, Sébastien et al. (2017). "Eddy-induced carbon transport across the Antarctic Circumpolar Current." In: *Global Biogeochemical Cycles* 31.9, pp. 1368–1386. DOI: https://doi.org/10.1002/2017GB005669.

Morgan, Sean, Sara Wong, Tyler Byrne, Adam Comeau, Brian Ward, Mark Barry, and Dariia Atamanchuk (2025). "Wave Glider-Based Measurements and Corrections of Near-Surface pCO_2 Gradients in the Coastal Ocean." In: *Global Biogeochemical Cycles* 39.7, e2024GB008396. DOI: https://doi.org/10.1029/2024GB008396.

Mortenson, Eric, Andrew Lenton, Elizabeth H. Shadwick, Thomas W. Trull, Matthew A. Chamberlain, Ramkrushnbhai Patel, Xuebin Zhang, and Rik Wanninkhof (2025). "Meridional asymmetry in the evolution of the Southern Ocean carbon sink over the 21st century in a high-resolution model." In: *Frontiers in Marine Science* Volume 12 - 2025. ISSN: 2296-7745. DOI: 10.3389/fmars.2025.1589735.

Müller, Jens Daniel et al. (2023). "Decadal Trends in the Oceanic Storage of Anthropogenic Carbon From 1994 to 2014." In: *AGU Advances* 4.4, e2023AV000875. DOI: https://doi.org/10.1029/2023AV000875.

Müller, W. A. et al. (2018). "A Higher-resolution Version of the Max Planck Institute Earth System Model (MPI-ESM1.2-HR)." In: *Journal of Advances in Modeling Earth Systems* 10.7, pp. 1383–1413. ISSN: 1942-2466. DOI: 10.1029/2017MS001217.

Nababan, B., D. Ulfah, and J. P. Panjaitan (2021). "Light propagation, coefficient attenuation, and the depth of one optical depth in different water types." In: *IOP Conference Series: Earth and Environmental Science* 944.1. Publisher: IOP Publishing, p. 012047. DOI: 10.1088/1755-1315/944/1/012047.

Naegler, Tobias (2009). "Reconciliation of excess $^{1}4$C-constrained global CO_2 piston velocity estimates." In: *Tellus B* 61.2, pp. 372–384. DOI: https://doi.org/10.1111/j.1600-0889.2008.00408.x.

Newton, Ja, Ra Feely, Eb Jewett, P Williamson, and J Mathis (2015). *Global Ocean Acidification Observing Network: Requirements and Governance Plan.* Report. URL: https://archimer.ifremer.fr/doc/00651/76343/ (visited on 06/06/2025).

Ni, Qinbiao, Xiaoming Zhai, Xuemin Jiang, and Dake Chen (2021). "Abundant Cold Anticyclonic Eddies and Warm Cyclonic Eddies in the Global Ocean." In: *Journal of Physical Oceanography* 51.9. Place: Boston MA, USA Publisher: American Meteorological Society, pp. 2793 –2806. DOI: 10.1175/JPO-D-21-0010.1.

Nicholson, S.-A., T. J. Ryan-Keogh, S. J. Thomalla, N. Chang, and M. E. Smith (2025). "Satellite-derived global-ocean phytoplankton phenology indices." In: *Earth System Science Data* 17.5, pp. 1959–1975. DOI: 10.5194/essd-17-1959-2025.

Nicholson, S., T. Ryan-Keogh, S. Thomalla, N. Chang, and M. Smith (2023). *Global Phytoplankton Phenological Indices - 4km resolution (1.0)*. DOI: 10.5281/zenodo.8402932.

Nicholson, Sarah-Anne, Daniel B. Whitt, Ilker Fer, Marcel D. du Plessis, Alice D. Lebéhot, Sebastiaan Swart, Adrienne J. Sutton, and Pedro M. S. Monteiro (2022). "Storms drive outgassing of CO_2 in the subpolar Southern Ocean." In: *Nature Communications* 13.1, p. 158. ISSN: 2041-1723. DOI: 10.1038/s41467-021-27780-w.

Nickford, S., J. B. Palter, and L. Mu (2024). "The Importance of Contemporaneous Wind and pCO_2 Measurements for Regional Air-Sea CO_2 Flux Estimates." In: *Journal of Geophysical Research: Oceans* 129.6, e2023JC020744. DOI: https://doi.org/10.1029/2023JC020744.

Nielsen, David M., Fatemeh Chegini, Joeran Maerz, Sebastian Brune, Moritz Mathis, Mikhail Dobrynin, Johanna Baehr, Victor Brovkin, and Tatiana Ilyina (2024). "Reduced Arctic Ocean CO_2 uptake due to coastal permafrost erosion." In: *Nature Climate Change* 14.9. Publisher: Nature Publishing Group, pp. 968–975. ISSN: 1758-6798. DOI: 10.1038/s41558-024-02074-3.

Nielsen, David Marcolino, Fatemeh Chegini, Nuno Serra, Arjun Kumar, Nils Brüggemann, Cathy Hohenegger, and Tatiana Ilyina (2025). "Resolved tropical cyclones trigger CO_2 uptake and phytoplankton bloom in an Earth system model simulation." In: preprint. DOI: 10.31223/X5KF05.

Nocera, Ariadna C., Irene R. Schloss, and Gabriela N. Williams and (2024). "Phytoplankton bloom detection and trends in satellite inherent optical properties over the last two decades in a heterogeneous Patagonian coastal system." In: *International Journal of Remote Sensing* 45.17, pp. 5946–5977. DOI: 10.1080/01431161.2024.2383384.

Olafsson, J., S. R. Olafsdottir, T. Takahashi, M. Danielsen, and T. S. Arnarson (2021). "Enhancement of the North Atlantic CO_2 sink by Arctic Waters." In: *Biogeosciences* 18.5, pp. 1689–1701. DOI: 10.5194/bg-18-1689-2021.

Oliveira Carvalho, Andréa da Consolação de, Rodrigo Kerr, Virginia Maria Tavano, and Carlos Rafael B. Mendes (2022). "The southwestern South Atlantic

continental shelf biogeochemical divide." In: *Biogeochemistry* 159.2, pp. 139–158. ISSN: 1573-515X. DOI: 10.1007/s10533-022-00918-8.

Oliver, H., K. M. Krumhardt, D. J. McGillicuddy Jr., C. Mitchell, and W. M. Balch (2024). "Mechanisms Regulating Coccolithophore Dynamics in the Great Calcite Belt in the Southern Ocean in the Community Earth System Model." In: *Journal of Geophysical Research: Oceans* 129.11, e2024JC021371. DOI: https://doi.org/10.1029/2024JC021371.

Olivier, Léa et al. (2022). "Wintertime process study of the North Brazil Current rings reveals the region as a larger sink for CO_2 than expected." In: *Biogeosciences* 19.12, pp. 2969–2988. ISSN: 1726-4170. DOI: 10.5194/bg-19-2969-2022.

Orselli, Iole B. M., Rodrigo Kerr, José L. L. de Azevedo, Felippe Galdino, Moacyr Araujo, and Carlos A. E. Garcia (2019). "The sea-air CO_2 net fluxes in the South Atlantic Ocean and the role played by Agulhas eddies." In: *Progress in Oceanography* 170, pp. 40–52. ISSN: 0079-6611. DOI: https://doi.org/10.1016/j.pocean.2018.10.006.

Orsi, Alejandro H., Thomas Whitworth, and Worth D. Nowlin (1995). "On the meridional extent and fronts of the Antarctic Circumpolar Current." In: *Deep Sea Research Part I: Oceanographic Research Papers* 42.5, pp. 641–673. ISSN: 0967-0637. DOI: https://doi.org/10.1016/0967-0637(95)00021-W.

Oschlies, Andreas and Véronique Garçon (1998). "Eddy-induced enhancement of primary production in a model of the North Atlantic Ocean." In: *Nature* 394.6690, pp. 266–269. ISSN: 1476-4687. DOI: 10.1038/28373.

Ostle, Clare, Peter Landschützer, Martin Edwards, Martin Johnson, Sunke Schmidtko, Ute Schuster, Andrew J. Watson, and Carol Robinson (2022). "Multidecadal changes in biology influence the variability of the North Atlantic carbon sink." In: *Environmental Research Letters* 17.11. Publisher: IOP Publishing, p. 114056. ISSN: 1748-9326. DOI: 10.1088/1748-9326/ac9ecf. (Visited on 11/22/2022).

Park, Geun-Ha, Rik Wanninkhof, Scott C. Doney, Taro Takahashi, Kitack Lee, Richard A. Feely, Christopher L. Sabine, Joaquin Triñanes, and Ivan D. Lima (2010). "Variability of global net sea–air CO_2 fluxes over the last three decades using empirical relationships." In: *Tellus B: Chemical and Physical Meteorology*. DOI: 10.1111/j.1600-0889.2010.00498.x.

Park, Y.-H. et al. (2019). "Observations of the Antarctic Circumpolar Current Over the Udintsev Fracture Zone, the Narrowest Choke Point in the Southern Ocean." In: *Journal of Geophysical Research: Oceans* 124.7, pp. 4511–4528. ISSN: 2169-9291. DOI: 10.1029/2019JC015024.

Patterson, Ruth G. et al. (2025). "Uncrewed surface vehicles in the Global Ocean Observing System: a new frontier for observing and monitoring at the air-sea

interface." In: *Frontiers in Marine Science* Volume 12 - 2025. ISSN: 2296-7745. DOI: 10.3389/fmars.2025.1523585.

Paulsen, Hanna, Tatiana Ilyina, Katharina D. Six, and Irene Stemmler (2017). "Incorporating a prognostic representation of marine nitrogen fixers into the global ocean biogeochemical model HAMOCC." In: *Journal of Advances in Modeling Earth Systems* 9.1, pp. 438–464. DOI: https://doi.org/10.1002/2016MS000737.

Pawlowicz, R. (2020). *M_Map: A Mapping Package for MATLAB*. URL: http://www.eoas.ubc.ca/rich/map.html.

Pegliasco, C., A. Delepoulle, E. Mason, R. Morrow, Y. Faugère, and G. Dibarboure (2022). "META3.1exp: a new global mesoscale eddy trajectory atlas derived from altimetry." In: *Earth System Science Data* 14.3, pp. 1087–1107. DOI: 10.5194/essd-14-1087-2022.

Perrot, Laurie, Francis Gohin, Diana Ruiz-Pino, Luis Lampert, Martin Huret, Aurélie Dessier, Pascale Malestroit, Christine Dupuy, and Paul Bourriau (2018). "Coccolith-derived turbidity and hydrological conditions in May in the Bay of Biscay." In: *Progress in Oceanography*. Multidisciplinary integrated surveys 166, pp. 41–53. ISSN: 0079-6611. DOI: 10.1016/j.pocean.2017.12.008.

Peter, R., J. Kuttippurath, N. Sunanda, and Kunal Chakraborty (2025). "Effect of thermal and non-thermal processes on the variability of ocean surface pCO_2 and buffering capacity in the north Indian Ocean." In: *Progress in Oceanography* 233, p. 103442. ISSN: 0079-6611. DOI: https://doi.org/10.1016/j.pocean.2025.103442.

Pezzi, Luciano P. et al. (2021). "Oceanic eddy-induced modifications to air–sea heat and CO_2 fluxes in the Brazil-Malvinas Confluence." In: *Scientific Reports* 11.1, p. 10648. ISSN: 2045-2322. DOI: 10.1038/s41598-021-89985-9.

Pfeil, B. et al. (2013). "A uniform, quality controlled Surface Ocean CO_2 Atlas (SOCAT)." In: *Earth System Science Data* 5.1, pp. 125–143. DOI: 10.5194/essd-5-125-2013.

Pierrot, Denis, Craig Neill, Kevin Sullivan, Robert Castle, Rik Wanninkhof, Heike Naigur, Truls Johannessen, Are Olsen, Richard Feely, and Catherine Cosca (2009). "Recommendations for autonomous underway pCO_2 measuring systems and data-reduction routines." In: *Deep Sea Research Part II: Topical Studies in Oceanography* 56, pp. 512–522. DOI: 10.1016/j.dsr2.2008.12.005.

Pollina, Thibaut, Adam G. Larson, Fabien Lombard, Hongquan Li, David Le Guen, Sébastien Colin, Colomban de Vargas, and Manu Prakash (2022). "PlanktoScope: Affordable Modular Quantitative Imaging Platform for Citizen Oceanography." In: *Frontiers in Marine Science* Volume 9 - 2022. ISSN: 2296-7745. DOI: 10.3389/fmars.2022.949428.

Poulton, Alex J., Stuart C. Painter, Jeremy R. Young, Nicholas R. Bates, Bruce Bowler, Dave Drapeau, Emily Lyczsckowski, and William M. Balch (2013). "The 2008 Emiliania huxleyi bloom along the Patagonian Shelf: Ecology, biogeochemistry, and cellular calcification." In: *Global Biogeochemical Cycles* 27.4, pp. 1023–1033. DOI: https://doi.org/10.1002/2013GB004641.

Prend, Channing J., Marcel D. du Plessis, Matthew R. Mazloff, Lovisa Sunnercrantz, Sebastiaan Swart, and Sarah T. Gille (2025). "Observing system requirements for measuring high-frequency air–sea fluxes in the Southern Ocean." In: *Elementa: Science of the Anthropocene* 13.1, p. 00061. ISSN: 2325-1026. DOI: 10.1525/elementa.2024.00061.

Project, Global Carbon (2022). *Supplemental data of Global Carbon Budget 2022 (Version 1.0)*. DOI: 10.18160/gcp-2022. URL: https://doi.org/10.18160/gcp-2022.

Pérez, Fiz F. et al. (2024). "An Assessment of CO_2 Storage and Sea-Air Fluxes for the Atlantic Ocean and Mediterranean Sea Between 1985 and 2018." In: *Global Biogeochemical Cycles* 38.4, e2023GB007862. ISSN: 1944-9224. DOI: 10.1029/2023GB007862.

Rajulapati, Chandra Rupa, Simon Michael Papalexiou, Martyn P. Clark, and John W. Pomeroy (2021). "The Perils of Regridding: Examples Using a Global Precipitation Dataset." In: *Journal of Applied Meteorology and Climatology* 60.11, pp. 1561–1573. DOI: 10.1175/JAMC-D-20-0259.1.

Rees, Andrew P., Ian Joint, and Kirsten M. Donald (1999). "Early spring bloom phytoplankton-nutrient dynamics at the Celtic Sea Shelf Edge." In: *Deep Sea Research Part I: Oceanographic Research Papers* 46.3, pp. 483–510. ISSN: 0967-0637. DOI: 10.1016/S0967-0637(98)00073-9. (Visited on 02/20/2025).

Reichstein, Markus, Gustau Camps-Valls, Bjorn Stevens, Martin Jung, Joachim Denzler, Nuno Carvalhais, and Prabhat (2019). "Deep learning and process understanding for data-driven Earth system science." In: *Nature* 566.7743, pp. 195–204. ISSN: 1476-4687. DOI: 10.1038/s41586-019-0912-1.

Resplandy, L., J. Boutin, and L. Merlivat (2014). "Observed small spatial scale and seasonal variability of the CO_2 system in the Southern Ocean." In: *Biogeosciences* 11.1. Publisher: Copernicus GmbH, pp. 75–90. ISSN: 1726-4170. DOI: 10.5194/bg-11-75-2014.

Reynolds, Richard W., Thomas M. Smith, Chunying Liu, Dudley B. Chelton, Kenneth S. Casey, and Michael G. Schlax (2007). "Daily High-Resolution-Blended Analyses for Sea Surface Temperature." In: *Journal of Climate* 20.22, pp. 5473–5496. ISSN: 0894-8755, 1520-0442. DOI: 10.1175/2007JCLI1824.1.

Ritter, R. et al. (2017). "Observation-based trends of the southern ocean carbon sink." In: *Geophysical Research Letters* 44, pp. 12,339–12,348. ISSN: 0094-8276. DOI: 10.1002/2017GL074837.

Robinson, Kelly L., Su Sponaugle, Jessica Y. Luo, Miram R. Gleiber, and Robert K. Cowen (2021). "Big or small, patchy all: Resolution of marine plankton patch structure at micro- to submesoscales for 36 taxa." In: *Science Advances* 7.47, eabk2904. DOI: 10.1126/sciadv.abk2904.

Rödenbeck, C., D. C. E. Bakker, N. Metzl, A. Olsen, C. Sabine, N. Cassar, F. Reum, R. F. Keeling, and M. Heimann (2014). "Interannual sea–air CO_2 flux variability from an observation-driven ocean mixed-layer scheme." In: *Biogeosciences* 11.17, pp. 4599–4613. DOI: 10.5194/bg-11-4599-2014.

Rödenbeck, C. et al. (2015). "Data-based estimates of the ocean carbon sink variability – first results of the Surface Ocean pCO_2 Mapping intercomparison (SOCOM)." In: *Biogeosciences* 12.23, pp. 7251–7278. ISSN: 1726-4170.

Rödenbeck, Christian, Tim DeVries, Judith Hauck, Corinne Le Quéré, and Ralph F. Keeling (2022). "Data-based estimates of the ocean carbon sink variability – first results of the Surface Ocean pCO_2 Mapping intercomparison (SOCOM)." In: *Biogeosciences* 19.10, pp. 2627–2652. ISSN: 1726-4189. DOI: 10.5194/bg-19-2627-2022.

Rodgers, Keith B. et al. (2023). "Seasonal Variability of the Surface Ocean Carbon Cycle: A Synthesis." In: *Global Biogeochemical Cycles* 37.9, e2023GB007798. DOI: https://doi.org/10.1029/2023GB007798.

Roemmich, Dean et al. (2019). "On the Future of Argo: A Global, Full-Depth, Multi-Disciplinary Array." In: *Frontiers in Marine Science* 6. ISSN: 2296-7745. DOI: 10.3389/fmars.2019.00439.

Romero, Silvia I., Alberto R. Piola, Marcela Charo, and Carlos A. Eiras Garcia (2006). "Chlorophyll-a variability off Patagonia based on SeaWiFS data." In: *Journal of Geophysical Research: Oceans* 111.C5. DOI: https://doi.org/10.1029/2005JC003244.

Roobaert, A., P. Regnier, P. Landschützer, and G. G. Laruelle (2024). "A novel sea surface pCO_2-product for the global coastal ocean resolving trends over 1982–2020." In: *Earth System Science Data* 16.1, pp. 421–441. DOI: 10.5194/essd-16-421-2024. URL: https://essd.copernicus.org/articles/16/421/2024/.

Roobaert, Alizee, Goulven Laruelle, Peter Landschützer, and Pierre Regnier (2018). "Uncertainty in the global oceanic CO_2 uptake induced by wind forcing: Quantification and spatial analysis." In: *Biogeosciences* 15. DOI: 10.5194/bg-15-1701-2018.

Roobaert, Alizée, Goulven G. Laruelle, Peter Landschützer, Nicolas Gruber, Lei Chou, and Pierre Regnier (2019). "The Spatiotemporal Dynamics of the Sources and Sinks of CO_2 in the Global Coastal Ocean." In: *Global Biogeochemical Cycles* 33.12, pp. 1693–1714. DOI: https://doi.org/10.1029/2019GB006239.

Rouault, Mathieu, Pierrick Penven, and Benjamin Pohl (2009). "Warming in the Agulhas Current system since the 1980's." In: *Geophysical Research Letters* 36.12. DOI: https://doi.org/10.1029/2009GL037987.

Rustogi, Paridhi, Peter Landschützer, Sebastian Brune, and Johanna Baehr (2023). "The impact of seasonality on the annual air-sea carbon flux and its interannual variability." In: *npj Climate and Atmospheric Science* 6.1, p. 66. ISSN: 2397-3722. DOI: 10.1038/s41612-023-00378-3.

Sabine, C. L. et al. (2013). "Surface Ocean CO_2 Atlas (SOCAT) gridded data products." In: *Earth System Science Data* 5.1, pp. 145–153. ISSN: 1866-3508. DOI: 10.5194/essd-5-145-2013.

Sabine, Chris, Ducklow Hugh, and Maria Hood (2010). "International Carbon Coordination: Roger Revelle's Legacy in the Intergovernmental Oceanographic Commission." In: *Oceanography* 23. DOI: 10.5670/oceanog.2010.23.

Sabine, Christopher et al. (2020). "Evaluation of a New Carbon Dioxide System for Autonomous Surface Vehicles." In: *Journal of Atmospheric and Oceanic Technology* 37.8, pp. 1305–1317. DOI: 10.1175/JTECH-D-20-0010.1.

Salinas-Matus, M., N. Serra, F. Chegini, and T. Ilyina (2025). "Mesoscale eddies heterogeneously modulate CO_2 fluxes in eddy-rich regions of the Southern Ocean." In: *EGUsphere* 2025, pp. 1–20. DOI: 10.5194/egusphere-2025-3067.

Sarmiento, Jorge L. and Nicolas Gruber (2006b). "Carbon Cycle, CO_2, and Climate." In: *Ocean Biogeochemical Dynamics*. Princeton University Press, pp. 392–458. ISBN: 9780691017075. DOI: 10.2307/j.ctt3fgxqx.14.

— (2006a). "Carbon Cycle." In: *Ocean Biogeochemical Dynamics*. Princeton University Press, pp. 318–358. ISBN: 9780691017075. DOI: 10.2307/j.ctt3fgxqx.12.

Sarmiento, Jorge L. et al. (2023). "The Southern Ocean carbon and climate observations and modeling (SOCCOM) project: A review." In: *Progress in Oceanography* 219, p. 103130. ISSN: 0079-6611. DOI: https://doi.org/10.1016/j.pocean.2023.103130.

Schloss, Irene, Gustavo Ferreyra, Martha Ferrario, Gastón Almandoz, Raul Codina, Alejandro Bianchi, Carlos Balestrini, Héctor Ochoa, Ruiz Diana, and Alain Poisson (2007). "Role of plankton communities in sea–air variations in pCO_2 in the SW Atlantic Ocean." In: *Marine Ecology Progress Series* 332, pp. 93–106. DOI: 10.3354/meps332093.

Schneider, B., S. Kaitala, and P. Maunula (2006). "Identification and quantification of plankton bloom events in the Baltic Sea by continuous pCO_2 and chlorophyll a measurements on a cargo ship." In: *Journal of Marine Systems* 59.3, pp. 238–248. ISSN: 0924-7963. DOI: https://doi.org/10.1016/j.jmarsys.2005.11.003.

Schoderer, Mirja, Henry Bittig, Birgit Klein, Ramona Hägele, Tobias Steinhoff, Karel Castro-Morales, Leticia Cunha, Anna-Katharina Hornidge, and Körtzinger Arne (2024). "From Individual Observations to Global Assessments: Tracing the Marine Carbon Knowledge Value Chain." In: *Ocean and Society* 2. DOI: 10.17645/oas.8891.

Schulz, E. W., S. A. Josey, and R. Verein (2012). "First air-sea flux mooring measurements in the Southern Ocean." In: *Geophysical Research Letters* 39.16. ISSN: 1944-8007. DOI: 10.1029/2012GL052290.

Sebille, E. van, A. Biastoch, P. J. van Leeuwen, and W. P. M. de Ruijter (2009). "A weaker Agulhas Current leads to more Agulhas leakage." In: *Geophysical Research Letters* 36.3. DOI: https://doi.org/10.1029/2008GL036614.

Shadwick, E. H., C. A. Wynn-Edwards, R. S. Eriksen, P. Jansen, X. Yang, G. Woodward, and D. Davies (2024). "The Southern Ocean Time Series: A climatological view of hydrography, biogeochemistry, phytoplankton community composition, and carbon export in the Subantarctic Zone." In: *EGUsphere* 2024, pp. 1–33. DOI: 10.5194/egusphere-2024-3887.

Shutler, J. D., P. E. Land, C. W. Brown, H. S. Findlay, C. J. Donlon, M. Medland, R. Snooke, and J. C. Blackford (2013). "Coccolithophore surface distributions in the North Atlantic and their modulation of the air-sea flux of CO_2 from 10 years of satellite Earth observation data." In: *Biogeosciences* 10.4. Publisher: Copernicus GmbH, pp. 2699–2709. ISSN: 1726-4170. DOI: 10.5194/bg-10-2699-2013.

Shutler, Jamie D, Nicolas Gruber, Helen S Findlay, Peter E Land, Luke Gregor, Thomas Holding, Richard P Sims, Hannah Green, Jean-Francois Piolle, Bertrand Chapron, et al. (2024). "The increasing importance of satellite observations to assess the ocean carbon sink and ocean acidification." In: *Earth-Science Reviews* 250, p. 104682.

Shutler, Jamie D, Rik Wanninkhof, Philip D Nightingale, David K Woolf, Dorothee CE Bakker, Andy Watson, Ian Ashton, Thomas Holding, Bertrand Chapron, Yves Quilfen, et al. (2020). "Satellites will address critical science priorities for quantifying ocean carbon." In: *Frontiers in Ecology and the Environment* 18.1, pp. 27–35.

Siegel, D. A., P. Peterson, D. J. McGillicuddy Jr., S. Maritorena, and N. B. Nelson (2011). "Bio-optical footprints created by mesoscale eddies in the Sargasso Sea." In: *Geophysical Research Letters* 38.13. DOI: https://doi.org/10.1029/2011GL047660.

Siegel, D.A. et al. (2013). "Regional to global assessments of phytoplankton dynamics from the SeaWiFS mission." In: *Remote Sensing of Environment* 135, pp. 77–91. ISSN: 0034-4257. DOI: https://doi.org/10.1016/j.rse.2013.03.025.

Silvy, Y. et al. (2024). "AERA-MIP: Emission pathways, remaining budgets and carbon cycle dynamics compatible with 1.5°C and 2°C global warming stabilization." In: *EGUsphere* 2024, pp. 1–47. DOI: 10.5194/egusphere-2024-488.

Six, Katharina D. and Ernst Maier-Reimer (1996). "Effects of plankton dynamics on seasonal carbon fluxes in an ocean general circulation model." In: *Global Biogeochemical Cycles* 10.4, pp. 559–583. ISSN: 1944-9224. DOI: 10.1029/96GB02561.

Sloyan, Bernadette M. et al. (2019). "The Global Ocean Ship-Based Hydrographic Investigations Program (GO-SHIP): A Platform for Integrated Multidisciplinary Ocean Science." In: *Frontiers in Marine Science* Volume 6 - 2019. ISSN: 2296-7745. DOI: 10.3389/fmars.2019.00445.

Smith, Shawn R. et al. (2019). "Ship-Based Contributions to Global Ocean, Weather, and Climate Observing Systems." In: *Frontiers in Marine Science* 6. ISSN: 2296-7745. DOI: 10.3389/fmars.2019.00434.

Smith, T. G., S.-A. Nicholson, F. A. Engelbrecht, N. Chang, N. P. Mongwe, and P. M. S. Monteiro (2023). "The Heat and Carbon Characteristics of Modeled Mesoscale Eddies in the South–East Atlantic Ocean." In: *Journal of Geophysical Research: Oceans* 128.12, e2023JC020337. DOI: https://doi.org/10.1029/2023JC020337.

Song, Hajoon, John Marshall, David R. Munro, Stephanie Dutkiewicz, Colm Sweeney, D. J. McGillicuddy Jr., and Ute Hausmann (2016). "Mesoscale modulation of air-sea CO_2 flux in Drake Passage." In: *Journal of Geophysical Research: Oceans* 121.9, pp. 6635–6649. DOI: https://doi.org/10.1002/2016JC011714.

Song, Ruiming, Tim DeVries, Renjian Li, Adrienne Sutton, Uwe Send, and Helena C. Frazão (2025). "High-Frequency Correlations Between Winds and pCO_2 Change the California Coastal Upwelling System From a CO_2 Sink to a Source." In: *Geophysical Research Letters* 52.14, e2025GL115470. DOI: https://doi.org/10.1029/2025GL115470.

Souza, Márcio Silva de, Carlos Rafael Borges Mendes, Virgínia Maria Tavano Garcia, Ricardo Pollery, and Vanda Brotas (2012). "Phytoplankton community during a coccolithophorid bloom in the Patagonian Shelf: microscopic and high-performance liquid chromatography pigment analyses." In: *Journal of the Marine Biological Association of the United Kingdom* 92.1, pp. 13–27. DOI: 10.1017/S0025315411000439.

Steinhoff, Tobias et al. (2025). "The ICOS OTC pCO_2 instrument inter-comparison." In: *Limnology and Oceanography: Methods*. submitted, pp. 1–66. ISSN: 1541-5856. URL: https://oceanrep.geomar.de/id/eprint/62199/.

Storey, John D. (2002). "A direct approach to false discovery rates." In: *Journal of the Royal Statistical Society: Series B (Statistical Methodology)* 64.3, pp. 479–498. ISSN: 13697412, 14679868. DOI: 10.1111/1467-9868.00346.

Su, Jiaoyang, Peter G. Strutton, and Christina Schallenberg (2021). "The subsurface biological structure of Southern Ocean eddies revealed by BGC-Argo floats." In: *Journal of Marine Systems* 220, p. 103569. ISSN: 0924-7963. DOI: https://doi.org/10.1016/j.jmarsys.2021.103569.

Sutton, A. J., N. L. Williams, and B. Tilbrook (2021). "Constraining Southern Ocean CO_2 Flux Uncertainty Using Uncrewed Surface Vehicle Observations." In: *Geophysical Research Letters* 48.3, e2020GL091748. ISSN: 1944-8007. DOI: 10.1029/2020GL091748.

Sutton, A. J. et al. (2014). "A high-frequency atmospheric and seawater pCO_2 data set from 14 open-ocean sites using a moored autonomous system." In: *Earth System Science Data* 6.2, pp. 353–366. DOI: 10.5194/essd-6-353-2014.

Sutton, A. J. et al. (2019). "Autonomous seawater pCO_2 and pH time series from 40 surface buoys and the emergence of anthropogenic trends." In: *Earth System Science Data* 11.1, pp. 421–439. DOI: 10.5194/essd-11-421-2019.

Sutton, Adrienne and Christopher Sabine (2023). "Emerging Applications of Longstanding Autonomous Ocean Carbon Observations." In: *Oceanography*. DOI: 10.5670/oceanog.2023.209.

Suykens, K., B. Delille, L. Chou, C. De Bodt, J. Harlay, and A. V. Borges (2010). "Dissolved inorganic carbon dynamics and air-sea carbon dioxide fluxes during coccolithophore blooms in the northwest European continental margin (northern Bay of Biscay)." In: *Global Biogeochemical Cycles* 24.3. ISSN: 1944-9224. DOI: 10.1029/2009GB003730.

TRICUSO (2024). *Three Research Infrastructures together: Carbon Uptake Southern Ocean (TRICUSO)*. Funded by the European Union under the Horizon Europe program, Call: HORIZON-INFRA-2024-TECH-01, Topic: HORIZON-INFRA-2024-TECH-01-01, Type of Action: HORIZON-RIA, with Proposal Number: 101188028. Type of Model Grant Agreement: HORIZON Action Grant Budget-Based. Available at: https://tricuso.eu and https://ec.europa.eu/info/funding-tenders/opportunities/portal/screen/opportunities/projects-details/43108390/101188028/HORIZON.

Takahashi, Taro (1961). "Carbon dioxide in the atmosphere and in Atlantic Ocean water." In: *Journal of Geophysical Research (1896-1977)* 66.2, pp. 477–494. DOI: https://doi.org/10.1029/JZ066i002p00477.

Takahashi, Taro, Richard A Feely, Ray F Weiss, Rik H Wanninkhof, David W Chipman, Stewart C Sutherland, and Timothy T Takahashi (1997). "Global air-sea flux of CO_2: An estimate based on measurements of sea–air pCO_2 dif-

ference." In: *Proceedings of the National Academy of Sciences* 94.16, pp. 8292–8299.

Takahashi, Taro et al. (2002). "Global sea–air CO_2 flux based on climatological surface ocean pCO_2, and seasonal biological and temperature effects." In: *Deep Sea Research Part II: Topical Studies in Oceanography* 49.9. The Southern Ocean I: Climatic Changes in the Cycle of Carbon in the Southern Ocean, pp. 1601–1622. ISSN: 0967-0645. DOI: https://doi.org/10.1016/S0967-0645(02)00003-6.

Takahashi, Taro et al. (2009). "Climatological mean and decadal change in surface ocean pCO_2, and net sea–air CO_2 flux over the global oceans." In: *Deep Sea Research Part II: Topical Studies in Oceanography*. Surface Ocean CO_2 Variability and Vulnerabilities 56.8, pp. 554–577. ISSN: 0967-0645. DOI: 10.1016/j.dsr2.2008.12.009.

Takao, Shintaro, Shin-Ichiro Nakaoka, Fuminori Hashihama, Keishi Shimada, Hisayuki Yoshikawa-Inoue, Toru Hirawake, Jota Kanda, Gen Hashida, and Koji Suzuki (2020). "Effects of phytoplankton community composition and productivity on sea surface pCO_2 variations in the Southern Ocean." In: *Deep Sea Research Part I: Oceanographic Research Papers* 160, p. 103263. ISSN: 0967-0637. DOI: https://doi.org/10.1016/j.dsr.2020.103263.

Talley, Lynne D., George L. Pickard, William J. Emery, and James H. Swift (2011). "Chapter 13 - Southern Ocean." In: *Descriptive Physical Oceanography (Sixth Edition)*. Ed. by Lynne D. Talley, George L. Pickard, William J. Emery, and James H. Swift. Sixth Edition. Boston: Academic Press, pp. 437–471. ISBN: 978-0-7506-4552-2. DOI: https://doi.org/10.1016/B978-0-7506-4552-2.10013-7.

Tanhua, Toste, Sören B. Gutekunst, and Arne Biastoch (2020). "A near-synoptic survey of ocean microplastic concentration along an around-the-world sailing race." In: *PLOS ONE* 15.12, pp. 1–11. DOI: 10.1371/journal.pone.0243203. URL: https://doi.org/10.1371/journal.pone.0243203.

Tanhua, Toste et al. (2019). "What We Have Learned From the Framework for Ocean Observing: Evolution of the Global Ocean Observing System." In: *Frontiers in Marine Science* 6. ISSN: 2296-7745. DOI: 10.3389/fmars.2019.00471.

Telszewski, M. et al. (2009). "Estimating the monthly pCO_2 distribution in the North Atlantic using a self-organizing neural network." In: *Biogeosciences* 6.8. Publisher: Copernicus GmbH, pp. 1405–1421. ISSN: 1726-4170. DOI: 10.5194/bg-6-1405-2009.

Titchner, H. A. and N. A. Rayner (2014). "The Met Office Hadley Centre sea ice and sea surface temperature data set, version 2: 1. Sea ice concentrations."

In: *Journal of Geophysical Research: Atmospheres* 119, pp. 2864–2889. DOI: 10.1002/2013JD020316.

Ulibarrena, Javier and Victor H. Conzonno (2015). "Mechanisms involved in the proliferation and distribution of phytoplankton in the Patagonian Sea, Argentina, as revealed by remote sensing studies." In: *Environmental Earth Sciences* 74.1, pp. 439–449. ISSN: 1866-6299. DOI: 10.1007/s12665-015-4052-0.

Umbert, Marta, Nina Hoareau, Jordi Salat, Joaquín Salvador, Sébastien Guimbard, Estrella Olmedo, and Carolina Gabarró (2022). "The Contribution of the Vendée Globe Race to Improved Ocean Surface Information: A Validation of the Remotely Sensed Salinity in the Sub-Antarctic Zone." In: *Journal of Marine Science and Engineering* 10.8. ISSN: 2077-1312. DOI: 10.3390/jmse10081078.

United Nations Framework Convention on Climate Change (2015). *Paris Agreement*. URL: https://unfccc.int/sites/default/files/resource/parisagreement_publication.pdf (visited on 10/12/2023).

Waite, A. M., S. Pesant, D. A. Griffin, P. A. Thompson, and C. M. Holl (2007). "Oceanography, primary production and dissolved inorganic nitrogen uptake in two Leeuwin Current eddies." In: *Deep Sea Research Part II: Topical Studies in Oceanography* 54.8, pp. 981–1002. ISSN: 0967-0645. DOI: https://doi.org/10.1016/j.dsr2.2007.03.001.

Wang, Xiaojing, Bo Han, Gong Zhang, Changwei Liu, and Qinghua Yang (2025a). "Sub-monthly Processes Contribute Significantly to CO_2 Uptake in the South China Sea." In: *Advances in Atmospheric Sciences*. ISSN: 1861-9533. DOI: 10.1007/s00376-025-4439-0.

Wang, Yujie, Yadong Gao, Rui He, Yangyang Gao, Ziyang Xu, Changjie Wang, and Fenfen Liu (2025b). "Global ocean surface pCO_2 retrieval and the influence of mesoscale eddies on its performance." In: *Science of The Total Environment* 993, p. 179856. ISSN: 0048-9697. DOI: https://doi.org/10.1016/j.scitotenv.2025.179856.

Wanninkhof, Rik (1992). "Relationship between wind speed and gas exchange over the ocean." In: *Journal of Geophysical Research: Oceans* 97.C5, pp. 7373–7382. ISSN: 2156-2202. DOI: 10.1029/92JC00188.

Wanninkhof, Rik et al. (2019). "A Surface Ocean CO_2 Reference Network, SOCONET and Associated Marine Boundary Layer CO_2 Measurements." In: *Frontiers in Marine Science* 6. ISSN: 2296-7745. DOI: 10.3389/fmars.2019.00400.

Waterman, L. S., P. P. Tans, T. Aten, C. D. Keeling, and T. A. Boden (1996). "Quasi-simultaneous CO_2 Measurements in the Atmosphere and Surface Ocean

Waters from Scripps Institution of Oceanography DOWNWIND, MONSOON, and LUSIAD Expeditions, 1957-1963." In: Draft report, p. 38.

Watson, Andrew J., C. Robinson, J. E. Robinson, P. J. le B. Williams, and M. J. R. Fasham (1991). "Spatial variability in the sink for atmospheric carbon dioxide in the North Atlantic." In: *Nature* 350.6313, pp. 50–53. ISSN: 1476-4687. DOI: 10.1038/350050a0.

Watson, Andrew J., Ute Schuster, Jamie D. Shutler, Thomas Holding, Ian G. C. Ashton, Peter Landschützer, David K. Woolf, and Lonneke Goddijn-Murphy (2020). "Revised estimates of ocean-atmosphere CO_2 flux are consistent with ocean carbon inventory." In: *Nature Communications* 11.1, p. 4422. ISSN: 2041-1723. DOI: 10.1038/s41467-020-18203-3.

Watson, Andrew et al. (2009). "Tracking the Variable North Atlantic Sink for Atmospheric CO_2." In: *Science (New York, N.Y.)* 326, pp. 1391–3. DOI: 10.1126/science.1177394.

Wei, Yanzhou, Sarah T. Gille, Matthew R. Mazloff, Veronica Tamsitt, Sebastiaan Swart, Dake Chen, and Louise Newman (2020). "Optimizing Mooring Placement to Constrain Southern Ocean Air–Sea Fluxes." In: *Journal of Atmospheric and Oceanic Technology* 37.8. Place: Boston MA, USA Publisher: American Meteorological Society, pp. 1365 –1385. DOI: 10.1175/JTECH-D-19-0203.1.

Weiss, R. (1974). "Carbon dioxide in water and seawater: the solubility of a non-ideal gas." In: *Marine Chemistry* 2.3, pp. 203–215.

Whitt, Christopher et al. (2020). "Future Vision for Autonomous Ocean Observations." In: *Frontiers in Marine Science* 7. ISSN: 2296-7745. DOI: 10.3389/fmars.2020.00697.

Williams, N. L. et al. (2017). "Calculating surface ocean pCO_2 from biogeochemical Argo floats equipped with pH: An uncertainty analysis." In: *Global Biogeochemical Cycles* 31.3, pp. 591–604. ISSN: 1944-9224. DOI: 10.1002/2016GB005541.

Williams, NL, LW Juranek, RA Feely, JL Russell, KS Johnson, and B Hales (2018). "Assessment of the carbonate chemistry seasonal cycles in the Southern Ocean from persistent observational platforms." In: *Journal of Geophysical Research: Oceans* 123.7, pp. 4833–4852.

Williams, Richard G. and Michael J. Follows (2011a). "Carbonate chemistry fundamentals." In: *Ocean Dynamics and the Carbon Cycle: Principles and Mechanisms*. Cambridge University Press, 125–156.

— (2011b). "Fundamentals." In: *Ocean Dynamics and the Carbon Cycle: Principles and Mechanisms*. Cambridge University Press, 41–42.

Williams, Richard G., Andrew J. S. Meijers, Vassil M. Roussenov, Anna Katavouta, Paulo Ceppi, Jonathan P. Rosser, and Pietro Salvi (2024). "Asymmetries in

the Southern Ocean contribution to global heat and carbon uptake." In: *Nature Climate Change* 14.8. Publisher: Nature Publishing Group, pp. 823–831. ISSN: 1758-6798. DOI: 10.1038/s41558-024-02066-3.

Woolf, D. K., P. E. Land, J. D. Shutler, L. M. Goddijn-Murphy, and C. J. Donlon (2016). "On the calculation of air-sea fluxes of CO_2 in the presence of temperature and salinity gradients." In: *Journal of Geophysical Research: Oceans* 121.2, pp. 1229–1248. DOI: https://doi.org/10.1002/2015JC011427.

Woolf, D.K. et al. (2019). "Key Uncertainties in the Recent Air-Sea Flux of CO_2." In: *Global Biogeochemical Cycles* 33.12, pp. 1548–1563. DOI: https://doi.org/10.1029/2018GB006041.

Wu, Yingxu and Di Qi (2022). "Inconsistency between ship- and Argo float-based pCO_2 at the intense upwelling region of the Drake Passage, Southern Ocean." In: *Frontiers in Marine Science* Volume 9 - 2022. ISSN: 2296-7745. DOI: 10.3389/fmars.2022.1002398.

Wunsch, Carl, Raymond W. Schmitt, and D. James Baker (2013). "Climate change as an intergenerational problem." In: *Proceedings of the National Academy of Sciences* 110.12, pp. 4435–4436. DOI: 10.1073/pnas.1302536110.

Yang, Xiang, Cathryn A. Wynn-Edwards, Peter G. Strutton, and Elizabeth H. Shadwick (2024). "Drivers of Air-Sea CO_2 Flux in the Subantarctic Zone Revealed by Time Series Observations." In: *Global Biogeochemical Cycles* 38.1, e2023GB007766. DOI: https://doi.org/10.1029/2023GB007766.

Yun, Jeongmin, Junjie Liu, Kevin W. Bowman, Laure Resplandy, and Dustin Carroll (2024). "The potential of the Orbiting Carbon Observatory-2 column CO_2 measurements to constrain air-sea CO_2 fluxes." In: *ESS Open Archive eprints* 389, p. 172252933.38918992. DOI: 10.22541/essoar.172252933.38918992/v1.

Zhang, D., M. F. Cronin, C. Meinig, J. T. Farrar, R. Jenkins, D. Peacock, J. Keene, A. Sutton, and Q. Yang (2019). "Comparing air-sea flux measurements from a new unmanned surface vehicle and proven platforms during the SPURS-2 field campaign." In: *Oceanography* 32.2, pp. 122–133. DOI: 10.5670/oceanog.2019.220.

Zhang, Dongxiao et al. (2023). "Observing Extreme Ocean and Weather Events Using Innovative Saildrone Uncrewed Surface Vehicles." In: *Oceanography* issue$_v$*olume*. DOI: 10.5670/oceanog.2023.214.

Zhong, Guorong et al. (2024). "The Southern Ocean carbon sink has been overestimated in the past three decades." In: *Communications Earth & Environment* 5.1. Publisher: Nature Publishing Group, pp. 1–12. ISSN: 2662-4435. DOI: 10.1038/s43247-024-01566-6.

EIDESSTATTLICHE VERSICHERUNG
DECLARATION ON OATH

Hiermit erkläre ich an Eides statt, dass ich die vorliegende Dissertationsschrift selbst verfasst und keine anderen als die angegebenen Quellen und Hilfsmittel benutzt habe. Sofern im Zuge der Erstellung der vorliegenden Dissertationsschrift generative Künstliche Intelligenz (gKI) basierte elektronische Hilfsmittel verwendet wurden, versichere ich, dass meine eigene Leistung im Vordergrund stand und dass eine vollständige Dokumentation aller verwendeten Hilfsmittel gemäß der Guten wissenschaftlichen Praxis vorliegt. Ich trage die Verantwortung für eventuell durch die gKI generierte fehlerhafte oder verzerrte Inhalte, fehlerhafte Referenzen, Verstöße gegen das Datenschutz- und Urheberrecht oder Plagiate.

I hereby declare and affirm that this doctoral dissertation is my own work and that I have not used any aids and sources other than those indicated. If electronic resources based on generative artificial intelligence (gAI) were used in the course of writing this dissertation, I confirm that my own work was the main and value-adding contribution and that complete documentation of all resources used is available in accordance with good scientific practice. I am responsible for any erroneous or distorted content, incorrect references, violations of data protection and copyright law or plagiarism that may have been generated by the gAI.

Hamburg, August 2025

Jacqueline Behncke

Hinweis / Reference

Die gesamten Veröffentlichungen in der Publikationsreihe des MPI-M
„Berichte zur Erdsystemforschung / Reports on Earth System Science“,
ISSN 1614-1199

sind über die Internetseiten des Max-Planck-Instituts für Meteorologie erhältlich:
https://mpimet.mpg.de/forschung/publikationen

All the publications in the series of the MPI -M
„Berichte zur Erdsystemforschung / Reports on Earth System Science“,
ISSN 1614-1199

are available on the website of the Max Planck Institute for Meteorology:
https://mpimet.mpg.de/en/research/publications